

**University of Belgrade
School of Medicine**

Jelena R. Potić, MD

**Characterization of the Mechanisms of
Photoreceptor Degeneration during Retinal
Detachment; the Evaluation of Postoperative
Anatomical and Functional Recovery**

Doctoral Dissertation

Belgrade, 2018.

Универзитет у Београду
Медицински факултет

Јелена Р. Потих

**Карактеризација механизма дегенерације
фоторецептора након аблације ретине;
евалуација анатомског и функционалног
постоперативног опоравка**

докторска дисертација

Београд, 2018.

Mentors

Prof. Yvan Arsenijevic, Professor of Neurobiology

Unit of Retinal Degeneration and Regeneration, Jules-Gonin Eye Hospital, Faculty of Biology and Medicine, University of Lausanne, Switzerland

Prof. Thomas J. Wolfensberger, Professor of Ophthalmology

Jules-Gonin Eye Hospital, Faculty of Biology and Medicine, University of Lausanne, Switzerland

Jury members

Prof. Vladimir Bumbaširević, Professor of Histology and Embryology,

Institute of Histology and Embryology, Faculty of Medicine, University of Belgrade, Serbia

Prof. Tatjana Pekmezović, Professor of Epidemiology

Institute of Epidemiology, Faculty of Medicine, University of Belgrade, Serbia

Prof. Milenko Stojković, Professor of Ophthalmology

Clinic for Eye Diseases, Clinical Center of Serbia, Faculty of Medicine, University of Belgrade, Serbia

Prof. Dragan Vuković, Professor of Ophthalmology

Clinic for Eye Diseases, Clinical Center of Serbia, Faculty of Medicine, University of Belgrade, Serbia

Prof. Francis Munier, Professor of Ophthalmology

Jules-Gonin Eye Hospital, Faculty of Biology and Medicine, University of Lausanne, Switzerland

Acknowledgments

Special thanks to my Swiss and Serbian professors for this opportunity, for precious advices, for knowledge, for unlimited support

Prof. Thomas J. Wolfensberger

Prof. Yvan Arsenijevic

Prof. Ivan Stefanovic

To my Swiss team who were essential power of the study:

Ciara Bergin, PhD

Dana Wanner

Clarice Giacuzzo, MD

To all the members of this project, this project wouldn't be possible to realize without them:

Prof. Francine Behar Cohen, PhD

Alejandra Daruich, MD

Lazaros Konstantinidis, MD

Jean-Antoine Pournaras, MD

Martial Mbefo, PhD

To my colleagues from the Clinic for Eye Diseases, Clinical Center of Serbia

To my parents and family who were always standing next to me, full of understanding and support.

“It is an unending story of a leaking break in a retinal detachment which has to be found and closed once and for all.”

PhD thesis information:

TITLE: Characterization of the Mechanisms of Photoreceptor Degeneration during Retinal Detachment; the Evaluation of Postoperative Anatomical and Functional Recovery

ABSTRACT

Introduction: Rhegmatogenous retinal detachment (RD) has diagnostically been divided into macula-OFF (OFF) or macula-ON (ON). Currently the only treatment for RD is surgery. Despite good anatomical surgical success in majority of cases, visual recovery varies a lot. Reduction in visual acuity (VA) has a direct effect on patient's quality of life (QoL). To date, few studies have reported QoL measures in patients with RD. The degree of visual loss is proportional to the degree of photoreceptor loss, which has been impossible to assess *in-vivo* until recently. If foveal photoreceptor alterations following RD can be observed and monitored using adaptive optics fundus camera (AO), and if these correlate with visual impairment, there is a strong case for a clinical application of this device. We previously identified that cell cycle proteins are reactivated in various rodent models of inherited retinal dystrophies as well as during light damage; this mechanism might overlap in RD as well. Therefore, we investigated human retina to have a better comprehension of the cell death mechanisms that may occur in patients affected by RD. The first step to develop an effective therapeutic agent is to determine the underlying disease mechanisms to identify the most appropriate means for intervention.

Aims: The aims of this study were: to describe the demographics and primary outcome of patients with RD following surgery with respect to the macular status, and to determine risk factors for macular involvement; to measure and compare preoperative and postoperative QoL in OFF and ON RD patients; to report new distinct type of RD: hemi-macular detachment (HMD); to evaluate the changes in choroidal thickness (CT) pre- and postoperatively in RD and among different RD types; to quantify the changes in cone density and topography using AO in RD, and to correlate (or not) these changes, macular involvement and changes in best corrected VA (BCVA) [logMAR]; and to reveal whether apoptosis, cell cycle reentry and epigenetic modifications, are also involved in an *in vitro* model of human RD, which was shown to activate different pathways during the initiation of photoreceptor degeneration.

Methods: This prospective, observational mono-centric cohort study was conducted at the Jules-Gonin Eye Hospital, from February 2015 until March 2017. 204 patients with primary

RD were enrolled but 194 were analyzed in the study. All patients underwent surgical treatment (scleral buckling or pars plana vitrectomy (PPV)) after baseline clinical examination and completing shorten validated version of National Eye Institute Visual Function Questionnaire (NEI VFQ-13). Composite score (CS) and subscale scores (short-form visual functioning scale (SFVFS) and short-form socioemotional scale (SFSES)) of NEI VFQ-13 were analyzed. Using EnFace optical coherence tomography (OCT) images, 9 cases had distinct subgroup of RD-HMD (4.4%). 54 eyes of 54 patients who underwent PPV with gas tamponade were suitable for CT analysis. They were divided into three groups according to the extension of the RD: peripheral macula-ON (>3 mm from the fovea, 14 eyes), paracentral ON (\leq 3 mm from the fovea; 14 eyes) and 26 OFF eyes. All eyes had CT measures at 1 month (M1) and 3 months (M3) on SD-OCT using enhanced depth images (EDI-OCT). Macula-ON RDs also had a CT measurement prior to surgery. The difference between treated (TE) and fellow eye (FE) was calculated. At M1 and M3 post-vitrectomy, patients underwent AO imagery in both eyes, at five locations, that were matched between time-points using anatomical landmarks. 22 patients (10 OFF and 12 ON) had matched and analyzable AO images. The dataset was analyzed using descriptive and analytic statistics. We used analysis of variance for repeated measures. In addition, we made an *in vitro* model of human RD, dividing explants into two groups: with and without RPE. The tissue was studied at different time points and immunohistochemical analyses for TUNEL, CDKs, H3K27me³, caspase3 and AIF expression were performed.

Results: 52.6% of patients presented with OFF RD. Mean age were 63.9 ± 12.0 vs. 59.7 ± 11.2 years in OFF and ON group, respectively. There were 129 men (66.5%) and 65 (33.5%) women, and there were significantly more right eyes affected (right vs. left eyes 123 (63.4%) vs. 71 (36.6%), $p=0.000$). Significantly more myopes ($<-3D$) presented with an ON RD ($p=0.04$). There were more phakic patients in the cohort (55.7%), and phakic eyes were more likely to present with ON RD ($p=0.01$). Multivariate modeling showed that pseudophakic lens status and eyes with axial length (AL) $< 25\text{mm}$ ($p=0.06$) are independent predictive factors for OFF RD ($p=0.02$), whereas sex and laterality were no risk factors for macular involvement. BCVA was significantly different between OFF and ON RDs at baseline: $2.0[2.3-0.95]$ vs $0[0.1-0]$; at M1 $0.35[0.5-0.1]$ vs $0.05[0-0.1]$ and at M3 $0.25[0.3-0.1]$ vs $0[0-0]$. 47 patients completed NEI VFQ-13 (26 ON RD and 21 OFF RD) in all time-points. In the OFF group, QoL scores improved from pre-operative to M1 and again at M3-6. In the ON group, QoL scores at M1 decreased in comparison to preoperatively, but recovered at M3-6. Preoperatively, there was a significant difference between ON and OFF RD in QoL scores

($p < 0.03$) with SFSES being the most sensitive. At M1 no difference in QoL was noted between ON and OFF groups. At M3-6 QoL was again significantly different between groups, in both CS and SFSES ($p = 0.03$, $p = 0.002$), but not in the SFVFS subscale ($p = 0.10$). A large improvement in BCVA in OFF group throughout follow-up coincided with improvement in QoL scores, but didn't reach the significance. In the ON group, there was a significant improvement in BCVA between M1 and M3-6 ($p = 0.03$), this coincided with a significant increase in the SFSES score ($p = 0.006$). Pre-operatively, BCVA and QoL were poorly correlated ($R^2 < 0.20$). Post-operatively, in the OFF group there was positive correlation between BCVA and QoL, the strongest at M3-6 in SFSES score ($p < 0.001$, $R^2 = 0.58$). In the ON group there was the correlation with BCVA only in SFVFS score at M3-6 ($p < 0.001$, $R^2 = 0.41$). In HMD, preoperatively, subretinal fluid (SRF) formed a circular sub-foveal pocket ($85 \pm 85 \mu\text{m}$), decreasing at peripheral border of the fovea ($82.9 \pm 55.4 \mu\text{m}$ at $200 \mu\text{m}$). Shallow RD persisted para-centrally ($113.2 \pm 66.4 \mu\text{m}$ at $500 \mu\text{m}$) until vascular arcades, where SRF height increased ($548.1 \pm 348.8 \mu\text{m}$ at $3000 \mu\text{m}$). Postoperative BCVA was $0.1 [0.2-0.0]$ logMAR, yet patients described visual disturbances. Hypo-reflective zones within ellipsoid layer were visible on EnFace OCT, forming a watermark along former RD border in coronal images. In peripheral RD the inter-eye difference in CT at the sub-foveal location showed a thickening throughout follow up (pre op: $19.6\% \pm 43.9$, M1: $22.9\% \pm 27.5$, M3: $18.2\% \pm 35.6$). In the paracentral RD, the inter-eye difference in CTs sub-foveally showed a thinning over FE throughout follow-up (pre-op: $-7.8\% \pm 21.9$, M1: $-5.5\% \pm 26.1$, M3: $-9.3\% \pm 19.4$). In the OFF RD, the inter-eye difference indicated more marked CT thinning throughout follow-up (at the sub-foveal location: M1 = $-14.1\% \pm 18.7$, M3 = $-9.9\% \pm 15$). The inter-eye difference in sub-foveal CT between peripheral ON and paracentral ON and between peripheral ON and OFF eyes was statistically different at M1 ($p = 0.00$, $p = 0.00$) and at M3 ($p = 0.00$, $p = 0.00$). With AO, we observed that cone density was: stable in FE between M1 and M3 ($p = 0.67$); decreased in TE than in FE ($p < 0.05$); increased postoperatively in ON ($p = 0.02$) but not in the OFF group ($p = 0.97$). BCVA and RD type were independently correlated with cone density ($p = 0.004$, $p = 0.000$).

The *in vitro* model of RD mimics the kinetic of cell death described *in vivo*. Indeed, the number of TUNEL positive cells, compared between 1DIV and 7DIV, increased with time in retina with (1DIV: 1.50 ± 0.00 vs 7DIV: 7.67 ± 0.00) and without RPE (1DIV: 2.83 ± 1.03 vs 7DIV: 15.84 ± 1.73 , $p = 0.02$) with a peak at 3DIV (wRPE 0.75 ± 0.30 vs noRPE: 11.83 ± 6.68). CDK4-positive cells, were poorly expressed in both groups at 1DIV (wRPE: 0.00 ± 0.00 vs noRPE: 2.01 ± 0.75 , $p = 0.02$) and at 7 DIV (wRPE: 1.58 ± 0.12 vs 4.73 ± 0.86 , $p = 0.02$).

H3K27me3 positive cells were present at all time points with the peak at 5DIV (wRPE 1.35 ± 0.08 vs. noRPE 12.68 ± 2.06). AIF positive cells are present at 1DIV in a lesser amount, having a peak at 3DIV in concomitance to the peak of TUNEL positive cells.

Conclusion: Pseudophakia and AL < 25 mm are independent predictive factors for OFF RD. While pseudophakia is a recognized risk factor for RD, shorter AL has not been previously identified as a risk factor for the OFF RD. There is significant difference in QoL CS and more importantly SFSES and SFVFS between ON and OFF RD. This difference is pronounced pre-operatively, but also throughout follow-up. In ON patients there is a notable drop of patients' QoL at M1 while in the OFF patients there is a positive progression in their QoL in the whole postoperative period. The biggest changes in QoL are present in SFSES subscale. HMD occurs in 4% of primary RD. Pre-operatively, SRF was shallow within vascular arcades, markedly more bullous immediately outside these limits. Post-operatively these eyes had good VA recovery despite persistent visual disturbances.

Peripheral ON RD showed different recovery paths in comparison with OFF RD and with paracentral ON group, with respect to CT changes. The origin and clinical implications of these changes are not yet known. Further studies are necessary to clarify the relationship between the circulatory alterations, the effect of PPV, cryotherapy/laser therapy and the RD itself to the changes in CT. Post-operative cone density was markedly reduced in OFF RD. Surprisingly cone density was also reduced in ON RD although the drop recovered during the 3 months follow-up. Cone density was significantly correlated with both BCVA and type of RD measured at both time points. These AO baseline measurements may prove to be useful in the future to follow-up subclinical changes at cellular level and to help document cellular recovery to therapeutic agents as well as predict postoperative functional outcome.

In the human *in vitro* model of RD, CDK4, H3K27me3 and AIF are expressed. The peak of TUNEL positive cells is observed at 3DIV with the peak of AIF positive cells. This suggests that AIF mediates the first process of cell death. H3K27me3 positive cells are present with the peak at 5DIV and being stable at 7DIV, suggesting that at a later stage of degeneration the cell death may be related to epigenetic modification. CDK4 positive cells are present also, but in small amount and at a later stage than the peak of TUNEL positive cells at 5-7DIV, suggesting that the re-entrance into the cell cycle is not the main pathway of photoreceptors' death in RD. The characterization and the interactions of the different cell death pathways occurring in human retina after RD is required to give adapted medication in the future if surgery cannot be performed during the early event of RD.

KEYWORDS: retinal detachment; macular status; adaptive optics; cone mosaic; choroidal thickness; EnFace OCT; vision-related quality of life; cell death; *in vitro* human retina

FIELD OF SCIENCE: medicine

SPECIFIC FIELD OF SCIENCE: epidemiology/ophthalmology/cellular biology

Подаци о докторској дисертацији

НАСЛОВ: Карактеризација механизма дегенерације фоторецептора након аблације ретине; евалуација анатомског и функционалног постоперативног опоравка

РЕЗИМЕ

Увод

Регматогене аблације ретине (АР) се анатомски могу поделити на АР са захваћеном макулом (макула-ОФ) и оне са незахваћеном макулом (макула-ОН). Тренутно једини начин лечења АР је хирургија. Међутим, и поред доброг анатомског успеха операције, у већини случајева, опоравак вида је веома различит. Смањење видне оштрине (ВО) [logMAR] има директан утицај на квалитет живота (КвЖ) пацијената. До данас, ретке су студије које су истраживале КвЖ код болесника са АР. Степен губитка вида пропорционалан је степену губитка фоторецептора, што није било могуће испитати *in-vivo* (*уживо*) до скоро. Уколико алтерације фоторецептора током АР могу бити забележене користећи „адаптив оптикс фундус камеру (АО)“, и уколико се ове промене могу повезати са губитком вида, отварају се врата клиничкој примени АО апарата. Раније је доказано да се протеини ћелијског циклуса реактивирају у различитим експерименталним моделима ретиналних дистрофија на глодарима, као и у току оштећења ретине светлости. Постоји могућност да се ови механизми преклапају и у моделу АР. Стога, у овој студији је рађено истраживање на хуманој ретини у циљу бољег разумевања механизма ћелијске смрти који се одигравају код болесника са АР. Први корак ка развоју ефикасног лека је да се дефинише механизам болести у циљу препознавања најбољег начина лечења.

Циљ

Циљеви студије су: дефинисати демографске карактеристике болесника са АР, као и примарни исход хирургије АР у односу на захваћеност макуле, дефинисати факторе ризика за захваћеност макуле са АР; анализирати преоперативни и постоперативни КвЖ код пацијената са ОН или ОФ АР; истакнути постојање посебне подгрупе АР: хеми-макуларна аблација ретине (ХМАР); анализирати промене у дебљини хориоиде (ДХ) пре и после операције АР и између различитих типова АР; квантификација промена у густини чепања и топографији фоторецептора код АР помоћу АО, као и повезати ове промене са захваћеношћу макуле и променама у ВО; и испитати да ли су

апоптоза, поновни улазак фоторецептора у ћелијски циклус и епигенетске модификације такође присутни у *in vitro* експерименталном моделу хумане ретине.

Методe

Ова проспективна, обсервациона моноцентрична кохортна студија је спроведена на Клиници за очне болести Jules-Gonin, у периоду од фебруара 2015. До марта 2017. Гдоине. 204 болесника са примарном АР су укључени у студију, а детаљно је анализирано 194 болесника. Сви болесници су били подвргнути хируршком лечењу АР (класична операција АР (КО) или парс плана витректомија (ППВ)) након преоперативног клиничког прегледа и попуњавања скраћене валидиране верзије Упитника Националног Института за испитивање видне функције (УВФ-13). Анализиран је композитни скор (КС) као и скор подскала (скраћена скала видне функције (ССВФ) и скраћена социоемотивна скала (ССЕС)) УВФ-25. Помоћу АнФас слика оптичке кохерентне томографије (ОЦТ), утврђено је да 9 болесника припада посебној подгрупи АР – ХМАР (4.4%). 54 очију (54 болесника) који су подвргнути ППВ са тампонадом гасом задовољавали су карактеристике за анализу ДХ. Болесници су били подељени у три групе у зависности од простирања АР: периферна макула-ОН АР (>3 mm од фовее, 14 очију), парацентрална макула-ОН АР (≤ 3 mm удаљеност од фовее, 14 очију) и 26 очију са макула-ОФ АР. Свима је ДХ мерена 1 месец (М1) и 3 месеца након операције (М3) на ОЦТ-у, користећи опцију за дубинско снимања (ЕДИ-ОЦТ). Болесници са макула-ОН АР су имали и преоперативна мерења. Анализирана је разлика између оперисаног ока (ОО) и контралатералног ока (КО). АО снимање је спроведено на болесницима са АР 1М и 3М након ППВ. Снимљена су оба ока, на 5 различитих локација, које су међусобно повезане према времену сликања и анатомским обележјима. 22 болесника (10 макула-ОФ и 12 макула-ОН) су поседовали АО слике које су биле одговарајуће за анализу. Подаци су анализирани методама дескриптивне и аналитичке статистике. Анализа варијансе за поновљена мерења је такође коришћена. Направљен је *in vitro* модел хумане АР. Експлантациони материјали су били подељени у две групе: са и без ретиналног пигментног епитела (РПЕ). Ткиво је испитивано у различитим временским размацима и подвргнуто имунохистохемијским анализама: TUNEL, CDKs, H3K27me³, caspase3 и AIF.

Резултати

У студији је учествовало 52.6% болесника са макула-ОФ АР. Просечна старост болесника износила је 63.9 ± 12.0 vs. 59.7 ± 11.2 година у групи са макула-ОФ, одн. макула-ОН АР. Било је 129 мушкараца (66.5%) и 65 (33.5%) жена. Статистички

значајно више су биле заступљене десне очи (десне очи: леве очи 123 (63.4%) vs. 71 (36.6%), $p=0.000$). Статистички значајно више болесника са миопијом ($<-3D$) је имало макула-ОН АР ($p=0.04$). Факни болесници су били значајно више заступљени у кохорти (55.7%), а такође значајно више болесника са факним очима су презентовали макула-ОН АР ($p=0.01$). Мултиваријантна анализа је показала да су псеудофакија и очи са аксијалном дужином (АЛ) $< 25mm$ ($p=0.06$) независни предиктивни фактор за настанак макула-ОФ АР ($p=0.02$), док пол и страна (десно/лево) не представљају фактор ризика за захваћеност макуле. ВО је била статистички значајно различита између макула-ОФ и макула-ОН АР преоперативно: $2.0[2.3-0.95]$ vs $0[0.1-0]$; М1 $0.35[0.5-0.1]$ vs $0.05[0-0.1]$ и М3 $0.25[0.3-0.1]$ vs $0[0-0]$.

47 болесника је попунило упитник УВФ-13 (26 макула-ОН и 21 макула-ОФ) у свим временским интервалима. У макула-ОФ групи, скорови КвЖ су се побољшали након М1 у односу на пре операције, а ово побољшање се наставило и након М3-6. У макула-ОН групи, скор КвЖ се погоршао након М1, али се поправио након М3-6. Преоперативно, уочена је значајна разлика у КвЖ између макула-ОН и макула-ОФ група ($p<0.03$), а најосетљивија подскала за ове промене је била ССЕС. Након М1 није уочена значајна разлика између група. Након М3-6 поново је уочена значајна разлика између група, како у КС тако и у ССЕС подскали ($p=0.03$, $p=0.002$), али не и у ССВФ ($p=0.10$). Значајано побољшање у ВО у макула-ОФ групи кроз постоперативно праћење се подударало са побољшањем у КвЖ, иако није забележена статистичка значајност. У макула-ОН групи, забележено је статистички значајно побољшање у ВО између М1 и М3-6 ($p=0.03$), што се подударало са значајним побољшањем ССЕС скорa ($p=0.006$). Преоперативно, ВО и КвЖ нису показали значајну повезаност ($R^2<0.20$). Постоперативно, у макула-ОФ групи, присутна је позитивна корелација између ВО и КвЖ, највише изражена након М3-6 и то у ССЕС подскали ($p<0.001$, $R^2=0.58$). У макула-ОН групи уочена је позитивна корелација између ВО и ССФВ након М3-6 ($p<0.001$, $R^2=0.41$). Код ХМАР преоперативно, субретинална течност (СРТ) формира циркуларно субфовеални џеп ($85\pm 85\mu m$), снижавајући се код периферне ивице фовее ($82.9\pm 55.4\mu m$; $200\mu m$ од фовее). Плитка АР перзистира парацентрално ($113.2\pm 66.4\mu m$ на $500\mu m$ од фовее) до васкуларне аркаде, када се висина СРТ нагло повећава ($548.1\pm 348.8\mu m$ на $3000\mu m$ од фовее). Постоперативна ВО је износила $0.1[0.2-0.0]$ logMAR, иако су се болесници жалили на сметње у виду. Хипорефлективне зоне у нивоу елипсоидног слоја ретине биле су видљиве на АнФас ОЦТ-у, правећи отисак на месту некадашње ивице АР, на короналним снимцима. Код периферних АР, разлика

између оперисаног и неоперисаног ока у ДХ субфовеоларно је показала задебљавање током периода праћења (преоперативно: $19.6\% \pm 43.9$, М1: $22.9\% \pm 27.5\%$, М3: $18.2\% \pm 35.6\%$). Насупрот овоме, код парацентралних АР, уочена разлика између оперисаног и неоперисаног ока у ДХ субфовеално показала је истањење хириоиде у односу на здраво, неоперисано око (преоперативно: $-7.8\% \pm 21.9$, М1: $-5.5\% \pm 26.1$, М3: $-9.3\% \pm 19.4$). Макула-ОФ АР праћене су значајним истањењем ДХ субфовеално и М1 ($-14.1\% \pm 18.7\%$) и након М3 ($-9.9\% \pm 15\%$). Разлика између оперисаног и здравог, неоперисаног ока у ДХ мерено субфовеално између периферних макула-ОН АР и парацентралних макула-ОН АР као и између периферне макула-ОН АР и макула-ОФ АР, била је статистички значајно другачија на М1 ($p=0.00$, $p=0.00$) и М3 ($p=0.00$, $p=0.00$). Помоћу АО уочено је да је густина чепића стабилна/непромењена кроз време (М1 и М3) код неоперисаног здравог ока ($p=0.67$); снижена код оперисаних очију ($p<0.05$); повећана постоперативно код макула-ОН АР ($p=0.02$), али не и у макула-ОФ групи ($p=0.97$). ВО и тип АР су независно позитивно повезани са густином чепића ($p=0.004$, $p=0.000$).

Потврђено је да *in vitro* модел хумане АР имитира кинетику ћелијске смрти која је описана на *in vivo* моделима. Број ТУНЕЛ-позитивних ћелија, ако се упореди након 1 дан *in vitro* (1 ДИВ) и 7 дана *in vitro* (7 ДИВ) се повећао са временом у ретиналном експланту са РПЕ (1ДИВ: 1.50 ± 0.00 vs 7ДИВ: 7.67 ± 0.00) и без РПЕ (1ДИВ: 2.83 ± 1.03 vs 7ДИВ: 15.84 ± 1.73 , $p=0.02$), а пик позитивности је забележен након 3ДИВ (саРПЕ: 0.75 ± 0.30 vs безРПЕ: 11.83 ± 6.68). CDK4-позитивне ћелије су биле слабо присутне у обе групе након 1 ДИВ (саРПЕ: 0.00 ± 0.00 vs безРПЕ: 2.01 ± 0.75 , $p=0.02$), и након 7 ДИВ (саРПЕ: 1.58 ± 0.12 vs безРПЕ: 4.73 ± 0.86 , $p=0.02$). НЗК27 me^3 позитивне ћелије су биле присутне све време, али су највише биле изражене након 5ДИВ (саРПЕ 1.35 ± 0.08 vs безРПЕ 12.68 ± 2.06). АИГ позитивне ћелије су биле слабо присутне након 1ДИВ, док су након 3ДИВ достигле свој максимум, пратећи пик TUNEL – позитивних ћелија.

Закључак

Псеудофакија и АЛ < 25 μm представљају независне предикторне факторе за настанак макула-ОФ АР. Док је псеудофакија већ препознат фактор ризика за настанак АР, краћа АЛ није раније била идентификована као фактор ризика за настанак макула-ОФ АР. Уочена је значајна разлика у КС КвЖ али, што је још значајније, и у подскалама ССЕС и ССФВ између болесника са макула-ОН и макула-ОФ АР. Ова разлика је уочљива преоперативно, али такође и током постоперативног праћења. У макула-ОН групи уочен је пад КвЖ након М1, док је код макула-ОФ болесника забележена позитивна

прогресија у њиховом КвЖ током постоперативног периода. Као најсензитивнија скала показала се ССЕС подскала, која је забележила највеће промене у КвЖ. ХМАР се јавља у око 4% болесника са примарном АР. Преоперативно, СРТ је плитка, у оквиру васкуларне аркаде, и постаје значајно булознија одмах изван ових граница. Постоперативно, ови болесници имају добру ВО упркос присутним видним сметњама. Уочена је другачија путања опоравка, у односу на дебљину хориоидее, код болесника са периферном макула-ОН АР и код болесника са макула-ОФ АР и парацентралном макула-ОН АР. Узрок ових промена је још увек непознат. Потребна су даља истраживања да би се разјаснила повезаност између поремећаја у циркулацији, утицаја ППВ, криопексије / ендоласерфотокоагулације као и саме АР на промене у дебљини хориоидее. Постоперативно, густина чепића је била значајно снижена код макула-ОФ АР. Међутим, густина чепића је такође била снижена код макула-ОН АР, иако се овај пад у густини чепића опоравио током наредна три месеца праћења. Густина чепића је значајно повезана и са ВО и са типом АР, мерено на М1 и М3. Снимање и анализа АО слика могу бити врло важни у будућности за праћење субклиничких промена у оквиру болести на ћелијском нивоу, такође, АО може омогућити праћење опоравка ћелија након лечења, а може имати улогу и у предикцији постоперативног функционалног опоравка. У хуманом *in vitro* моделу АР, CDK4, H3K27me3 и AIF су експримирани. Највећи пик TUNEL-позитивних ћелија је уочен након 3ДИВ, што је праћено и пиком AIF-позитивних ћелија. Ово указује да је AIF највероватније медијатор првих промена које воде ћелијској смрти. H3K27me³ позитивне ћелије су присутне и имају пик након 5ДИВ, који се одржава и након 7ДИВ. Ови резултати указују да је у дуготрајнијим АР ћелијска смрт повезана са епигенетским модификацијама. CDK4 позитивне ћелије су такође присутне, у знатно мањем броју који је израженији након пика TUNEL-позитивних ћелија, након 5-7ДИВ. Ово указује да постоје заједнички путеви ћелијске смрти који се одигравају код дегенерација ретине и код АР, али да поновни улазак фоторецептора у ћелијски циклус не представља главни пут њиховог умирања код АР. Карактеризација и испитивање интеракција различитих путева ћелијске смрти који се одигравају у хуманој ретини након АР је неопходно наставити и у будућности да би се утврдио прави механизам и могући лек уколико хирургију није могуће извести одмах након почетка АР.

КЉУЧНЕ РЕЧИ : аблација ретине; макуларни статус; адаптив оптикс; мозаик чепића; дебљина хориоидее; АнФас ОЦТ; квалитет живота; ћелијска смрт; *in vitro* људска ретина

НАУЧНА ОБЛАСТ: медицина

УЖА НАУЧНА ОБЛАСТ: епидемиологија/офталмологија/ћелијска биологија

Summary

1. INTRODUCTION.....	1
1.1. ANATOMY AND HISTOLOGY OF A NORMAL EYE	3
1.1.1. The eye	3
1.1.2. Histology of the retina	4
1.1.3. Photoreceptors	6
1.1.4. Retinal pigment epithelium	7
1.2. RETINAL DETACHMENT	8
1.2.1. Definition and types	8
1.2.2. Rhegmatogenous retinal detachment (RD).....	8
1.2.3. Anatomical and functional recovery (risk factors and visual acuity)	9
1.2.3.1. Epidemiology of retinal detachment	11
1.2.4. The cause of rhegmatogenous retinal detachment.....	14
1.2.5. Pathogenesis of the retinal detachment	15
1.2.5.1. Subretinal fluid in rhegmatogenous retinal detachment	15
1.2.5.2. Macula-ON vs Macula-OFF retinal detachment	16
1.2.6. Treatment of retinal detachment.....	17
1.2.6.1. Scleral buckle surgery	18
1.2.6.2. Pars plana vitrectomy	18
1.3. IMPORTANCE OF RETINAL DETACHMENT	19
2. AIMS AND WORKING HYPOTHESIS.....	20
3. METHODS OVERVIEW	21
3.1. Clinical and epidemiology study protocol.....	21
3.1.1. Subject selection.....	21
3.1.2. Statistical analysis	22
3.1.3. Processing of personal data	23
3.2. Basic research and experimental study protocol	24
3.2.1. Statistical analysis	24
4. RESULTS.....	25
4.1. CLINICAL ASPECTS OF RHEGMATOGENOUS RETINAL DETACHMENT	25
4.1.1. Introduction	25
4.1.2. The study design.....	25
4.1.3. The baseline data	26
4.1.3.1. Patients	26
4.1.3.2. Age and gender distribution	26
4.1.3.3. Myopia (spherical equivalence and axial length).....	27
4.1.3.4. Lens status	27
4.1.3.5. Relation of age with lens status and myopia	27
4.1.3.6. Laterality	28
4.1.3.7. Retinal detachment characteristics	28
4.1.3.8. Multivariate model	28
4.1.4. Discussion	30
4.1.5. Conclusion.....	31
4.2. RETINAL DETACHMENT AND ITS IMPACT ON VISUAL ACUITY AND VISION-RELATED QUALITY OF LIFE	32
4.2.1. Introduction	32
4.2.1.1. Quality of life (QoL)	32
4.2.1.2. Instruments of QoL: development, adaptation and analysis.....	33
4.2.1.3. How to select the appropriate QoL instrument?.....	34
4.2.1.4. Appropriateness of NEI VFQ-25: Validity, reliability and responsiveness	35
How are the items measured: Likert-style scale.....	36
Does this scale measure what it is supposed to: Rasch analysis	36
4.2.1.5. Implementation of Rasch analysis.....	40
4.2.2. QoL study design.....	41

4.2.2.1.	Patients	41
4.2.2.2.	NEI VFQ-13	41
4.2.2.3.	Statistical Analyses.....	41
4.2.3.	QoL results	42
4.2.3.1.	Baseline characteristics	42
4.2.3.2.	NEI-VFQ-13 scores.....	43
4.2.3.3.	Relationship between QoL and BCVA	45
4.2.4.	QoL discussion	48
4.2.5.	QoL conclusion	50
4.3.	CLINICAL IMAGING IN PATIENTS WITH RETINAL DETACHMENT.....	51
4.3.1.	Introduction	51
4.3.1.1.	Optical coherence tomography (OCT)	52
Tissue visualization	54	
4.3.1.2.	“EnFace” Optical Coherence Tomography	56
4.3.1.3.	Macular area visualization and characteristics	59
4.3.1.4.	Choroid visualization.....	59
Reflectivity	60	
4.3.1.5.	Quantitative Analysis	60
Frontal and “EnFace” Measurement	60	
Quantitative segmentation	60	
Quantitative choroid measurements	61	
Retinal Mapping.....	61	
Retinal and choroidal volume.....	61	
4.3.2.	Study design	62
4.3.2.1.	Patients	62
4.3.2.2.	Imaging characteristics.....	62
4.3.2.3.	EnFace OCT image	62
4.3.2.4.	Measurement on OCT	63
4.3.2.5.	Choroidal thickness measurements and analysis.....	63
4.3.2.6.	Measurements repeatability.....	63
4.3.2.7.	Statistical analyses.....	64
4.3.3.	Data overview.....	64
4.3.3.1.	Hemi-macular detachment - a distinct new subgroup of RD	64
Baseline characteristics	64	
Retinal detachment	65	
EnFace OCT images.....	65	
Impact on quality of vision.....	66	
4.3.3.2.	The role of choroidal thickness in retinal detachment patients	69
Baseline characteristics	69	
Mean sub-macular choroidal thickness in groups with different extents of RD	71	
Inter-eye difference	73	
4.3.4.	Discussion	75
4.3.4.1.	Hemi-macular detachment.....	75
4.3.4.2.	Choroidal thickness	76
4.3.5.	Conclusion.....	79
4.4.	EXPERIMENTAL IMAGING IN RETINAL DETACHMENT	80
4.4.1.	Introduction	80
4.4.1.1.	Adaptive Optics	81
4.4.1.2.	Adaptive Optics Fundus Camera in patients with retinal detachment.....	85
4.4.2.	Study design	86
Patients	86	
Adaptive Optics Retinal Camera	87	
Alignment methodology and image analysis by AO Detect Mosaic.....	87	
Spectral domain optical coherence tomography (SD-OCT).....	90	
Inter-eye difference (left eye – right eye).....	91	

Statistics	91
4.4.3. Results	91
Baseline characteristics	91
Photoreceptor changes between treated and fellow eye during follow-up	92
Foveal microstructure changes (SD-OCT)	94
Correlation between visual acuity and cone density in treated eyes	94
4.4.4. Discussion	95
4.4.5. Conclusion	98
4.5. EXPERIMENTAL BASIC SCIENCE RESEARCH IN RETINAL DETACHMENT	99
4.5.1. Introduction	99
4.5.1.1. CELL DEATH	101
Types of cell death	102
Apoptosis	103
Necrosis	103
Autophagy	104
4.5.1.2. THE CELL-CYCLE	104
The cell-cycle control system	105
Cyclin-dependent protein kinases (CDKs)	106
Polycomb group and epigenetic modifications	107
H3K27me ³	108
4.5.1.3. Human retina	109
4.5.2. Experimental study design	111
4.5.2.1. Protocol for preparing human retinal explants	111
Procedure of eye dissection	111
4.5.2.2. Immunohistochemistry	112
TUNEL staining	112
H3K27me ³ staining	112
CDK4 DAB staining	112
Active Caspase 3 staining	113
AIF staining	113
4.5.2.3. Statistical analysis	113
4.5.3. Results	114
4.5.3.1. Number of photoreceptors' layers	114
4.5.3.2. TUNEL staining; cell death marker	117
4.5.3.3. Caspase-3 expression	119
4.5.3.4. Apoptosis-inducing factor (AIF) staining	119
4.5.3.5. CDK4 staining; marker of cell cycle re-entrance	121
4.5.3.6. H3K27me ³ ; epigenetic modifications	123
4.5.4. Discussion	125
4.5.5. Conclusion	128
5. DISCUSSION	129
6. CONCLUSIONS	134
7. REFERENCES	136

List of legends (tables and figures)

TABLE 1-1. REFERRAL PROCEDURE FOR RD (ADAPTED FROM (WILLIAMSON, SHUNMUGAM ET AL. 2013).....	17
TABLE 1-2. CHANCE OF 0.3 LOGMAR OR BETTER VISUAL ACUITY AFTER FOVEA-OFF RD, ADAPTED FROM (HASSAN, SARRAFIZADEH ET AL. 2002).....	17
TABLE 3-1. PROTOCOL OF THE STUDY	27
TABLE 4-1. BASELINE CHARACTERISTICS OF PATIENTS WITH PRIMARY RHEGMATOGENOUS RETINAL DETACHMENT.....	34
TABLE 4-2. BASELINE CHARACTERISTICS AND BEST CORRECTED VISUAL ACUITY PRE-OPERATIVELY, 1 MONTH (M1) AND 3-6 MONTHS (M3-M6) AFTER SURGERY IN PATIENTS WITH MACULA-ON (ON) AND MACULA-OFF (OFF) RETINAL DETACHMENT.....	43
TABLE 4-3. QUALITY OF LIFE SCORES PRE-OPERATIVELY, 1 MONTH (M1) AND 3-6 MONTHS (M3-M6) AFTER SURGERY IN PATIENTS WITH MACULA-ON (ON) AND MACULA-OFF (OFF) RETINAL DETACHMENT.....	44
TABLE 4-4. COMPARISON OF QUALITY OF LIFE SCORES REPORTED BY PATIENTS WITH MACULA-ON AND MACULA-OFF RETINAL DETACHMENT, BETWEEN TIME POINTS: PRE-OPERATIVELY, 1 MONTH (M1) AND 3-6 MONTHS (M3-M6) AFTER SURGERY (WILCOXON-PAIRED TEST).....	45
TABLE 4-5. LINEAR REGRESSION ANALYSIS TO EXAMINE THE RELATIONSHIP BETWEEN QUALITY OF LIFE SCORES AND BEST CORRECTED VISUAL ACUITY AT EACH TIME-POINT DURING FOLLOW-UP. PEARSON CORRELATION COEFFICIENT AND CORRESPONDING P-VALUE.	46
TABLE 4-6. COMPARISON OF TD-, SD- AND SS-OCT DEVICES, ADAPTED FROM (GABRIELE, WOLLSTEIN ET AL. 2011).....	53
TABLE 4-7. LIST OF OCT LAYERS AS AGREED ON BY THE INTERNATIONAL NOMENCLATURE FOR OCT PANEL (STAURENGHI, SADDI ET AL. 2014).....	55
TABLE 4-8. CHARACTERISTICS OF STUDY PATIENTS AT BASELINE (PRE-OPERATIVELY) AND 1 MONTH POST-OPERATIVELY	65
TABLE 4-9. BASELINE CHARACTERISTICS OF THE PATIENT COHORT IN RELATION TO RETINAL DETACHMENT EXTENSION.....	69
TABLE 4-10. MEAN CHOROIDAL THICKNESS VALUES AND PERCENTAGE OF CHANGE IN CT OVER FELLOW EYES IN PERIPHERAL, PARACENTRAL AND MACULA-OFF RD. THE LIGHTLY SHADED AREAS DENOTE A GENERAL THINNING OF THE CHOROID, WHEREAS A DARKER SHADE DENOTES THICKENING OF THE CHOROID.	71
TABLE 4-11. SUMMARY STATISTICS FOR MEAN CT BETWEEN FE AND TE, MEAN CT IN FE AND THE PERCENTAGE OF CHANGE IN CT OVER FE IN PERIPHERAL RD, PARACENTRAL RD AND MACULA-OFF RD.	73
TABLE 4-12. BASELINE CHARACTERISTICS AND VISUAL ACUITY	92
TABLE 4-13. SUMMARY MEASURES OF CONE TOPOGRAPHY IN FELLOW-EYES, MACULA-ON AND MACULA-OFF GROUPS AT MONTH 1 AND MONTH 3 AFTER SURGERY	93
TABLE 4-14. THE MAJOR CYCLINS AND CDKS OF VERTEBRATES.....	106
TABLE 4-15. LIST OF PRIMARY AND SECONDARY ANTIBODIES FOR IMMUNOCHEMISTRY	113
TABLE 4-16. MANN-WHITNEY TEST P-VALUES OF COMPARISON OF THE NUMBER OF PHOTORECEPTOR LAYERS BETWEEN EACH TIME-POINT IN THE GROUP OF <i>IN VITRO</i> RD EXPLANTS (WITHOUT RPE), *p<0.05	114
TABLE 4-17. MEAN NUMBER OF POSITIVE CELLS IN EACH DAY OF FIXATION, IN BOTH GROUPS.	115
TABLE 4-18. MANN-WHITNEY TEST P-VALUES OF COMPARISON OF THE NUMBER OF TUNEL POSITIVE CELLS BETWEEN EACH TIME-POINT IN THE GROUP OF <i>IN VITRO</i> RD EXPLANTS (WITHOUT RPE), *p<0.05	119
TABLE 4-19. MANN-WHITNEY TEST P-VALUES OF COMPARISON OF THE NUMBER OF CDK4 POSITIVE CELLS BETWEEN EACH TIME-POINT IN THE GROUP OF <i>IN VITRO</i> RD EXPLANTS (WITHOUT RPE), *p<0.05	121
TABLE 4-20. MANN-WHITNEY TEST P-VALUES OF COMPARISON OF THE NUMBER OF H3K27ME ³ POSITIVE CELLS BETWEEN EACH TIME-POINT IN THE GROUP OF <i>IN VITRO</i> RD EXPLANTS (WITHOUT RPE), *p<0.05.....	124

FIGURE 1-1 SCHEMATIC DIAGRAM OF A HUMAN EYE, ADAPTED FROM (FORRESTER, DICK ET AL. 2015)	3
.....	
FIGURE 1-2 HISTOLOGICAL CUT OF ADULT HUMAN RETINA.	4
FIGURE 1-3 DIVISION OF RETINA. HTTPS://EN.WIKIPEDIA.ORG/WIKI/MACULA_OF_RETINA, HTTPS://WWW.SLIDESHARE.NET/SAJJANSANGAI/ANATOMY-OF-RETINA-75005025	5
FIGURE 1-4 PHOTORECEPTORS' DISTRIBUTION	6
FIGURE 1-5 SCHEMATIC DIAGRAM OF THE EYE WITH RETINAL DETACHMENT. ADAPTED FROM (BOWLING 2015).....	8
FIGURE 1-6. DIFFERENT TYPES OF MACULA-OFF RHEGMATOGENOUS RETINAL DETACHMENT, DEFINED WITH PREOPERATIVE OCT: ADAPTED FROM (WOLFENSBERGER AND GONVERS 2002)	9
FIGURE 1-7. LINCOFF RULES OF TEAR LOCALIZATION IN RETINAL DETACHMENT (LINCOFF AND GIESER 1971, KOROBELNIK JEAN-FRANÇOIS 2014).....	15
FIGURE 1-8. PRE-OPERATIVE AND POSTOPERATIVE OCT FOLLOW-UP OF THE SAME PATIENT. ADAPTED FROM (WOLFENSBERGER AND GONVERS 2002)	16
FIGURE 4-1. PATIENTS' APPRECIATION OF THEIR QOL, ADAPTED FROM (YUZAWA, FUJITA ET AL. 2013)	32
.....	
FIGURE 4-2. ADAPTED FROM PESUDOV'S ET AL (PESUDOV'S, GOTHWAL ET AL. 2010), SUMMARY OF ITEMS INCLUDED IN EACH REVISED VERSION OF THE NEI-VFQ. RED CIRCLES DENOTING THE ITEMS USED IN THE SHORTEN REENGINEERED NEI-VFEQ VERSION	39
FIGURE 4-3. THE RELATIONSHIP BETWEEN QUALITY OF LIFE SCORES AND BEST CORRECTED VISUAL ACUITY PRE-OPERATIVELY (CS) AND AT MONTH 3-6 (SFVFS SCORE)	47
FIGURE 4-4. OCT IMAGE OF RETINAL LAYERS. NOMENCLATURE FOR NORMAL ANATOMIC LANDMARKS SEEN ON SD-OCT IMAGES PROPOSED AND ADOPTED BY THE INTERNATIONAL NOMENCLATURE FOR OPTICAL COHERENCE TOMOGRAPHY PANEL.....	55
FIGURE 4-5. RELATIVE ORIENTATION OF THE AXIAL SCAN (A SCAN), TRANSVERSE SCAN (T SCAN), LONGITUDINAL SLICE (B SCAN) AND ENFACE OR TRANSVERSE SLICE (C SCAN). ADAPTED FROM (LUMBROSO, HUANG ET AL. 2013).....	57
FIGURE 4-6. DIFFERENT MODES OF OPERATION OF THE THREE SCANNERS IN A 3D IMAGING SYSTEM AND THE TWO MODALITIES OF CREATING ENFACE IMAGE. ADAPTED FROM (LUMBROSO, HUANG ET AL. 2013).....	58
FIGURE 4-7 A-D OCT IMAGES OF PATIENT 1 AT TWO TIME POINTS BASELINE/PREOPERATIVELY AND AT ONE MONTH AFTER SURGERY.	67
FIGURE 4-8 A-D OCT IMAGES OF PATIENT 2 AT TWO TIME POINTS BASELINE/PREOPERATIVELY AND ONE MONTH AFTER SURGERY SHOWING AN IDENTICAL SITUATION TO PATIENT 1 WITH A SUB-FOVEAL POCKET OF SUBRETINAL FLUID (A+B) AND THE HYPOREFLECTIVE LESIONS IN THE ELLIPSOID LAYER CORRESPONDING TO THE RIDGE-LIKE STRUCTURE VISIBLE ON ENFACE OCT (C+D).....	68
FIGURE 4-9. EDI SD-OCT REPRESENTING CHOROIDAL THICKNESS (CT) IN PATIENTS WITH PERIPHERAL RD, PARACENTRAL RD AND MACULA-OFF RD 1 MONTH AFTER SURGERY.	70
FIGURE 4-10. CHOROIDAL THICKNESS IN PERIPHERAL RD, PARACENTRAL RD AND MACULA-OFF RD	72
FIGURE 4-11. INTER-EYE DIFFERENCE IN CHOROIDAL THICKNESS IN PERIPHERAL RD, PARACENTRAL RD AND MACULA-OFF RD.....	74
FIGURE 4-12.....	81
FIGURE 4-13. SCHEMATIC DIAGRAM OF AN ADAPTIVE OPTICS (AO) RETINAL IMAGING SYSTEM AND PARALLEL WITH OCT IMAGING SYSTEM. OCT USES LOW-COHERENCE INTERFEROMETRY TO ACHIEVE HIGH AXIAL RESOLUTION. AO MEASURES THE OCULAR ABERRATIONS WITH A WAVE-FRONT SENSOR AND CORRECTS FOR THEM (CORNEA, LENS, AND OPTICAL MEDIA) WITH A WAVE-FRONT CORRECTOR TO ACHIEVE THE COMPLEMENTARY HIGH LATERAL RESOLUTION. ADAPTED FROM (MILLER, KOCAOGLU ET AL. 2011)	82
FIGURE 4-14. SCHEMATIC DIAGRAM OF LATERAL AND AXIAL RESOLUTIONS IN DIFFERENT RETINAL IMAGING SYSTEMS COMMERCIAL CONFOCAL SCANNING LASER OPHTHALMOSCOPE (CSLO), CONFOCAL SCANNING LASER OPHTHALMOSCOPE WITH ADAPTIVE OPTICS (AO-CSLO), FLOOD ILLUMINATION WITH ADAPTIVE OPTICS, COMMERCIAL OCT, ULTRAHIGH-RESOLUTION OCT	

(UHR-OCT), ULTRAHIGH-RESOLUTION OCT WITH ADAPTIVE OPTICS (UHR- AO-OCT), OPTICAL SYSTEM IS LIMITED BY THE DIFFRACTION OF LIGHT WAVES 0.013 ARCSEC. PRACTICAL LIMIT TO RESOLUTION IS ONLY ABOUT 1 ARCMIN (~5 μ M) DUE TO RESIDUAL DISTORTIONS. ADAPTED FROM (MILLER, KOCAOGLU ET AL. 2011).....	83
FIGURE 4-15. AO-OCT VOLUME ACQUIRED OVER A 1° RETINAL REGION LOCATED TEMPORAL OF THE FOVEA, AS ILLUSTRATED BY THE RECTANGLE IN THE FUNDUS PHOTOGRAPH. THE IMAGES ON THE RIGHT ARE ENFACE VIEWS OF PARTICULAR RETINAL LAYERS EXTRACTED FROM THE AO-OCT VOLUME. RETINAL LAYERS FROM TOP TO BOTTOM ARE: NERVE FIBER LAYER (NFL), GANGLION CELL LAYER (GCL), OUTER PLEXIFORM LAYER (OPL), AND OUTER SEGMENT LAYER OF PHOTORECEPTORS (OS). ADAPTED FROM (MILLER, KOCAOGLU ET AL. 2011).....	84
FIGURE 4-16. ENFACE OCT IMAGE (PREOPERATIVELY AND POST-OPERATIVELY) AND ADAPTIVE OPTICS (POSTOPERATIVELY) OF THE SAME REGION IN A PATIENT WITH RD	86
FIGURE 4-17. A-D MATCHING ROIS BETWEEN TREATED EYE AT 1 MONTH POST-OPERATIVELY AND FELLOW EYE.....	88
FIGURE 4-18. A-L MATCHING ROIS BETWEEN TREATED EYE AT 1 AND 3 MONTHS POST-OPERATIVELY AND FELLOW EYE AT THE SAME TIME-POINTS (CONE-TRACKING)	89
FIGURE 4-19. ANALYSED MATCHING REGION OF INTERESTS (ROIS) FOR DENSITY (D), SPACING (S), AND VORONOI (V) BETWEEN TREATED AND FELLOW EYE AT 1 MONTH (M1) AND AT 3 MONTHS (M3) POST-OPERATIVELY, IN MACULA-OFF AND MACULA-ON PATIENT. NOTE THE IMPROVEMENT OF CELL DENSITY AND THE REDUCTION IN CELL SPACING OVER THE 2 MONTH PERIOD.	90
FIGURE 4-20. CHANGE IN DISTRIBUTION OF THE NUMBER OF NEIGHBORS AS COMPARED TO FELLOW EYE (VORONOI).....	93
FIGURE 4-21. THE RELATIONSHIP BETWEEN LOG CONE DENSITY, TYPE OF RD (MACULA-ON OR MACULA-OFF) AND BCVA OVER TIME (MONTH 1 AND MONTH 3). THE IMPROVEMENT IN LOG CONE DENSITY IS EVIDENT BETWEEN MONTH 1 AND MONTH 3 IN MACULA-ON EYES. BCVA AND RD TYPE ARE INDEPENDENTLY CORRELATED WITH LOG CONE DENSITY (P=0.004, P=0.000).	95
FIGURE 4-22. HISTOLOGY OF THE NORMAL RETINA (A) AND DETACHED RETINA (B), ADAPTED FROM (CAPUTO, METGE ET AL. 2012).....	102
FIGURE 4-23. CELL CYCLE PHASES AND REGULATORS. PHASES ARE CONTROLLED BY MANY FACTORS, MOSTLY A SUBSET OF PROTEINS, SUCH AS CYCLINS, CYCLIN-DEPENDENT KINASES (CDKS), RETINOBLASTOMA PROTEIN (RB) TOGETHER WITH OTHER PROTEINS (P107 AND P130), AND THE E2F FAMILY OF TRANSCRIPTION FACTORS. ADAPTED FROM (HERRUP AND YANG 2007)	105
FIGURE 4-24 A-B. FIGURES SHOWING SUMMARY DATA OF ALL FOUR HUMAN RETINAL EXPLANTS, IN TWO GROUPS: <i>IN VITRO</i> CONTROL GROUP (A) AND <i>IN VITRO</i> RD GROUP (B) FOR ALL FIVE FOLLOWED PARAMETERS. NOTE THE SIGNIFICANT DIFFERENCE BETWEEN GROUPS FOR ALL FIVE PARAMETERS BUT AT DIFFERENT TIME POINTS. THE MOST IMPORTANT DIFFERENCES ARE ESPECIALLY FOR AN INCREASE OF TUNEL- AND H3K27ME3-POSITIVE PHOTORECEPTORS OVER TIME IN THE RD GROUP, AIF HAD A PEAK AT 3DIV, FOLLOWING THE PEAK OF TUNEL POSITIVE CELLS, WHILE THE CDK4 IS MODERATELY MORE EXPRESSED IN RD GROUP, SUGGESTING THE CELL-CYCLE RE-ENTRANCE IN CERTAIN CELLS.	116
FIGURE 4-25. COMPARISON OF TUNEL-POSITIVE CELLS BETWEEN CONTROL GROUP (HUMAN RETINAL EXPLANTS WITH RPE) AND <i>IN VITRO</i> MODEL OF RD (HUMAN RETINAL EXPLANTS WITHOUT RPE). NOTE THE IMPORTANT DIFFERENCE IN TUNEL POSITIVE CELLS BETWEEN GROUPS IN ALL TIME POINTS, NOTABLY HIGHLY EXPRESSED SINCE 3 RD DAY <i>IN VITRO</i> . N = 0.75 FOR THE CONTROL GROUP, AND N = 11.83 FOR THE GROUP WITHOUT RPE.....	117
FIGURE 4-26.....	118
FIGURE 4-27. AIF POSITIVE CELLS AT 3DIV IN THE HUMAN <i>IN VITRO</i> MODEL OF RETINAL DETACHMENT. AT 5DIV THERE IS ONLY ONE AIF POSITIVE CELL. <i>ONL</i> : OUTER NUCLEAR LAYER, <i>INL</i> : INNER NUCLEAR LAYER.....	120
FIGURE 4-28. COMPARISON OF AIF-POSITIVE CELLS BETWEEN CONTROL GROUP (HUMAN RETINAL EXPLANTS WITH RPE) AND <i>IN VITRO</i> MODEL OF RD (HUMAN RETINAL EXPLANTS WITHOUT RPE). NOTE THE IMPORTANT DIFFERENCE IN AIF POSITIVE CELLS BETWEEN GROUPS AT 3DIV, WHEN THEY WERE NOTABLY HIGHLY EXPRESSED. N = 0.60 FOR THE CONTROL GROUP, AND N = 8.60 FOR THE GROUP WITHOUT RPE.....	120

FIGURE 4-29. COMPARISON OF CDK4 POSITIVE CELLS BETWEEN CONTROL GROUP (HUMAN RETINAL EXPLANTS WITH RPE) AND <i>IN VITRO</i> MODEL OF RD (HUMAN RETINAL EXPLANTS WITHOUT RPE). NOTE THE VERY LOW NUMBER OF CDK4 POSITIVE CELLS AFTER 1 DIV IN THE CONTROL GROUP, AS WELL AS ITS LITTLE INCREASE OVER TIME IN THE RD GROUP. N=1.65 AT 3DIV FOR THE CONTROL GROUP, AND N=3.70 AT 3DIV AND N=4.73 AT 7DIV FOR THE GROUP WITHOUT RPE.....	121
FIGURE 4-30. CDK4 POSITIVE CELLS (ARROWS) IN THE HUMAN <i>IN VITRO</i> MODEL OF RETINAL DETACHMENT (HUMAN RETINAL EXPLANTS WITHOUT RPE) AND CONTROL GROUP (HUMAN RETINAL EXPLANTS WITH RPE), AT 1DIV AND AT 7DIV. <i>ONL</i> : OUTER NUCLEAR LAYER, <i>INL</i> : INNER NUCLEAR LAYER. MAGNIFICATION: 400X. CALIBRATION BAR: 20 μ M.....	122
FIGURE 4-31. COMPARISON OF H3K27ME3 POSITIVE CELLS BETWEEN CONTROL GROUP (HUMAN RETINAL EXPLANTS WITH RPE) AND <i>IN VITRO</i> MODEL OF RD (HUMAN RETINAL EXPLANTS WITHOUT RPE). NOTE THE INCREASE IN H3K27ME3 POSITIVE CELLS LEVEL IN RD MODEL STARTING AT 5 DIV. N=1.35 FOR THE CONTROL GROUP, AND N=12.68 FOR THE GROUP WITHOUT RPE.....	123
FIGURE 4-32. H3K27ME ³ POSITIVE CELLS AT 1DIV AND AT 7DIV, IN THE HUMAN <i>IN VITRO</i> MODEL OF RD (WITHOUT RPE) AND HUMAN <i>IN VITRO</i> MODEL OF RETINAL TISSUE WITH RPE <i>ONL</i> : OUTER NUCLEAR LAYER, <i>INL</i> : INNER NUCLEAR LAYER, <i>RPE</i> : RETINAL PIGMENT EPITHELIUM. MAGNIFICATION: 400X CALIBRATION BAR: 20 μ M	124

1. INTRODUCTION

Retinal detachment (RD) is the separation of sensory retina from the retinal pigment epithelium (RPE), due to the presence of fluid in the subretinal space. (Bowling 2015) Subretinal fluid (SRF) can fill the subretinal space in several different ways, causing different types of retinal detachment (e.g. macula-OFF, inverted fovea etc). (Wolfensberger and Gonvers 2002) The incidence of RD is estimated to be 1:10,000 per year, increasing to about 3.5% to 5.8% in the first year after the primary RD and 10% within 4 years in the second eye. (Mitry, Charteris et al. 2010) Retinal tears, the root cause of most rhegmatogenous RD, are the result of dynamical vitreoretinal traction on susceptible peripheral retina, (Bowling 2015) with SRF filling the subretinal space. Currently the only treatment for RD is surgery, depending on the indications: either scleral buckling or pars plana vitrectomy will be performed. Both of these have the same purpose: drainage/reabsorption of SRF to allow anatomical retinal reattachment in order to regain/maintain visual function. (Bowling 2015)

Retinal degeneration is associated with RD, and in order to optimize postoperative recovery a better understanding of the mechanisms involved in the photoreceptor cell death is needed. Cellular pathways of photoreceptor death in retinal diseases, i.e. apoptosis, necrosis and autophagy, have been studied, and the important roles of cyclin-dependent kinases as well as the role of epigenetic modifications and other apoptotic factors have been identified. (Murakami, Notomi et al. 2013) The role of these cell cycle proteins as described in models of retinal degeneration may be similar to role played in RD. (Menu dit Huart, Lorentz et al. 2004, Wenzel, Grimm et al. 2005, Zencak, Schouwey et al. 2013)

Visual acuity (VA) is directly related to the density of photoreceptors in the central retina (macula). (Ratnam, Carroll et al. 2013) The post-operative improvement in VA has been associated with duration of RD, degree of myopia (axial length of the globe), age and persistence of SRF. (Wolfensberger and Gonvers 2002) Since photoreceptor cell death starts within the first twelve hours and peaks at 2-3 days following RD, it is important to perform surgery as quickly as possible, especially when the macula is at risk. (Cook, Lewis et al. 1995, Hisatomi, Sakamoto et al. 2001, Arroyo, Yang et al. 2005) Myopia is associated with vitreous liquefaction, posterior vitreous detachment (PVD), common lattice degeneration and thinner retina, therefore, retinal breaks are larger, occur earlier and more frequently in myopic eyes. (Kaluzny 1970, Yonemoto, Ideta et al. 1994, Mitry, Singh et al. 2011, Morgan, Ohno-Matsui et al. 2012) Myopia of up to -3 diopters (D) quadruples the risk of RD, and myopia of more than -3D increases the risk of RD tenfold. (Mitry, Singh et al. 2011, Morgan, Ohno-Matsui et

al. 2012) Myopia is a relevant risk factor because of increased prevalence; every third European adult is now myopic. (Pan, Ramamurthy et al. 2012) Younger eyes have been shown to have more persistent SRF. (Edmund 1968, Takeuchi, Kricorian et al. 1996)

The recent exploitation of the birefringent properties of the retina with optical coherence tomography (OCT) device, has allowed *in-vivo* high resolution imaging of the retinal layers. Following the proper segmentation of these layers, the integrity of the retinal structure can be examined. Modifications to the retinal structure have been shown to be a predictive factor for visual recovery in patients after successful surgery. (Schocket, Witkin et al. 2006, Wakabayashi, Oshima et al. 2009, Murakami, Notomi et al. 2013) OCT images can also be used to quantify and monitor the amount, configuration and localization of SRF. (Wolfensberger and Gonvers 2002) Adaptive optics fundus camera (AO) is a modified OCT device, which attempts to correct for optical aberrations in order to deliver a representation of the microscopic retina. These images can be used to examine cone morphology *in-vivo*. Therefore, AO imagery could potentially be used to monitor foveal photoreceptor cellular alterations following RD. (Zawadzki, Jones et al. 2005, Zhang, Rha et al. 2005, Zawadzki, Choi et al. 2007)

Reduction in VA has a direct effect on patient's quality of life (QoL). (Okamoto, Okamoto et al. 2010) However, to date, few studies have reported QoL measures in RD patients. (Okamoto, Okamoto et al. 2008, Okamoto, Okamoto et al. 2010) The most commonly used questionnaire for quantitative assessment of QoL with respect to vision is National Eye Institute Visual Function Questionnaire (NEI VFQ-25). (Rossi, Milano et al. 2003, Fukuda, Okamoto et al. 2009, Okamoto, Okamoto et al. 2010, Nassiri, Mehravaran et al. 2013, Aydin Kurna, Altun et al. 2014) There is only one report that compares the QoL of macula-ON versus macula-OFF patients, here despite a large significant difference in final VA being reported between patients groups, there was no significant difference in the post-operative QoL observed. This is most likely due to the inadequate statistical power of this study (n=18 macula-ON) and is likely misrepresentative of the true impact of RD. Moreover, if the type of RD or the persistence of SRF is related to post-operative VA and QoL, this may have important implications for clinical patient management.

1.1. ANATOMY AND HISTOLOGY OF A NORMAL EYE

1.1.1. The eye

The main role of the eye is to transform the incoming light energy (falling on the retina) from the environment, into nerve action potentials that are traveling via specialized cells (photoreceptors) and optic nerve to the brain, developing the consciousness about vision. All the eye structures are in the service of this function (Forrester, Dick et al. 2015).

The eye is positioned in the anterior orbit, being closer to the lateral wall and to the orbital roof (Forrester, Dick et al. 2015). The axial length is usually about 24 mm, with some still physiological inter-individual variations (21-26mm) and the volume of about 6.5 ml. The eye contains three layers (tunics): corneo-scleral layer (it has the protective role); the uveal tract consisted of choroid, ciliary body and iris and has the metabolic role; and the neural layer (retina) with the role of vision (**Figure 1-1**). These layers are surrounding the inner eye structures: lens, aqueous humour and vitreous body (Bowling 2015, Forrester, Dick et al. 2015).

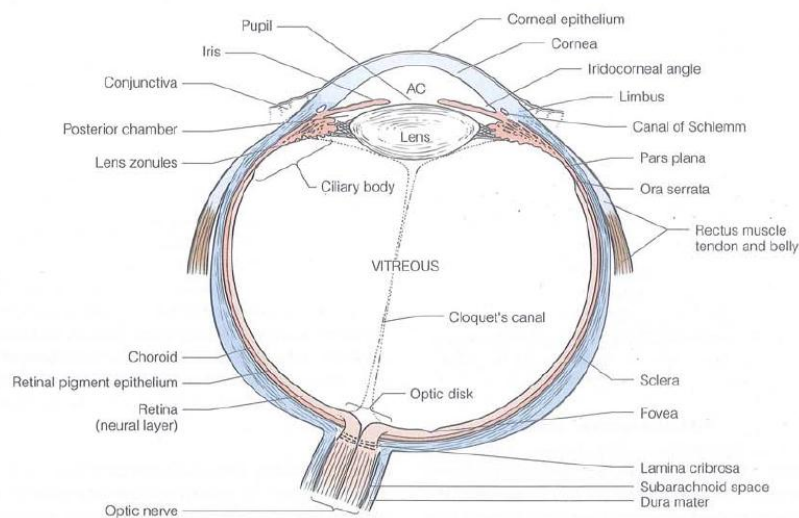


Figure 1-1 Schematic diagram of a human eye, adapted from (Forrester, Dick et al. 2015)

1.1.2. Histology of the retina

The retina is a neural tissue made of highly specialized cells that are organized in several layers. Retina has the role to capture the surrounding light energy and to process it as the “first order signal”. (Sancho-Pelluz, Arango-Gonzalez et al. 2008) The human retina is made of two layers: the inner neurosensory layer and outer simple epithelium, the retinal pigment epithelium (**Figure 1-2**). Between these two layers there is a potential space, “subretinal space”, where the two layers must have strong adhesion. This adhesion is kept by negative pressure, electrostatic forces and viscous proteoglycans in the subretinal space. (Forrester, Dick et al. 2015) The attachments of neurosensory retina are solid anteriorly, at the ora serrata and at the margins of the optic nerve head. Internally, retina is in the contact with vitreous while exteriorly is in contact with Bruch’s membrane. (Forrester, Dick et al. 2015)

The retina is consisted of ten layers (**Figure 1-2**): the inner limiting membrane (**ILM**), the nerve fiber layer (**NFL**), the ganglion cell layer (**GCL**), the inner plexiform layer (**IPL**), the inner nuclear layer (**INL**), the outer plexiform layer (**OPL**), the outer nuclear layer (**ONL**), the outer limiting membrane (**OLM**), the photoreceptor layer (**PL**), and the retinal pigmented epithelium (**RPE**) monolayer. (Bowling 2015, Forrester, Dick et al. 2015) Roughly, the retina can be divided on outer and inner nuclear layers, with **OPL** being a “border” between the two parts. (Sancho-Pelluz, Arango-Gonzalez et al. 2008, Forrester, Dick et al. 2015) The **ONL** of the retina contains rod and cone photoreceptor nuclei which are responsible for vision in dim lighting and for color and daylight vision, respectively. The cells of the **INL** are responsible for trophic support, signal processing, and signal transmission to the ganglion cell layer. Axons of ganglion cells form the optic nerve transmit visual information to the brain. (Kolb 2003, Sancho-Pelluz, Arango-Gonzalez et al. 2008)

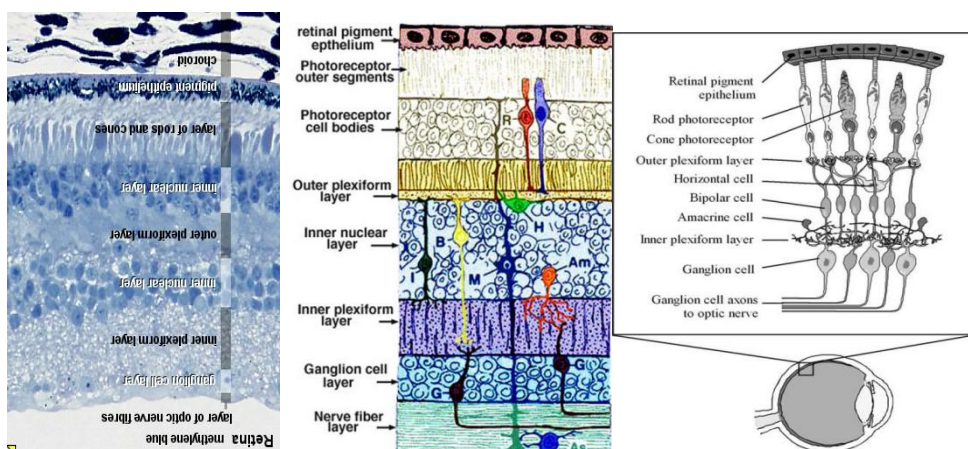


Figure 1-2 Histological cut of adult human retina.

<http://webvision.med.utah.edu/book/part-i-foundations/gross-anatomy-of-the-eye/>

Retina is covering the area of about 1250 mm² and varies in thickness from 100 μm (periphery) to 230 μm (near the optic nerve head). In everyday practice, retina is divided into five important zones (**Figure 1-3**) (Forrester, Dick et al. 2015):

1. **Posterior pole or central retina** represents the area between vascular arcades, normally 5-6mm in diameter, and it is cone-dominated.
2. **The macula lutea (fovea)**, which is located in the posterior pole, 3mm temporally to the optic disc, a region of 1.5mm in diameter, filled with cones. **Fovea centralis or foveola** is a central 0.35mm wide zone in the macula, representing the area of the highest density of cones. In this area the inner retinal layers are moved laterally. This is avascular zone, having metabolic processes via the choriocapillaris.
3. **The optic nerve disc** is 1.8mm in diameter and localized on the posterior pole. This area represents “blind spot” with ganglion cell axons penetrating the sclera to enter the optic nerve. The central retinal vessels arise at the optic disc center.
4. **The peripheral retina** is the rest of the retina, laterally to posterior pole. Temporally, the distance to ora serrata is about 23-24 mm, while nasally this distance is a bit shorter of 18.5 mm. On the opposite of the posterior pole retina, the rods are dominant on the periphery.
5. **The ora serrata** represents the anterior border of the neurosensory retina, the “transition zone”. Here, neuroretina is continuous with the non-pigmented epithelial cells of the pars plana. It is 1 mm closer to the limbus nasally than temporally.

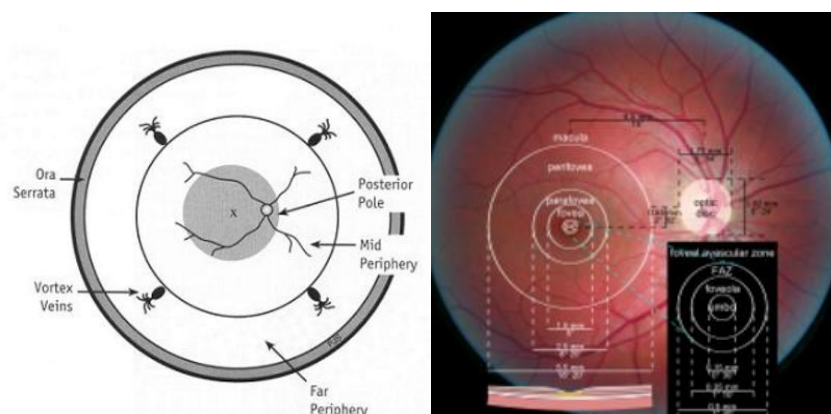


Figure 1-3 Division of retina. https://en.wikipedia.org/wiki/Macula_of_retina, <https://www.slideshare.net/sajjansangai/anatomy-of-retina-75005025>

1.1.3. Photoreceptors

There are two types of **photoreceptors** in the human eye: rods and cones. They are located in the outer layers of the neurosensory retina. There are approximately 115 million rods and 6.5 million cones in the human eye. Rods are responsible for sensing contrast, brightness and motion, while cones are responsible for final resolution, spatial resolution and color vision. The photoreceptors' (rods and cones) density vary in different retinal zones, depending on the periphery. In the periphery, rods are dominating ($30000/\text{mm}^2$) while cone density increases nearer the macula ($150000/\text{mm}^2$ at the fovea), the fovea containing exclusively cones (**Figure 1-4**). (Osterberg 1935, Curcio, Sloan Jr et al. 1987, Curcio, Sloan et al. 1990, Forrester, Dick et al. 2015)

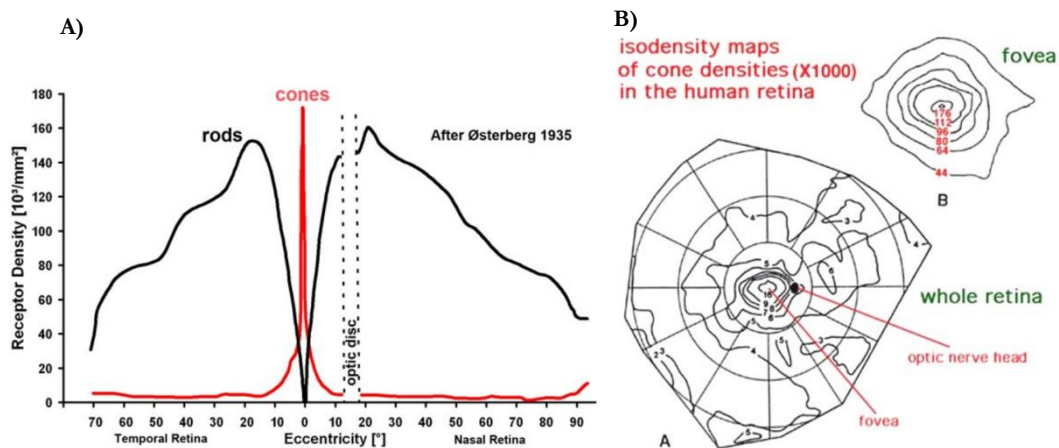


Figure 1-4 Photoreceptors' distribution

A) Density of rods and cones along the horizontal meridian (Osterberg 1935)

B) Cone densities in human retina as revealed in whole mount. (Curcio, Sloan Jr et al. 1987)

1.1.4. Retinal pigment epithelium

Retinal pigment epithelium (RPE) is consisted of one layer of cuboidal epithelial cells, spreading from optic nerve head until ora serrata, where it is continuous with the pigment epithelium of the pars plana (**Figure 1-2**). The role of RPE is essential in the vision process, having physical, optical, metabolic and transport functions. RPE is preserving adhesion with the neurosensory retina, playing a selectively permeable barrier between neurosensory retina and choroid. RPE is having a role in photoreceptors' outer segment phagocytosis, especially rods, and less important in cones. RPE is important for the synthesis of the interphotoreceptor matrix, absorption of light and reduction of light scatter within the eye, hence improving image resolution; and transport plus storage of metabolites and vitamins (especially vitamin A). (Forrester, Dick et al. 2015) RPE is playing a role in the retinoid acid cycle and is involved in the continuous regeneration of visual pigments. (Sancho-Pelluz, Arango-Gonzalez et al. 2008)

1.2. RETINAL DETACHMENT

1.2.1. Definition and types

RD is the separation of neurosensory retina from the RPE, due to the presence of fluid in the subretinal space (**Figure 1-5**). (Bowling 2015) Depending on the mechanism of SRF accumulation, RDs have been classified into rhegmatogenous, tractional, and exudative RD. In the origin of tractional RDs is traction on the retina, usually from a scar tissue on the retina's surface contracting and causing retina to pull away (i.e. proliferative diabetic retinopathy with tractional retinal detachment). Exudative RD is secondary RD most commonly occurring in other comorbidities such as inflammatory diseases, intraocular tumors etc. The most common type of RD is rhegmatogenous RD. The root cause is a tear formation (*rhegma*, gr) in the retina. Retinal tear is the result of dynamical vitreoretinal traction and predisposing peripheral retinal degeneration. (Bowling 2015)

1.2.2. Rhegmatogenous retinal detachment (RD)

The incidence of RD is estimated to be 1:10,000 per year, increasing to about 3.5% to 5.8% in the first year after the primary RD and 10% within 4 years in the second eye. (Mitry, Charteris et al. 2010) Retinal tears, the root cause of most RD, are the result of dynamical vitreoretinal traction on susceptible peripheral retina (Bowling 2015), with SRF filling the subretinal space.

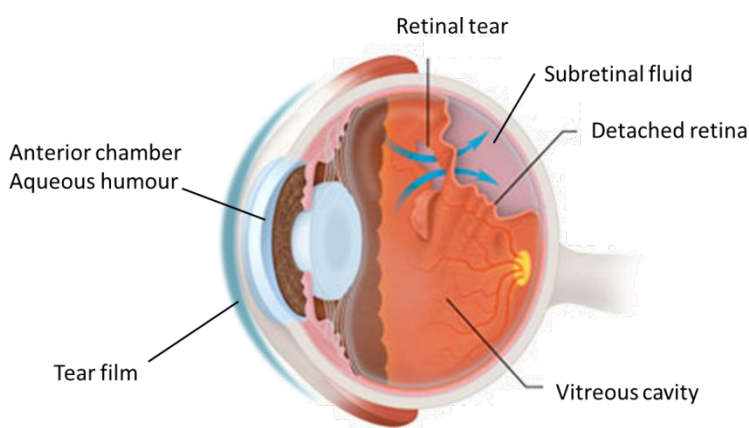


Figure 1-5 Schematic diagram of the eye with retinal detachment. Adapted from (Bowling 2015)

SRF can fill the sub retinal space in several different ways, causing different types of RD (e.g. macula-OFF, inverted fovea etc.) (**Figure 1-6**). (Wolfensberger and Gonvers 2002) Currently the only treatment for RD is surgery, depending on the indications: either scleral buckling or pars plana vitrectomy will be performed. Both of these have the same purpose: drainage/reabsorption of SRF to allow anatomical retinal reattachment in order to regain/maintain visual function. (Bowling 2015)

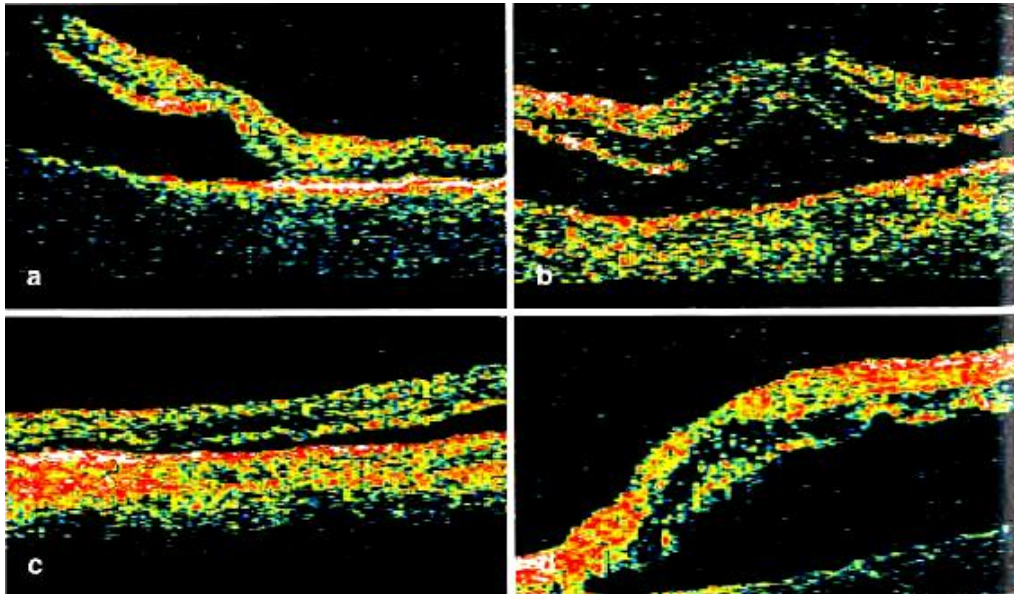


Figure 1-6. Different types of macula-OFF rhegmatogenous retinal detachment, defined with preoperative OCT: Adapted from (Wolfensberger and Gonvers 2002)

A) **Class I:** a detached macula with a retina of normal thickness and a retained, though inverted, foveal depression. B) **Class II:** a detached macula with normal retinal thickness but with loss of the foveal depression. C) **Class III:** widespread edema in the external plexiform layer of the detached retina and a retained foveal depression. D) **Class IV:** widespread retinal edema in the external plexiform layer with loss of the foveal depression

1.2.3. Anatomical and functional recovery (risk factors and visual acuity)

Visual function, expressed as VA is directly related to the density of photoreceptors in the central retina (macula). The post-operative improvement in VA has been associated with duration of RD, degree of myopia (axial length of the globe), age and persistence of SRF. (Wolfensberger and Gonvers 2002) Following RD, the photoreceptors' cell death starts in the first twelve hours and peaks at 2-3 days; thus it is important to perform surgery as quickly as possible, especially when the macula is at risk. (Cook, Lewis et al. 1995, Hisatomi, Sakamoto et al. 2001, Arroyo, Yang et al. 2005) Myopia is associated with vitreous liquefaction, PVD, common lattice degeneration and thinner retina, therefore, retinal breaks are larger, occur earlier and more frequently in myopic eyes. (Kaluzny 1970, Yonemoto, Ideta et al. 1994,

Mitry, Singh et al. 2011, Morgan, Ohno-Matsui et al. 2012) Myopia of up to -3 diopters (D) quadruples the risk of RD, and myopia of more than -3D increases the risk of RD tenfold. (Mitry, Singh et al. 2011, Morgan, Ohno-Matsui et al. 2012) Myopia is a significant risk factor because of increased prevalence; every third European adult is now myopic. (Pan, Ramamurthy et al. 2012) Younger eyes have been shown to have more persistent SRF. (Edmund 1968, Takeuchi, Kricorian et al. 1996) Veckeneer et al. have hypothesized that SRF composition, such as increased outer segment fragments and cellularity, may influence the SRF persistence which would correspond with the more viscous vitreous observed in young eyes. (Veckeneer, Derycke et al. 2012)

Two modifiable factors essential in the recovery of visual function after RD are the pre-operative duration of the macular detachment (i.e. a longer duration will result in a lower VA), (Tani, Robertson et al. 1981, Mitry, Awan et al. 2012) and the preoperative height of the macular detachment (i.e. an increase in height will result in a lower postoperative BCVA). (Ross, Lavina et al. 2005, van de Put, Hoeksema et al. 2014) Non-modifiable factors influencing the postoperative recovery of visual function include age, refractive error, and preoperative VA. (Kreissig, Lincoff et al. 1981, Tani, Robertson et al. 1981) Traditionally, quality in ophthalmic care has been assessed by measures of VA. (Brown 1999) There are several visual measurement charts. The Snellen classification is the most widely used in clinical practice, while other systems, such as the logMAR chart, are also utilized. (Ferris, Kassoff et al. 1982) Clinical studies (e.g. treatment success) usually rely on measuring the change, or absence of change, in VA. (Brown 1999)

1.2.3.1. Epidemiology of retinal detachment

A. Intrinsic risk factors

A.1. Age, gender, laterality

RD is very rare before the age of 20 years. After that age, its incidence is increasing gradually over time, with two peaks in frequency: one is between the age 20 and 29 in phakic patients, high myopes and without PVD and the second one is, much more significant, between the age 60 and 79 in patients with PVD. (Mitry, Chalmers et al. 2010) Men present more often and earlier than women patients, and right eyes are more often involved than left eyes. (Mitry, Charteris et al. 2010, Mitry, Charteris et al. 2010)

A.2. Refraction

Depending on the level of myopia, myopes are 4 to 10 times more at the risk of developing RD compared to non-myopes. The origin of this “rule” is that the liquefaction of vitreous is more often in high myopes, as well as presence of lattice retinal degenerations. They have the tendency to develop RD earlier and bilateral. (Mitry, Charteris et al. 2010) This is the reason why myopes represent 50% of phakic RDs and about 60% of all RDs. (Burton 1989, Mitry, Charteris et al. 2010) The cumulative risk of myopia importance is 1.6-9.3% compared to 0.3% of the cumulative risk for non-myopes. (Burton 1989)

A.3. Lattice retinal degeneration

There are retinal degenerations that represent the risk to develop RD. Among them, the eyes with the highest risk to develop RD are those with lattice degeneration that are frequently myopes. The lattice degeneration is present in about 30% of eyes with RD and in up to about 60% of young patients with high myopia, phakic and without PVD. (Carvounis and Holz 2005)

A.4. Hereditary variations with vitreoretinal anomalies

A.4.1. Autosomal-dominant vitreoretinopathies and other rare hereditary vitreoretinal anomalies

There are vitreoretinopathies that are recognized as the risk factors for RD. Stickler syndrome is the least rare and associate ocular anomaly where high myopia and systemic anomalies are present with variable expression. Early RD is present in more than 40% of cases and can be even bilateral, in 1:2 cases. (Korobelnik Jean-François 2014)

Marfan syndrome and homocystinuria should be mentioned as well. The risk to develop RD in these patients is increased to 8-19%. Patients with Marfan syndrome are usually high myopes; they have lattice degeneration and ectopic lens. The risk for RD is linked also with the surgery for the ectopic lens. (Korobelnik Jean-François 2014)

A.5. Antecedents with RD

A.5.1. Familial antecedents

Presence of a familial antecedent with RD is fully a risk factor, even in case of absence of hereditary vitreoretinal anomalies, except myopia. The cumulative risk for close relatives is evaluated to be 7.7%. (Go, Hoyng et al. 2005)

A.5.2. Personal antecedents

If one eye has RD, it represents an important risk factor for the other eye; bilateralism is present in 6-11% of patients, according to current studies. (Carvounis and Holz 2005) The risk for the other eye is often (but not always) linked with myopia, familial antecedents, hereditary vitreoretinopathies and giant tears. (Carvounis and Holz 2005, Mitry, Charteris et al. 2010, Mitry, Charteris et al. 2010)

A.6. Socio-economical level

The study has shown that the more elevated socio-economical level, the higher risk for RD is present. (Mitry, Charteris et al. 2010) This strong positive relationship is explained with the presence of myopia, as there is strong positive correlation between myopia and education level: more myopes are present among highly educated people. (Mitry, Charteris et al. 2010)

B. Extrinsic risk factors

B.1. Eye surgery

B.1.1. Cataract surgery

Patients that have undergone the cataract surgery have a 5 times increased risk to develop RD during several years after surgery. (Mitry, Charteris et al. 2010) It was shown that the prevalence was 2.3% of RDs over 8 years after cataract surgery. (Sheu, Ger et al. 2010) Aphakic or pseudophakic patients represent 25-33% of cases with RD, with continuing increase. (Mitry, Charteris et al. 2010, Sheu, Ger et al. 2010) Myopia, especially high myopia, young age, male gender, history of RD in the other eye and perioperative rupture of posterior lens capsule are the recognized risk factors for RD. The role of secondary capsulotomy with YAG (yttrium aluminum garnet) laser is still not clear. (Sheu, Ger et al. 2010) Children, who underwent surgery for congenital cataract, have also the elevated risk to develop RD, but the frequency is more difficult to estimate without noise, as RD happens many years after surgery. The prevalence has variations from 2 to 25% in series, usually in myopic eyes. (Korobelnik Jean-François 2014)

B.1.2. Vitrectomy

Patients who had underwent a vitrectomy have also the elevated risk to develop RD. RD usually appear not because of overlooked little retinal tears while surgery, but because of postoperative retinal tears due to secondary (peri/postoperative) vitreoretinal tractions in the basis of vitreous. The reported prevalence is 1.7 to 13.3%. (Koh, Cheng et al. 2007, Ramkissoon, Aslam et al. 2010) The maximal risk is estimated to be in case of dissection of posterior hyaloid or in some indications such as rupture of posterior lens capsule with lens fragments in vitreous. (Korobelnik Jean-François 2014)

B.1.3. Refractive surgery for myopes

There are different types of refractive surgery. The risk for RD is elevated in the case of clear lens extraction in high myopes. A prospective study has shown that there is the risk of 8.1% 7 years following surgery. Secondary YAG laser capsulotomy, frequent in young patients, has the important role. (Colin, Robinet et al. 1999) However, it is not certain that lens additive surgery is an independent risk factor for RD. (Korobelnik Jean-François 2014) It is the same for the corneal surgery although the Lasik can induce a PVD. (Carvounis and Holz 2005)

B.1.4. Intravitreal injections

Intravitreal injection of the expansive gas is also recognized as the risk for RD, e.g. the RD prevalence is 3% after pneumatic displacement of sub-macular hemorrhage. (Chen, Hooper et al. 2007) On the opposite, the risk to develop RD after the injection of corticoids or anti-VEGF is very low. (Chen, Hooper et al. 2007)

B.2. Eye contusions

Serious eye contusions can be complicated with RD in 5.5% of cases, often with retinal dialysis near ora serrata. (Eagling 1974) In the anamnesis, mentioning of some type of traumatism is present in 6.3% up to 12.2% of cases with RD. On the opposite, some studies showed that the incidence of trauma is not very high; this might be due to the weak definition of trauma. (Mitry, Charteris et al. 2010) The possibility to develop RD after indirect eye traumatism is still a controversy. (Korobelnik Jean-François 2014)

1.2.4. The cause of rhegmatogenous retinal detachment

Rhegmatogenous RD appears as the consequence of the presence of a retinal break. The retinal break is a full-thickness interruption of neuroepithelium. The current theory is that the fluid from vitreous is passing through the retinal break into subretinal space and thus provoking the RD. According to the origin of retinal breaks, they can be divided into “tears” (due to dynamic vitreoretinal traction) and “holes” (due to localized retinal disintegration or atrophy). (Williamson, Shunmugam et al. 2013)

The retinal tears are appearing after the “dynamic vitreous traction” following or during PVD, after the rotational energy (generated by saccadic contraction of the extraocular muscles) is forwarded from the eye coats to the vitreous and back. (Cheng, Yen et al. 2004, Williamson, Shunmugam et al. 2013) As the vitreous have strong adhesions to the retina in some points, this energy is transmitted to every area of vitreoretinal contact. After PVD, the vitreous base originates the energy while the posterior vitreous is transmitting this energy through remarkable movements. In this situation, if there is any “abnormal” vitreoretinal adhesion, the energy will provoke the dynamic traction on the retina, causing the retinal tear, commonly U-shaped. (Williamson, Shunmugam et al. 2013)

Firstly, the posterior edge of the tear appears and then, the vitreous detaches and tears retina towards the vitreous base, anteriorly. The round tear is formed after the complete separation

of the vitreous and retinal flap together (the piece of avulsed neurosensory retina floating in the vitreous as the operculum). (Williamson, Shunmugam et al. 2013)

In young myopic patients, rhegmatogenous RD can happen without PVD, due to atrophic retinal holes or by retinal dialysis at the ora serrata. (Williamson, Shunmugam et al. 2013)

1.2.5. Pathogenesis of the retinal detachment

Following the formation of the retinal break, the SRF is completing the subretinal space, firstly around the tear, progressively extending and forming a real RD. (Williamson, Shunmugam et al. 2013) The progression of RD (extending of SRF) has been estimated at 1.8 disc diameters/day (Ho, Fitt et al. 2006); so that fovea-ON patients can become fovea-OFF by the time of surgery. If the globe is immobilized at an early stage, or the patient is positioned, the retina may partially or even completely reattach. (Williamson, Shunmugam et al. 2013) This is most probably due to inhibiting the dynamic vitreoretinal traction by stopping eye movements and energy transmission. (Hammer, Burch et al. 1986, Williamson, Shunmugam et al. 2013)

1.2.5.1. Subretinal fluid in rhegmatogenous retinal detachment

Subretinal fluid (SRF) can fill the subretinal space in several different ways, causing different types of RD (e.g. macula-OFF, inverted fovea etc.). (Wolfensberger and Gonvers 2002) Gravity encourages spread of the SRF. (Williamson, Shunmugam et al. 2013) The pattern of the SRF spread is described by Lincoff, used to identify the localization of breaks, **Figure 1-7.** (Lincoff and Gieser 1971)

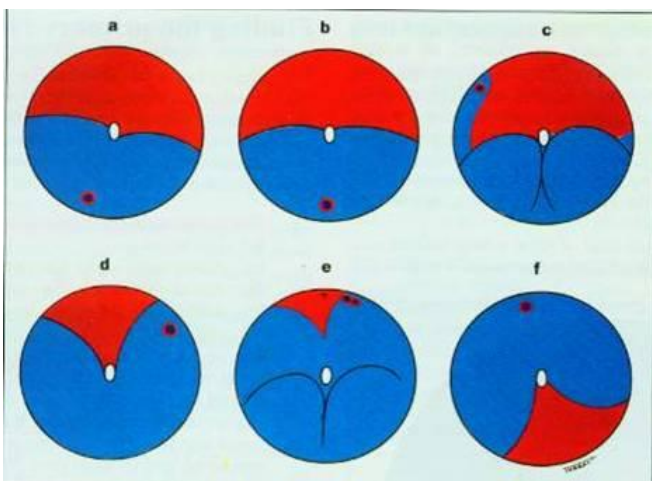


Figure 1-7. Lincoff rules of tear localization in retinal detachment (Lincoff and Gieser 1971, Korobelnik Jean-François 2014)

1.2.5.2. Macula-ON vs Macula-OFF retinal detachment

Depending on the SRF spreading (**Figure 1-7**) and consequently detaching macula and fovea, rhegmatogenous RDs are divided into two groups: macula-ON (with macula attached) and macula-OFF (with detached macula). (Bowling 2015) It has been proved that the VA is directly related to the density of photoreceptors in the macular region. There are several factors that might influence the post-operative improvement in VA, such as the duration of RD, the degree of myopia (axial length of the globe), the age and the persistence of SRF (**Figure 1-8**). (Wolfensberger and Gonvers 2002) It is important to perform surgery as soon as possible, especially when the fovea is at risk of detachment, as the photoreceptors' cell death begins within the first twelve hours, with its peak at 2-3 days following RD. (Cook, Lewis et al. 1995, Hisatomi, Sakamoto et al. 2001, Arroyo, Yang et al. 2005)

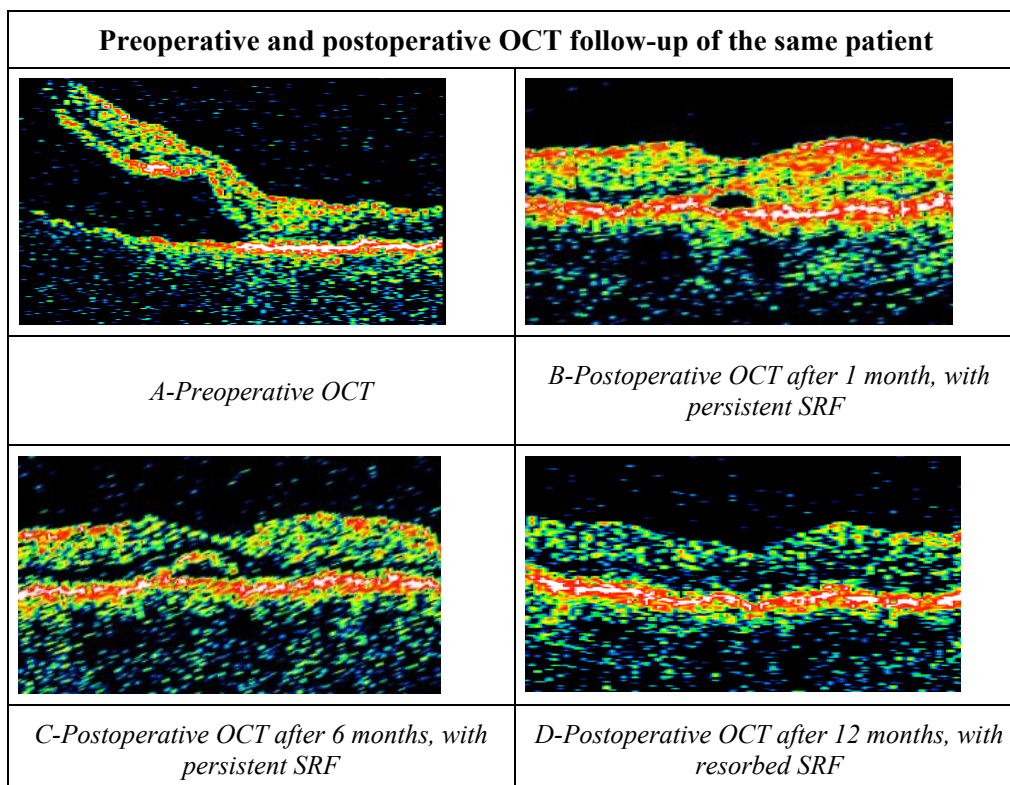


Figure 1-8. Pre-operative and postoperative OCT follow-up of the same patient. Adapted from (Wolfensberger and Gonvers 2002)

In the macula-OFF patients (when fovea is detached), the chances of return of the preoperative VA with good central vision are decreased, especially after the first week following RD. As a “rule of thumb”, the urgency to perform the surgery for RD is equal to the number of days that the fovea has been detached, i.e. if the fovea has been detached for 2

days, the surgery should be performed within 2 days (**Table 1-1, Table 1-2**). (Hassan, Sarrafizadeh et al. 2002, Williamson, Shunmugam et al. 2013)

Table 1-1. Referral procedure for RD (adapted from (Williamson, Shunmugam et al. 2013)

Condition	Characteristics	Referral	Why?
RD with PVD	Macula-ON	Immediate	Prevent macula-detaching
	Macula-OFF less than 1 week	1-3 days	Macula should recover fully
	Macula-OFF 1-2 weeks	1 week	Macula should recover well
	Macula-OFF 2-6 weeks	1-2 weeks	Macula will show moderate recovery
	Macula-OFF >6 weeks	2-3 weeks	Macula unlikely to recover well
RD without PVD		1-2 weeks	Slow progression

Patients with macula-OFF RD have higher probability to be concerned about their postoperative vision and consequently they report more often slight changes in vision such as distortions. Therefore, it is preferable to avoid the detachment of the fovea by performing surgery on macula-ON RD promptly. (Williamson, Shunmugam et al. 2013)

Table 1-2. Chance of 0.3 logMAR or better visual acuity after fovea-OFF RD, adapted from (Hassan, Sarrafizadeh et al. 2002)

10 days or less	71%
11 days to 6 weeks	27%
More than 6 weeks	14%

1.2.6. Treatment of retinal detachment

The father of vitreoretinal surgery and of the treatment of RD was Jules Gonin, who first introduced the technique called ignipuncture: *“all retinal holes must be closed definitively, this interrupts the passage of fluid under the retina and it resolves by accumulation”*. (Gonin 1930) After Gonin, Custodis, Schepens, Arruga continued to develop retinal surgery.

Currently the only treatment for RD is surgery. As the definition of rhegmatogenous RD is a retinal break with SRF, the identification and closure of the retinal break or breaks is the primary aim of surgery.

Depending on the indications there are two types of surgery that can be performed: scleral buckling or pars plana vitrectomy. Both of these have the same purpose: drainage/reabsorption of SRF to allow anatomical retinal reattachment in order to regain/maintain visual function. (Bowling 2015)

1.2.6.1. Scleral buckle surgery

Scleral buckle surgery (SB) is the extraocular procedure that aims to close retinal breaks through external scleral indentation. (Ophthalmology 2016) In this surgery, trans-scleral cryopexy is used to create a permanent adhesion between the detached retina and the RPE at the sites of retinal breaks. (Ophthalmology 2016) The buckling material is then carefully positioned to support the causative breaks by scleral indentation. There exist several SB techniques: encircling, segmental, radial placement of the sponge. In order to decide which buckling type to use, several factors should be considered: localization and number of retinal breaks, extent of RD, as well as correlated vitreoretinal findings (e.g. lattice degeneration, vitreoretinal traction, aphakia).

The simple SB surgery can be followed by the drainage of the SRF (e.g. in chronic, long-standing RDs with viscous SRF), or intraocular air or gas tamponade (e.g. in the case of large retinal breaks, bullous RDs). (Ophthalmology 2016)

1.2.6.2. Pars plana vitrectomy

Pars plana vitrectomy (PPV) is the intraocular procedure that among other indications is used also in patients with RD. Its aim is to reattach retina and to drain the SRF. The name relates to the fact that the eye is “opened” at pars plana (3.5-4.0 mm from the limbus); most commonly on three places (three sclerotomies, so called three-port approach). This entrance is followed with vitrectomy; i.e. the vitreous removal. PPV consists of vitreous removal, release of vitreous traction, internal drainage of SRF, endolaser retinopexy or cryotherapy of retinal breaks, and internal tamponade with air or gas or silicon oil on completion of surgery. (Narendran, Kothari et al. 2014)

1.3. IMPORTANCE OF RETINAL DETACHMENT

RD is a condition that results in blindness in 100% of cases if left untreated. Time taken to seek treatment will affect the surgical outcome and visual recovery. Potentially the final visual outcome can have important socio-economic consequences in terms of mobility and independence. Quantifying the influence of vision on QoL in these patients will help underline problem areas. Better understanding of the predictive factors, such as cellular/retinal morphology and risks associated with different types of RD (based on retinal appearance/structure) will provide more realistic information for patients preoperatively, ultimately resulting in better clinical management.

The work of this thesis aims to identify a photoreceptor cell death pathway on the human *in vitro* RD model. If successful this work will report cell death pathways in humans and as such should motivate further research in this area, including addition *in vitro* models to identify additional pathways. Ultimately this type of research aims to identify new treatment options.

2. AIMS AND WORKING HYPOTHESIS

Working Hypothesis:

- Better characterization of the cell cycle proteins and cell death pathways of photoreceptors *in situ* and cellular/retinal morphology of RD could help predict post-operative anatomical/functional recovery and subsequently patients QoL

The aims of the study

1. To investigate the cell cycle proteins and other cell death pathways *in situ* during photoreceptor degeneration after RD
2. To characterize the postoperative anatomical recovery following RD with sequential 3D and cellular *in vivo* imaging
3. To investigate the postoperative functional recovery of patients following RD with sequential VA assessment
4. To investigate the QoL of RD patients using the validated NEI VFQ-13 QoL instrument

3. METHODS OVERVIEW

3.1. Clinical and epidemiology study protocol

This prospective observational, non-randomized, cohort study was conducted at the Department for Vitreoretinal Surgery of the Jules-Gonin Eye Hospital, in the period from February 2015 until March 2017.

The study followed the tenets of the Declaration of Helsinki and was approved by the Ethical Committee of Canton Vaud, Switzerland (protocol No. 483/14) and by the Ethical Committee of Medical Faculty, University of Belgrade (protocol No. 29/II-31). Written informed consent was obtained from participants.

3.1.1. Subject selection

Subject recruitment was performed at the Department for Vitreoretinal Surgery, following their first examination. Patients, who have consented to vitreoretinal surgery and were eligible for the study, they were approached by the investigators. The study purpose has been clearly explained to patients and the patient information sheet was distributed. Patients had at least 24 hours to reflect before consenting to participate in the study.

Inclusion criteria:

1. Patients with primary rhegmatogenous retinal detachment (RD)

Excluding criteria:

1. People not able to consent
2. Patients older than 99 years and younger than 18 years
3. Patients with RD that has lasted for more than 30 days
4. Patients with ocular comorbidity (including: retinal vascular occlusions, diabetic retinopathy, age related macular degeneration, proliferative vitreoretinopathy grade C or more)

Clinical judgment criteria

Changes on the following clinical measures were assessed: best corrected visual acuity (BCVA), fundus exam on the slit lamp, Fundus photo, optical coherence tomography (OCT), ultrasound examinations. In addition to the standard method of analysis of SD-OCT images, the images were post-processed to account for the curvature of the globe,

in suitable images the height of SRF was calculated and compared over follow-up (**Table 3-1**). In addition, AO *in vivo* images of the cellular configuration were collected on patients with good optical quality (20%), allowing the assessment of the cellular changes post-operatively. Combined these measures permitted the retinal morphology in RD patients pre and post operatively to be more accurately characterized. To quantify the possible changes to QoL during follow-up, shortened; modified National Eye Institute Visual Functioning Questionnaire (NEI VFQ-13 questionnaire) was administered four times. The QoL outcomes were compared preoperatively and one, three and six months postoperatively (**Table 3-1**).

Table 3-1. Protocol of the study

Number of visits	Time of visits (day, month, year)	Description of procedures	Additional patient time
1	Preoperatively (recruitment)	Standard clinical exam §	0 min
2	Operation day (Enrollment consent)	NEI VFQ-13 * Performing surgery (scleral buckle or pars plana vitrectomy)	10 min 0 min
3	Month 1	Standard clinical exam § AO * NEI VFQ-13 *	20 min
4	Month 3	Standard clinical exam § AO * NEI VFQ-13 *	20 min
5	Month 6	Standard clinical exam § AO * NEI VFQ-13*	20 min

* Not part of standard clinical exam

§ Standard clinical exam: BCVA measurement on Snellen optotype, IOP measurement, Fundus examination, Fundus photo and SD-OCT

3.1.2. Statistical analysis

Pre and post-operative measures were compared using a paired two-sample t-test. The differences between subgroups (e.g. type of RD) were compared using a two-sample test for comparing variables between two groups. Statistical significance was examined at the 5% level. Multilevel modeling was used to examine the predictive factors (baseline VA, type of RD etc.) of visual recovery and QoL scores.

Statistical power

In this study we aimed to examine if there was a significant difference in the QoL of different RD subtypes. Okomoto et al reported that there is a 4.4 point difference in the composite score between the macula-ON and the macula-OFF subtypes of RD. In patients with RD the standard deviation in QoL composite score was estimated to be 12.1 points. Therefore to have 80% power of detecting a significant change at the 5% significant level between these groups we require 48 patients in each group. Allowing for 20% dropout this would equate to 118 patients in total.

3.1.3. Processing of personal data

Personal and medical data were collected in this study. However, they have been made anonymous, which means associated with a code. The code list have been prepared and stored by third party, independent of the study. Only anonymous data were accessible to specialists for scientific evaluation. Patient privacy is strictly guaranteed throughout the study and during the above controls. The names of the patients will not under any circumstances be published in reports or publications arising from this study.

3.2. Basic research and experimental study protocol

The experimental basic research study was conducted on human retinal explants as an *in vitro* model of RD. The complete globe was obtained during organ retrieval, following the preparation of the cornea, while the remaining materials were considered biological waste. Where appropriate (no history of ocular disease) the retina was retained for medical research purposes, according to the ethical approval (protocol No 340-15). Therefore the required explants were recuperated from cornea organ donor eyes. The experiments were conducted at the Research Pole in Ophthalmology, UGTSCB (Unit of Gene Therapy and Stem Cell Biology) at the Jules-Gonin Eye Hospital, University of Lausanne, Switzerland. This study lasted from February 2015 until March 2017.

The human retinal explants were prepared as the *in vitro* model of the RD: group without RPE and the group with retained RPE. Immunohistochemical analyses were performed according to standard protocol, on a series of 14 µm-thick cryosections.

3.2.1. Statistical analysis

Statistical analysis of data was done using the methods of descriptive and analytic statistics. For the statistical importance, the value of $p < 0.05$ was considered, repeated measures were accounted.

4. RESULTS

4.1. CLINICAL ASPECTS OF RHEGMATOGENOUS RETINAL DETACHMENT

4.1.1. Introduction

The incidence of RD is estimated to be 1/10,000 inhabitants per year, increasing to about 3.5% to 5.8% for recurrences within the first year after a primary RD and 10% within 4 years for the second eye. (Mitry, Charteris et al. 2010) The macula-ON and macula-OFF statuses in RD are considered different stages; however, the risk factors for progression to macular involvement in RD have not been extensively studied. The majority of studies comparing RD based on macular status used retrospectively collected data, which limit the available information especially regarding risk and retinal features. The aim of this study was to describe the demographics of RD patients and primary outcomes after surgery with respect to macular status in a cohort of consecutive prospectively enrolled patients.

4.1.2. The study design

Patients

All patients presenting with primary RD were invited to participate in the study, if they fulfilled the inclusion/exclusion criteria (please refer to **Table 3-1** and the paragraph **3.1**). A total of 204 patients were recruited in the study, with 194 included in the analysis.

Clinical examination

All patients underwent a baseline/preoperative standard clinical examination and follow up at 1, 3 and 6 months after surgery (**Table 3-1**). The macular involvement preoperatively was confirmed by a preoperative OCT. The included patients with primary RD were divided into two groups: macula-ON (with preserved macula) and macula-OFF (with detached macula).

Surgical procedure

Patients underwent scleral buckling surgery (n=7) or pars plana vitrectomy (n=187). A scleral buckle was performed in young phakic patients who hadn't yet developed a PVD. Depending on the RD and retinal tear localization, we used a 240 silicone band or a 5 mm

radial sponge explant (Labtician, Oakville, Ont. Canada). For all scleral buckle surgeries, we performed cryotherapy around tears and external SRF drainage, as described previously. (Wolfensberger 2004)

Most patients were treated with PPV, cryotherapy and/or endolaser, and tamponade (complete or partial fluid-gas exchange with 23% sulfahexafluoride [SF6], 12% octafluoropropane [C3F8], or 5500 cs silicone oil tamponade [FCI, France]) (**Table 4-1**). Patients were operated on in turn by a group of vitreoretinal surgeons in the institution. Patients were positioned after surgery to reinforce the absorption of SRF. All patients received a local treatment of antibiotics and corticosteroids for one month after surgery. Total retinal reattachment, determined by binocular indirect ophthalmoscopy and OCT, was considered a complete surgical success, as described previously. (Wolfensberger 2004)

Statistics

Proportionality differences, including trends, were calculated with the χ^2 statistic. Continuous data, such as age, were compared between groups using the Wilcoxon non-paired t-test. All reported probabilities (p) are based on two-sided tests. A p-value <0.05 was considered statistically significant. Statistics were calculated using R version 3.1.3.

4.1.3. The baseline data

4.1.3.1. Patients

This study included 194 eyes from 194 patients, 102 (52.6%) patients presented with a RD that extended through the macula (macula-OFF) and 92 (47.4%) patients had a more peripheral RD (macula-ON). The mean age was significantly older in the macula-OFF group (63.9 ± 12.0 years) compared with the macula-ON group (59.7 ± 11.2 years, $p=0.01$, Wilcoxon non-paired t-test Table 4-1. In our study group, three patients developed RD in the fellow eye during the follow-up period (3/194, 1.5%).

4.1.3.2. Age and gender distribution

The difference in the mean age between men and women was not significant (62.5 ± 10.9 vs. 60.9 ± 13.3 years, respectively). The gender distribution was imbalanced with 65 (33.5%) women and 129 (66.5%) men. The confidence interval with a probability of 95% for men was calculated to be 59-73%; while, it was 27-41% for women ($p=0.000$ chi-square test)

(Table 4-1). In both subgroups, this trend remained with 35 women vs. 57 men (38% vs. 62%) in the macula-ON group and 30 women vs. 72 men (29.4% vs. 70.6%) in the macula-OFF group (Table 4-1). Primary surgical failure occurred in 11% of eyes.

4.1.3.3. Myopia (spherical equivalence and axial length)

To measure myopia, we used spherical equivalence (SE) in diopters (D). We divided our patients in groups of low myopia ($<-3D$), medium myopia ($-3D$ to $-6D$) and high myopia ($>-6D$). Most patients had low myopia (94/194, 48.5%), while medium and high myopia occurred less frequently (27/194, 13.9% and 19/194, 9.8%, respectively). In addition, 12.4% (24/194) were emmetropes and 11.8% (23/194) were hypermetropes. For two patients, the preoperative SE and AL were not available. There was a significantly greater proportion of myopes, with a SE $<-3D$, in the macula-ON group (n=30) than in the macula-OFF group (n=19) (p=0.04, chi-square test) (Table 4-1). As some patients had undergone cataract surgery or refractive surgery, we also investigated the relationships with AL. We evaluated a cut-off value of >25 mm, which corresponds to a refractive error of approximately $-3D$. We demonstrated there was greater proportion of eyes with AL >25 mm in the macula-ON group (p=0.04, chi-square test). There was no significant difference in mean AL between women (24.8 ± 1.6 mm) and men (25.2 ± 1.6 mm), p=0.11 (Table 4-1).

4.1.3.4. Lens status

There were 108 (55.7%) phakic and 86 (44.3%) pseudophakic patients. Among men with RD, there were 66 (51.2%) phakic patients and 63 (48.8%) pseudophakic; while, the distribution was less balanced among women with 42 (64.6%) phakic and 23 (35.4%) pseudophakic. The RD eyes of phakic patients were more often macula-ON (60/92, 65.2%) than macula-OFF (48/102, 47.1%). There were few pseudophakic myopes with SE $<-3D$ (n=6) and they were split equally between the macula-ON (n=3) and macula-OFF (n=3) subgroups (Table 4-1).

4.1.3.5. Relation of age with lens status and myopia

The mean age of pseudophakic patients (n=86) was 67.1 ± 10.2 years, while phakic (n=108) patients were younger (57.8 ± 11.3 years). The oldest patients were pseudophakic medium myopes with a mean age of 73.8 ± 10.7 years, while the youngest population was represented by highly myopic phakic patients (48.6 ± 16.1 years).

4.1.3.6. Laterality

In our study group, RD was present significantly more in right eyes (OD, n=123) than left eyes (OS, n=71) (63.4% [CI 56-70%] vs. 36.6% [30-44%], $p=0.000$ chi-squared test). This was evident in both men (OD:OS=82:47, $p=0.002$) and women (OD:OS=41:24, $p=0.03$). In the macula-ON and macula-OFF subgroups, this relationship persisted, with RD occurring significantly more often in right eyes ($p=0.05$, $p=0.001$) and men ($p=0.02$, $p=0.000$) respectively (**Table 4-1**).

4.1.3.7. Retinal detachment characteristics

We analyzed the following RD characteristics in our cohort: RD localization (superior, inferior, nasal, or temporal), RD extension (expressed in clock hours), number, and localization of retinal breaks. The majority of eyes with nasal RD had preserved macula (97%), while eyes presenting with temporal or temporal and nasal RD were more often macula-OFF ($p<0.001$) (**Table 4-1**). There was no statistically significant difference between inferior and superior RD ($p=0.34$). The mean number of retinal breaks and their localization was not statistically significant ($p=0.08$) (**Table 4-1**). Macula-OFF eyes presented with RD that was extended for more clock-hours than eyes in the macula-ON group (5.94 ± 1.94 vs. 3.97 ± 1.37 , $p<0.001$) (**Table 4-1**).

4.1.3.8. Multivariate model

A stepwise logistic regression was performed. All parameters that had a p -value <0.2 following univariate analysis were included in this analysis. Pseudophakic lens status ($p=0.02$) and eyes with an AL <25 mm ($p=0.06$) were independent predictive factors for macula-OFF detachments.

Table 4-1. Baseline characteristics of patients with primary rhegmatogenous retinal detachment

	Macula-OFF	Macula-ON	p-value
No. of patients	102 (52.6%)	92 (47.4%)	p=0.47
Mean age (years)	63.9 ± 12.0	59.7 ± 11.2	p=0.01
Men vs. women	129 vs. 65 (66.5% vs. 33.5%)		p=0.000
Proportion of men	72 (70.6%)	57 (62%)	p=0.26
Right eyes vs. left eyes	123 vs. 71 (63.4% vs. 36.6%)		p=0.000
Proportion of right eyes	61 (59.8%)	62 (67.4%)	p=0.34
Systemic factors:			
-Diabetes	2 (2%)	3 (3%)	p=0.98
-Hypertension	33 (32%)	23 (25%)	p=0.26
-Hyperlipidemia	16 (16%)	8 (9%)	p=0.15
-Smoker	2 (2%)	2 (2%)	p=0.92
Mean SE (D)	-1.40 ± 3.04	-2.34 ± 3.10	p=0.31
Medium/high myopes (SE>-3D)	19 (18.8%)	30 (33.0%)	p=0.04
Mean axial length (mm)	24.85 ± 1.7 (FE 24.92±1.7)	25.28 ± 1.6 (FE 25.18±1.5)	p=0.106
- Men	25.04 ± 1.66	25.39 ± 1.63	p=0.231
- Women	24.30 ± 1.80	25.10 ± 1.47	p=0.086
Eyes with AL >25.0mm	38 (37.6%)	49 (53.8%)	p=0.04
Phakic vs. Pseudophakic	108 vs. 86 (55.7% vs. 44.3%)		p=0.114
Proportion of phakic eyes	48 (47.1%)	60 (65.2%)	p=0.01
Median BCVA (logMAR) [IQR]	2.0 [0.8 to 2.3] (FE 0.0 [0. to 0.1])	0.1 [0 to 0.2] (FE 0.0 [0.0 to 0.01])	p=0.00 p=0.59
Median IOP TE (mmHg)	12 [10 to 16]	14 [12 to 16]	p=0.09
FE	14 [13 to 17]	14 [12.5 to 16]	p=0.54
FE-TE	1 [-1 to 2]	1 [-1 to 4]	p=0.03
Central macular thickness (µm)	466.17 ± 528.78 (FE 283.72 ± 29.73)	283.36 ± 79.04 (FE 285.81 ± 26.51)	p<0.001
- In men	469.43 ± 574.57	285.79 ± 88.52	p<0.001
- In women	458.67 ± 413.15	279.34 ± 61.29	p<0.001
- In phakic eyes	356.91 ± 349.49	281.24 ± 70.61	p<0.001
- In pseudophakic eyes	564.92 ± 637.32	287.27 ± 93.74	p<0.001
Subfoveal fluid height (µm)	361.11 ± 419.45	0	p<0.001
RD type			
Nasal/Temporal/Both	1/53/43	28/45/19	p<0.001
Inferior/Superior/Both	20/24/35	24/52/16	p=0.34
Mean No. of RD extensions (Clock hours) (±SD)	5.94 (±1.94)	3.97 (±1.37)	p<0.001
Mean No. of retinal breaks	1.91 (±1.24)	2.27 (±1.52)	p=0.08
Surgery type			
Scleral buckling	2	5	
Pars plana vitrectomy	100	87	
- SF6	48	55	
- C3F8	18	23	
- Silicone oil	34	9	p<0.001
Primary surgical failure	9	21/194 (10.8%) 12	p=0.46

Macula-OFF: retinal detachment that involves the macula, Macula-ON: retinal detachment with the macula preserved; SE: spherical equivalence; AL: axial length; BCVA: best corrected visual acuity expressed as interquartile range [IQR]; IOP: intraocular pressure; TE: Treated eye; FE: fellow eye; RD: retinal detachment; SF6: 23% sulfahexafluoride; C3F8: 12% octafluoropropane

4.1.4. Discussion

In our 2-year prospective study, 194 patients had primary RD that affected significantly more right eyes than left eyes (63.4% vs. 36.6%). Moreover, there were twice as many men with RD than women. These relationships were evident for both the macula-ON and macula-OFF subtypes. Age, lens status, AL, and SE were associated with macula status by univariate analysis. However, the multivariate model indicated that a shorter AL and pseudophakic lens status were the only independent risk factors for macula-OFF RD. Right eye predominance has been noted in RD in several studies (i.e. 54.9% vs. 43.4%; $p < 0.0001$) with an incidence of up to 1.36:1. (Laatikainen, Tolppanen et al. 1985, Mitry, Tuft et al. 2011) A meta-analysis of previous studies showed the right eye incidence in RD was between 53.5% and 56.7% ($p < 0.0001$). (Mitry, Charteris et al. 2010) In our study group, we also observed significantly more right eyes with RD. The reason for the right eye being more predisposed to RD is still unknown. Mitry et al. hypothesized this was because the right eye was the dominant eye in many patients (Cheng, Yen et al. 2004, Mitry, Tuft et al. 2011) and it is generally assumed that the dominant eye is more myopic. (Cheng, Yen et al. 2004) Another hypothesis could be that repeated rubbing of the right eye in a predominantly right-handed population could have an effect on the pathogenesis of retinal detachment. A similar effect has been shown in keratoconus. (Coyle 1984, Ioannidis, Speedwell et al. 2005)

We observed that there were statistically significantly fewer macula-OFF detachments in medium to high myopes than macula-ON. Additionally, there were fewer eyes with an $AL > 25$ mm in the macula-OFF group. This may be due to providing high myope patients with better information on RD during standard care. Alternatively, a thinner choroid may restrict retinal perfusion, inhibiting accumulation of subretinal fluid and resulting in slower progression of RD; thus, the negative relationship between AL and choroidal thickness may contribute to the higher rate of macula-OFF RD in shorter eyes. (Flores-Moreno, Lugo et al. 2013, Alshareef, Khuthaila et al. 2017, Iwase, Kobayashi et al. 2017, Sayman Muslubas, Hocaoglu et al. 2017)

In our study group, there were slightly more phakic than pseudophakic eyes. The lens status is a recognized risk factor for RD and is due to induced vitreous tractional forces; however, the relationship between the RD type and the lens status has not been previously reported. (Mitry, Charteris et al. 2010) In this study, we observed that phakic eyes presented more often with the macula-ON RD subtype. Perhaps those tractional forces induced by cataract surgery also increase the risk of macula-detachment; however, this requires further investigation. Moreover, women were more often phakic. A Taiwanese study showed a higher

risk for RD in men after cataract surgery (Wang, McLeod et al. 2003, Sheu, Ger et al. 2007, Sheu, Ger et al. 2010, Chen, Lian Ie et al. 2016) and this also may be associated with potential differences in the anatomy of vitreoretinal adhesions at the vitreous base. (Wang, McLeod et al. 2003) The combination of lens status and AL as predictive risk factors for RD has not been previously reported.

Several studies have reported a population-based incidence of RD, with age, gender, refractive error (i.e. myopia), lens status (i.e. pseudophakia), and socioeconomic status identified as risk factors. (Mitry, Charteris et al. 2010, Mitry, Charteris et al. 2010, Van de Put, Hooymans et al. 2013, Chen, Lian Ie et al. 2016, Park, Cho et al. 2017) Mitry reported a male to female ratio of 1.68:1, while other authors have reported ratios up to 2.3:1. (Rosman, Wong et al. 2001, Van de Put, Hooymans et al. 2013, Chen, Lian Ie et al. 2016, Howie, Darian-Smith et al. 2016) In our study, the male to female ratio was 1.98:1. Meta-estimations of previous studies have found the male incidence in RD to be between 52% and 59%. In our study group, the interval of confidence for men was 59-73%. The origin of these gender differences has been associated with differences in AL, since males tend to be more myopic. (Lee, Klein et al. 2009, Mitry, Charteris et al. 2010, Mitry, Charteris et al. 2010) An alternative hypothesis is that men may be at greater risk to develop RD due to differences in the anatomy of vitreoretinal adhesions at the vitreous base. This contributes to a higher frequency of retinal breaks after posterior vitreous detachment. (Wang, McLeod et al. 2003) There was no difference in the gender distribution between the macula-ON and macula-OFF groups.

There are some weaknesses of this study. First, the study is mono-centric and not population based; therefore, the data were subject to selection bias. While every effort was made to include all possible patients at our center, the patient mix from our tertiary referral center may have been systematically more complex. With a sample size of almost 200 eyes, the analysis was limited to detecting only the largest contributing factors to macular involvement. Thus, there may be additional risk factors that were not observed in this analysis. Additional studies are required to confirm these results.

4.1.5. Conclusion

The results of this study indicate that a pseudophakic lens status and shorter AL were associated with macula-OFF RD. While pseudophakic lens status is a recognized risk factor for RD, a shorter AL has not been previously identified.

4.2. RETINAL DETACHMENT AND ITS IMPACT ON VISUAL ACUITY AND VISION-RELATED QUALITY OF LIFE

4.2.1. Introduction

4.2.1.1. Quality of life (QoL)

In 1948, the World Health Organization defined health as “the state of complete physical, mental and social well-being and not merely the absence of disease or infirmity”. Since then, quality of life (QoL) has become increasingly important in health-care practice and research, however it is a complex concept for which no universally accepted definition is available. (Fayers and Machin 2013) What is recognized is the very important role that vision plays in patients’ appreciation of their QoL, with patients with reduced vision reporting comparable scores to those patients with stroke or advanced cancer (**Figure 4-1**). Many instruments for measuring different aspects of QoL have been developed; the majority of them have two central components. Firstly, they are multidimensional, including multiple measures on: physical, emotional and social aspects, this can be correlated with a particular disease or treatment. (Globe, Levin et al. 2002) Secondly, instruments include both objective and subjective perspectives in each field assessed. (Fayers and Machin 2013, Turner and Gellman 2013)

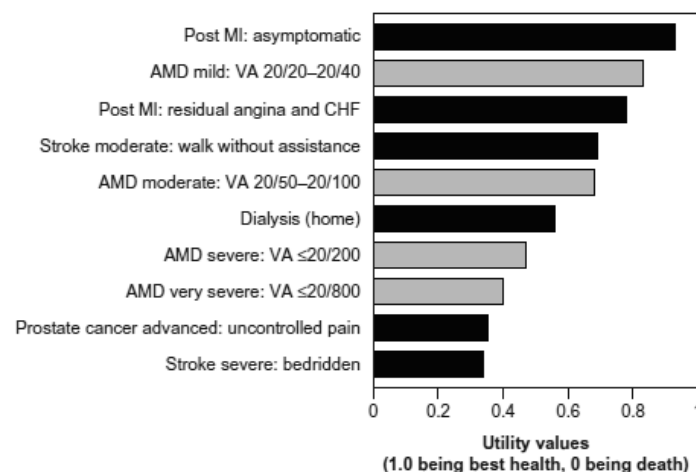


Figure 4-1. Patients’ appreciation of their QoL, adapted from (Yuzawa, Fujita et al. 2013)

In ophthalmology, the impact of chronic eye disease on health related QoL has been explored for diabetic retinopathy, (Lee, Whitcup et al. 1995, Klein, Klein et al. 1998) corneal transplantation, (Musch, Farjo et al. 1997) cataract, (Steinberg, Tielsch et al. 1994, Steinberg, Tielsch et al. 1994) glaucoma, (Parrish, Gedde et al. 1997) retinal disorders, (Linder, Chang et

al. 1999) and macular degeneration. (Globe, Levin et al. 2002, Mackenzie, Chang et al. 2002). In these studies a reduction in VA was observed to have a negative effect on patients' QoL (Parrish, Gedde et al. 1997, Linder, Chang et al. 1999, Okamoto, Okamoto et al. 2010, Zou, Zhang et al. 2011, Lina, Xuemin et al. 2016).

Rhegmatogenous RD will result in blindness if not surgically repaired, but successful anatomical reattachment is achieved in more than 95% of cases. (Tani, Robertson et al. 1981, Grizzard, Hilton et al. 1994, Pastor, Fernandez et al. 2008, van de Put, Hoeksema et al. 2014) Surgical success is assessed on postoperative VA, (Burton 1982, Grizzard, Hilton et al. 1994, Ross and Kozy 1998, Hassan, Sarrafizadeh et al. 2002, Mitry, Awan et al. 2013) however a patients' appreciation of success may diverge significantly from this assessment. (Stangos, Petropoulos et al. 2004, Wickham, Connor et al. 2004, Weichel, Martidis et al. 2006, Falkner-Radler, Myung et al. 2011, Smretschmig, Falkner-Radler et al. 2016). To the best of our knowledge there are six studies which have tried to assess QoL measures in patients following RD (Okamoto, Okamoto et al. 2008, Okamoto, Okamoto et al. 2010, Zou, Zhang et al. 2011, van de Put, Hoeksema et al. 2014, Lina, Xuemin et al. 2016, Smretschmig, Falkner-Radler et al. 2016), of which only two compare preoperative type of RD and patients' QoL preoperatively and during several time-points follow up. Contrary to clinical observation, to date the published literature indicates that there is no significant difference in health-related QoL post-operatively between patients with macula-ON against macula-OFF RD. However, a recent publication by Pesudovs et al, indicates that the instrument used in these studies may have been ill-conceived to measure this. (Pesudovs, Gothwal et al. 2010)

4.2.1.2. Instruments of QoL: development, adaptation and analysis

Instruments of QoL have changed the way we assess the impact of disease and treatment, extending our understanding beyond the traditional limits of symptoms, signs, morbidity, and mortality. Including additional dimensions, such as patient's physical, social, and emotional wellbeing, provides a more global evaluation of person with the disease. (Pesudovs, Burr et al. 2007) Given the large number of instruments available; selecting the appropriate instrument is difficult, especially as implementation in multiple medical fields has changed the format and purpose of the instruments. Care needs to be taken in this selection process as inappropriate changes in the design and application of an instrument can invalidate it; and measures for assessing validity of changes have only recently been applied in ophthalmology. (Pesudovs, Burr et al. 2007)

The National Eye Institute Visual Function Questionnaire (NEI VFQ) is a good example of this type adaption by specialty; to date three variants have been published. (Mangione, Berry et al. 1998) and have been used to evaluate the degree of disability secondary to ocular diseases. (Alonso, Espallargues et al. 1997, Gutierrez, Wilson et al. 1997, Parrish, Gedde et al. 1997) To overcome the lack of generalized applicability across specialties, some investigators have incorporated more generalized medical QoL measurement indices. (Parrish, Gedde et al. 1997) The most commonly used instrument for quantitative assessment of QoL with respect to vision is NEI VFQ-25. (Rossi, Milano et al. 2003, Fukuda, Okamoto et al. 2009, Okamoto, Okamoto et al. 2010, Orr, Rentz et al. 2011, Nassiri, Mehravaran et al. 2013, Aydin Kurna, Altun et al. 2014) The NEI VFQ-25 was developed to test the general well-being of patients with diseases that cause vision loss, i.e., vision-related QoL (Mangione, Lee et al. 1998, Mangione, Lee et al. 2001). The instrument with its 25 questions is reported to provide reliable and valid QoL scores for patients with a variety of eye diseases. (Klein, Moss et al. 2001, Deramo, Cox et al. 2003, Nordmann, Viala et al. 2004, Sugawara, Sato et al. 2011)

4.2.1.3. How to select the appropriate QoL instrument?

Once the dimensions for assessment have been identified (i.e. socio-emotional) and where the research protocol permits (pre and post treatment), in order to select the highest quality instrument the researcher must consider (1) how accurately the content (items) was developed and (2) how exhaustively the instruments were psychometrically tested. (Pesudovs, Burr et al. 2007)

The quality of a QoL instrument is determined by a large number of criteria that include steps taken in the development and identification of the initial content. (Pesudovs, Burr et al. 2007) The following important parameters should be considered when assessing the QoL instruments: (Khadka, McAlinden et al. 2013)

- **Validity;** a degree to which a QoL instrument measures the concept it is supposed to measure. (Lundström and Wendel 2006, Pesudovs, Burr et al. 2007)
- **Reliability;** the feature that any significant results obtained from a QoL instrument are repeatable, and not just a one-off phenomenon. (Khadka, McAlinden et al. 2013)

- **Responsiveness;** the capability of a QoL instrument to capture a change in participants who had modifications in their ability over a period. (Lundström and Wendel 2006, Pesudovs, Burr et al. 2007)

4.2.1.4. Appropriateness of NEI VFQ-25: Validity, reliability and responsiveness

The original NEI VFQ consisted of 51 questions (known as items in questionnaire research). (Mangione, Berry et al. 1998, Mangione, Lee et al. 1998) A shorter 26-item version (NEI VFQ-25) with 13 additional optional items placed in an appendix (NEI VFQ-39) was developed. (Mangione, Lee et al. 2001) The NEI VFQ-39 has 39 items grouped into the following 12 vision-specific subscales: general health, general vision, ocular pain, near activities, distance activities, social functioning, mental health, role difficulties, dependency, driving, color vision, and peripheral vision. The NEI VFQ-25 consists of 26 items; 25 are used to compute the overall score, grouped into the same 12 vision-specific subscales, although 8 have fewer items. (Mangione, Lee et al. 2001, Pesudovs, Gothwal et al. 2010).

As the instrument that is better positioned than others, NEI VFQ-25 and its subscales should fulfil the appropriate features. NEI VFQ-25 is supposed to measure vision-related QoL (validity), a vast construct; even though its name is suggesting that the main construct is visual functioning. Tested with Rasch analysis for the validity, it assumed testing for unidimensionality, as the main validity feature. NEI VFQ-25 overall as well as its subscales failed to satisfy Rasch analysis for validity, it is not clear what was measured, as it has characteristics of multidimensional instrument. (Pesudovs, Gothwal et al. 2010) Reliability of the NEI VFQ, i.e. the reproducibility of the results satisfied the Rasch criteria and testing. (Pesudovs, Gothwal et al. 2010) The reliability was confirmed also in the studies that used NEI VFQ in eye diseases. (Lee, Whitcup et al. 1995, Klein, Klein et al. 1998), (Musch, Farjo et al. 1997), (Parrish, Gedde et al. 1997), (Linder, Chang et al. 1999, Globe, Levin et al. 2002, Mackenzie, Chang et al. 2002) NEI VFQ showed also a good person separation reliability, but, many patients showed to have better abilities than the items in the instrument permitted. Responsiveness, failed to satisfy the required criteria. It was not sensitive enough to capture all the changes in patients; this was visible also through the items that were not good targeted to the persons.

How are the items measured: Likert-style scale

Standard scoring consists of using the Likert-style scale data. This means that each rating category (e.g., little difficulty) has the same value across all items, and the difference between each category is exactly the same. The use of a composite score and statistical analyses that assume interval-, rather than ordinal, scaled data is not a valid method for analyzing subject response data. (Massof and Rubin 2001, Trevor and Fox 2007) The most frequently used scoring method for NEI VFQ-25 is the one published with the original instrument. (Group 2003, Dougherty and Bullimore 2010) The original published scoring method involves assigning an integer value to the subject's responses, summing those values, and then generating a *composite score* between 0 and 100 that is meant to be a measure of the subject's visual ability. The published scoring methods also allow for groups of items to be scored as subscales that are intended to be used as an indicator of ability in specific areas such as near visual tasks or distance visual tasks. This published scoring method has been criticized because it does not produce interval-scaled estimates of visual ability. (Massof and Rubin 2001)

Does this scale measure what it is supposed to: Rasch analysis

The two essential features of a measurement instrument are:

- ***Unidimensionality*** (i.e., the scale should measure only a single underlying construct) and
- ***Interval-level measurement*** (the steps along the measurement continuum are the same size). (Mallinson 2007, Khadka, McAlinden et al. 2013)

When two dimensions are combined, meaningful information is lost in noise; it is more meaningful if an instrument only measures a single underlying construct (i.e., unidimensional concept). The simple algebraic summary scores obtained from first-generation instruments include noise that damages the sensitivity of the instrument to make meaningful comparisons between patients or clinical intervention outcomes. (Khadka, McAlinden et al. 2013) An instrument that provides interval-level measurement (i.e., when the steps along the measurement continuum are the same size at all points) is more useful in making meaningful comparisons and comparing between clinical parameters. (Mallinson 2007) A critical step forward for a QoL instrument is the conversion of raw scores into interval-level scoring. (Khadka, McAlinden et al. 2013)

Rasch analysis is a statistical approach to the measure of human performance, attitudes and perceptions. It is named after its inventor, the Danish mathematician Georg

Rasch and was published in 1960. (Tesio 2003) Rasch analysis was considered as a psychometric tool for use in the social sciences. In the last ten years it has become increasingly applied to medical and rehabilitation research. In order to understand the general principles of Rasch analysis, asking “what to measure” should precede asking “how to measure”. (Tesio 2003)

Several authors have advocated the use of Rasch analysis for producing **interval-scaled estimates** of visual ability from Likert scale data. (Massof and Fletcher 2001, Pesudovs 2010) Rasch analysis uses subjects’ responses to the items of an instrument to produce person measures meant to serve as an indicator of visual ability for each subject and item measures that are indicators of the difficulty of each item. (Trevor and Fox 2007) The other important indicators of instrument performance are generated including **person separation reliability**— higher values representing better ability to discriminate among subjects. Values of at least 0.8 are considered acceptable. (Pesudovs, Burr et al. 2007) The Rasch model is seen as a template that “*operationalizes the formal axioms which strengthen measurement*” (Karabatsos 2001) and against which the data from the scale may be tested.

Fitting data to the Rasch model allows several key methodological aspects associated with scale development and construct validation to be addressed. (Pallant and Tennant 2007) Rasch analysis transforms raw questionnaire data, which are composed of nominal numeric values applied to response options, into a continuous scale with interval-level measurement properties (like a ruler). (Rasch 1960, Wright and Mok 2000) This transformation is important for scoring because it reduces noise and enables valid parametric statistical analysis of the output. These attributes have led to growing recognition of the value of Rasch analysis in the development or **revalidation** of questionnaires, (Pesudovs, Burr et al. 2007) and the method is now used in ophthalmology. (Pesudovs, Caudle et al. 2008). Ad hoc attempts have been made to shorten the NEI VFQ (Ryan and MARGRAIN 2008), however Pesudovs et al provided new guidance on how to approach this question. The authors tested following key-characteristics (Pesudovs, Gothwal et al. 2010):

- the response category,
- the person separation reliability,
- subscales (same requirements for validity as the overall instrument; therefore, they must be individually tested),
- unidimensionality and
- item fit to the construct.

Their analysis of **response categories** demonstrated disordered thresholds in NEI VFQ-25 (they suggested that the missing category be removed and the two pre-existing categories be combined see **Annex 1**). (Pesudovs, Gothwal et al. 2010) The **person separation reliability** didn't contain satisfactory targeting. None of the NEI VFQ-25 **subscales** functioned satisfactorily. Additionally, NEI VFQ-25 showed **multidimensionality** (principal were visual functioning items but with mix of mental health, role difficulties and dependency social functioning, color vision). With the absence of unidimensionality, it was unclear what the **construct under measurement** was (partly visual functioning and partly another construct). Based on these results, Pesudovs et al reengineered the questionnaire. The question selection is shown at the **Figure 4-2**. From these 2 short-form versions (SFV): short-form visual functioning scale (SFVFS) and short-form socioemotional scale (SFSES) were produced. The SFVFS contained 6 items and SFSES contained 7 items, both had acceptable person separation reliability and were unidimensional, with better targeting than the long versions (**Figure 4-2**). (Pesudovs, Gothwal et al. 2010)

Item	Description	NEI VFQ-39/NEI VFQ-25 Version*					
		LFVFS ₃₉	LFSES ₃₉	LFVFS ₂₅	LFSES ₂₅	SFVFS	SFSES
1	Health	-	-	-	-	-	-
2	Eyesight	+	-	+	-	+	-
3	Worry	-	-	-	-	-	-
4	Pain or discomfort	-	-	-	-	-	-
5	Read ordinary print in newspapers	+ (near)	-	+	-	+	-
6	See well up close	+ (near)	-	+	-	+	-
7	Find something on a crowded shelf	+ (near)	-	+	-	+	-
8	Read street signs or the names of stores	+ (distance)	-	+	-	+	-
9	Going down steps, stairs, or curbs in dim light or at night	+ (distance)	-	+	-	+	-
10	Notice objects off to the side while walking	+	-	+	-	-	-
11	See how people react to things	-	+	-	+	-	-
12	Pick and match own clothes	+	-	-	-	-	-
13	Visiting with people in their homes, or at parties, or in restaurants	-	+	-	+	-	+
14	Go out to see movies, plays, or sports events	+ (distance)	-	+	-	-	-
15c	Drive during daytime in familiar places	-	-	-	-	-	-
16	Drive at night	-	-	-	-	-	-
16a	Drive in difficult conditions	-	-	-	-	-	-
17	Accomplish less	-	+ (role)	-	+	-	+
18	Limited	-	+ (role)	-	+	-	+
19	Pain around eyes	-	-	-	-	-	-
20	Stay home most of the time	-	+	-	+	-	+
21	Frustrated	-	-	-	+	-	-
22	Much less control	-	+	-	+	-	+
23	Rely too much on what other people tell	-	+	-	+	-	+
24	Need a lot of help	-	+	-	+	-	-
25	Do things that will embarrass	-	+	-	+	-	+
A1	Overall health	-	-	-	-	-	-
A2	Eyesight now	-	-	-	-	-	-
A3	Read small print in a telephone book, on a medicine bottle, or on legal forms	+ (near)	-	-	-	-	-
A4	Figure out whether bills received are accurate	+ (near)	-	-	-	-	-
A5	Doing things like shaving, styling hair, or putting on makeup	+ (near)	-	-	-	-	-
A6	Recognize people across a room	+ (distance)	-	-	-	-	-
A7	Take part in active sports or other outdoor activities	+ (distance)	-	-	-	-	-
A8	See and enjoy programs on TV	+ (distance)	-	-	-	-	-
A9	Entertain friends and family in home	-	-	-	-	-	-
A11a	Have more help	-	+ (role)	-	-	-	-
A11b	Limited	-	+ (role)	-	-	-	-
A12	Irritable	-	-	-	-	-	-
A13	Don't go out of home alone	-	+	-	-	-	-

+ = item used in version; - = item not used in version; LFSES₂₅ = long-form socioemotional scale derived from NEI VFQ-25; LFVFS₂₅ = long-form visual functioning scale derived from NEI VFQ-25; LFSES₃₉ = long-form socioemotional scale derived from NEI VFQ-39; LFVFS₃₉ = long-form visual functioning scale derived from NEI VFQ-39; NEI VFQ-25 = 25-item National Eye Institute-Visual Functioning Questionnaire; NEI VFQ-39 = 39-item National Eye Institute-Visual Functioning Questionnaire; SFSES = short-form socioemotional scale; SFVFS = short-form visual functioning scale
*Items parentheses indicate those from valid subscales (near activities, distance activities, role difficulties) on the LFVFS₃₉ and LFSES₃₉.

Figure 4-2. Adapted from Pesudovs et al (Pesudovs, Gothwal et al. 2010), Summary of items included in each revised version of the NEI-VFQ. Red circles denoting the items used in the shorten reengineered NEI-VFEQ version

4.2.1.5. Implementation of Rasch analysis

Given the result of the Rasch analysis published by Pesudovs et al, we were convinced that the most appropriate instrument for our study population (RD patients) was the new shortened version of NEI-VFQ, with only 13 items and 4 categories and two subscales (NEI-VFQ-13). (Pesudovs, Gothwal et al. 2010, Mangione, Lee et al. 2001)

To date there are only two reports that compare the QoL of macula-ON versus macula-OFF patients. In one study, despite a large significant difference in final VA being reported between patients' groups did not detect a significant difference in the post-operative QoL. Clinically we observe that patients with macula-OFF detachment are less satisfied than macula-ON patients with surgical outcomes, therefore not seeing the reflection of this difference in patients' reported QoL is surprising. (Okamoto, Okamoto et al. 2008) However, perhaps this study was underpowered or given the outcomes of Pesudovs et al, perhaps it was due to the inappropriateness of the instrument used for this study. In a second study QoL was compared preoperatively and after long-term follow up of up to 3 years, again no statistical significance was observed. However, here a mixture of macula-ON and macula-OFF patients were included, and several different surgery types were used. In this case the QoL composite score contains more variability because of mixed variables. Combined these aspects undermine the ability of the instrument to detect changes.

Given these observations and results, the aim of our study was to evaluate the use of the NEI VFQ-13 in RD patients following PPV with gas tamponade, and to compare the outcomes of Macula-ON and Macula OFF patients, pre- and post-operatively.

4.2.2. QoL study design

4.2.2.1. Patients

A total of 204 patients were recruited and 194 patients were included in the study. All patients underwent a baseline/preoperative standard clinical exam (please refer to **Table 3-1** and to the **paragraph 3.1**). They were asked to answer the shorten version of the validated NEI VFQ-25 following the protocol of Nordmann in French language, administrator administered preoperatively, as well as at 1, 3 and 6 months post-operatively (**Table 3-1**). (Nordmann, Viala et al. 2004) The study team explained the questionnaire to the patients and supplied assistance when required. The participants indicated the response that best fitted.

NEI VFQ-13 full datasets were available for 47 patients who underwent 23G pars plana vitrectomy with gas tamponade (SF6) and attended m1, m3 and m6 appointments. Of these 21 presented with macula-OFF RD and 26 with macula-ON RD.

4.2.2.2. NEI VFQ-13

To analyze the instrument NEI VFQ-13, we respected the rules of Rasch analysis, as Pesudovs et al demonstrated in their study (**Figure 4-2**). (Pesudovs, Gothwal et al. 2010) As it is composed of 13 questions separated into two subscales: visual functioning scale and socioemotional scale, we report both, the composite score and the subscales scores: subscale 1 = SFVFS score, of 6 items and subscale 2 = SFSES score of 7 items. Every item contained 4 categories (**Annex 1**). (Mangione, Lee et al. 2001, Pesudovs, Gothwal et al. 2010)

4.2.2.3. Statistical Analyses

The NEI VFQ-13 questionnaire data were summarized according to the instructions in the test manual, resulting in a subscales sum score and the total score with the possible range of values equals 0 to 100. The answers to each of the 13 questions were converted to a 100-point scale, in which 100 represented the best possible QoL score and 0 the worst. The composite and subscale scores were calculated as the mean score of the respective items. (Sugawara, Hagiwara et al. 2010, Sugawara, Sato et al. 2011) Composite score and subscales' scores were also converted into Rasch scores using the available kit for transforming raw data into Rasch score, published by Pesudovs et al. (Pesudovs, Gothwal et al. 2010)

Patients were asked to complete questionnaire in 4 time-points (pre-operatively, and after 1, 3, 6 months after surgery). In this study we report QoL scores on 3 time-points: preoperatively, 1 month after surgery and the best QoL score between 3 and 6 months after

surgery. The reason to report data on such a way is that some of patients even though they had a successfully operated RD, they developed cataract in the period 3-6 months after surgery. In order to avoid bias linked to cataract development, we decided to combine these two time-points and to report better QoL score between the two, as well as BCVA.

For descriptive purposes, mean and standard deviation were calculated for the QoL scores, for age, and visual acuity. The mean QoL subscales' and composite scores were compared between macula-ON and macula-OFF groups, as well as over time, using Mann-Whitney test and Wilcoxon paired test. Linear regression analysis was used to assess the correlation between BCVA and QoL scores. A p-value of less than 0.05 was considered to be statistically significant. Statistics were calculated using R version 3.1.3.

4.2.3. QoL results

4.2.3.1. Baseline characteristics

47 patients (21 with macula-OFF RD and 26 with macula-ON RD) completed the QoL assessment using the NEI VFQ-13 instrument at all time-points. These patients all had the same type of surgery and tamponade (pars plana vitrectomy with SF6 gas tamponade). There were 33 men and 14 women; mean age of patients at baseline was 62.45 ± 8.96 years (**Table 4-2**). Data from patients with RD in 31 right and 16 left eyes were analyzed (**Table 4-2**). There were 27 phakic eyes and 20 eyes had previously undergone cataract surgery (**Table 4-2**). The mean axial length was 24.90 ± 1.71 mm (**Table 4-2**). The median (interquartile range) logMAR visual acuity at baseline was 0.1 [0.2-0.0] in the macula-ON group and 2 [2.0-0.8] in the macula-OFF group. At month one postoperatively, BCVA had improved to 0.1 [0.1-0.0] in the macula-ON group and to 0.3 [0.4-0.1] logMAR in the macula-OFF group. Final (at 3-6 months) BCVA was 0 [0.1-0.0] logMAR in the macula-ON group and 0.1 [0.3-0.1] logMAR in the macula-OFF group (**Table 4-2**).

Table 4-2. Baseline characteristics and best corrected visual acuity pre-operatively, 1 month (M1) and 3-6 months (M3-M6) after surgery in patients with macula-ON (ON) and macula-OFF (OFF) retinal detachment						
		Macula-ON		Macula-OFF		p-value (ON vs OFF)
Baseline characteristics	Age	62.85 ± 7.97 years		61.96 ± 10.24 years		p>0.05
	Gender	10 women and 16 men		4 women and 17 men		
	Operated eye	16 right eyes and 10 left eyes		15 right eyes and 6 left eyes		
	Lens status	17 phakic and 9 pseudophakic		10 phakic and 11 pseudophakic		
	Axial length	24.76 ± 1.53 mm		25.06 ± 1.94 mm		p>0.05
Time point		Mean	p-value time-point vs pre-op	Mean	p-value time-point vs pre-op	p-value (ON vs OFF)
Visual acuity [logMAR]	Pre-op	0.1 [0.2-0.0]		2 [2.0-0.8]		p=0.000
	Post-op M1	0.1 [0.1-0.0]	p=0.45	0.3 [0.4-0.1]	p=0.000	p=0.009
	Post-op M3-M6	0 [0.1-0.0]	p=0.18	0.1 [0.3-0.1]	p=0.000	p=0.051
	M1 vs M3 – M6		p=0.03		p=0.001	

4.2.3.2. NEI-VFQ-13 scores

In both groups, the QoL scores changed over time. In the macula-OFF group, the composite score (CS) preoperatively was 68% ± 26%, while the subscale 1 (SFVFS) score was 67% ± 27%, and subscale 2 (SFSES) score was 69% ± 28%. At month 1 after surgery QoL scores improved (CS 75% ± 17%, SFVFS 74% ± 16%, SFSES 76% ± 20%); and again at 3-6 months after surgery (CS 79% ± 17%, SFVFS 76% ± 20%, SFSES 81% ± 20%) (**Table 4-3**). In the macula-ON group, preoperative CS was 86% ± 17%, while SFVFS score was 83% ± 15% and SFSES was 89% ± 19%. One month after surgery QoL scores decreased (CS 79% ± 21%, SFVFS 78% ± 20%, SFSES 79% ± 22%) but recovered at 3-6 months postoperatively (CS 87% ± 19%, SFVFS 82% ± 20%, SFSES 90% ± 21%) (**Table 4-3**).

We observed a statistically significant difference preoperatively between ON and OFF group in QoL scores (p<0.03), with SFSES being the most sensitive. One month postoperatively no difference in QoL was noted between ON and OFF groups (**Table 4-3, Table 4-4**). At 3-6 months postoperatively QoL was again significantly different between groups, in both CS and SFSES (p=0.03, p=0.002), but not in the SFVFS subscale (p=0.10) (**Table 4-3, Table 4-4**).

Table 4-3. Quality of life scores pre-operatively, 1 month (M1) and 3-6 months (M3-M6) after surgery in patients with macula-ON (ON) and macula-OFF (OFF) retinal detachment

			Macula ON	Macula OFF	
	Time point		Mean score	Mean score	p-value (ON vs OFF)
Composite Score	Pre-op		86% ± 17%	68% ± 26%	p=0.007
	Post-op M1		79% ± 21%	75% ± 17%	p=0.15
	Post-op M3 – M6		87% ± 19%	79% ± 17%	p=0.03
Subscale 1 (SFVFS)	Pre-op	%	83% ± 15%	67% ± 27%	p=0.03
		R	-3.7 ± 1.7	-2.1 ± 3.1	
	Post-op M1	%	78% ± 20%	74% ± 16%	p=0.10
		R	-3.4 ± 2.3	-3.3 ± 1.7	
	Post-op M3-M6	%	82% ± 20%	77% ± 17%	p=0.10
		R	-3.9 ± 2.2	-3.5 ± 1.7	
Subscale 2 (SFSES)	Pre-op	%	89% ± 19%	69% ± 28%	p=0.002
		R	1.9 ± 1.2	0.8 ± 1.6	
	Post-op M1	%	79% ± 22%	76% ± 20%	p=0.24
		R	1.2 ± 1.3	1.0 ± 1.4	
	Post-op M3-M6	%	90% ± 21%	81% ± 20%	p=0.006
		R	2.0 ± 1.1	1.4 ± 1.2	

% - the QoL score is expressed in %, where 0 represents the worst and 100 the best value, R – QoL score transformed to Rasch scale, SFVFS – short form visual functioning scale, SFSES – short form socioemotional scale

In the macula-OFF group there was no statistically significant difference in QoL scores during follow-up (**Table 4-4**). In the macula-ON group, a significant reduction in QoL on the SFSES was observed 1 month postoperatively (p=0.03), however this then reversed between month 1 and 3-6 months postoperatively, with a significant improvement in QoL (CS p=0.03 and SFSES p=0.006). This resulted in little overall change in QoL in Macula-ON patients between baseline and 3-6months postoperatively (p>0.25) (**Table 4-4**).

Table 4-4. Comparison of quality of life scores reported by patients with macula-ON and macula-OFF retinal detachment, between time points: pre-operatively, 1 month (M1) and 3-6 months (M3-M6) after surgery (Wilcoxon-paired test).

	Time point	Macula ON	Macula OFF
Composite score	Pre-op vs M1	p=0.06	p=0.27
	Pre-op vs M3-M6	p=0.37	p=0.11
	M1 vs M3 – M6	<i>p=0.03*</i>	p=0.18
SFVFS	Pre-op vs M1	p=0.18 (0.30)	p=0.31 (0.30)
	Pre-op vs M3-M6	p=0.40 (0.32)	p=0.13 (0.13)
	M1 vs M3 – M6	p=0.12 (0.12)	p=0.27 (0.33)
SFSES	Pre-op vs M1	<i>p=0.03* (0.02)</i>	p=0.27 (0.40)
	Pre-op vs M3-M6	p=0.26 (0.30)	p=0.10 (0.11)
	M1 vs M3 – M6	<i>p=0.006** (0.006)</i>	p=0.19 (0.16)

SFVFS – short form visual functioning scale, SFSES – short form socioemotional scale, *p<0.05, **p<0.01

4.2.3.3. Relationship between QoL and BCVA

A large improvement in preoperative BCVA was noted in the macula-OFF group postoperatively, at month 1 ($p<0.001$) and at 3-6 months ($p<0.001$). This coincided with an improvement in QoL scores (CS and SFSES), however these did not reach significance. In the macula-ON group, 1 month post-operatively despite having no change in BCVA, there was a significant reduction observed in the SFSES score. Subsequently there was a significant improvement in BCVA between month 1 and month 3-6 ($p=0.03$), this coincided with a significant increase in the SFSES score ($p=0.006$). Preoperatively the BCVA and QoL scores are poorly correlated ($R^2<0.20$) (Table 4-5, Figure 4-3). Postoperatively the QoL reported by patients with macula OFF detachment was positively correlated with BCVA in the composite and subscale scores, and this correlation was strongest at 3-6months post-operatively in the QoL SFSES score ($p<0.001$, $R^2=0.58$) (Table 4-5, Figure 4-3). QoL measures in patients with macula ON RD did not have a positive correlation with BCVA, with the single exception of SFVFS subscale at month 3-6 ($p<0.001$, $R^2=0.41$) (Table 4-5, Figure 4-3).

Table 4-5. Linear regression analysis to examine the relationship between quality of life scores and best corrected visual acuity at each time-point during follow-up. Pearson correlation coefficient and corresponding p-value.

	Time point	Macula ON	Macula OFF
Composite score	Pre-op	$R^2 = 0.08; p=0.15$	$R^2 = 0.12; p=0.13$
	M1	$R^2 = 0.06; p=0.22$	$R^2 = 0.25; p=0.02$
	M3 – M6	$R^2 = 0.12; p=0.08$	$R^2 = 0.55; p<0.001$
SFVFS	Pre-op	$R^2 = 0.07; p=0.19$	$R^2 = 0.03; p=0.44$
	M1	$R^2 = 0.02; p=0.44$	$R^2 = 0.16; p=0.07$
	M3 – M6	$R^2 = 0.41; p<0.001$	$R^2 = 0.39; p=0.003$
SFSES	Pre-op	$R^2 = 0.08; p=0.15$	$R^2 = 0.19; p=0.05$
	M1	$R^2 = 0.10; p=0.12$	$R^2 = 0.25; p=0.02$
	M3 – M6	$R^2 = 0.09; p=0.14$	$R^2 = 0.58; p<0.001$

SFVFS – short form visual functioning scale, SFSES – short form socioemotional scale, M1 – month 1 follow up, M3-M6 – three to six months follow up, R^2 – Pearson correlation coefficient value

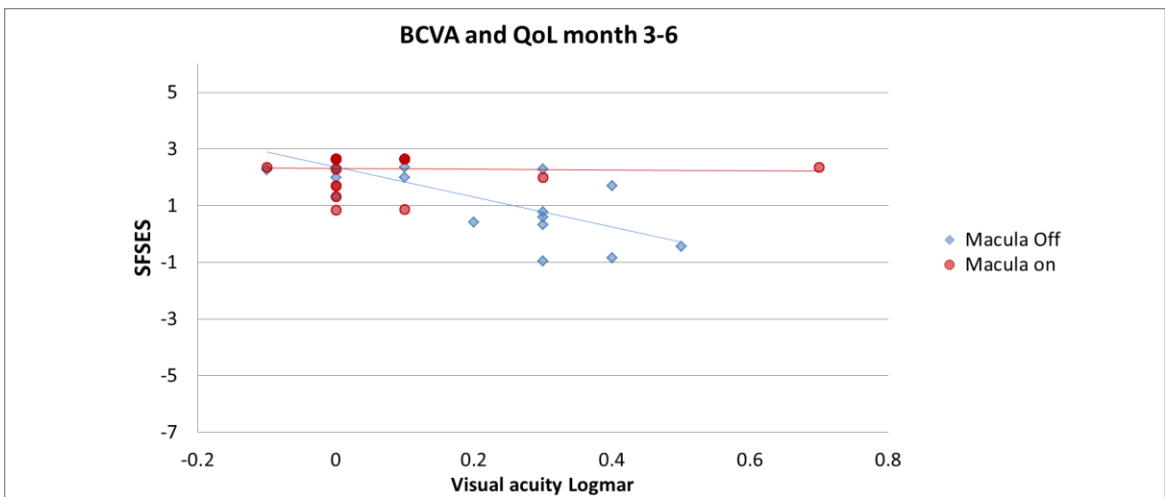
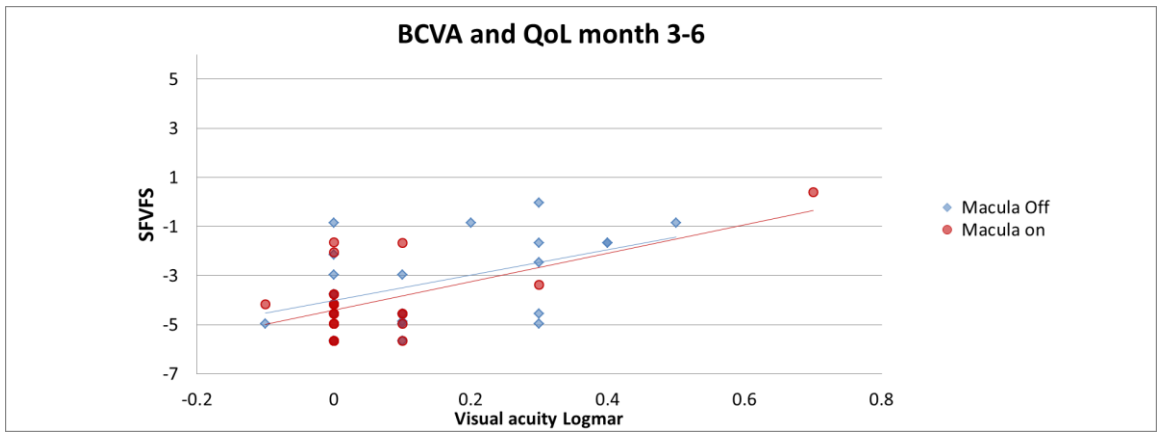
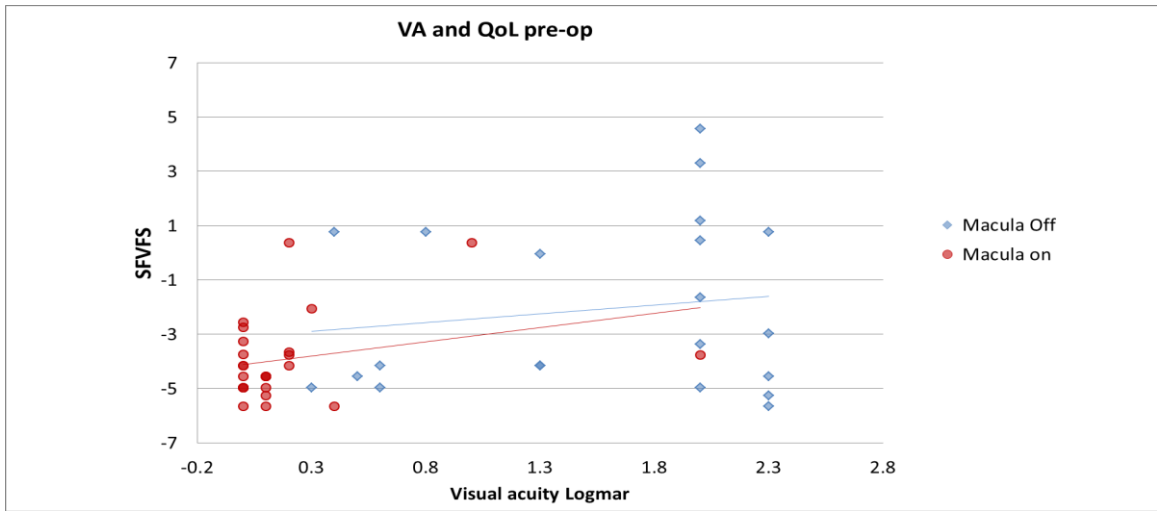


Figure 4-3. The relationship between quality of life scores and best corrected visual acuity pre-operatively (CS) and at month 3-6 (SFVFS score)

4.2.4. QoL discussion

This is the first article to report assessment using the SFVFS and SFSES subscales from the NEI-VFQ instrument. (Pesudovs et al. 2010) In this study, we observed a statistically significant reduction in QoL of patients with Macula OFF RD as compared to Macula ON RD, particularly in the SFSES subscale. Furthermore, QoL in patients with macula ON RD was significantly negatively affected by surgery but this effect was of short duration, returning to preoperative values by month 3-6. Postoperative QoL and BCVA were correlated, in macula OFF patients this relationship was stronger in the socio-emotional subscale, and macula ON patients we observed that this relationship existed only for the visual functioning subscale of the instrument at month 3-6.

Previous studies identified a relationship between postoperative BCVA and postoperative QOL as measured by the NEI VFQ-25 in patients operated on for various vitreoretinal disorders, including RD. (Mangione, Berry et al. 1998, Mangione, Lee et al. 1998, Mangione, Lee et al. 2001, Okamoto, Okamoto et al. 2008, Okamoto, Okamoto et al. 2010, Zou, Zhang et al. 2011) Zou and colleagues reported that postoperative QoL was reduced for patients presenting with macula-OFF RD as compared to macula-ON RD. (Zou, Zhang et al. 2011) These results are corresponding well with our results. In Okamoto's study, postoperative BCVA differed significantly between macula-ON and macula-OFF RD, while scores on the NEI VFQ-25 were similar in both groups of patients. (Okamoto, Okamoto et al. 2008) This is the first study to use the shorten version of the NEI VFQ-25 instrument, with items selected based statistical evidence from Rasch analysis rather than ad hoc, and with Rasch scores used for the response categories that are aimed to ensure equal interval levels measurement. (Pesudovs et al. 2010) We used this instrument to assess QoL of patients with macula ON and macula OFF RD at several time-points during follow-up. We included only data from a homogenous group in terms of surgical procedure in order to minimize noise. Our results showed that the composite score (CS) of NEI VFQ-25 was statistically significantly different between macula-ON and macula-OFF groups preoperatively and post-operatively at month 3-6. It is perhaps due to this more considerate approach that we observed a statistically significant difference in QoL between patients with Macula-ON and Macula-OFF RD in a similar number of patients to that of Okamoto (Okamoto, Okamoto et al. 2008).

Smretschmig et al assessed QoL in patients with RD at 6-months postoperatively, as compared to healthy controls. (Smretschmig, Falkner-Radler et al. 2016) In the multiple regression model, BCVA in operated and fellow eye, age and gender were identified as independent risk factors for reduced QoL, whereas macula detachment was not. Okamoto et

al, also used the composite score to examine the pre-operative BCVA, number of retinal breaks and clock hours as risk factors for poor QoL post-operatively. Patients had either macula-ON or macula-OFF RD yet macula involvement was not a significant risk factor. This may be due to the choice of the composite score as the parameter include in the analysis, whereas we have observed that the socioemotional subscale was more sensitive to changes experienced by patients with macula OFF. Any regression analysis that attempts to correlate post-operative QoL with either post-operative measures (such as LogMar BCVA) or preoperative values (days with symptoms) should take this into consideration. By contrast Zou et al used a visual function questionnaire, and observed that at 3 years better QoL score was associated with better post-operative BCVA and macula ON type RD.

Reduced BCVA has been identified as a significant risk factor for reduced QoL, as such many ophthalmologists use BCVA as a parameter to determine success of RD surgery. However, BCVA alone is a poor measure to summarize visual function. (Klein, Moss et al. 2001, Nassiri, Mehravaran et al. 2013, Renieri, Pitz et al. 2013, van de Put, Hoeksema et al. 2014) In the literature a QoL CS score following PPV for RD have been reported of between 76% and 80% at 3-6 months after surgery in macula OFF patients (87% macula ON patients in our study at 3-6 months) increasing to 89% at one year post-operatively in macula OFF eyes. (Smretschning, Falkner-Radler et al. 2016) In other retinal diseases treated with vitreous surgery comparable scores have been reported following macular hole surgery (mean CS 79-82%) and epiretinal membrane surgery (79-83%) but much lower scores were recorded in age-related macular degeneration depending on disease severity and the proportion of days that restricted activity was experienced (44-80%).(Van de Put et al 2014, Muzyka-Woźniak et al 2011, Yuzawa et al 2011).

Smretschning et al. observed significant differences between RD patients and normal controls in five subscales: general vision, mental health, social functioning, driving, and color vision. (Smretschning, Falkner-Radler et al. 2016) In contrast to their findings concerning the subscales, Okamoto et al reported lower results in near activities, distance activities, peripheral vision, dependency, and mental health in their studies on RD patients. (Okamoto, Okamoto et al. 2008, Okamoto, Okamoto et al. 2010). This lack of repeatability between the outcomes of these two studies may be a reflection of the differences between the study groups. However these differences may also be a reflection of the previous lack of validity of these subscales with problems with multidimensionality, person separation and misfitting items. (Pesudovs et al. 2010)

There are several limitations of this study, the small sample size and the short term follow-up limits the observations that we are able to make. For example, Smretschnig et al found that QoL improved between 3 months and 12 months postoperatively. (Smretschnig, Falkner-Radler et al. 2016) and Van de Put has reported a very high CS score in patients with macula OFF RD at 12 months postoperatively (van de Put, Hoeksema et al. 2014) Interestingly, mean CS was 88.9 in their study, which is considerably higher than the mean CS of 76.3 in macula-OFF RD patients in the study of Smretschnig et al. or of the 79% observed in our study patients (Van de Put, Hooymans et al. 2013, Smretschnig, Falkner-Radler et al. 2016) This finding may indicate a possible gain in QoL between 6 and 12 months postoperatively.(Van de Put, Hooymans et al. 2013). In addition the targeting of the NEI-VFQ questionnaire meaning that there is poor patient separation for those with good visual function/ability, therefore following the patients' long term and detecting any changes becomes more difficult as visual outcomes improve.

4.2.5. QoL conclusion

The QoL assessment is of increasing importance, particularly in the 4.0 model of the health-care system. Using the scale and models that facilitate the acquisition of the best quality data and produce the most statistically robust results will be one of the greatest challenges in the coming years. In the field of QoL instruments, Rasch analysis offers a simple and elegant approach to identify and redress several of limitations the existing instruments. In this study we have adopted the remediated NEI-VFQ-25 instrument. Our results have shown that there is a statistical significance in QoL CS and more importantly the socioemotional and visual functioning subscale' between patients with macula-ON and macula-OFF RD. This difference is pronounced pre-operatively, as well as in the postoperative period. In the macula-ON patients there is a notable drop of patients' satisfaction one month after surgery while in the macula-OFF patients there is a positive progression in their satisfaction in the whole postoperative period. The biggest changes in QoL are present in the socioemotional subscale. This is important because even though there is a good anatomical success after RD surgery, and good postoperative BCVA, (representative of part of the visual function), patients still report impediments post-operatively, which can have important consequences in terms of mobility and independence.

4.3. CLINICAL IMAGING IN PATIENTS WITH RETINAL DETACHMENT

4.3.1. Introduction

Visual recovery after RD can be compromised (Ross and Kozy 1998, Williamson, Shunmugam et al. 2013) by many factors depending on the RD extension, height and duration as well as on the degree of retinal edema in the detached macula shown on optical coherence tomography (OCT). (Wolfensberger and Gonvers 2002) Primary anatomical surgical success is achieved in 81-92% of uncomplicated cases (Tani, Robertson et al. 1981, Grizzard, Hilton et al. 1994, Pastor, Fernandez et al. 2008, Williamson, Shunmugam et al. 2013) but despite retinal reattachment and a good anatomical outcome, there is no guarantee of complete visual recovery. (Grizzard, Hilton et al. 1994, Ross and Kozy 1998, Salicone, Smiddy et al. 2006) Post-operative prognostic factors for the degree of visual recovery are the OCT appearance (Wolfensberger 2004) as well as the integrity of the external limiting membrane (ELM). (Park, Choi et al. 2017)

The velocity of RD progression has been associated with the location of retinal tears and the location of the RD. (Lincoff and Gieser 1971, Ho, Fitt et al. 2006) The risk of macular detachment is, for example, linked to the extension of the RD, particularly when extension reaches the vascular arcade in the presence of a superior temporal retinal break. (Ho, Fitt et al. 2006, Williamson, Shunmugam et al. 2013, Kontos and Williamson 2016) Those patients with RD within the macula but not involving the fovea are theoretically at highest risk of complete macular detachment. Clinically it is difficult to identify these cases and pre-operative OCT imaging may provide a more definitive characterization of these patients who are in need of urgent treatment. The aim of this study was thus to investigate and report clinical and spectral domain optical coherence tomography (SD-OCT) characteristics (B-scan and EnFace OCT) of a distinct subgroup of RD patients, with hemi macular-detachment (HMD) and the associated post-operative anatomical and visual evolution.

By delivering nutrients and removing waste products, the choroid circulatory system plays an essential role in the pathogenesis of multiple diseases of the posterior segment of the eye. (Kur, Newman et al. 2012) Enhanced depth imaging in optical coherence tomography (EDI-OCT) provides cross-sectional images of the retina, which extend to the posterior border of the choroid. From these images, the choroidal thickness (CT) can be measured reliably. (Mrejen and Spaide 2013) The CT has been correlated with the axial length of the eye and

patient age. (Margolis, Coyne et al. 2002, Ruiz-Medrano, Flores-Moreno et al. 2014) Moreover, based on OCT images, associations have been established between the CT and chorio-retinal diseases, such as central serous retinopathy and age-related maculopathy. (Imamura, Fujiwara et al. 2009, Koizumi, Yamagishi et al. 2011) During retinal detachment (RD), many metabolic processes are disrupted, which may affect choroid circulation. (Sayman Muslubas, Karacorlu et al. 2016, Sayman Muslubas, Hocaoglu et al. 2017) Modifications in choroidal circulation have been shown to modify the CT in the fovea. (Nickla and Wallman 2010) Preoperative observations in patients with RD have shown modifications in the CT. (Kimura, Nishimura et al. 2012, Sayman Muslubas, Karacorlu et al. 2016) Postoperatively, after both PPV and scleral buckling treatments, changes in the sub-foveal CT have been observed, which have been attributed to surgical inflammation and/or RD. (Kimura, Nishimura et al. 2012, Miura, Arimoto et al. 2012, Akkoyun and Yilmaz 2014)

Previous studies have indicated that disruptions in retinal metabolism, due to RD and/or subsequent surgical interventions, could induce transient choroidal thickening. However, this process has not been well characterized. The present study aimed to investigate morphologic changes in CT by measuring the thickness pre- and post-operatively over a much more extended area (51 loci across the central 5 mm of the retina) than previously studied. Additionally, this report was the first to compare the effect of RD on CT between three disease groups; eyes with peripheral macula-ON RD; eyes with paracentral macula-ON RD, and eyes with macula-OFF RD.

4.3.1.1. Optical coherence tomography (OCT)

Optical coherence tomography (OCT) is a noninvasive cross-sectional imaging of the tissue's inner structures, by measuring their optical reflections. (Huang, Swanson et al. 1991) In ophthalmology, OCT is a scan of retinal layers and, sometimes, it includes also choroid and anterior segment. The technology used in OCT is a low-coherence interferometry. On this way, using the optical scattering from the microstructures of the internal tissue, a two-dimensional image is formed. The image obtained is analogous to ultrasonic pulse-echo imaging. The lateral and spatial resolution of the OCT is about few micrometers; reflected signals as small as $\sim 10\mu\text{m}$ can be detected.

The first OCT technology to obtain retinal image was time-domain OCT (TD-OCT). Over time, OCT hardware and software have been improving; especially in better axial length resolution (from 10 μm up to 2 μm) and faster scanning speed (backscattered depth information at a given location can be collected without the movement of a reference mirror).

(Drexler, Morgner et al. 1999, de Boer, Cense et al. 2003, Wojtkowski, Srinivasan et al. 2005, Zhang, Rao et al. 2005)

To obtain frequency information, the broad-band width light source is needed as well as charge-coupled device (CCD) camera, and a spectrometer. (de Boer, Cense et al. 2003, Wojtkowski, Srinivasan et al. 2005) This technology is used in spectral-domain OCT (SD-OCT). The other possibility to obtain frequency information is by sweeping a narrow-bandwidth source through a broad range of frequencies with a photodetector, which is used in swept-source OCT (SS-OCT). (Zhang, Rao et al. 2005) In both OCT-technologies, A-scans (representing the intensity profiles) are acquired using a Fourier-transform of the detected frequencies on a fast way. The OCT technology using the frequency domains has improved the scanning speed and has higher detection sensitivity (higher signal-to-noise ratio). (Choma, Sarunic et al. 2003, Leitgeb, Hitzenberger et al. 2003) Different OCT detection techniques are listed in **Table 4-6**. Broadband volumetric retinal imaging with SD-OCT at speeds of up to 312,500 A-scans/s and SS-OCT at 249,000 A-scans/s has been demonstrated. (Gabriele, Wollstein et al. 2011) Nowadays, most systems in clinical practice function at an acquisition rate of around 27,000 A-scans/s and an axial resolution of 5 to 6 μm . (Gabriele, Wollstein et al. 2011)

Table 4-6. Comparison of TD-, SD- and SS-OCT devices, adapted from (Gabriele, Wollstein et al. 2011)

	Light source	Primary Advantages	Primary Disadvantages
TD-OCT	Broadband width	Intensity information acquired in time domain; no complex conjugate image	Moving reference mirror required limiting acquisition rate
SD-OCT	Broadband width	No moving reference mirror required; higher sensitivity than TD-OCT; high scanning speed and axial resolution have been attained	Noticeable signal drop-off with depth
SS-OCT	Narrow band, swept through broad image	No moving reference mirror required; Higher sensitivity than TD-OCT very high scanning speeds can be attained; minimal signal drop-off with depth	Most ophthalmic systems operating at longer wave lengths ($\lambda=1-1.3\mu\text{m}$), with lower axial resolution

Tissue visualization

Histologically, retina is composed of 10 different layers (**Figure 1-2**). (Bowling 2015, Forrester, Dick et al. 2015) The recent exploitation of the birefringent properties of the retina with OCT device, has allowed *in-vivo* high resolution imaging of the retinal layers (**Figure 4-4**).

Following the proper segmentation of these layers, the integrity of the retinal structure can be examined. Modifications to the retinal structure have been shown to be a predictive factor for visual recovery in patients after successful surgery. (Schocket, Witkin et al. 2006, Wakabayashi, Oshima et al. 2009, Murakami, Notomi et al. 2013) OCT images can also be used to quantify and monitor the amount, configuration and localization of SRF. (Wolfensberger and Gonvers 2002)

Despite a notable development of OCT devices, the interpretation and understanding of visualized retinal layers persisted to be based on histological findings for a long period of time. In 2014, there was the International Nomenclature for Optical Coherence Tomography Panel, where a different aspect for analysis was included; the anatomical findings were correlated to the new OCT findings, and with the disease pathophysiology, especially with vitreoretinal diseases and imaging. The evidences were reviewed and agreed on the anatomic correlations of the zones and layers seen in OCT scans (**Figure 4-4, Table 4-7**). (Staurenghi, Sadda et al. 2014)

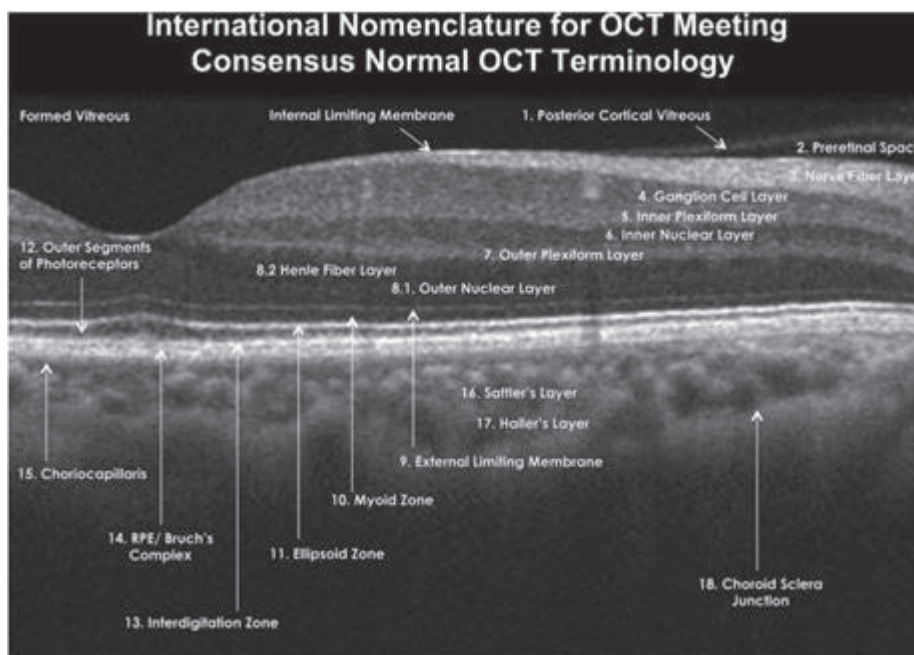


Figure 4-4. OCT image of retinal layers. Nomenclature for normal anatomic landmarks seen on SD-OCT images proposed and adopted by the International Nomenclature for Optical Coherence Tomography Panel. Healthy retina imaged using Heidelberg Spectralis. RPE $\frac{1}{4}$ retinal pigment epithelium. (Staurenghi, Sadda et al. 2014)

Table 4-7. List of OCT layers as agreed on by the International Nomenclature for OCT panel (Staurenghi, Sadda et al. 2014)

Layer No.	OCT description	Consensus Nomenclature
1	Hyperreflective	Posterior cortical vitreous
2	Hyporeflective	Pre-retinal space
3	Hyperreflective	Nerve fiber layer
4	Hyporeflective	Ganglion cell layer
5	Hyperreflective	Inner plexiform layer
6	Hyporeflective	Inner nuclear layer
7	Hyperreflective	Outer plexiform layer
8	Hyporeflective band	Inner half: Henle's nerve fiber layer; outer half: outer nuclear layer
9	Hyperreflective	External limiting membrane
10	Hyporeflective	Myoid zone of the photoreceptors
11	Hyperreflective	Ellipsoid zone of the photoreceptors
12	Hyporeflective	Outer segments of the photoreceptors
13	Hyperreflective	Cone interdigitation with RPE
14	Hyperreflective band	RPE/Bruch's membrane complex. On occasion this can be separated into more than 1 band
15	Thin layer of moderate reflectivity in inner choroid	Choriocapillaris
16	Thick layer of round or oval-shaped hyperreflective profiles with Hyporeflective cores in mid-choroid	Sattler's layer
17	Thick layer of oval-shaped hyperreflective profiles with hyporeflective cores in outer choroid	Haller's layer
18	Zone at the outer choroid with a marked change in texture in which large circular or ovoid profiles abut a homogenous region of variable reflectivity	Choroidal-scleral juncture

4.3.1.2. “EnFace” Optical Coherence Tomography

EnFace OCT represents a technology to obtain and visualize frontal scans adapted to the concavity of posterior pole of the eye. The acquired frontal scans are parallel to ideal RPE, at a constant depth in the retina or choroid; thus it is possible to study each retinal and choroidal layer separately. (Drexler and Fujimoto 2008) This lateral information about retinal details is not available on clinical exam or with normal OCT scans or photos.

In order to gather 3D information about the retina, any imaging system contains three scanning means: one to scan the object in depth and two others to scan the object transversally. (Podoleanu and Rosen 2008) One-dimensional (1D) and two-dimensional (2D) scans are known. One-dimensional scans are labeled as A and T scans, while 2D scans are labeled as B and C scans (**Figure 4-5**):

- **A-scan** is a reflectivity profile in depth; it is used clinically to assess the eye length.
- **T-scan** is the reflectivity profile in transverse, i.e. obtained by scanning the beam transversally across the target.
- **B-scan** is a cross section image, a (lateral X depth) map. This type of image could be obtained by grouping T-scans together from different depth values or A-scans together for different lateral positions, both in use in the OCT practice.
- **C-scan** represents a raster image, with the same orientation as a TV image or image provided by microscopy, a (lateral x lateral) scanned map. C scans are made from many T scans along different coordinates (X , Y , ρ or θ coordinates), repeated for different values of the other transverse coordinate (Y , X , θ or ρ respectively in the transverse plane, mostly along X-axis). To gather 3D image, several transversal slices are collected at different depths. (Drexler and Fujimoto 2008, Podoleanu and Rosen 2008, Lumbroso, Huang et al. 2013)

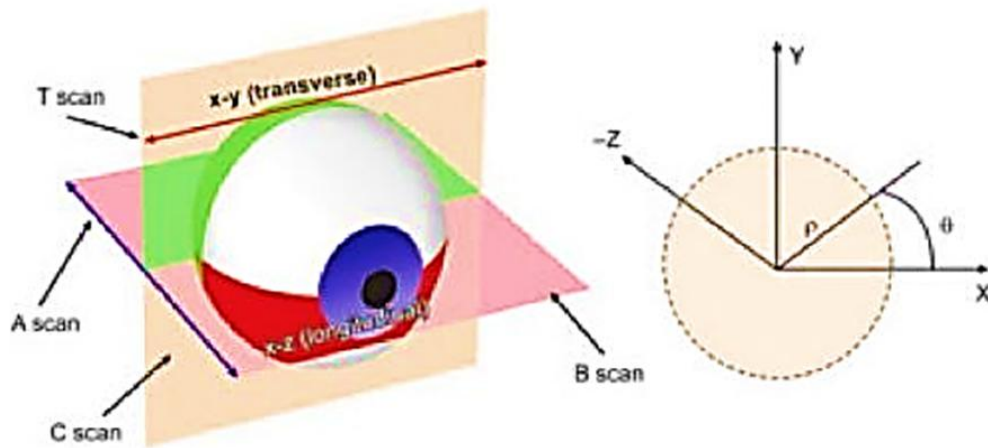


Figure 4-5. Relative orientation of the axial scan (A scan), transverse scan (T scan), longitudinal slice (B scan) and EnFace or transverse slice (C scan). Adapted from (Lumbroso, Huang et al. 2013)

The 3D data set is usually shown in a series of 2D cross-sectional images in any orientation desired. The most common cross – sectional images are:

- B scan images (B scans in X-Z plane and in Y-Z plane) where the cross-sections are about to be perpendicular to the retinal surface (**Figure 4-6**) and
- EnFace images (EnFace image in X-Y plane, **Figure 4-6**), in which the cross-sections are approximately parallel to the retinal surface. (Drexler and Fujimoto 2008, Podoleanu and Rosen 2008, Lumbroso, Huang et al. 2013)

EnFace scan, instead of making a section, can be produced following a natural surface contour. The thickness of EnFace scan is usually uniform. The particularity of EnFace images is that they are reformed to the cup-shaped retina and this is the improvement on plane scans for clinical and research purposes. With EnFace OCT images, it is possible to analyze and assess the retina and choroid, whose shape and curvature is corrected and parallel to the following RPE, obtained by the frontal scan. Frontal scans generated to follow a retinal surface contour or adapted to RPE shape are placed at constant depth in the retina or choroid and parallel to RPE. (Lumbroso, Huang et al. 2013) The 3D cube allows retinal segmentation and delineating the individual retinal layers. EnFace scans help diagnose retinal and choroidal diseases. (Drexler and Fujimoto 2008, Lumbroso, Huang et al. 2013)

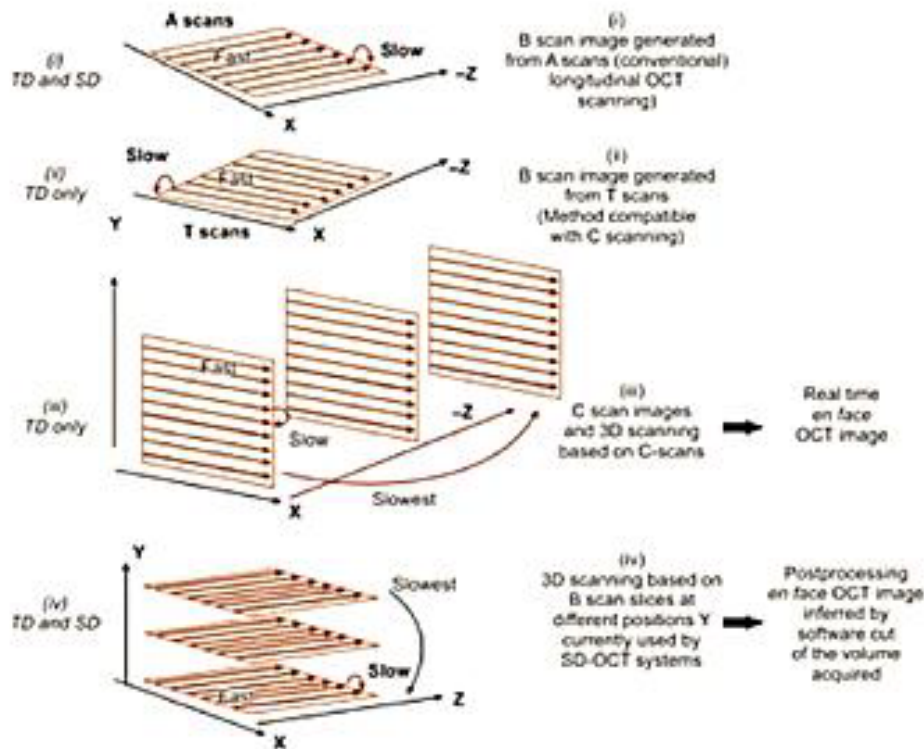


Figure 4-6. Different modes of operation of the three scanners in a 3D imaging system and the two modalities of creating EnFace image. Adapted from (Lumbroso, Huang et al. 2013)

The new generation SD-OCT software has the possibility to visualize volume scans in many different ways: the transverse sections that are aligned parallel to structures such as the RPE. The transverse section module (firstly made by Heidelberg Engineering, Spectralis) allows acquiring OCT volume scans with a B scan distance of only 11 microns. With this acquisition it is possible to get an isotropic transverse section image of 11 microns lateral resolution. (Drexler and Fujimoto 2008, Podoleanu and Rosen 2008, Lumbroso, Huang et al. 2013)

Standard retina and macula analysis nowadays should always include EnFace analysis. The possibility to study and map photoreceptor lesions represents one of the major achievements of EnFace OCT. (Podoleanu, Rogers et al. 2000, Drexler and Fujimoto 2008, Podoleanu and Rosen 2008)

4.3.1.3. Macular area visualization and characteristics

The macula, usually 150-190 μm thick and 1200 μm in diameter, is located at the center of the posterior pole, where it forms a slight depression centered on the fovea and the foveola (**Figure 1-3**). Inside the macular area, there are the *avascular area* (450-500 μm in diameter, limited by a ring of fine anastomoses of the peri-foveal vascular network, made of a single layer of capillaries), *fovea* (350 μm in diameter, inside the avascular zone) and *foveola* (“macular center”, 120-150 μm). Inside the macular area there is a network of retinal capillaries of 5-10 μm in diameter. (Drexler and Fujimoto 2008, Podoleanu and Rosen 2008, Lumbroso, Huang et al. 2013)

Outside the macular area the thickness of the retina is 270-280 μm . The interpapillomacular region is slightly thicker.

4.3.1.4. Choroid visualization

The choroid that was difficult to analyze and assess became available for examination from RPE to suprachoroidal space, with the development of modern OCTs in more than 80% of eyes. With the development of OCT, the visualization behind retina; to the level of sclera and Tenon’s capsule; became possible in patients with low pigmentation or myopia or who are affected by atrophic retinal diseases. (Drexler and Fujimoto 2008, Podoleanu and Rosen 2008, Lumbroso, Huang et al. 2013)

On the OCT, the choriocapillaris is thin and hyper-reflective. It is placed at the innermost limit of the choroid and consists of a single layer of polygonal vascular lobules which independently receive blood from the short posterior ciliary arteries. The venous blood is drained from the smaller veins into the vortex veins, of which there are one or two per quadrant.

The larger vessels of the choroid are hypo-reflective on the OCT. They form the *Sattler (small vessels)* and *Haller (large vessels) layers* of the choroid (**Figure 4-4, Table 4-7**). The connective tissue between vessels has a low to high reflectivity depending on age and vascular sclerosis, and pigment deposits. The walls of blood vessels normally are not visible. Choroidal vessels have different aspects depending upon depth (**Figure 4-4, Table 4-7**). Their contents are not always seen. (Drexler and Fujimoto 2008, Podoleanu and Rosen 2008, Lumbroso, Huang et al. 2013)

In young people, the choroid has a thickness of about 320 microns. Thickness decreases with aging after 25 years. Choroid thickness decreases also with myopia. It increases in hypermetropia.

Reflectivity

The reflectivity is very important OCT characteristic; it can be high or low. Reflectivity represents the strength of the signal reflected by the tissue. The strength of the signal depends on the amount of light arriving at a specific layer, and it depends on the light absorption tissue characteristics, as some of the light is absorbed by the interposed tissues. The amount of light reflected that reaches the measuring device, after being attenuated by the interposed tissues is visible on OCT scan. Reflectivity may be increased or reduced. (Drexler and Fujimoto 2008, Podoleanu and Rosen 2008, Lumbroso, Huang et al. 2013)

Vertical structures, such as photoreceptors, are less reflective than the horizontal structures, such as nerve fibers. Structure and reflectivity are frequently correlated in the normal retina as each structure has normally a given reflectivity. Based on a reflectivity OCT detects retinal boundaries (**Figure 4-4**). Loss of structure normally implies loss of reflectivity, and loss of reflectivity implies loss of structure and disappearance of boundaries. (Drexler and Fujimoto 2008, Podoleanu and Rosen 2008, Lumbroso, Huang et al. 2013)

4.3.1.5. Quantitative Analysis

Frontal and “EnFace” Measurement

The macular cube can be analyzed using raster scan of linear B-scan. The macular cube analysis can be assessed by cutting planar flat scans or by scans adapted to the RPE cup-shaped concavity. The quantitative analysis of the outer and inner retina, as well as the full-thickness retina is available with the new generations of OCT. Different anatomical alterations can be seen, analyzed, followed, such as drusen morphology, surface and volume, or RPE alterations. On some OCT devices it is possible to examine deeper layers, choroid or even sclera. (Drexler and Fujimoto 2008, Podoleanu and Rosen 2008, Lumbroso, Huang et al. 2013)

Quantitative segmentation

The most used segmentation is the nerve fiber layer segmentation that is available on all OCT devices. Quantitative segmentation gives also data on the inner and outer retina, inner retina, ganglion cell complex, outer retina between epithelium and inner plexiform layer. Segmentation allows measurements of the inner and outer retina thickness and volume, but

retinal alterations may strongly interfere with segmentation. (Drexler and Fujimoto 2008, Podoleanu and Rosen 2008, Lumbroso, Huang et al. 2013)

Quantitative choroid measurements

Choroid thickness measurement can be obtained in more than 80% of the normal eyes and in more than 90% of the myopic eyes.

Retinal Mapping

The tissue cube (bordered by ILM and RPE) obtained in most OCT devices is 4x4 mm, with 100-200 horizontal parallel scans. Most SD-OCT devices get 60 B-scans per second, achieving a good resolution. The topographic map of the cube is subdivided in sectors with indications of the thickness and standard deviation from a normal database. Thickness of different retinal layers can be obtained (e.g. thickness of NFL and its map). (Drexler and Fujimoto 2008, Podoleanu and Rosen 2008, Lumbroso, Huang et al. 2013)

Retinal and choroidal volume

Every OCT device can calculate the retinal volume for each map. The most common weakness of OCT devices in everyday clinical use is that in most of unhealthy eyes all the retinal layers should be drawn and assessed manually.

4.3.2. Study design

4.3.2.1. Patients

A total of 204 patients were recruited and 194 patients were included in the study. All patients respected the inclusion and exclusion criteria (please refer to the chapter **3.1**). Here, we also excluded patients when the OCT images were low-quality or blurred, and the chorio-scleral interface could not be traced. We excluded patients with a spherical equivalent (SE) higher than -12 diopters and patients without a complete set of images. All the patients underwent a baseline/preoperative standard clinical exam and at 1 and 3 months after surgery (please refer to **Table 3-1** and to the **paragraph 3.1**).

4.3.2.2. Imaging characteristics

SD-OCT scans were performed on all patients, using EnFace and B-scan OCT imaging. General parameters were set to “high speed resolution mode”; scan focus was adjusted depending on the spherical equivalence of the patient. Reflectance image characteristics were as following: scan angle 30 degrees, A-scans were 1536x496 pixels resolution, ART mode was activated with 12 images averaged. OCT image characteristics were as following: scan angle 20 degrees, A-scans with 1024x496 pixels resolution, ART mode activated (12 images averaged), eye length adjusted to the patients’ eye with a quality of ≥ 25 dB. OCT scan pattern was: 193 B-scans, pattern size was $20^\circ \times 20^\circ$ (5.8 x 5.8 mm) and separation between B-scans was 30 μ m. A single horizontal EDI scans through the fovea were also obtained for each eye.

Patients with low-quality or blurred OCT images in which the chorio-scleral interface could not be traced were also excluded from this part of the study. We excluded patients with a spherical equivalent (SE) higher than 12 and patients that withdrew from the study before completion (lack of images). Fellow eyes were used as control eyes.

4.3.2.3. EnFace OCT image

EnFace OCT images were analyzed after the alignment of retinal layers in all 193 B-scans. When automatic alignment was not appropriate, the layers were corrected manually. After verifying the position of the fovea through all images, the retinal layers such as Bruch’s membrane (BM), inner limiting membrane (ILM) and outer retina (OR) were assessed on horizontal scans within the volume stack and on the transverse image. The same alignment and analysis method were used preoperatively and at one month postoperatively.

4.3.2.4. Measurement on OCT

For all patients, central macular thickness (CMT) and height of subretinal fluid (SRF) were measured, preoperatively and one month postoperatively. CMT was measured using the Spectralis incorporated software after verifying and adjusting the position of fovea, using the reflectance image and corresponding B-scan image. By assessing individually each horizontal scan the maximal SRF height was determined for the following 8 radii from the fovea (0 μm (sub-foveal), 100 μm , 200 μm , 300 μm , 400 μm , 500 μm , 1000 μm and 3000 μm). At each radius, the SRF height was measured using digital calipers within the proprietary software.

4.3.2.5. Choroidal thickness measurements and analysis

OCT images were taken pre-operatively in macula-ON groups, and at 1 and 3 months postoperatively in all eyes. A single horizontal EDI-OCT scan through the fovea was obtained for each eye. Fellow eyes served as control eyes. The extent of RD was measured manually with an OCT map scan (Spectralis HRA+OCT, Heidelberg, 30° ART, 5.9×5.9 mm). The CT was measured with proprietary software, using the horizontal line scan in the area between 2.5 mm nasal and 2.5 mm temporal from the fovea. Briefly, we aligned the external limiting membrane (ELM) segmentation to the posterior choroidal boundary and assessed the “outer retinal layer” to extract the CT systematically (the distance between Bruch’s membrane and the outer border of the choroidal stroma).

CT measurements were compared between those taken at baseline and those taken at each postoperative visit. We also compared measurements between treated and fellow eyes. CTs were measured at 51 points that spanned the central 5 mm, from -2.5 mm to +2.5 mm, with a horizontal separation of 0.1 mm. We defined three regions: the nasal macular region, which comprised 11 points, starting at 1 mm and ending at 2 mm from the fovea, respectively, on the nasal side; the temporal macular region, which comprised 11 points, starting at 1 mm and ending at 2 mm from the fovea, on the temporal side (-2 mm to -1 mm); and the sub-foveal region, which comprised 5 points along the 0.4-mm diameter of the fovea (-0.2 mm to 0.2 mm).

4.3.2.6. Measurements repeatability

The repeatability of CT measurements was assessed by two trained observers that measured CTs on the same images, manually, from 10 patients that represented the range of RD types at all 51 loci. No significant differences were found between observers ($p=0.89$). Henceforth, all CT measures were performed by a single observer (MANOVA)

4.3.2.7. Statistical analyses

Statistical analyses were performed to assess data on sex, age, lens status, symptom duration, extent of RD, macular condition, changes in the logMAR of the BCVA, refractive errors, axial length, IOP, retinal thickness, and CT measured pre-operatively, at 1 month, and at 3 months post-surgery. The multiple measures in each region for each patient were evaluated with the analysis of variance (ANOVA) for repeated measures. We considered p-values below 0.05 as statistically significant. Mean and standard deviations are given for all parameters with the exception of LogMAR visual acuity, where median and interquartile range (IQR) is reported.

4.3.3. Data overview

4.3.3.1. Hemi-macular detachment - a distinct new subgroup of RD

Among 194 patients, 9 eyes presented with a hemi macular detachment (HMD). HMD was defined as a partially detached macula on preoperative OCT, with subretinal fluid up to half of the foveal region and extending continuously towards the retinal periphery.

All 9 patients underwent 23-gauge pars plana vitrectomy with gas (n=5) or silicone oil tamponade (n=4) for primary RD (two with longstanding RDs and PVR and two patients living at greater altitude than 1500m above sea level). The surgery was performed on the same day or within 24h after patients' presentation. Patients were examined preoperatively and one month postoperatively with best corrected visual acuity (BCVA) (logMAR), intraocular pressure (IOP) and fundus exam. All patients were systematically questioned at their postoperative follow-up exam if they have had blurred vision or visual distortions in their central field of view.

Baseline characteristics

Nine patients with HMD were reviewed. There were 6 men and 3 women (mean age 70 ± 12 years). There were 6 right and 3 left eyes involved. The mean axial length of treated eyes was 24.8 ± 1.2 mm. There were five phakic patients and 4 who had undergone cataract surgery before. The median (interquartile range) LogMAR visual acuity at baseline was 0.4 [range: 0.2-0.4]. At month one postoperatively, BCVA had improved to 0.1 [range: 0.2-0.0] LogMAR (**Table 4-8**).

Table 4-8. Characteristics of study patients at baseline (pre-operatively) and 1 month post-operatively		
Baseline characteristics	Mean age	70 ± 12 years
	Number of eyes/patients	of 9
	Sex	6 men and 3 women
	Axial length	24.8 (± 1.2) mm
	Lens status	5 phakic and 4 pseudophakic
Duration of symptoms		9 ± 11 days
BCVA median logMAR [IQR]	Baseline	0.4 [0.2-0.4]
	Post-op	0.1 [0.2-0.0]
Mean CMT	Baseline	339.9 ± 61.7 µm
	Post-op	274.4 ± 42.1 µm
Mean SRF height at baseline	0 µm	85.0 ± 84.6 µm
	100 µm	78.56 ± 68.1 µm
	200 µm	82.9 ± 55.4 µm
	300 µm	81.8 ± 54.3 µm
	400 µm	88.0 ± 55.2 µm
	500 µm	113.2 ± 66.4 µm
	1000 µm	122.0 ± 81.6 µm
3000 µm	548.1 ± 348.8 µm	
SRF height post-op	1 patient had persistent postoperative SRF of 45 µm	
<i>SRF: subretinal fluid, CMT: central macular thickness, BCVA: best corrected visual acuity, IQR: interquartile range</i>		

Retinal detachment

The mean duration of symptoms, was 9 ± 11 days (range was from 1 to 28 days). Seven out of nine patients presented with superior temporal RD and two patients had mainly inferior RD. In all patients, retinal breaks were localized in the superior temporal quadrant. Patients with long-standing symptoms had inferior RD, however most patients had symptoms of a short duration (3-5 days) at presentation, with superior-temporal RD.

EnFace OCT images

All 9 patients had the same presentation on EnFace OCT preoperatively. On transverse images, a pocket of subretinal fluid (SRF) accumulation up to the half of foveal region was visible. The mean CMT was 339.9±61.7 µm. On EnFace OCT this shallow RD had the appearance of a circular sub-foveal pocket of fluid (85.0±84.6 µm at fovea) with a slight decrease in SRF at the border of the fovea in most cases (78.56 ± 68.1 µm at 100 µm,

82.9 ± 55.4 μm at 200 μm, 81.8 ± 54.3 μm at 300 μm). Typically, the RD remained shallow para-centrally (88.0 ± 55.2 μm at 400 μm, 113.2±66.4 μm at 500 μm). A slight but restrained elevation of SRF was observed with continuously low height until beyond the vascular arcade to a region (i.e between 1000 μm and 3000 μm), where the RD became more bullous (122.0±81.6μm at 1000μm and 548.1±348.8 μm at 3000 μm from the fovea) (**Table 4-8**).

At 1 month, the average CMT was reduced to 274.4±42.1 μm and there was one case with persistent SRF under the fovea (45μm). The former limit of the extension of the RD remained visible with modifications on the reflectance image appearing as a gray line passing through the fovea. This intra-retinal disturbance corresponded to changes in the outer retinal layers presenting as a hypo-reflectivity within the ellipsoid layer visible on B-scan, while EnFace OCT shows a ridge-like tissue densification which corresponds to ellipsoid layer changes evident on B-scans (**Figure 4-7, Figure 4-8**).

Impact on quality of vision

The changes in the outer retinal layers did not correlate with an obvious measurable change in postoperative visual acuity which increased by 0.1 [range: 0.2-0.0] LogMAR units. However, direct questioning of the patients elicited the presences of subjective visual disturbances such as metamorphopsia (5/8 patients), while 6/8 patients reported blurred vision in eight out of the nine patients.

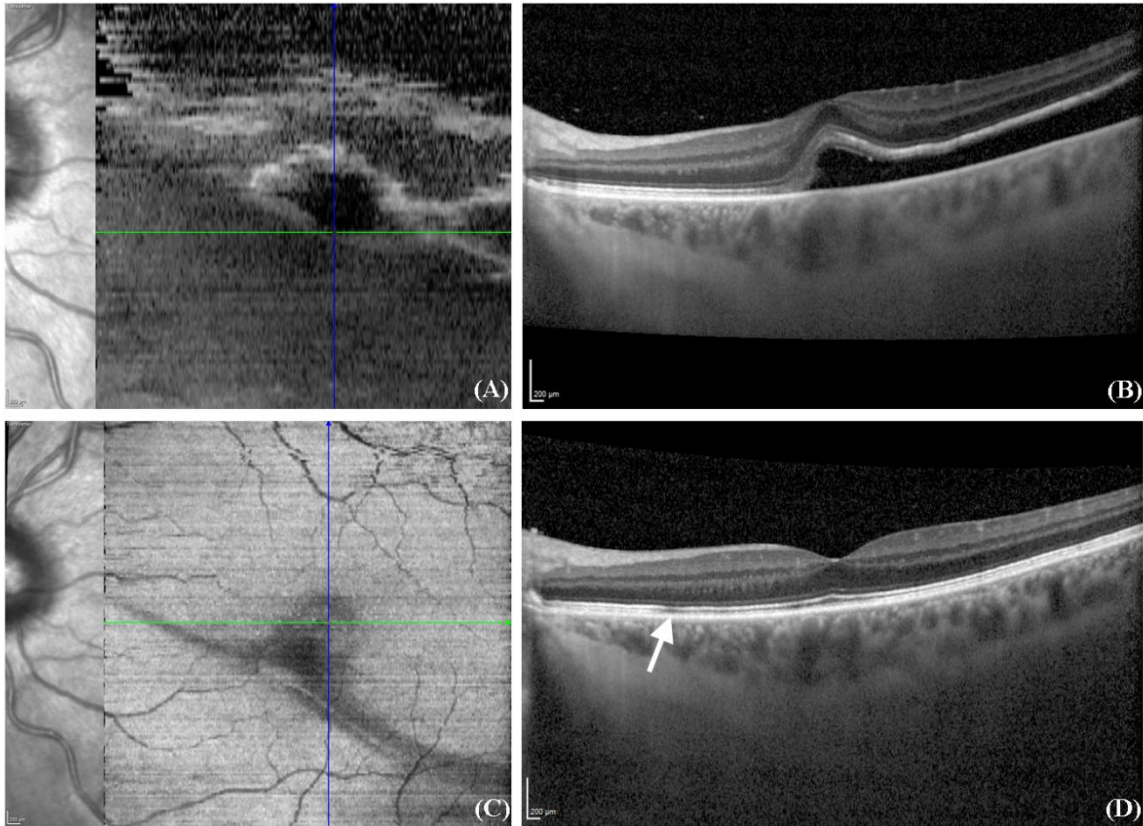


Figure 4-7 A-D OCT images of patient 1 at two time points baseline/preoperatively and at one month after surgery.

A) Preoperative EnFace OCT image demonstrating a circular sub-foveal pocket of subretinal fluid, followed by a shallow RD that is continuously slowly increasing until RD extension is beyond the vascular arcade (gray zone), after which RD height is much greater and OCT imaging becomes impossible

B) Preoperative B-scan demonstrating hemi-macular detachment with cross section of the circular peri-foveal pocket

C) 1 month postoperative EnFace OCT image demonstrating a ridge-like tissue densification that matches with previous border of the RD and previous pocket of subretinal fluid

D) 1 month postoperative B-scan showing hyporeflective lesions in the ellipsoid layer (white arrow) which correspond to ridge evident on EnFace image.

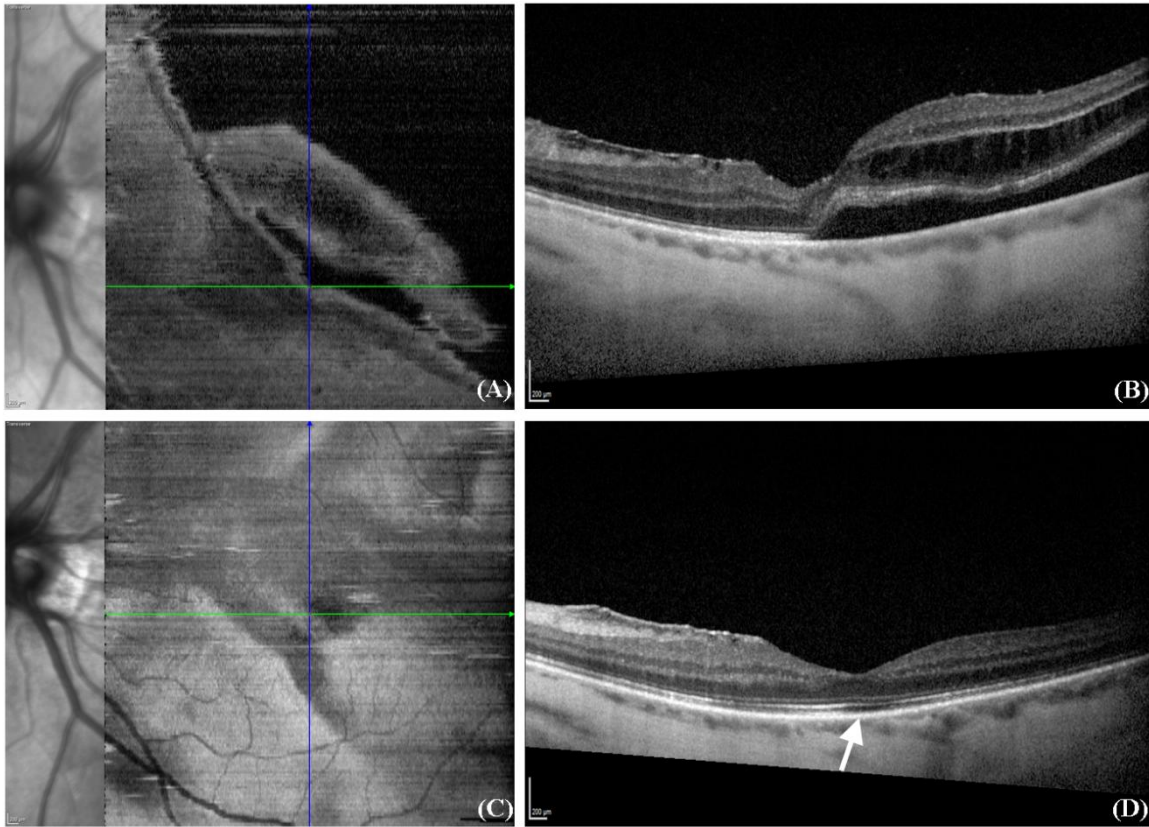


Figure 4-8 A-D OCT images of patient 2 at two time points baseline/preoperatively and one month after surgery showing an identical situation to patient 1 with a sub-foveal pocket of subretinal fluid (A+B) and the hyporeflective lesions in the ellipsoid layer corresponding to the ridge-like structure visible on EnFace OCT (C+D).

4.3.3.2. The role of choroidal thickness in retinal detachment patients

A total of 54 eyes of 54 patients were included in analysis. The patients were divided into three groups, according to the extent of RD, as follows: peripheral RD with macula-ON (>3 mm from the fovea, n=14); paracentral RD with macula-ON (fovea-sparing, ≤3 mm from the fovea, n=14); and macula-OFF RD (central RD, involving the fovea, n= 26) (**Figure 4-9**).

Baseline characteristics

The demographic and clinical characteristics of patients are shown in **Table 4-9**. In the peripheral RD group, the mean age at the onset of RD was 63.4 ±8.5 years. The median BCVA was 0 [IQR 0 to 0.1], both before and after surgery (p=0.37). In the paracentral RD group, the mean age was 55.1 ±6.0 years, and the median pre-operative BCVA was 0.08 [IQR 0 to 0.2], which improved to a postoperative BCVA of 0 [IQR 0 to 0.1], p=0.08. In the macula-OFF RD group, the mean age at the onset of RD was 60.5 ± 9.6 years, and the BCVA improved significantly from 2 [IQR 1.3 to 2.3] pre-operatively to 0.2 [IQR 0.1 to 0.3] postoperatively (p<0.001). The BCVA in fellow eyes remained stable at 0.0 [IQR: 0.0 to 0.1] throughout the follow-up.

Table 4-9. Baseline characteristics of the patient cohort in relation to retinal detachment extension.

Baseline characteristics with respect to retinal detachment extension						
	Peripheral (ON)		Paracentral (ON)		Macula-OFF	
Age (Mean Y± SD)	63.4±8.5		55.1±6		60.5 ±9.6	
Male (%)	74.1		63		67.4	
Duration of symptoms (days)	9.4 (range 0-23)		8.7 (range 0-26)		6.4 (range 1-21)	
patients with > 6 clock hours detachment % (N°)	14% (2/14)		21% (3/14)		50% (13/26)	
Phakic (%)	71		85		61.5	
	TE	FE	TE	FE	TE	FE
SE (Mean D± SD)	-1.6±2.8	-1.7±3	-2.8±2.1	-1.9±1.8	2.51±4	1.60±3.9
AL (Mean mm± SD)	25.6±1.9	25.1±1.7	25.5±1.2	25.4 ±1.1	24±5.2	23.8±5.6
IOP (Mean mmHg± SD)	14.7±3	15.6±4.8	16.3±3.2	16.3±1.8	13.9±4.3	15.6±4.8

Y = years, D= diopters, TE=treated eye; FE=fellow eye; SE=spherical equivalent; AL=axial length; IOP=intraocular pressure, SD= standard deviation

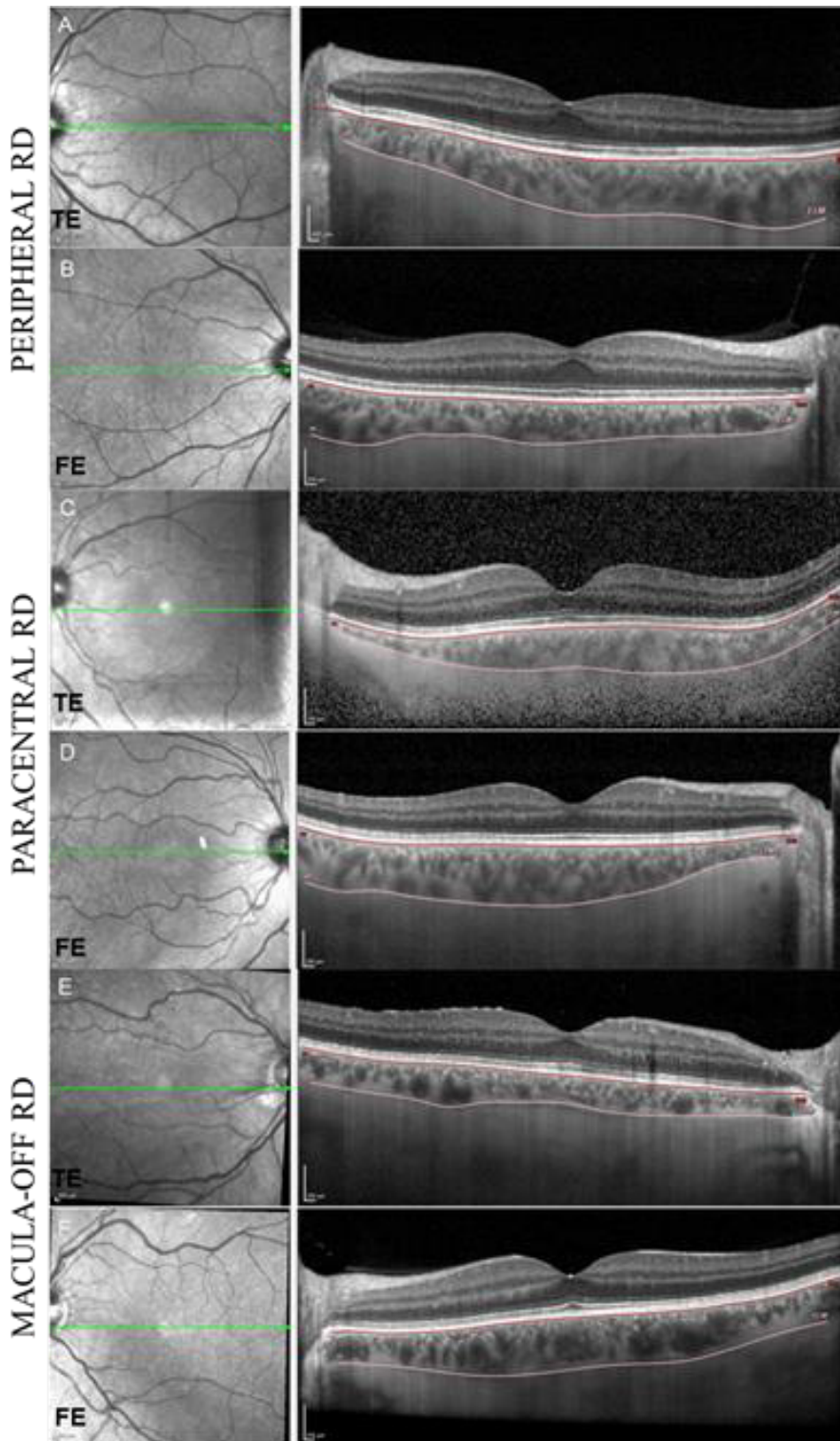


Figure 4-9. EDI SD-OCT representing choroidal thickness (CT) in patients with peripheral RD, paracentral RD and macula-OFF RD 1 month after surgery.

- a.** CT in the affected eye of peripheral RD
- b.** CT in the fellow eye of peripheral RD. The CT in TE is thicker than the FE.
- c.** CT in the affected eye of paracentral RD
- d.** CT in the fellow eye of paracentral RD. The CT in TE is thinner than the FE.
- e.** CT in the affected eye of macula-OFF RD
- f.** CT in the fellow eye of macula-OFF RD. The CT in TE is thinner than the FE

Mean sub-macular choroidal thickness in groups with different extents of RD

The preoperative mean CT at the sub-foveal location in the peripheral RD group was $202 \pm 75.5 \mu\text{m}$, and the postoperative mean sub-foveal CTs at months 1 and 3 were $208.4 \pm 57.8 \mu\text{m}$ and $200.2 \pm 61.4 \mu\text{m}$, respectively. In the paracentral RD group, the mean CT was thicker at the sub-foveal location preoperatively ($220.9 \pm 74.5 \mu\text{m}$) than in the peripheral RD group, but similar to that of the peripheral RD group at 1 and 3 months postoperatively ($204.8 \pm 68.7 \mu\text{m}$ and $206 \pm 72.7 \mu\text{m}$, respectively). The mean sub-foveal CTs in the macula-OFF RD group at 1 and 3 months were also similar to those of the peripheral RD group postoperatively ($201.3 \pm 70.9 \mu\text{m}$ and $210.3 \pm 67.1 \mu\text{m}$, respectively). In the fellow eyes, the mean sub-foveal CT was thinner in the peripheral RD group ($172.7 \pm 42.2 \mu\text{m}$) than in the paracentral or macula-OFF RD groups ($230.6 \pm 81.0 \mu\text{m}$ and 235.2 ± 70.3 , respectively; $p < 0.01$ and $p < 0.01$ respectively; **Table 4-10**). In the fellow eyes, no significant differences were found in the preoperative, 1 month, and 3 month examinations. The mean CTs at the foveal, nasal, and temporal locations in the three different groups at the three different pre- and postoperative time points are summarized in **Table 4-10** and in **Figure 4-10**.

Table 4-10. Mean choroidal thickness values and percentage of change in CT over fellow eyes in peripheral, paracentral and macula-OFF RD. The lightly shaded areas denote a general thinning of the choroid, whereas a darker shade denotes thickening of the choroid.

		Extension of retinal detachment								
		Peripheral (ON)			Paracentral (ON)			Macula-OFF		
		Macula region			Macula region			Macula region		
		Temporal	Sub-foveal	Nasal	Temporal	Sub-foveal	Nasal	Temporal	Sub-foveal	Nasal
Mean CT values (μm)	FE	188.5 ± 41.8	172.7 ± 42.2	148.1 ± 47.0	236.5 ± 74.3	230.6 ± 81.0	181.6 ± 70.4	234.6 ± 57.9	235.2 ± 70.3	198.3 ± 71.6
	Preop TE	200.3 ± 66.0	202.0 ± 75.5	160.9 ± 59.6	225.5 ± 86.1	220.9 ± 74.5	181.8 ± 78.1			
	M1 TE	210.1 ± 71.4	208.4 ± 57.8	158.3 ± 68.8	220.9 ± 80.3	204.8 ± 68.7	170.7 ± 65.4	198.6 ± 60.4	201.3 ± 70.9	171.6 ± 72.7
	M3 TE	205.5 ± 78.1	200.2 ± 61.4	161.2 ± 59.7	226.4 ± 81.4	206.0 ± 72.7	170.2 ± 61.6	207.7 ± 58.8	210.3 ± 67.1	178.6 ± 73.5
		Peripheral (ON)			Paracentral (ON)			Macula-OFF		
		Macula region			Macula region			Macula region		
		Temporal	Sub-foveal	Nasal	Temporal	Sub-foveal	Nasal	Temporal	Sub-foveal	Nasal
Percentage change in CT over FE	Pre-op	7.5 ± 22.2	19.6 ± 43.9	14.2 ± 36.3	-7.7 ± 24.9	-7.8 ± 21.9	-3.2 ± 14.3			
	M1	11.8 ± 26.8	22.9 ± 27.5	9.2 ± 22.2	-5.4 ± 22.4	-5.5 ± 26.1	1.1 ± 33.6	-15.7 ± 15.0	-14.1 ± 18.7	-11.8 ± 22.8
	M3	9.4 ± 33.4	18.2 ± 35.6	9.5 ± 21.4	-1.8 ± 25.7	-9.3 ± 19.4	-2.1 ± 28.5	-11.2 ± 17.0	-9.9 ± 15.0	-7.5 ± 27.0

*blue=peripheral RD, green= paracentral RD, red= macula-OFF RD

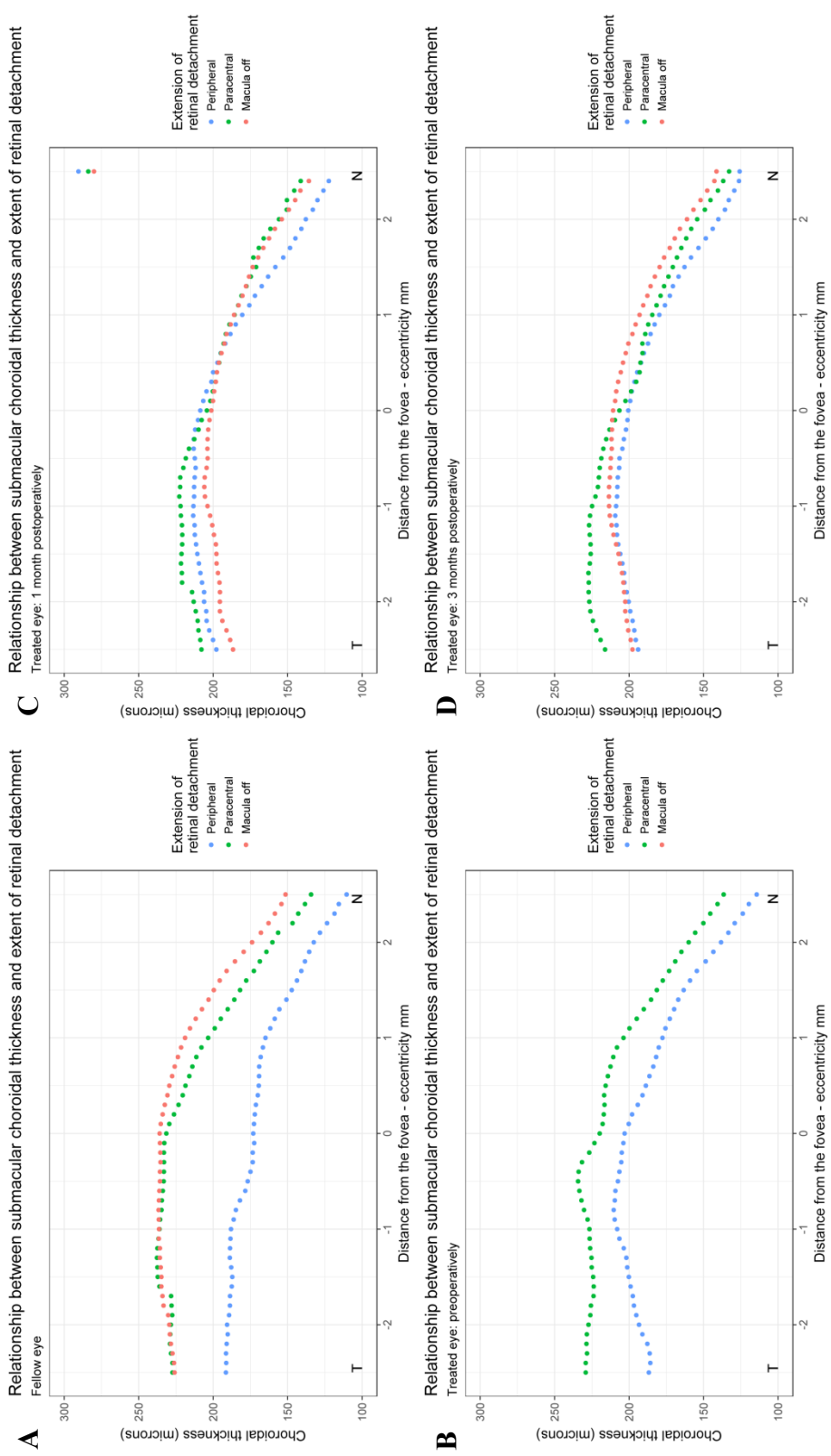


Figure 4-10. Choroidal thickness in peripheral RD, paracentral RD and macula-OFF RD

A. FE

B. TE pre-op

C. TE at M1

D. TE at M3

(TE=treated eye, FE= fellow eye, M1= 1 month post-op, M3=3 months post-op)

Inter-eye difference

In the peripheral RD group, the inter-eye difference in CTs at the sub-foveal location showed a thickening throughout follow up (preoperative = $19.6 \pm 43.9\%$, 1 month = $22.9 \pm 27.5\%$, 3 months = $18.2 \pm 35.6\%$). In the paracentral RD group, the inter-eye difference in sub-foveal CTs showed a thinning throughout follow up (preoperative = $-7.8 \pm 21.9\%$, 1 month = $-5.5 \pm 26.1\%$, 3 months = $-9.3 \pm 19.4\%$). In the macula-OFF RD group, the inter-eye difference in sub-foveal CTs showed a more pronounced thinning at 1 month ($-14.1 \pm 18.7\%$) and 3 months ($-9.9 \pm 15\%$). The inter-eye differences in mean CTs at the sub-foveal, nasal and temporal locations and in the three different groups at different pre- and postoperative time points are summarized in **Table 4-10** and in **Figure 4-11**.

At one month postoperatively, the peripheral RD group showed a significant thickening in the sub-foveal CT ($p < 0.01$) compared to fellow eyes. Conversely, the paracentral and macula-OFF RD groups showed significant thinning in the sub-foveal CTs ($p = 0.04$, $p < 0.01$, **Table 4-10**, **Table 4-11**).

The summary statistics show the significance of the observed differences in the mean CT values between the treated eyes and the fellow eyes and the significance of the percentage of change in CTs in the peripheral, paracentral, and macula-OFF RD groups compared to the corresponding fellow eyes **Table 4-11**.

Table 4-11. Summary statistics for mean CT between FE and TE, mean CT in FE and the percentage of change in CT over FE in peripheral RD, paracentral RD and macula-OFF RD.

		Extension of retinal detachment								
		Peripheral (ON)			Paracentral (ON)			Macula-OFF		
		Macula region			Macula region			Macula region		
		Temporal	Sub-foveal	Nasal	Temporal	Sub-foveal	Nasal	Temporal	Sub-foveal	Nasal
Mean CT values (μm)	FE vs TE at M1	0.001	0.000	0.16	0.10	0.04	0.27	0.000	0.000	0.000
		Peripheral vs Paracentral			Paracentral vs Macula-OFF			Macula-OFF vs Peripheral		
		Macula region			Macula region			Macula region		
		Temporal	Sub-foveal	Nasal	Temporal	Sub-foveal	Nasal	Temporal	Sub-foveal	Nasal
Percentage change in CT over FE	Pre-op	0.000	0.000	0.000						
	M1	0.000	0.000	0.23	0.000	0.002	0.75	0.000	0.000	0.62
	M3	0.000	0.000	0.02	0.004	0.10	0.82	0.09	0.000	0.06

Submacular choroidal thickness vs extent of retinal detachment

Inter eye difference ((TE-FE)/FE): Postoperative month 3 measures

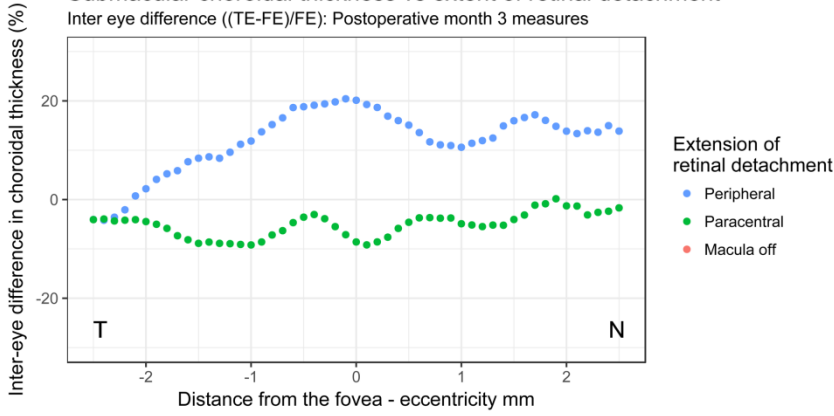
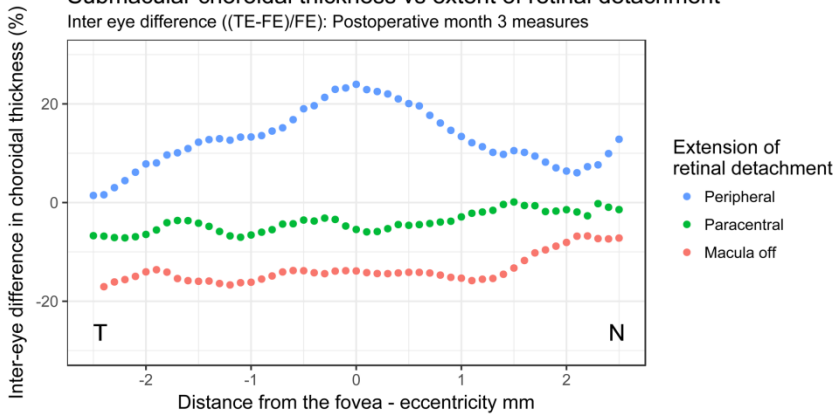


Figure 4-11. Inter-eye difference in choroidal thickness in peripheral RD, paracentral RD and macula-OFF RD

- A. Pre-op
- B. M1
- C. M3

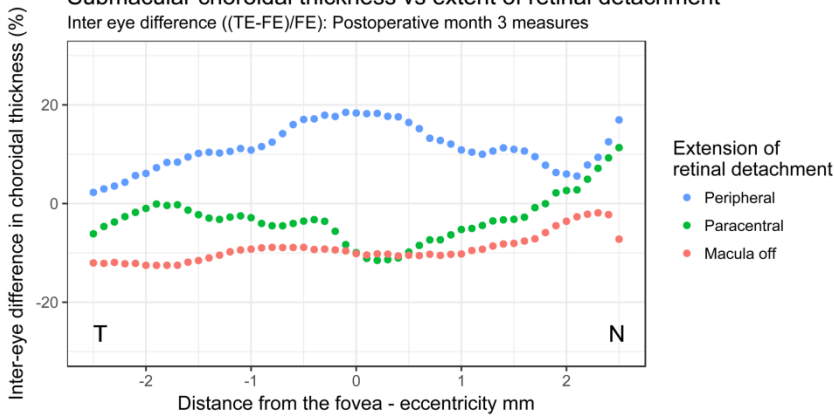
Submacular choroidal thickness vs extent of retinal detachment

Inter eye difference ((TE-FE)/FE): Postoperative month 3 measures



Submacular choroidal thickness vs extent of retinal detachment

Inter eye difference ((TE-FE)/FE): Postoperative month 3 measures



4.3.4. Discussion

4.3.4.1. Hemi-macular detachment

The present study describes novel aspects of SD-OCT characterization of HMD as a sub-type of retinal detachment with characteristic and well defined pre- and post-operative image patterns. It appears that this particular type of RD with a half-off/half-on fovea is associated with superior temporal retinal breaks and SRF distribution in both temporal quadrants following the Lincoff rules. (Lincoff and Gieser 1971) More interestingly, both pre- and post-operative reflectance images, B-scans and EnFace OCT images of the fovea showed characteristic signs such as a circular sub-foveal fluid pocket as well as hypo-reflective zones within the ellipsoid layer and tissue densification selectively at the border of the RD between the attached and detached retina. These structural modifications in the retina may correspond to direct mechanically induced alterations as this location acts like a hinge between the attached and detached retina. A further factor could be a delayed localized glial reaction to the kinking of the retina along the line between attached and detached retina. (Fisher, Lewis et al. 2005) Although post-operative VA increased despite these tissue modifications almost all patients reported subjective visual disturbances in the form of metamorphopsia and blurred vision.

It has been known for some time that demarcation lines may occur in RD. Tani et al. described a cohort of 173 eyes with macula on RD, in which more than 40% had long standing RD (>1month), and one third had an evident demarcation line. The authors hypothesized that these patients belonged to a more benign RD subgroup, with lower likelihood of RD expansion. (Tani, Robertson et al. 1980) Our cases with HMD represent a more defined subgroup of these patients as the diagnosis of the fovea on/off situation can only be made using OCT, and it is likely that the patients with HMD fall into the category of RDs with low progression potential. Ho et al estimated the mean rate of RD extension as 1.80 disc diameters per day, although up to 87% of macula-ON patients showed no progression in the first few days. (Ho, Fitt et al. 2006) The main risk factor for macular detachment was described as the distance of SRF within one disc diameter from the fovea at presentation, (Ho, Fitt et al. 2006) and the rate of conversion from a macula-ON to a macula-OFF RD while awaiting surgery was 1%. In the series reported by Kontos et al, 9/10 cases which converted had a superior temporal retinal break, 5 of these eyes converted within several hours of presentation. (Kontos and Williamson 2016) In our cohort this distinction was less clear-cut as 2 patients had long standing RD, 3 had RD of medium duration (5-8 days) and 4 had a RD

of short duration (1-3 days). There was no clear separation between “benign” and “high risk” HMD patients, irrespective of the duration.

From a pathophysiological point of view the exact reasons for the progression of a macula-ON to a macula-OFF RD are still not completely known and both retinal and indeed choroidal factors may play a role. Some potential anatomical and physiological impediments to complete retinal detachment were first described in animal models, where fluid was injected into the subretinal space to induce a complete RD. (Machemer and Steinhorst 1993) Similar barriers were subsequently observed in humans during macular translocation surgery (Machemer and Steinhorst 1993, Mruthyunjaya, Stinnett et al. 2004) and it became evident that the adhesion between the neurosensory retina and the retinal pigment epithelium may be sufficiently strong in certain situations to prevent rapid RD extension and conversion into a total RD.

It is interesting to note in this context that the foveal RD remained very shallow in all patients (approximately 80 μm) and that it only increased considerably in the area more peripheral to the vascular arcades. We could express this observation in the descriptive term of a para-foveal ring of resistance to sub-macular fluid accumulation. The post-operative reflectance images, B-Scans and EnFace images could delineate the former limit of RD extension clearly as modifications in the outer retinal layers. These intra-retinal changes may be due to a photoreceptor outer segment degeneration or apoptotic cell death during RD. (Guerin, Lewis et al. 1993, Arroyo, Yang et al. 2005) Other modifications such as parafoveal thinning, hyporeflectivity and/or pigment migrations in the ellipsoid layer have been described in patients with RD but only using standard OCT. (Saleh, Debellemanni et al. 2014) In macula-OFF RD, changes to the inner and outer nuclear layers such as an absent or interrupted inner segment/outer segment junction line in the ellipsoid layer have also been reported both using SD-OCT (Lecleire-Collet, Muraine et al. 2006) and foveal densitometry. (Liem, Keunen et al. 1994) These changes were associated with poorer visual function and, in particular, with persistent metamorphopsia, which corresponds well with our current observations. (Liem, Keunen et al. 1994)

4.3.4.2. Choroidal thickness

In this study, we characterized the correlation between the extent of RD and the CT by measuring 51 loci across the macula, pre- and postoperatively. We observed that, when RD extended towards the macula (paracentral RD), the CT was thinner than in fellow eyes; moreover, when RD caused the macula-OFF condition, the CT was even thinner (relative to

fellow eye). Conversely, in peripheral RD, we observed that the CT was thicker than in fellow eyes. Furthermore, in the fellow eyes of patients with peripheral RD, the CT was markedly thinner than in the fellow eyes of patients with either paracentral or macula-OFF RD. Thus, patients with peripheral RD may be at lower risk of developing macula-OFF RD, due to the thinner baseline CT.

The architecture of the choroidal vasculature might partly explain the recovery trajectories observed. Previously, Nickla and Wallman demonstrated that modulations in ion and fluid flow across the retina and retinal pigment epithelium into the choroid modulated the CT. (Nickla and Wallman 2010) Similarly, RD was shown to disrupt retinal metabolism and ionic transfer into the choroid, resulting in CT modifications, which resolved once the retina was reattached. Several studies have shown that the CT increased immediately after surgery, and that resolution was achieved within 3 months of surgery. (Kimura, Nishimura et al. 2012, Miura, Arimoto et al. 2012, Akkoyun and Yilmaz 2014) Those findings were consistent with our hypothesis that, after retinal reattachment, the CT will return to the measurements observed in the fellow eye. Akkoyun and Yilmaz studied patients that underwent different types of surgical interventions for RD. (Akkoyun and Yilmaz 2014) They showed that a transient increase in sub-foveal CT occurred 1 week postoperatively, after both PPV and scleral buckling. This transient increase in CT may have been induced by scleral and choroidal inflammation after laser photocoagulation in the PPV group, and with scleral compression reducing blood flow and increasing hemostasis in the choroidal circulation in the scleral buckling group. (Akkoyun and Yilmaz 2014)

Somewhat surprisingly, we observed that CT changes were very different in eyes with peripheral RD than in those with paracentral or macula-OFF RD. In particular, the CT in fellow eyes was significantly thinner in the peripheral RD group than in the paracentral and macula-OFF RD groups (**Table 4-10**). This finding suggested that either systemic factors influenced the extent of RD or that eyes with peripheral RD were at lower risk of extensive RD, due to the thinner baseline CT. Following PPV with a silicone oil tamponade for treating RD, the sub-foveal CT decreased after surgery. (Sayman Muslubas, Karacorlu et al. 2016) This thinning might have been related to increased uveo-scleral outflow and intraocular inflammation caused by the RD. However, that study conducted a global analysis of a group of patients with macula-ON and macula-OFF RD (63% vs. 37%). Our results indicate that there would be patients with significant increases (peripheral RD) and decreases in CT (macula-OFF RD), as such changes in CT would be masked in this mixed cohort.

Another study suggested that the width and size of the buckling material could affect changes in the choroidal circulation, which could result in long-term increases in the sub-foveal CT in patients with macula-OFF RD. (Odrobina, Laudanska-Olszewska et al. 2013) Finally, a randomized clinical trial of cryotherapy vs. laser photocoagulation in scleral buckle surgery showed that the postoperative aqueous flare was higher after cryotherapy than after laser photocoagulation. (Veckeneer, Van Overdam et al. 2001) All our patients were treated with cryotherapy, except one that was treated only with laser photocoagulation in the paracentral RD group. Therefore, the different patterns in CT evolution that we observed among the three different RD groups were not related to the laser treatment used.

Margolis et al showed that the CT was thickest under the fovea in a healthy population. (Margolis and Spaide 2009) That finding was correlated with the vascular architecture, which is shaped to sustain the high metabolic demand of the macula. Also, the CT in healthy eyes is thinner in the nasal macula compared to the sub-foveal and temporal locations. (Ruiz-Medrano, Flores-Moreno et al. 2014) The outer retina in the nasal macula is relatively thin, due to increases in the overlying layers of nerve fibers in this region; consequently, a significant component of the nasal macula is sustained by the retinal vasculature. Accordingly, the nasal macula places lower metabolic demand on the choroidal vasculature; indeed, it has been shown that this area had a thinner CT than other areas of the macula. (Margolis and Spaide 2009) In our study, the healthy fellow eyes in the peripheral macula-ON RD group showed, a sub-macular CT that was thinner than the average measurements found in the literature. This unexpected finding could not be explained by the mean age, axial length, or SE.

Similar to other groups, we observed a high inter-observer correlation, high repeatability, and high inter-visit reproducibility in the CT measurements. (Spaide, Koizumi et al. 2008, Ikuno, Maruko et al. 2011, Rahman, Chen et al. 2011, Vuong, Moisseiev et al. 2016) The mean inter-eye CT difference in the peripheral RD group was elevated across the central 0.4 mm, and that elevation began to resolve at 3 months after surgery. In the paracentral RD group, at 1 month post-vitreotomy, the CT was thinner than that of the fellow eye, mainly in the foveal region. At 3 months, the inter-eye CT difference continued to resolve temporally and nasally, but not centrally. In the macula-OFF RD group, at 1 month postoperatively, the mean inter-eye CT difference showed significant thinning compared to fellow eye at all locations, particularly the sub-foveal and temporal locations. This thinning also started to resolve at 3 months postoperatively.

While the results of this study are exciting, there are several limitations that should be highlighted. First, we analyzed a small number of patients. Future studies with larger sample sizes are needed to confirm the different patterns of CT evolution that we observed before and after RD treatment. Furthermore, several studies have reported that the CT undergoes diurnal fluctuations of 8.5-13.9%. (Brown, Flitcroft et al. 2009, Chakraborty, Read et al. 2011) All our patients were imaged shortly after presentation, with no systematic selection bias for the RD type or imaging time. Therefore, although diurnal fluctuation might be a likely source of noise, it was not likely to mask the observed CT changes associated with RD type. However, ideally, all imaging should be performed at approximately the same time of day. Furthermore, there is currently no automated software that can segment and automatically extract CT measurements. In many eyes, the chorio-scleral interface is blurred on OCT images, which makes measuring the CT more challenging. However, this obstacle may be removed in the future with the recent advances in imaging technology, particularly the use of longer wavelength light sources, which allow deeper penetration. Lastly, since the fovea relies exclusively on the choroidal vascular system, greater changes in the choroid may represent larger impacts on retinal health, with negative consequences on visual acuity, in patients with RD. (Kur, Newman et al. 2012)

4.3.5. Conclusion

SD-OCT allows defining and characterizing more precisely HMD as a distinct subgroup of RDs, which occurs in 4.4% of primary retinal detachments. Pre-operative EnFace OCT allows the identification of a circular sub-foveal pocket of fluid with a shallow height within the zone demarcated by the vascular arcades, the RD only becoming more bullous further into the periphery. It is not yet clear why the expansion of HMD stalls in this particular fashion. Post-operatively HMD is highly likely to be associated with a watermark at the border of the detachment in the macular area presenting as hyporeflective zones or tissue densifications in the ellipsoid layer. VA recovery in HMD is good, although most patients report residual visual disturbances in their central visual field most probably induced by the changes in the outer retina along the demarcation line through the fovea.

This study was the first to report CT changes associated with RDs in the sub-foveal and sub-macular choroid. We found that the CT varied significantly, depending on the extent of RD, both before and after successful surgical treatment. The origin and clinical implications of these different recovery pathways remain unknown, but influencing factors might include effects from circulatory alterations, treatment choice, and the extent of RD.

4.4. EXPERIMENTAL IMAGING IN RETINAL DETACHMENT

4.4.1. Introduction

Visual sensitivity is proportional to the density of cone photoreceptors in the retina which reach their peak at the fovea. (Wassle, Grunert et al. 1990, Ratnam, Carroll et al. 2013) Visual recovery after RD has been shown to be associated with duration and height of RD, persistence of SRF, age, degree of myopia (axial length of the globe), macular involvement and form of the detached retina. (Cook, Lewis et al. 1995, Hisatomi, Sakamoto et al. 2001, Wolfensberger and Gonvers 2002, Arroyo, Yang et al. 2005) Analysis of foveal microstructure using SD-OCT has correlated worse visual recovery with loss of integrity of the ellipsoid zone, interdigitation zone and the external limiting membrane. (Wakabayashi, Oshima et al. 2009, Delolme, Dugas et al. 2012, Rashid, Pilli et al. 2013)

The detached retina is under metabolic, hypoxic and oxidative stress due to change in microenvironment; lack of nutrients, (Linsenmeier and Padnick-Silver 2000) and disruption of the outer retinal barrier after a loss of contact of the outer segments with the RPE. (Anderson, Stern et al. 1983, Chen, Rajapakse et al. 2016) Clinical observations have demonstrated sizeable intersubject variation between responses to this stress (e.g., the degree of visual recovery) that is not well explained by the identified risk factors. Photoreceptor cell death starts within the first twelve hours and peaks at 2-3 days following RD. (Cook, Lewis et al. 1995, Hisatomi, Sakamoto et al. 2001, Arroyo, Yang et al. 2005, Fisher, Lewis et al. 2005) The degree of visual loss is proportional to the degree of photoreceptor loss, which has been impossible to assess *in-vivo* until recently. (Miller, Williams et al. 1996, Liang, Williams et al. 1997, Hofer, Artal et al. 2001, Roorda and Williams 2002, Fernandez and Artal 2003)

OCT is the current imaging tool of transverse sections of the retina, but the recent advent of adaptive optics fundus camera (AO) allows visualization of photoreceptor morphology *in vivo* for the first time. If foveal photoreceptor alterations following RD can be observed and monitored using AO imaging, and if these correlate with visual impairment, there is a strong case for a clinical application of this device. (Zawadzki, Jones et al. 2005, Zhang, Rha et al. 2005, Zawadzki, Choi et al. 2007) There exist two studies analyzing RD patients with detached macula post-operatively, measured in one location using an AO fundus camera. (Saleh, Debellemanni et al. 2014, Ra, Ito et al. 2017) Saleh prospectively evaluated 21 patients at six weeks, after PPV with gas tamponade, (Saleh, Debellemanni et al. 2014) and Ra et al. retrospectively investigated 21 patients who underwent scleral buckle surgery with a long-term follow up of 12 months. (Ra, Ito et al. 2017) To the best of our knowledge,

AO has not been used to evaluate post-operative recovery of RD patients without macular detachment. Therefore the aim of this study was to quantify the changes in cone density postoperatively measured on five different matching loci using the AO fundus camera, in patients following RD with and without macular detachment, and to examine the relationship with functional recovery.

4.4.1.1. Adaptive Optics

Adaptive optics fundus camera (AO) is a modified OCT device, which attempts to correct for optical aberrations in order to deliver a representation of the microscopic retina **Figure 4-12**. These images can be used to examine cone morphology *in-vivo*. Therefore, AO imagery could potentially be used to monitor foveal photoreceptor cellular alterations following RD. (Zawadzki, Jones et al. 2005, Zhang, Rha et al. 2005, Zawadzki, Choi et al. 2007)

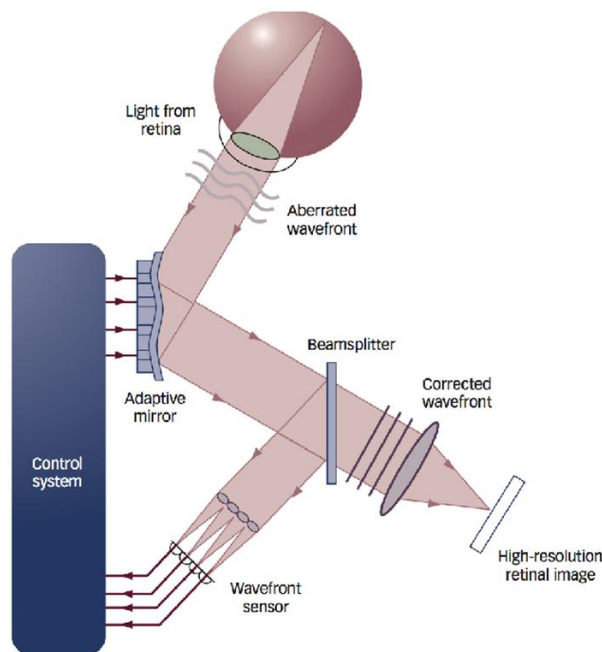


Figure 4-12. Schematic diagram of an adaptive optics retinal imaging system. Adapted from (Carroll, Kay et al. 2013)

Fundus imaging using AO has been developed in the last two decades by several teams in the world. Adaptive optics is basically an optoelectronic technique based on the dynamic adaptation of a deformable mirror to match the optical aberrations of the ocular milieu; this increases the lateral (though not the axial) resolution of images (**Figure 4-12**, **Figure 4-13**). Technically, AO may be combined to any fundus imaging system; either flood

imaging, scanning laser ophthalmoscopy or optical coherence tomography (OCT) (**Figure 4-13, Figure 4-14**). Current AO systems for fundus images allow a 1-5 μm lateral resolution. The actual resolution depends on a number of factors, among them the number of actuators of the deformable mirror.

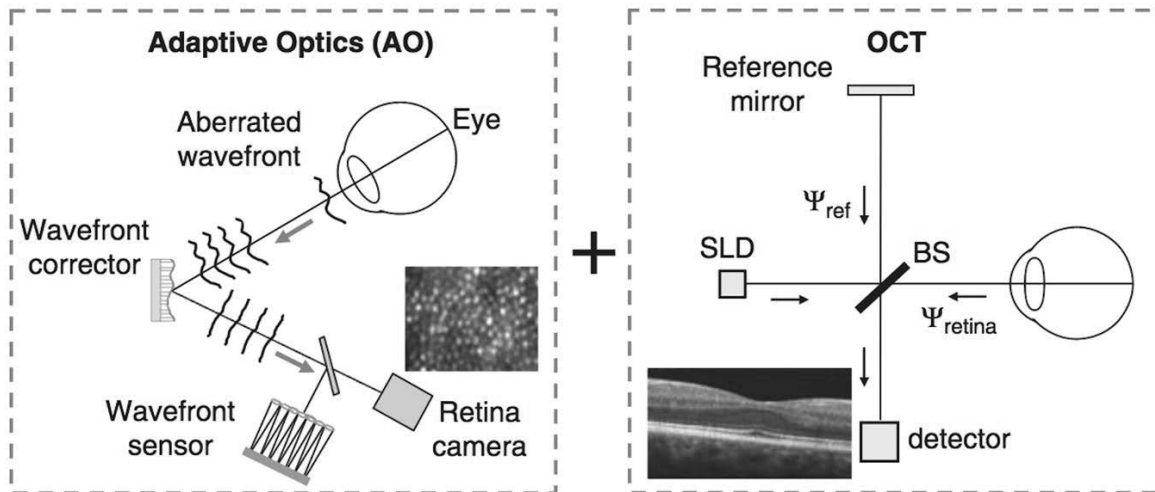


Figure 4-13. Schematic diagram of an adaptive optics (AO) retinal imaging system and parallel with OCT imaging system. OCT uses low-coherence interferometry to achieve high axial resolution. AO measures the ocular aberrations with a wave-front sensor and corrects for them (cornea, lens, and optical media) with a wave-front corrector to achieve the complementary high lateral resolution. Adapted from (Miller, Kocaoglu et al. 2011)

Adaptive optics technology is reaching technological maturity, hence it can be expected that commercially available systems will soon enter clinical routine. The primary contribution of AO to clinical retinal imaging has been the observation of the cone photoreceptor mosaic. (Liang, Williams et al. 1997)

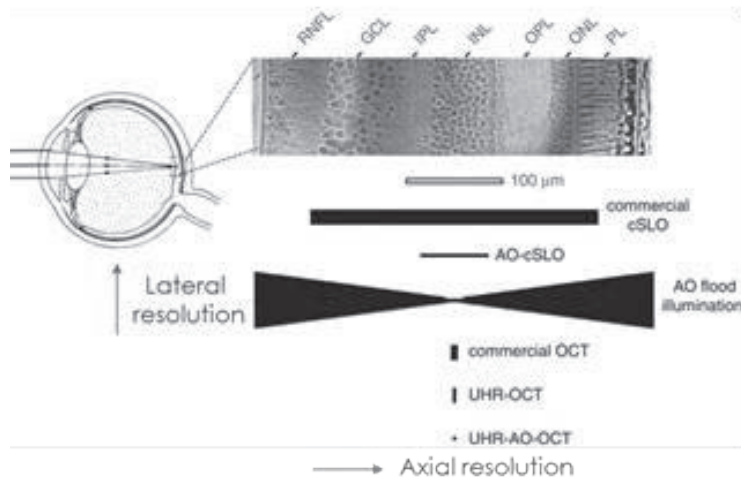


Figure 4-14. Schematic diagram of lateral and axial resolutions in different retinal imaging systems Commercial confocal scanning laser ophthalmoscope (cSLO), Confocal scanning laser ophthalmoscope with adaptive optics (AO-cSLO), Flood illumination with adaptive optics, Commercial OCT, Ultrahigh-resolution OCT (UHR-OCT), Ultrahigh-resolution OCT with adaptive optics (UHR-AO-OCT), Optical system is limited by the diffraction of light waves 0.013 arcsec. Practical limit to resolution is only about 1 arcmin ($\sim 5\mu\text{m}$) due to residual distortions. Adapted from (Miller, Kocaoglu et al. 2011)

Indeed, current concepts of the optical properties of the retina suggest that the outer segments of photoreceptors have a particularly high reflectance index as compared to other retinal structures; and, since in the posterior pole cones are larger than rods, the former are more easily detected (**Figure 4-15**). However, AO imaging has not yet entered routine clinical practice. This is partly due to the fact that interpretation of AO images in retinal diseases is not as straightforward as OCT; it is indeed sometime challenging because a number of factors may interfere with the obtained image. Among these factors are the level of pigmentation of fundus, the transparency of the retina, the presence of other sources of light dispersion in diseased retina, the spatial and temporal variability of photoreceptor reflectance, and the variable orientation of photoreceptor outer segments. Current softwares for photoreceptor counting are therefore affected by significant intersession variability.

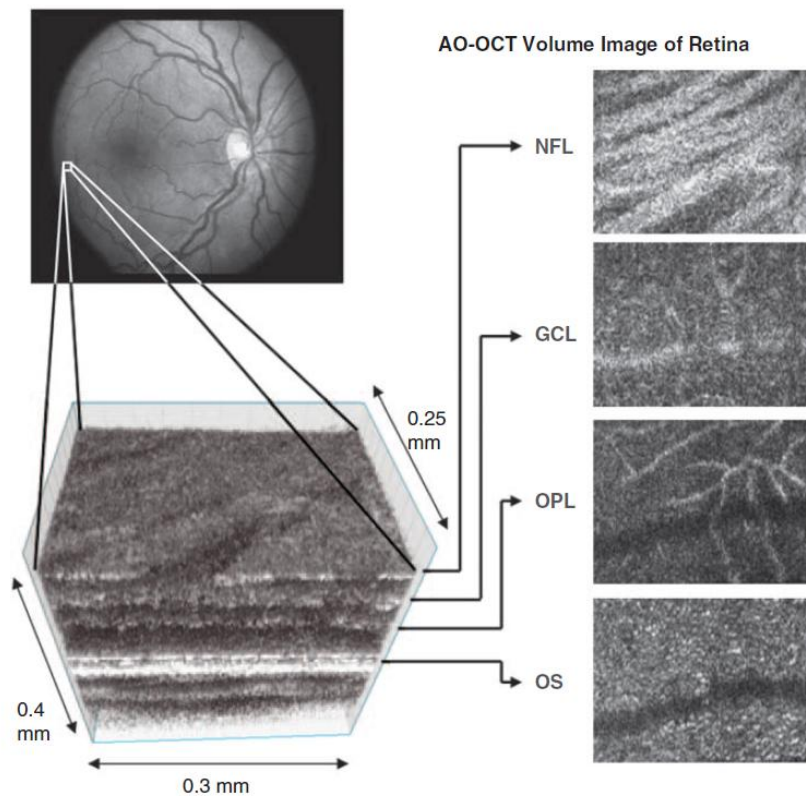


Figure 4-15. AO–OCT volume acquired over a 1° retinal region located temporal of the fovea, as illustrated by the rectangle in the fundus photograph. The images on the right are EnFace views of particular retinal layers extracted from the AO–OCT volume. Retinal layers from top to bottom are: nerve fiber layer (NFL), ganglion cell layer (GCL), outer plexiform layer (OPL), and outer segment layer of photoreceptors (OS). Adapted from (Miller, Kocaoglu et al. 2011)

Despite the above mentioned difficulties, most studies of AO imaging focused on photoreceptor imaging. This may have overshadowed other possible applications of AO imaging. Most AO imaging systems uses infrared light, which is highly absorbed by melanin. (Keilhauer and Delori 2006) It can be assumed that pigment redistribution reflect to some extent the degree of alteration of the RPE, as shown by histological studies. (Mrejen, Sato et al. 2014)

Cellular-level imaging has an increasing number of clinical applications as treatment options expand. Measurement of photoreceptor loss or rescue could be very useful in the evaluation of new pharmaceuticals, gene therapies or stem cell implants. The ability to reliably detect microscopic progression of geographic atrophy could also significantly help shorten clinical trials, limiting prolonged studies of dead-end approaches, saving time, money and effort.

The optics of the eye has been a major limiting factor in achieving lateral resolution capable of detecting cellular boundaries. Cones range in size from 4.0 microns down to 0.5 microns in the foveal center, while rods are typically 2.5 microns in diameter.

Williams, Liang, and Miller implemented adaptive optics, a technology first conceived for astronomy in 1953 to overcome atmospheric distortions, into an adaptive optics scanning laser ophthalmoscope (SLO) in 1997 (Liang, Williams et al. 1997, Williams 2011), allowing the visualization of the cone mosaic in the living eye (**Figure 4-15**). More recently, in 2011, Dubra and Carroll have advanced the optical design to 2 micron lateral resolution enabling clear images of rods (**Figure 4-14**). (Carroll, Kay et al. 2013)

Limitations of the technique are similar to those of any higher resolution system. Patients must have the ability to cooperate, possess clear media and a stable tear film. Operator skills are currently somewhat more demanding than standard systems and the very large data sets generated require adequate computer and storage capabilities.

The ability to zoom in on small lesions offers an unprecedented clinical view of histology and the OCT C scan tomographies allow dissection of the retina from a clinically familiar prospective. Refinement of the cellular density analysis holds the promise of earlier recognition of disease which will hopefully allow new proactive therapeutic interventions.

4.4.1.2. Adaptive Optics Fundus Camera in patients with retinal detachment

In many retinal diseases cone photoreceptors undergo degeneration, such as ARMD, or retinal dystrophies, like retinitis pigmentosa. Many retinal imaging systems have been used to visualize these changes on cones during the disease follow up (e.g. **Figure 4-16**). Other studies used histological cuts in order to understand better the pathogenesis of retinal diseases. With the development of AO system in ophthalmology, it has become possible to have the EnFace view of individual cones *in vivo*, using a non-invasive, alternative technique. With the AO imaging of cones, it became possible to monitor and to follow changes/disruptions in cone packing and brightness that occur with degeneration processes in photoreceptors. The OCT analyses of cone changes are mostly limited to eccentricities relatively distant from the fovea (greater than 4°), where cones are large and widely spaced (**Figure 1-4**). (Osterberg 1935, Miller, Kocaoglu et al. 2011)

In patients with RD, it is important to focus and to study changes in the photoreceptor level, especially in the macular region; i.e. cone changes (**Figure 4-16**). With the AO we were

able to access the outer segment layer of OCT (IS/OS zone; or ellipsoid zone) and to study several cone features:

- **Cone density** - the average number of cones in 1mm^2
- **Cone spacing** - average center-to-center distance in μm between two adjacent cones
- **Voronoi** - a summary of cone hexagonality where 6-sided cell shape is considered normal and consequently those cells with 3 or 9 neighbors are furthest away from normal

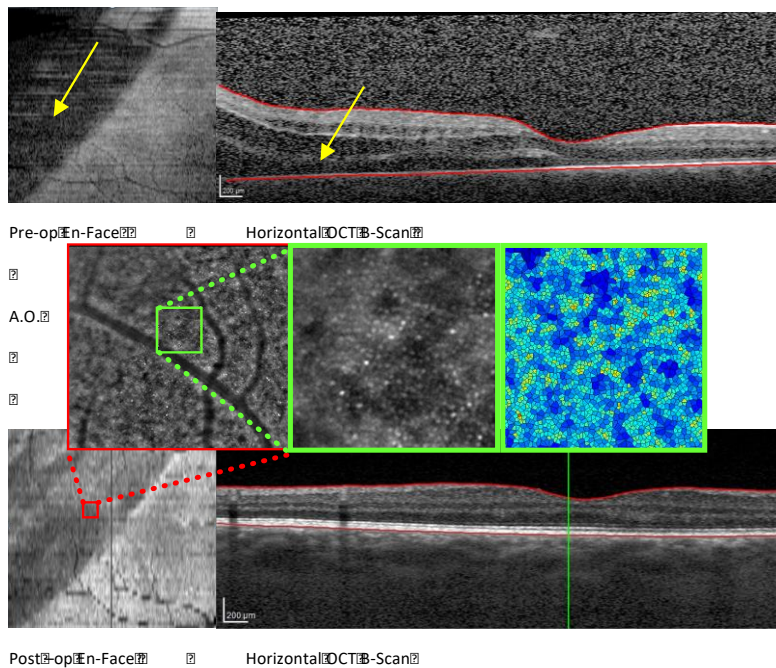


Figure 4-16. EnFace OCT image (preoperatively and post-operatively) and adaptive optics (postoperatively) of the same region in a patient with RD

4.4.2. Study design

Patients

All patients underwent a baseline/preoperative standard clinical exam: best corrected visual acuity (BCVA) measurement [logMAR]; intraocular pressure; fundus exam; SD-OCT scans were obtained using HEYEX software (version 1.7.1.0, Heidelberg Engineering, Heidelberg, Germany); axial length (using IOL Master 500, Carl Zeiss Meditec, Dublin, California, USA); and AO images (using RTX1, Imagine Eyes, Orsay, France). We created two groups depending on the preoperative macular status (as confirmed by OCT image): with detached macula (macula-OFF group) and with attached macula (macula-ON group). All

patients underwent transconjunctival 23g vitrectomy, cryocoagulation or endolaser and 23% SF6 gas tamponade and the same clinical assessment as before the surgery at one and three months postoperatively, as the visual acuity recovery is the fastest in this postoperative period. (Kobayashi, Iwase et al. 2017) In the early postoperative period, all patients underwent a steamroller maneuver to preclude subretinal fluid shift under the macula.

Adaptive Optics Retinal Camera

The device used for the study was rtx1™ Adaptive Optics Retinal Camera (software AOimage 2.0 version 002.000.20130111). The rtx1™ is an available camera based on a non-coherent flood-illuminated design with an 850-nm central illumination wavelength with a 4°×4° imaging field of view (1.2×1.2 mm on the retina) and a focusing range of 600 mm, allowing high-resolution imaging of cones. (Mrejen, Sato et al. 2014, Saleh, Debellemann et al. 2014)

We took AO images following full pupil dilatation (0.5% tropicamide), by adjusting the fixation target, and the imaging depth between 0 and -80µm. The spherical equivalence correction was used (between -12D and +10D). We took five images (central, 3°superiorly, 3°inferiorly, 3°nasally, 3°temporally) for each eye of each patient at month one and month three after surgery.

There were 204 patients recruited into the study, of them, 194 patients met the inclusion criteria. In 44 of the included 194 patients imaging with adaptive optics camera was not attempted, due to different reasons such as silicone oil tamponade, cataract, multifocal intraocular implants, bad lacrimal film, myopia > -12D, head trembling or nystagmus. Of the remaining 150 patients, only 22 patients had sufficiently good quality images such that the proprietary software was able to analyze the *region of interest* successfully in both eyes, at both time points (**ROI**; a square area 350x350µm of best image quality).

Alignment methodology and image analysis by AO Detect Mosaic

All included images had a signal to noise ratio of between 0.6 and 0.9 and were successfully analyzed with the proprietary software AO Detect Mosaic (v0.1, Imagine Eyes, Orsay, France). We used anatomical landmarks such as retinal vessels for manual alignment of overlapping AO images, fundus photography, and OCT images; a mosaic of available AO images was created using Photoshop (Photoshop CS6, Adobe System Inc., San Jose, CA). In this way, we were able to standardize the location, angle, and distance from the fovea between images and eyes (paired treated eye with fellow eye, and controls at month one and month

three on the same eye). We identified one ROI in each of the five images; at approximately the same degree (3 degrees) of retinal eccentricity from the foveal center in the same quadrant (**Figure 4-17, Figure 4-18**). (Curcio, Sloan et al. 1990, Lombardo, Serrao et al. 2013, Saleh, Debellemanni et al. 2014, Zhang, Godara et al. 2015) A trained observer performed the alignment and analysis of AO images.

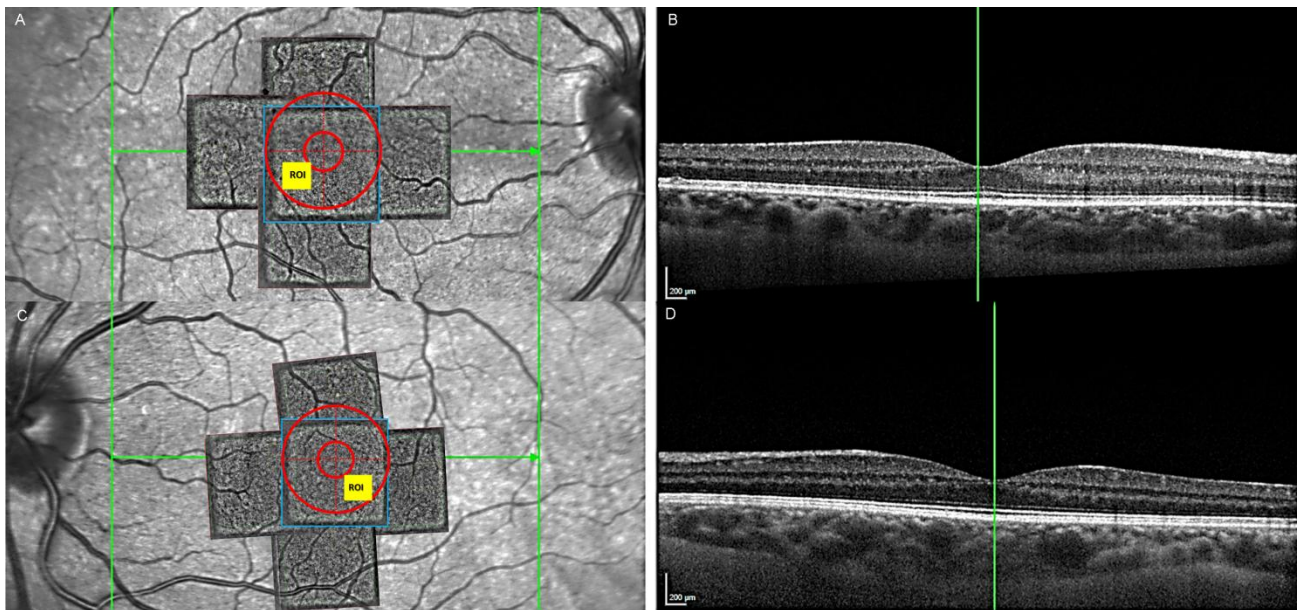


Figure 4-17. A-D Matching ROIs between treated eye at 1 month post-operatively and fellow eye **a)** Postoperative reflectance image used to determine the location of each AO image, the small and the large red circle denote the fovea and the macular region. The yellow square highlights the region of interest (ROI) in one AO image. **b)** Corresponding OCT image was used to denote exact location of the fovea and to center the red circle on the reflectance image **c)** Reflectance image and **d)** OCT image of the fellow eye used to denote fovea and to position AO images, matching with ROI location in affected eye (**1a**) with respect to location and eccentricity.

Of the 22 patients with AO images available in both eyes at M1 and M3, 11 had all 5 ROI, 6 with 4 ROI, 3 with 3 ROI, 2 with 1 ROI. There were multiple reasons for these exclusions such as the absence of complete overlap of images, selection of ROI inhibited by the presence of retinal vessels or due to poor image quality in a previously detached retina. We calculated the difference between the treated eye and the fellow eye and the difference between macula-OFF and ON RDs for the corresponding ROI. We performed this calculation for *cone density* (the average number of detectable cones in 1mm^2), *spacing* (spacing of cones is the average center-to-center distance in μm between two adjacent cones) and *Voronoi* (a summary of cone hexagonality where 6-sided cell shape is considered normal, and

consequently those cells with 3 or 9 neighbors are furthest away from normal) (**Figure 4-19**). Cone density, cone spacing, and Voronoi were analyzed by the proprietary software AO Detect Mosaic. This cell analysis incorporated the axial length for every eye of every patient.

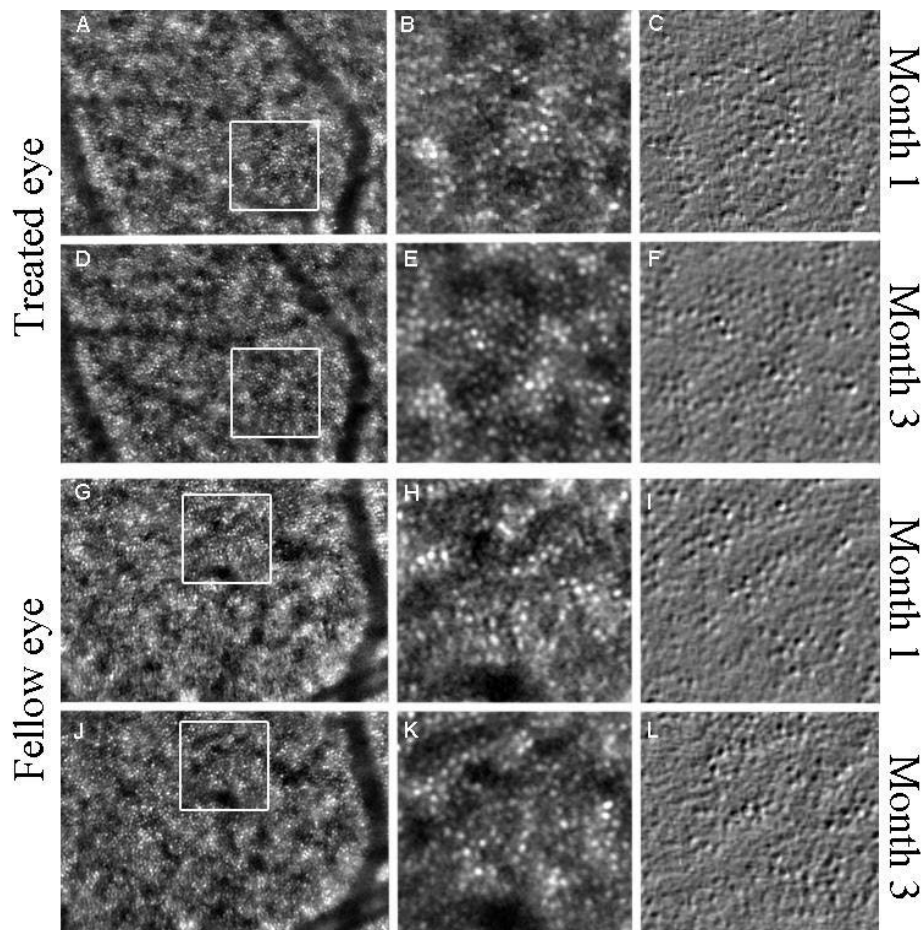


Figure 4-18. A-L Matching ROIs between treated eye at 1 and 3 months post-operatively and fellow eye at the same time-points (Cone-tracking)

A) Postoperative AO image at the treated eye, 1 month after surgery, with white square showing the region of interest (ROI) for analysis **B)** Enlarged ROI from the previous (1A) image **C)** The cone pattern at the selected ROI, from the previous (1B) image **D)** Postoperative AO image of the same treated eye at 3 months after surgery, with the white square demonstrating the ROI for analysis that is corresponding to the ROI from the 1a image, **E)** Enlarged ROI from 1D image, to be analyzed **F)** The cone pattern at the selected ROI, from the 1E image, demonstrating the same pattern as at the 1C image, showing the same cones to be followed and analyzed **G)** AO image from the fellow eye, at the same time-point taken as the treated eye (1 month after surgery of the treated eye), the AO image is matched with the AO image from the treated eye, using the vessels. The white square denotes the ROI to be analyzed, matching the same location as the ROI at the treated eye (1A image) **H)** Enlarged ROI from the 1G image **I)** The cone pattern of the Hh image, from the fellow eye **J)** AO image of the fellow eye matching the time-point with the 1D image of the treated eye, with the white square showing the ROI to be analysed. This ROI is matching with the ROI from the 1G image and is matching with 1D image (in eccentricity and orientation) from the treated eye **K)** Enlarged ROI from the 1J image, to be analysed **L)** The cone pattern from 1K image (ROI). This cone pattern is corresponding to the pattern at (1I) image, showing measurements of exactly the same cones over time.

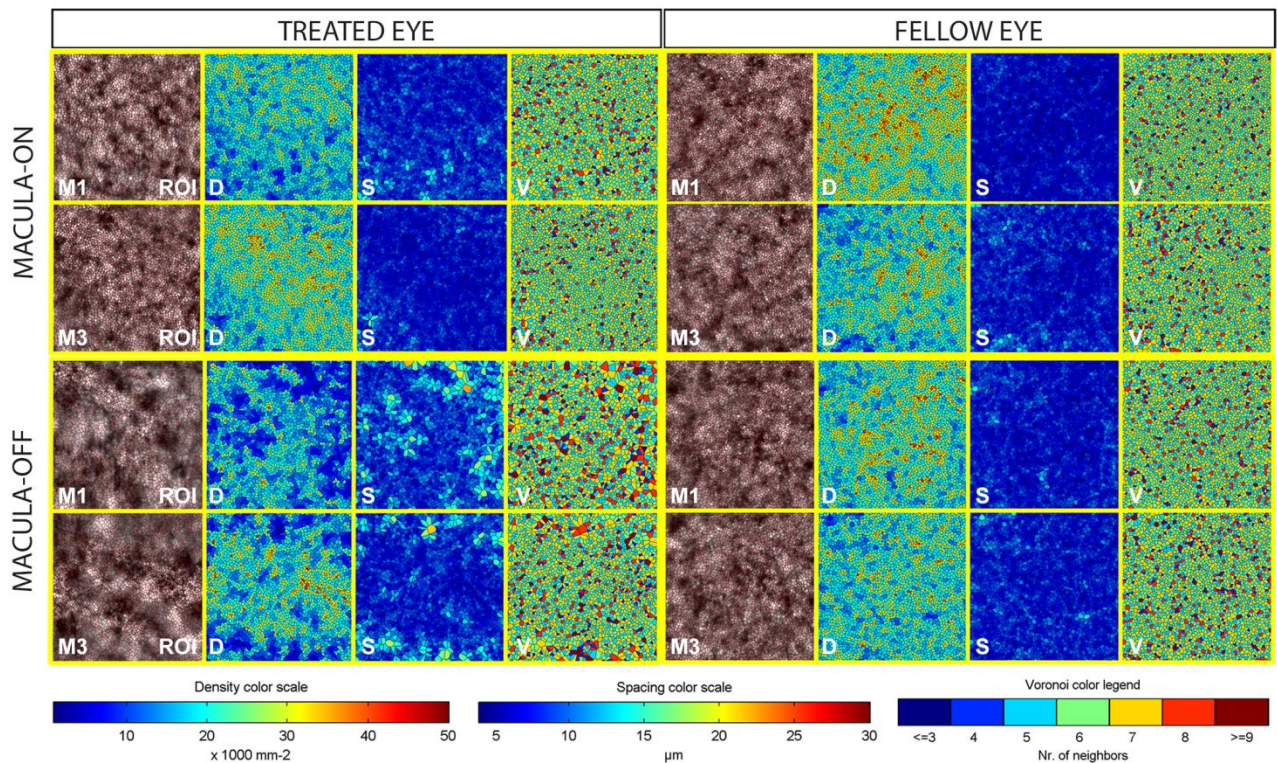


Figure 4-19. Analysed matching region of interests (ROIs) for density (D), spacing (S), and Voronoi (V) between treated and fellow eye at 1 month (M1) and at 3 months (M3) post-operatively, in macula-OFF and macula-ON patient. Note the improvement of cell density and the reduction in cell spacing over the 2 month period.

Spectral domain optical coherence tomography (SD-OCT)

All patients underwent SD-OCT imaging (EnFace and B-scans). We set the acquisition parameters to “high-speed resolution mode”; scan focus was corrected for the spherical equivalence of the patient. We selected the imaging pattern of 193 B-scans with 30µm separation and pattern size of 20° x 20° (5.8 x 5.8 mm). We analyzed the presence of microstructural foveal changes within 1mm in study patients. The following features were noted: disruption of the external limiting membrane (ELM); the presence of residual subretinal fluid (SRF); the presence of epiretinal membranes (ERM); and the presence of cystoid macular edema (CMO). (Wakabayashi, Oshima et al. 2009) Additionally we assessed a disruption of the photoreceptor interdigitation zone (IZ) at the central location which had been analyzed using AO.

Inter-eye difference (left eye – right eye)

Using histological counts Curcio et al. first described the widely varying peak in cone density between healthy post-mortem human retinas (high **inter-subject variability**). (Curcio, Sloan et al. 1990) More recently, using AO fundus camera *in vivo* in healthy subjects, Zhang et al. confirmed these results and described the comparatively low **inter-eye variability** and that there was no statistically significant **inter-eye difference**. (Curcio, Sloan et al. 1990, Zhang, Godara et al. 2015) **Inter-eye differences** are used in standard clinical care to detect bilateral asymmetric disease (e.g. glaucoma, diabetic retinopathy, keratoconus), and in monocular disease, a recent publication has reported postoperative recovery, with OCT, following macular hole surgery with the fellow eye as the control. (Yun, Ahn et al. 2017) In the majority of RD patients, only one eye is affected, and the fellow eye is considered “healthy” and thus the **inter-eye difference** is representative of damage due to RD. Given that **inter-eye variability** in cone density is markedly less than **inter-subject variability**, analyses using the **inter-eye differences** are more sensitive to detect any change due to RD.

Statistics

We examined the stability of the photoreceptor density and spacing measures of the fellow eye between month one and month three. We reported mean and standard deviations for all parameters apart from IOP and LogMAR BCVA, for these parameters we calculated median and interquartile range [IQR]. Analysis of variance (ANOVA) for repeated measures was used to assess the differences in cone spacing, cone density and Voronoi between groups (macula-ON vs. macula-OFF) and between time points (month one vs. month three). A p-value of less than 0.05 was considered to be statistically significant. Statistics were calculated using R version 3.1.3.

4.4.3. Results

Baseline characteristics

AO images of 22 patients (22 eyes with RD, 44 eyes in total) were suitable for analysis. There were 13 males and nine females included with a mean age of 53.3 ± 10.3 years. There was no statistically significant difference in age between macula-ON and OFF RDs ($p=0.85$). There were ten patients with macula-OFF RD and 12 in ON group. The mean axial length of the affected eye in the OFF group was 25.7 ± 1.8 mm and in the ON group 24.9 ± 1.4 mm. There were no significant differences in axial length between the type of RD

(macula-ON vs. macula-OFF) or between eyes (fellow vs. affected) (**Table 4-12**). The median BCVA at baseline was 2.0 [2.3-0.95] LogMAR in the OFF group, and 0 [0.1-0] in ON group, with a statistically significant difference between groups ($p < 0.001$) (**Table 4-12**). Postoperative follow-up showed improvement in BCVA in the OFF group: 0.35 [0.5-0.1] LogMAR at month one and 0.25 [0.3-0.1] LogMAR at month three ($p = 0.01$). In the ON group, BCVA was 0.05 [0-0.1] LogMAR at one month after surgery and improved to 0 [0-0] LogMAR three months after surgery (**Table 4-12**).

Table 4-12. Baseline characteristics and visual acuity

		Macula-ON (n=12)		Macula-OFF (n=10)	
Baseline characteristics	Mean age	53.3±10.3 years			
	Sex	13 men and 9 women			
	Axial length	24.9±1.4mm (TE)	24.9±1.3mm (FE)	25.7± 1.8 mm (TE)	25.9±1.7mm (FE)
No. patients		12		10	
BCVA median logMAR [IQR]	Pre-op	0 [0.1 to 0]		2 [2.3 to 0.95]	
	Post-op M1	0.05 [0.1 to 0]		0.35 [0.5 to 0.1]	
	Post-op M3	0 [0 to 0]		0.25 [0.3 to 0.1]	

TE: treated eye, **FE:** fellow eye, **BCVA:** best corrected visual acuity, **IQR:** interquartile range

Photoreceptor changes between treated and fellow eye during follow-up

The cone density of the fellow eyes remained stable at month one and month three, 15170 ± 3882 cones/mm² vs. 15023 ± 3629 cones/mm² ($p = 0.67$, paired t-test); in **Table 4-13** additional summary measures of the fellow eye indicate stability during follow-up. One month postoperatively there was a statistically significant difference in cone density between treated and fellow eye in both groups (macula-ON: $p = 0.001$, macula-OFF: $p = 0.01$) (**Table 4-13**). There was no significant inter-eye difference in photoreceptor density between month one and month three in OFF eyes ($p = 0.97$), but there was a statistically significant improvement observed in ON eyes ($p = 0.02$). There was a statistically significant improvement in spacing in macula-ON eyes over time ($p = 0.05$), but not in the macula-OFF group ($p = 0.73$) nor Voronoi ($p = 0.39$, $p = 0.58$) (**Table 4-13**). The changes in Voronoi measures are summarized graphically in **Figure 4-20**; we observed an increase of irregularly shaped cells and reduction in hexagonal cells between treated and the fellow eye for macula-OFF RD type.

Intereye difference in number of neighbouring cells (Voronoi)

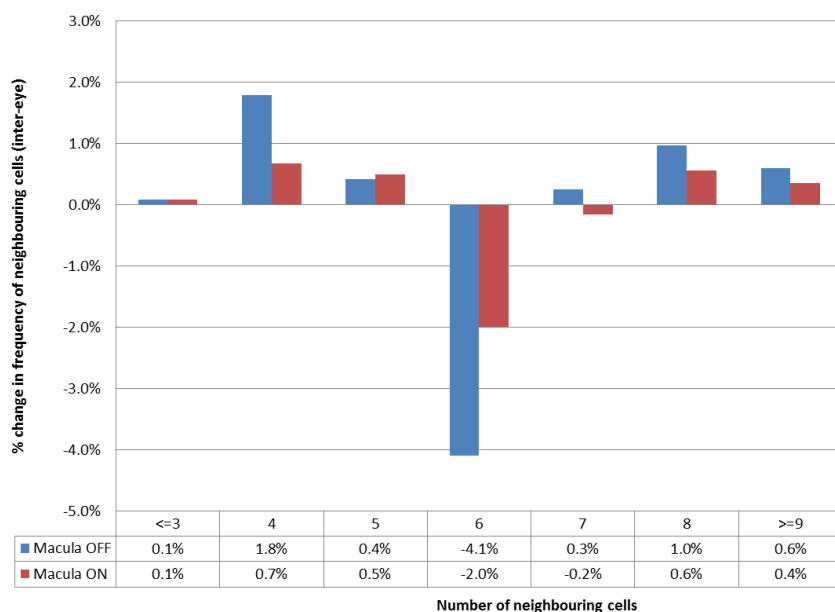


Figure 4-20. Change in distribution of the number of neighbors as compared to fellow eye (Voronoi)

In patients with macula-OFF RDs (blue) there is 4% reduction of hexagonal cells compared to the fellow eye, whereas in macula-ON RDs (red) this difference was only 2%. The differences in irregularly shaped cells with fewer or more than 6-sides were also more pronounced in the macula-OFF RDs.

Table 4-13. Summary measures of cone topography in fellow-eyes, macula-ON and macula-OFF groups at month 1 and month 3 after surgery

		Fellow eyes	Macula-ON			Macula-OFF		
	Time point	Mean values	Mean values TE	TE vs FE p-value	Inter-eye difference (TE-FE)	Mean values TE	TE vs FE p-value	Inter-eye difference (TE-FE)
Cone density (cones/mm ²)	Post-op M1	15170 ±3882	13261 ±3565	0.001	-1504 ±4068	11207 ±3183	0.005	-3676 ±3976
	Post-op M3	15023 ±3629	15517 ±3117	0.01	-698 ±4208	11058 ±3349	0.004	-3384 ±4408
	M1 vs M3 p-value	0.67	0.11		0.02	0.96		0.97
Cone spacing (µm)	Post-op M1	9.16 ±1.26	9.79 ±1.51	0.005	0.50 ±1.63	10.68 ±1.59	0.002	1.38 ±1.64
	Post-op M3	9.19 ±1.27	8.95 ±0.89	0.02	0.18 ±1.26	10.54 ±1.50	0.002	1.18 ±1.87
	M1 vs M3 p-value	0.68	0.12		0.05	0.95		0.73
Voronoi Ratio of irregular neighbors	Post-op M1	1.45 ±0.27	1.58 ±0.26	0.14	0.10 ±0.32	1.67 ±0.25	0.03	0.27 ±0.30
	Post-op M3	1.44 ±0.26	1.46 ±0.22	0.07	0.06 ±0.41	1.71 ±0.26	0.52	0.18 ±0.32
	M1 vs M3 p-value	0.83	0.16		0.39	0.64		0.58

Foveal microstructure changes (SD-OCT)

Foveal microstructure changes within 1mm radius from the fovea were reviewed. In the macula-OFF group, at one month after surgery, 3/10 presented with interruption of the ELM, 1/10 with ERM and 1/10 with 19 μ m SRF. At three months after surgery, only one patient had an interruption in ELM and 2/10 patients had ERM. There was no patient with cystoid macular edema. In the macula-ON group, none of the patients showed foveal microstructural changes at month one, and one patient developed ERM at month three after surgery.

Using the available OCT and AO images, the disruption of IZ, retinal thickness, and cone density were assessed at the central ROI, in both fellow and treated eyes. Significantly more treated eyes showed IZ disruption (14/22) than fellow eyes (4/22, $p=0.001$). Moreover, 5 of the macula-ON eyes presented with IZ disruption. We observed that the cone density was reduced with respect to IZ disruption, in fellow eyes (with IZ disruption 15570 ± 2023 cones/ mm^2 vs. without IZ disruption 17502 ± 4298 cones/ mm^2) and in treated eyes (with IZ disruption 12614 ± 3297 cones/ mm^2 vs. without IZ disruption 16484 ± 3206 cones/ mm^2). In eyes without IZ-disruption there was no significant difference in cone density between treated and fellow eyes ($p=0.63$), but there was a significant difference between the treated eyes with and without central IZ disruption ($p=0.025$). Retinal thickness was not correlated with cone density (R-squared=0.002) nor with presence of IZ disruption ($p=0.95$).

Correlation between visual acuity and cone density in treated eyes

We transformed cone density to a log scale for comparison with LogMAR BCVA. In **Figure 4-21** the relationship between log cone density and type of RD (macula-ON or macula-OFF) can be seen. Additionally, the improvement in log cone density between month 1 and month 3 in macula-ON eyes is evident. Furthermore, logMAR BCVA is dependent on the type of RD and the cone density. Using MANOVA for repeated measures, we observed that higher log cone density was positively significantly and independently correlated with better BCVA and RD without macular detachment ($p=0.004$, $p=0.000$).

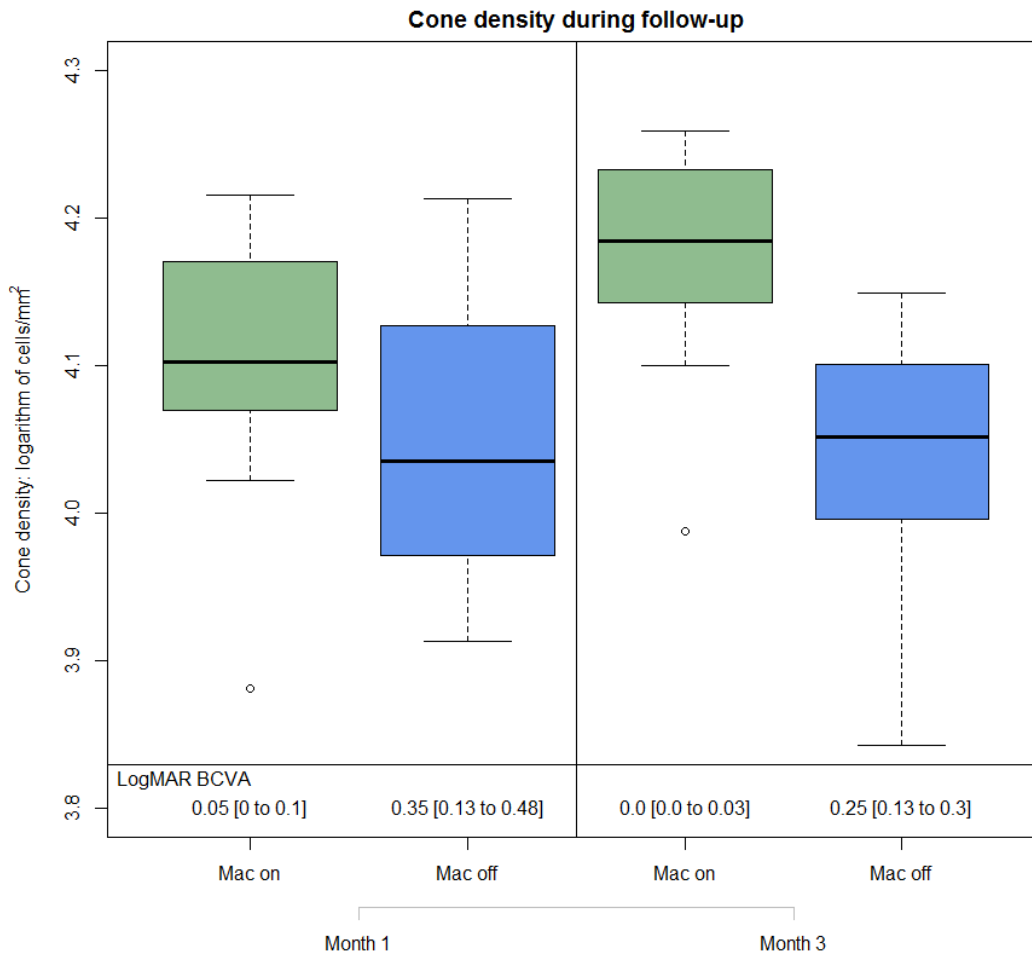


Figure 4-21. The relationship between log cone density, type of RD (macula-ON or macula-OFF) and BCVA over time (month 1 and month 3). The improvement in log cone density is evident between month 1 and month 3 in macula-ON eyes. BCVA and RD type are independently correlated with log cone density ($p=0.004$, $p=0.000$).

4.4.4. Discussion

In our study, we found that there is a statistically significant interocular difference between OFF and ON groups in both cone density and cone spacing following PPV. Furthermore, we observed a substantial improvement in cone density in ON group between month 1 and month 3 and positive correlation with BCVA.

Modifications in photoreceptor topography (density, spacing, and Voronoi) associated with retinal pathologies (AMD, macular dystrophies, and myopia), is an active area of current research. (Kitaguchi, Bessho et al. 2007, Mrejen, Sato et al. 2014, Ziccardi, Giannini et al. 2015) To date there are two reports on the use of AO fundus camera in eyes following macula-OFF RD but not in patients with macula-ON RD. (Saleh, Debellemanni et al. 2014, Ra, Ito et al. 2017) The two studies differ in patients' selection and methodology. The first

study included patients who underwent pars plana vitrectomy for RD with very short-term follow up, (Saleh, Debellemaniere et al. 2014) whereas the second study included only patients who underwent scleral buckle surgery for RD with long-term follow up. (Ra, Ito et al. 2017) Saleh et al. described a cone density loss of 30% over fellow eye at six weeks postoperatively (Saleh, Debellemaniere et al. 2014) while in the second study cone density increased between 6 and 12 months after surgery by 45% but remained significantly lower (39%) compared to fellow eye. (Ra, Ito et al. 2017) Cone density was also significantly correlated with VA in the treated eye. The results of our study correspond well with these reports.

What is new in this study using an AO fundus camera in patients with macula-ON and macula-OFF RD, is our observation that macula-ON eyes had a significant reduction in cell density over fellow eyes, but had significantly less reduction in cell density than macula-OFF eyes. Moreover, between month one and month three we observed a significant increase in cone density and a decrease in spacing of cones following macula-ON RD. The pattern of greater cellular damage in macula-OFF patients, shown in AO images analysis, corresponds well with our findings on SD-OCT and is consistent with previous reports. (Wakabayashi, Oshima et al. 2009, Okamoto, Sugiura et al. 2013)

The observed increase in cone density in macula-ON RDs between one and three months postoperatively was unexpected. Several mechanisms could explain these observations. Reports have shown that in healthy subjects, the misalignment with an off-axis illumination of cones will reduce cell estimations. (Stiles and Crawford 1933, Roorda, Romero-Borja et al. 2002, Miloudi, Rossant et al. 2015, Morris, Blanco et al. 2015) A similar effect could be present in RD patients in whom we observed reduction (density) and disorganization (spacing, Voronoi) of cone array as compared to fellow eyes, following both macula-ON and macula-OFF RD. The disorientation and disarray of photoreceptor cells may be due to changes in polarity of the cells. The origin of the distress is most probably mechanical and/or metabolic, such as the effect of surgery, the contact of the retina with the gas bubble, the tamponade composition or the type of RD. After retinal reattachment, the distress dissipates and cones become reorganized and realigned and hence again visible with AO imaging. (Roorda, Romero-Borja et al. 2002, Roorda and Williams 2002, Morris, Blanco et al. 2015) Some previous studies have demonstrated that “retina wants to stay attached,” i.e., the interphotoreceptor (cone) matrix very firmly adheres to the RPE. This adherence could explain our observations in macula-ON RD, where the cone sheaths became very stretched

but attached to the RPE surface, giving the impression of increasing cone density with time. (Hageman, Marmor et al. 1995) Our data correlate well with these observations.

Despite the surgical success, visual outcomes after RD involving the macula can be disappointing. To date, the precise cellular mechanisms that underlie vision loss associated with RD are not entirely understood. (Kubay, Charteris et al. 2005) Saleh et al. have reported a correlation between cellular changes and visual impairment. (Saleh, DeBellemaniere et al. 2014) This observation correlates well with our study findings, where clinically measurable visual acuity loss after RD repair (defined as a difference of more than 0.2 logMAR between both eyes) was associated with an inter-eye difference in cone density of >30%. A recent article by Yokota et al. with AO images taken after macular hole closure also reported a ratio of cone loss exceeding one-third, coinciding with a decrease in visual acuity. (Yokota, Ooto et al. 2013, Saleh, DeBellemaniere et al. 2014) Depending on the patient, postoperative interocular asymmetry in cone density may, however, not always manifest itself as visual acuity loss. A minor, yet significant reduction in cell density or disruptions in interdigitation zone and the external limiting membrane may be at the origin of postoperative metamorphopsias. (Murakami, Okamoto et al. 2017)

The high packing density in the foveal area is beyond the limitations of AO imaging as the current resolution of the rtx1 AO fundus camera is 4 μ which is insufficient to measure cone density at the foveola. (Muthiah, Gias et al. 2014) Also, the inter-subject variability in photoreceptor density is lower outside the central 2°, which increases the reliability of interocular comparisons. (Curcio, Sloan et al. 1990, Zhang, Godara et al. 2015) For these same reasons Saleh et al. and Ra et al. imaged cones at 2° of eccentricity. (Saleh, DeBellemaniere et al. 2014, Ra, Ito et al. 2017) We also respected this limitation of the device and concentrated our measures to the regions corresponding to between 3° and 10° from the fovea. This area will consist primarily of cones (>95%), limiting the risk of rods that can be erroneously marked as cones during the automated detection of cones. (Osterberg 1935, Curcio, Sloan et al. 1990)

In our study data, image quality was often poorer at month one than at three months postoperatively, and this may be due to the gas tamponade or the low contrast of the fixation device. In the future, this type of technical limitations of the AO fundus camera is expected to be reduced with the use of the split detector (AO-SLO) or improving AO fundus camera features. (Scoles, Flatter et al. 2016) Also, some of our patients developed a cataract postoperatively which reduced image quality at three months. An additional unforeseen impediment was that previously detached retina often had a blurred appearance on AO fundus

camera. This blurring may be due to an imperfect axonal realignment of the cones post-operatively or micro-deformations of the retina that allow a previously bullous detachment to reattach. All of these considerations impeded the performance of the AO Detect mosaic software. In turn, this restricted the analysis for the selection of the ROI on all images, matching M1 and M3. As we needed to compare the same area, with the same orientation and eccentricity, the loss of one image at a given time-point or orientation, resulted in the removal of one complete dataset (4 images) from the analysis. The majority of these issues can potentially be resolved with future versions of the software and device and should not restrict the clinical utility of this method in the long-term.

4.4.5. Conclusion

This study reports the clinical use of AO fundus camera in the diseased retina, with a two-time point follow up. Also, we observed the statistically significant and independent correlation between cone density, type of RD and postoperative BCVA over time. The AO fundus camera could quantify a more substantial reduction in cone density and an increase in cone spacing in the macular region of eyes following PPV for RD. Even at month three after complete reattachment and with no apparent changes in retinal layers on SD-OCT, the alterations in cone mosaic were visible in operated patients, especially in those who suffered from a macula-OFF RD. Surprisingly the post-operative macular cone density was also reduced in macula-ON RD although this drop recovered after three months.

AO fundus camera is thus capable of detecting subclinical changes of photoreceptors at a cellular level and may prove useful in the future as a tool to document cellular recovery following therapeutic agents or to predict the long-term postoperative functional outcome.

4.5. EXPERIMENTAL BASIC SCIENCE RESEARCH IN RETINAL DETACHMENT

4.5.1. Introduction

Retinal detachment (RD) is one of the most common causes of photoreceptor cell death worldwide. (Subramanian and Topping 2004) Photoreceptor cells die when they are physically separated from the underlying retinal pigment epithelium (RPE) and choroidal vessels, which provide metabolic support to the outer layers of the retina. Although various pathological changes occur in detached retina, (Anderson, Stern et al. 1981, Lewis, Guérin et al. 1994, Jablonski, Tombran-Tink et al. 2000) studies on experimental models have shown that photoreceptor cell death is immediately induced as early as 12h and peaks at around 2-3 days after RD. (Cook, Lewis et al. 1995, Hisatomi, Sakamoto et al. 2001, Arroyo, Yang et al. 2005) This indicates that early intervention could potentially preserve the photoreceptors, improving the visual acuity of patients who undergo both early- and late-stage reattachment procedures.

Currently, the knowledge of photoreceptors degeneration processes is not fully understood. Indeed, in rodent models of RD, cell death and apoptotic factors such as cytochrome C/caspase-9 and apoptosis inducing factor (AIF) were detected 3 days post detachment (Hisatomi, Sakamoto et al. 2001, Hisatomi, Sakamoto et al. 2002) Similar observations were obtained in RD human retina, (Hisatomi, Nakazawa et al. 2008) but the use of anti-apoptotic factors in clinical situation was poorly effective suggesting that other pathways are also activated during the cell death process. (Arroyo, Yang et al. 2005) Supporting this hypothesis, the combination of Z-VAD (pan-caspase inhibitor) with the anti-necrotic factor Necrostatin-1 (Nec-1) enhanced photoreceptor survival. (Trichonas, Murakami et al. 2010)

Photoreceptor cell death also underlies the pathology of other retinal disorders such as retinitis pigmentosa (RP), age-related macular degeneration (AMD), and also the light-damage of the retina; it is the basis for visual decline. (Sahaboglu, Paquet-Durand et al. 2013, Zencak, Schouwey et al. 2013, Farinelli, Perera et al. 2014) Although the causes and clinical characteristic of each retinal disorder differ, accumulating evidence suggests that some molecular pathways leading to photoreceptor cell death appear to be shared by these diseases at least in part. (Sancho-Pelluz, Arango-Gonzalez et al. 2008, Murakami, Notomi et al. 2013, Zencak, Schouwey et al. 2013)

The data from literature show an increasing amount of evidence to suggest that cell cycle events play a key role in neurons committed to apoptosis in several neurodegenerative diseases, (Herrup and Yang 2007) and clearly shows the importance of G1/S phase regulators in this process. (Al-Ubaidi, Hollyfield et al. 1992) Models of neurodegenerative disease show that neurons committed to cell death re-express cell-cycle related proteins, (Vincent, Rosado et al. 1996, Yang, Geldmacher et al. 2001, Nguyen, Boudreau et al. 2003, Höglinger, Breunig et al. 2007) where post-mitotic neurons start to express nuclear cyclin-dependent kinase 4 (CDK4), implicated in the re-entry into the cell cycle and in the transition from G1 into S-phase.

Another important pathway was recently identified to have the role in retinal degeneration – DNA methylation. (Wahlin, Enke et al. 2013) However, it is still poorly known how DNA methylation patterns vary between different genes in healthy and diseased tissues. (Barski, Cuddapah et al. 2007, Otteson 2011, Wahlin, Enke et al. 2013, Farinelli, Perera et al. 2014) Data of Farinelli et al show an increase in DNA methylation in dying photoreceptors in several RP animal models analyzed, suggesting DNA hypermethylation as a common denominator in the photoreceptor degeneration pathway. (Farinelli, Perera et al. 2014) Interestingly, interference with DNA methylation is beneficial for degenerating photoreceptors. Their findings thus suggest a complex relation between DNA methylation and retinal degeneration, which may include both disease-driving and disease-counteracting elements. (Farinelli, Perera et al. 2014)

In this study, we investigated human retina to have a better comprehension of the cell death mechanisms that may occur in patients affected by RD. This study aims to reveal whether apoptosis, cell cycle reentry and epigenetic modifications, are also involved in an *in vitro* model of human RD, which was shown to activate different pathways during the initiation of photoreceptor degeneration.

4.5.1.1. CELL DEATH

RD is a common cause of photoreceptor cell death. (Subramanian and Topping 2004) Studies in both humans and animal models have shown that photoreceptor cell death is induced as early as 12 hours after RD. (Zacks, Han et al. 2006, Yu, Peng et al. 2012) This timing indicates that early intervention could potentially preserve the photoreceptors, improving the visual acuity of patients who undergo both early- and late-stage reattachment procedures. Currently, the knowledge of photoreceptors degeneration process is very poorly understood. Therefore, the first step to develop an effective therapeutic agent is to determine the underlying disease mechanisms to identify the most appropriate means for intervention.

Photoreceptor cell death, as the consequence of different retinal disorders, such as RD, causes vision loss. There are different types of cell death but literature review suggests that the programmed cell death (i.e. apoptosis) pathway is activated in the most cases of photoreceptor death (e.g. in RD). (Murakami, Notomi et al. 2013) Different mechanisms can induce apoptosis. In experimental RD models it is observed that the central activation role belongs to the caspase family. On the contrary, it is reported that anti-caspase substances can't protect photoreceptors from inevitable cell death. This implies that some other mechanisms are also playing an important role. (Murakami, Notomi et al. 2013)

RD represents the separation of the neurosensory retina from the RPE and choroid; thus, the metabolism in the whole retina and even more in its outer parts is compromised, being without oxygen and nutrient support and bringing photoreceptors into the death.

The detached retina is exposed to different pathological changes (**Figure 4-22**), that don't appear at the same time. (Anderson, Stern et al. 1981, Lewis, Guérin et al. 1994, Jablonski, Tombran-Tink et al. 2000) In the experimental studies, mostly in rodent models, but also in a human retinal sample, is observed that the photoreceptors cell death starts already after 12 hours, and reaches its peak after 2-3 days from the RD. (Cook, Lewis et al. 1995, Hisatomi, Sakamoto et al. 2001, Arroyo, Yang et al. 2005)

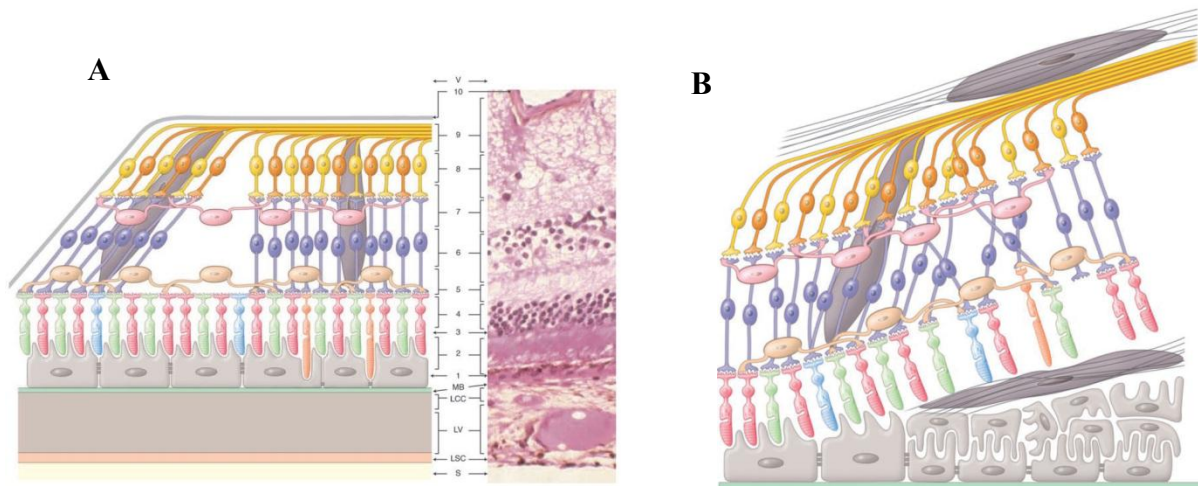


Figure 4-22. Histology of the normal retina (A) and detached retina (B), adapted from (Caputo, Metge et al. 2012)

A) Normal retina-layers: 1-retinal pigment epithelium, 2-outer photoreceptors' segments. 3-external limiting membrane, 4-external nuclear layer, 5-outer plexiform layer, 6-inner nuclear layer, 7-inner plexiform layer, 8-nuclear ganglion layer, 9-retinal nerve fiber layer, 10-inner limiting membrane

B) Alterations in the retina due to RD: retraction of the apices of the RPE microvilli, RPE cells proliferation, apoptosis of some photoreceptors, shortening of the "survivor" photoreceptors' outer parts, rounding of cones' synapsis, retraction of rods' synapsis, epiretinal and subretinal proliferation.

Visual loss due to photoreceptor cell death happens in many retinal diseases, apart from RD, such as retinitis pigmentosa, AMD. In these chronic disorders cell death pathways are better understood, but not solved; therefore, there might be overlapping with cell death pathway in patients with RD. This could be of great interest to identify key-role players, in order to find a new treating agent. (Murakami, Notomi et al. 2013)

Types of cell death

There are three described types of cell death: apoptosis, autophagy, and necrosis. Distinct cell morphological alterations demarcate each of them, (Kroemer, Galluzzi et al. 2009, Galluzzi, Vitale et al. 2012) as follows:

- *Autophagy*: is characterized by the changes in the cytoplasm, i.e. creation of autophagosomes and autolysosomes. There is no cellular – level changes (e.g. condensation and fragmentation are absent)
- *Apoptosis* is characterized by reduction of the cell size (volume) that is becoming more round and engulfing (due to a phagocyte) and key-important cytoplasm and nucleus that are becoming condensate.

- *Necrosis*, on the contrary of apoptosis, is characterized with the cellular bigger shape (increased volume), swelling of the cytoplasm and organelle around, and consequently the break of plasma membrane, and links with extracellular cavity (Murakami, Notomi et al. 2013).

Given that apoptosis and necrosis are present in photoreceptor degeneration in RD, it implies that the DNA degradation happens consequently followed by irreversible cellular changes. (Rowe, Erie et al. 1999, Yu, Peng et al. 2012, Matsumoto, Miller et al. 2013) After this event, it is not possible to regenerate a photoreceptor. Cell death prevention is a key in conserving retinal integrity.

The common question is why cell death occurs in RD patients; more precisely what is causing the death. Yu et al. observed in a vitreous sample (from RD patients) the up-regulation of inflammatory mediators (part of complement system). (Yu, Peng et al. 2012)

Apoptosis

Apoptosis, programmed cell death is characterized by specific cellular changes. (Alberts, Johnson et al. 2015) Apoptosis can start in two different ways: extrinsic (cell-death receptors on the cell surface) or intrinsic (mitochondrial) pathways (response to stress or developmental signals). Cellular surface bulges and becomes chemically transformed, so it can be quickly and easily eaten by a macrophage. If the cell is too big, it splits into apoptotic bodies. While apoptosis, the cytoplasm starts to condensate and collapse and the nucleus chromatin condensates as well and divides into fragments, while the nuclear envelope takes to pieces. Apoptosis doesn't cause the inflammatory response as the cell doesn't leak its content into the environment; microglia and macrophages digest it before that. (Alberts, Johnson et al. 2015) This is the reason why, even when many cells die via apoptosis, there are few dead cells to be seen, as they are devoured quickly. (Alberts, Johnson et al. 2015)

Necrosis

Cells dying as the consequence of a sudden event (eg. trauma, infarctus) usually activate necrosis pathway for the cell death. On the opposite to the clean programmed cell death (apoptosis) where the cell content can't be found in the environment, necrotic cells spill their content and cause the inflammatory reaction. Typically, these cells are swelling and rupturing. Necrosis starts as the consequence of the energy weakening, and is correlated with

disruption of ionic gradient that is, under normal circumstances, present in the cell membrane. Consequently, there is a problem in cell metabolism as well. (Alberts, Johnson et al. 2015)

Autophagy

Autophagy is a third described type of cell death. Commonly, it occurs as the answer to metabolic stress. (Chinskey, Zheng et al. 2014) The process that is typical for autophagy is forming a vacuoles of the cellular waist (demolished cell fragments) (i.e. creating autophagosomes) that are merged with lysosomes, destroyed with enzymes and metabolized back in the cell. (Besirli, Chinskey et al. 2011) Other authors reported that the autophagy in photoreceptors is present as part of a basal metabolism of rod outer segments (Remé and Sulser 1977), and in some models of retinal diseases. (Kunchithapautham and Rohrer 2007, Kunchithapautham and Rohrer 2007)

Interestingly, as autophagy is activated by the same mechanism as the apoptosis (Fas-dependent), its activation in RD models showed its protective role, at least at the beginning. (Besirli, Chinskey et al. 2011, Chinskey, Zheng et al. 2014) Being activated by the same mechanism, the studies showed that autophagy is activated as the protector of detached retinas from the apoptosis (blocking apoptosis), at least for the first 7DIV from RD, when there is a switch to apoptosis. The exact mechanisms are unknown and not fully understood. (Besirli, Chinskey et al. 2011, Chinskey, Zheng et al. 2014)

4.5.1.2. THE CELL-CYCLE

The cell cycle consists of several important phases, common for almost all the cells. (Herrup and Yang 2007, Alberts, Johnson et al. 2015) The appropriate timing to proceed over several cell cycle phases is crucial for every cell and consequently for the functioning of the whole organism. This timing is controlled by several factors, mostly proteins. There are four phases that are recognized as parts of cell cycle (**Figure 4-23**): (Alberts, Johnson et al. 2015)

- *G1 (Gap or Growth 1) phase* is the beginning of cell cycle. In this phase the cell is growing. There are many controllers of this phase that we can also divide on early G1, late G1 but also G0. In the early G1 the cells are growing. The late G1 phase is the preparation of the cell for DNA synthesis. This stage is controlled by tumor suppressor gene retinoblastoma (Rb) and transcription factor E2F1. G0 is a phase for the highly differentiated cells that normally don't divide (**Figure 4-23**). (Herrup and Yang 2007)

- *S phase (synthesis)*: replication of the complete genome, at the end of this phase there is a double content of DNA. (Herrup and Yang 2007)
- *G2 (Gap or Growth 2 or interphase) phase*, short phase, while organizing and collecting constituents that will organize the chromosomes and split the cell. (Herrup and Yang 2007)
- *M (Mitosis) phase* is the final aim of the cell cycle. It represents the division of the cell into two daughter cells that will now re-enter the G1 and re-start all the cell cycle. The process of cell division is very complex and is controlled by many factors in order to separate equally and gives same amount of the genetic material, to both daughters (Figure 4-23). (Herrup and Yang 2007)

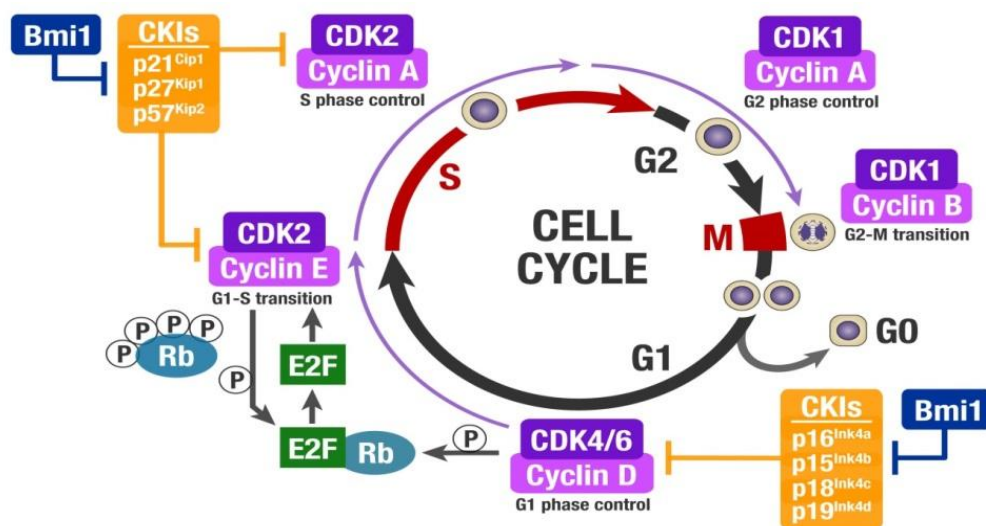


Figure 4-23. Cell cycle phases and regulators. Phases are controlled by many factors, mostly a subset of proteins, such as cyclins, cyclin-dependent kinases (CDKs), retinoblastoma protein (RB) together with other proteins (P107 and P130), and the E2F family of transcription factors. Adapted from (Herrup and Yang 2007)

The cell-cycle control system

The cell cycle control system is following the whole cell cycle in order to react and correct if there is any “mistake” (the cell might stop before finishing the entire cycle either the cell might be perturbed by uncomplimentary conditions) (Figure 4-23). The information about the “mistake” can be given by intra- or extra- cellular signals. (Alberts, Johnson et al. 2015)

Cyclin-dependent protein kinases (CDKs)

Cyclin-dependent protein kinases (CDKs) belong to important protein family to protect and control the cell cycle. Their activities are related to their activation through their cyclin subunits. Cyclin-CDK complexes might be different and might have alterations; thus, these complexes control different phases or steps in the cell cycle. (Lees 1995, Alberts, Johnson et al. 2015)

The CDKs are controlled by a variety of proteins/enzymes. CDKs are generally constantly present. The alterations of cyclical changes in cyclin levels depending on the cell cycle phase are the consequence of different activation and gathering of cyclin-CDK complexes.

Depending on the cell cycle phase, there are four types of cyclins that will bind with CDKs. In eukaryotic cells three of the following complexes are obligatory:

1. **G1/S – cyclins** are responsible for the “pledge” of the cell to enter the cell cycle. They are activated late in G1. The level is decreasing after G1.
2. **S-cyclins** are responsible for chromosome duplication phase, their level is high until mitosis; so they control the beginning of mitosis
3. **M-cyclins** is responsible for the G2/M switch. Their levels decrease during mitosis.

All four CDKs have their important role in vertebrate cells. They match with cyclins as follows: two CDKs link with G1-cyclins, one with G1/S- and S-cyclins; one with S- and one with M-cyclins (**Table 4-14**). (Alberts, Johnson et al. 2015)

Table 4-14. The major cyclins and CDKs of vertebrates

Cyclin-CDK complex	Cyclin	CDK-partner
G1-CDK	Cyclin D	CDK4, CDK6
G1/S-CDK	Cyclin E	CDK2
S-CDK	Cyclin A	CDK2, CDK1
M-CDK	Cyclin B	CDK1

According to current studies, cyclin D/CDK4/6 is responsible for the switch G1/S and the re-entrance of dormant cells. (Sherr and Roberts 1999, Sherr and Roberts 2004, Gil and Peters 2006)

Tumor suppressors contain a large group of proteins (such as Rb, p107, p130, known as “pocket proteins”) whose role is to control different phases of the cell cycle (**Figure 4-23**). They repress E2F transcription factor activity in order to block the cell cycle progression. There are present CDK inhibitors (CKIs), belonging to tumor suppressors group, that impede

CDK activity, either by building inactive complexes or by being competitive CDK ligand (**Figure 4-23**). (Sherr and Roberts 1999, Sherr and Roberts 2004, Sherr 2006)

The regulators of G1/S phase have proved to be very important for neurons entering in apoptosis in several neurodegenerative diseases. (Al-Ubaidi, Hollyfield et al. 1992)

The neuronal cells, such as the CNS neurons in adults, and photoreceptors, that are highly differentiated, are considered to be in G0 phase, or in constant post-mitotic phase. (Herrup and Yang 2007, Alberts, Johnson et al. 2015) It has been reported that even these highly differentiated cells always have to control their cell cycle. If this is not respected, these cells could re-enter the cell cycle and undergo some processes leading to cell death. This was proved in neurons at risk of neurodegeneration. Herrup and Yang have proved that the “mistakes” in neuronal cell cycle regulations, such as cells re-entering the cell cycle, can cause many neurodegenerative diseases and related changes. (Herrup and Yang 2007) This was seen in the model of Alzheimer disease, (Vincent, Rosado et al. 1996, Yang, Geldmacher et al. 2001) Parkinson’s disease, (Höglinger, Breunig et al. 2007) and amyotrophic lateral sclerosis. (Nguyen, Boudreau et al. 2003) In these diseases, where post-mitotic neurons re-enter the cell cycle, the key-role belongs to the regulators of G1/S phase, i.e. CDK4. But, these neuronal cells do not enter the complete cell cycle, but they undergo apoptosis after incomplete S phase. (Herrup and Yang 2007)

Polycomb group and epigenetic modifications

The polycomb group (PcG) proteins are stably silencing the expression of some specific target genes through chromatin modification. There exist two classes of complexes that they form: PRC1 (Polycomb repressive complex 1) and PRC2. PRC2 (histone methyltransferases) action is having as a result methylated histones and consequently silencing of target genomic regions. PRC1 is maintaining the repression of target genes. Mutations of PRC2 genes are lethal in embryonic stage, but the mutations of PRC1 genes are less severe. (Alberts, Johnson et al. 2015)

The role of PcG complexes is, during early development, to preserve pluripotency by repressing many target genes enrolled in pathways of differentiation (Boyer, Plath et al. 2006, Lee, Jenner et al. 2006) and to maintain “self-renewal ability” and multi-potency in different types of tissue-specific stem cells during development and in the adult organism. The PRC2 is also involved in cell differentiation during retinogenesis.

H3K27me³

Histone modifications are involved in manipulating gene expression and genome function by creating global chromatin environments and coordinating DNA-based biological processes. (Barski, Cuddapah et al. 2007)

Histones can undergo different post-translational changes: lysine acetylation, lysine and arginine methylation, serine/threonine/tyrosine phosphorylation, lysine ubiquitination. All these modifications regulate the histone-DNA interactions. As the consequence, these histone-alterations influence the structure and function of chromatin, but also by binding the effector proteins that can recognize the changed states of histone residues. (Jenuwein and Allis 2001, Sengoku and Yokoyama 2011)

The acetylation (ac) and methylation (me) of histone lysine (K) residues have distinct roles in regulating gene expression. (Ferrari, Scelfo et al. 2014) Acetylation has the important role in active transcription and lysine methylation correlates with either activation or repression of gene expression depending on the target residue and the level of its acquired methylation. (Berger 2007, Kouzarides 2007)

Histone lysine methylations, that are found in about five sites in H3 and in one site in H4, have different biological consequences, depending on their locations and methylation states (non-, mono-, di-, and trimethylations). (Kouzarides 2007) Different sites of histone lysine methylations act via different mechanisms and they target different genomic regions.

H3K27 trimethylation (me³) has the significant role in maintaining the gene transcriptional repression; working with PcG proteins with the aim to inhibit developmental genes. Thus, in pluripotent stem cells, developmental regulator genes are blocked/repressed by H3K27me³. (Boyer, Plath et al. 2006) The site of trimethylation is usually at CpG-dense promoters by the lysine methyltransferase activity of the PRC2. (Morey and Helin 2010) With the cell differentiation, some set of genes are losing the H3K27me³ to be able to begin the developmental programs. (Mikkelsen, Ku et al. 2007)

The direct methylation of the DNA (and not via chromatin modifications) (Mermoud, Rowbotham et al. 2011, Otteson 2011) represents a very potent module in epigenetic regulation of gene expression. (Farinelli, Perera et al. 2014) DNA methylation is thought to be correlated with repression of transcription. (Jones and Liang 2009) Apart being observed in gene promoters, the methylation can be observed also in intergenic noncoding regions as well as within genes. (Jones 2012)

The covalent addition of a methyl group on cytidines followed by guanosine in the DNA is performed by various DNA methyltransferases. (Aapola, Liiv et al. 2002)

The exact relationship between H3K27 methylation and DNA methylation is not yet clear enough. According to different studies, the non-methylated DNA in CpG islands can help recruiting H3K4 and H3K27 trimethylation, probably by making the chromatin environments exceptional and appropriated to gene regulatory elements that are capable to modify transcriptional states. (Rose and Klose 2014)

According to recent studies this epigenetic modification was reported in retinal degeneration and retinal development. (Wahlin, Enke et al. 2013) The exact connection between DNA methylation and degenerating photoreceptors is still unknown. (Farinelli, Perera et al. 2014) Farinelli et al. have observed an increase in DNA methylation in dying photoreceptors in different rodent models of retinitis pigmentosa. This indicates that DNA hypermethylation might be a common factor in the photoreceptor degeneration. (Farinelli, Perera et al. 2014)

To the best of knowledge, retinal degeneration is related to RD, and in order to optimize postoperative recovery a better understanding of the mechanisms involved in the photoreceptor cell death is needed. There have been many studies performed on different cell death mechanisms in retinal diseases. (Menu dit Huart, Lorentz et al. 2004, Wenzel, Grimm et al. 2005, Murakami, Notomi et al. 2013, Zencak, Schouwey et al. 2013)

4.5.1.3. Human retina

In the studies performed with *in vivo* models of RD in rodents, it was shown that photoreceptor cell apoptosis events may cause the reduced vision after RD. (Cook, Lewis et al. 1995, Hisatomi, Sakamoto et al. 2002, Lewis, Charteris et al. 2002, Murakami, Notomi et al. 2013) This implies that the new target therapeutic agents should be the ones that are blocking the apoptosis, in order to protect photoreceptors. (Arroyo, Yang et al. 2005) On the contrary, studies showed that caspase inhibition by Z-VAD (pan-caspase inhibitor) fails to fully prevent photoreceptor death, (Trichonas, Murakami et al. 2010) raising the idea of other mechanisms of cell death hidden behind.

New studies have reported the role of apoptosis-inducing factor (AIF) in RD as a novel mediator in apoptosis. Normally localized in mitochondria intermembrane space, while apoptosis AIF is translocating into nucleus. AIF is acting in a caspase-independent manner. (Hisatomi, Sakamoto et al. 2001)

Performing researches on different apoptosis pathways (e.g. caspase induced apoptosis), mostly in rodents models, studies revealed that apart apoptosis there is also some other type of cell death present – such as necrosis. (Hisatomi, Sakamoto et al. 2001, Hisatomi,

Sakamoto et al. 2002, Arroyo, Yang et al. 2005, Trichonas, Murakami et al. 2010) According to recent studies, some necrosis can be induced by regulated signal transduction pathways such as those mediated by receptor interacting protein (RIP) kinases, especially in conditions in which caspases are inhibited or cannot be activated efficiently. (Golstein and Kroemer 2007, Trichonas, Murakami et al. 2010)

There are few studies that are performed on human retina with RD. Arroyo et al studied the human retina obtained as retinal tissue fragments removed during vitreoretinal surgery for RD. The tissue was frozen, cut on 4 μ m cuts and then analyzed for apoptosis (TUNEL). They confirmed that the photoreceptor cells undergo apoptosis in response to RD on the same manner as reported in animal models. (Arroyo, Yang et al. 2005) Hisatomi et al assessed human retina with RD and healthy retina obtained from the pathology institute and eye banking specimen, according to the pathology report. They demonstrated that both the activation of caspase as well as mitochondrio-nuclear translocation of the caspase-independent death effector AIF occur in human retinas after RD. (Hisatomi, Nakazawa et al. 2008)

Zencak et al reported that in different mouse models of inherited retinal degeneration, the re-expression of cell cycle proteins such as cyclin-dependent kinases (CDKs) is the sign of photoreceptor cell death. Similar pathway has been reported in the rodent model of retinal light-damage. (Herrup and Yang 2007, Zencak, Schouwey et al. 2013) It was also noticed, by the same authors, that the epigenetic modifications, such as H3K27me³ were positive in these mouse models (unpublished data).

Our aim was to examine which cell death pathway(s) is activated in an *in vitro* model of RD in human retina.

4.5.2. Experimental study design

The study was conducted on human retinal explants as an *in vitro* model of RD. All procedures conformed to the tenets of the Declaration of Helsinki for biomedical research involving human subjects. Human globes received from the Lausanne Eye Bank were obtained after family consent for their use for research. The procedure was approved by the ethic committee of University of Lausanne (protocol No 340-15). The overall health of the donor before death was considered and tissue was rejected from donors with previous history or treatment that might damage the retina. The experiments were conducted at the Research Pole in Ophthalmology, UGTSCB (Unit of Gene Therapy and Stem Cell Biology) at the Jules-Gonin Eye Hospital, University of Lausanne, Switzerland. This study was performed from February 2015 until March 2017.

4.5.2.1. Protocol for preparing human retinal explants

Procedure of eye dissection

Following the donor cornea retrieval, the posterior segment was recovered; after removal of the vitreous, the sclera and retina were cut into a flower shape with 4 cuts. Next the retina was detached from the RPE, choroid and sclera, in order to achieve the *in vitro* model of RD. The RPE layer was preserved for the control group. The peripheral retina was dissected into small pieces, minimum 5mm x 5mm. Retinal explants were placed on Millipore membrane inserts (Millicell Culture Plate Inserts, MerckMillipore, Merck, Darmstadt, Germany), which were then placed in a 6 well plate (NalgeneNunc, Rochester, New York, USA), containing 1.5mL of medium per well. This medium included: B27 [1x]_f [50x]_i, FBS [1%]_f [100%]_i, P/S [100 x]_f [1x]_i, DMEM/F12 (please refer to **Annex 2**). The culture was maintained at 37°C, in 5% CO₂ and the medium was changed every 48 hours. During this protocol fixation was performed 1 day, 3 days, 5 days and 7 days after dissection, using 4% PFA. The explants were cryopreserved in 30% sucrose, with an intermediate step in 10% sucrose, then mounted using Yazulla and subsequently frozen at -20°C.

In order to mimic retinal detachment the retinal explants were held in this medium with the RPE for the control group (as previously described for mouse retina explant, (Zencak, Schouwey et al. 2013)) and without the RPE for the RD model.

There were four retinal explants that fulfilled the inclusion criteria (n=4). All 4 explants were negative on any eye or retinal disease. Each explant was divided in two groups: RD group (without RPE), n=4 and control group (with RPE), n=4 and served for all the time points analyzed.

4.5.2.2. Immunohistochemistry

Immunohistochemical analysis was performed according to standard protocol (see below), on a series of 14 µm-thick cryosections. TUNEL-positive cells were counted in the most central sections. All measurements were taken by Olympus BX6 fluorescence microscopy. The quantification of positive cells was performed on the pictures taken in the center of the retina in 10 different slices for each sample and then averaged.

Photoreceptor and cell death markers were studied in relation to cell cycle protein expression (CDK4), as well as epigenetic modifications (H3K27me3) and apoptotic markers Caspase-3 and apoptosis-inducing factor (AIF).

All primary antibodies, their source as well as their working dilutions are listed in **Table 4-15**. The standard protocol used for immunochemistry on cryostat sections included 1h of blocking with 10% Normal Goat Serum and 0.3% TritonX, followed, by overnight incubation with the primary antibody diluted in blocking solution and revelation with the appropriate secondary antibody incubated for 1h at room temperature (**Table 4-15**). On cryostat sections, nuclei were counter-stained with 4,6-diamidino-2-phenylindole (DAPI) (**Annex 4**).

TUNEL staining

To visualize dying cells on sections, a TUNEL (Terminal deoxynucleotidyl Transferase Biotin-dUTP Nick End Labeling) staining on cryostat sections was performed. For retinal explants a TUNEL assay kit conjugated with TMR red from Roche Diagnostics was used and performed as stated in the instructions. Negative controls consisted of omitting the terminal deoxynucleotidyl transferase enzyme from the labelling, and gave no staining at all (**Annex 3**).

H3K27me³ staining

The H3K27me³ was performed according to standard protocol (please refer to the **chapter 9.3**). To the standard protocol, in order to enhance the signal, we added antigen retrieval, which consists of 10 mM citrate buffer pH 6.0 home made. The cryosections were firstly heated in a microwave oven 5mn at 696W and then cooled down for 30mn at room temperature (RT) (**Annex 5**).

CDK4 DAB staining

DAB staining requires blocking endogenous peroxidase with 0.3% H₂O₂ for 5 min at RT. After incubation with anti-CDK4 we added 1/200 biotinylated goat anti-rabbit for 1h and then the ABC substrate 30 min. DAB revelation lasted 2 min at RT (please refer to the **Annex 6**).

Active Caspase 3 staining

The Caspase-3 staining was performed according to protocol (referred to the **Annex 7**).

AIF staining

The AIF staining was performed according to protocol (referred to the **Annex 8**).

Table 4-15. List of primary and secondary antibodies for immunochemistry

Primary antibody	Species	Source	Working dilution/incubation time
Cdk4	Rabbit	Santa Cruz, SC-601	1/100 ON
H3K27me3	Rabbit	MerckMillipore #07-449	1/200 ON
Caspase-3	Rabbit	BD Pharmingen #559969	1/75 ON
AIF	Rabbit	Abcam #ab32516	1/250 ON
Secondary antibody	Species	Source	Working dilution/incubation time
Alexa Fluor 633 Goat anti-Rabbit IgG		Invitrogen A21072	1/2000, 1h, RT
ON=overnight, RT=room temperature			

4.5.2.3. Statistical analysis

All the data are expressed as mean \pm standard error of the mean (SEM). Data were analyzed using the Mann-Whitney U-test. For the statistical importance, the value of $p < 0.05$ was considered, repeated measures were accounted.

4.5.3. Results

4.5.3.1. Number of photoreceptors' layers

In all four explants, the number of photoreceptor layers was quite stable in the control group, while there was a slight decrease in the RD group over time. In this group, at 5DIV and 7DIV, the number of photoreceptors rows was decreased by around 25% in comparison to 1DIV ($p < 0.04$). The difference between groups analyzed in every time-point, was not statistically significant, except after 1DIV (**Figure 4-24 A-B, Table 4-17**) where the RD group showed a high number of photoreceptors at the beginning of the experiment. This reveals that, although the retina pieces from a same donor were distributed between the two groups, some heterogeneity exists in a same explant. Nonetheless, each group contained retina with similar numbers of photoreceptor rows (see SEM bars in **Figure 4-24**). Thus the evolution of photoreceptor number in the same group better reveals the health of retina. To note, the RD retina showed a decline in photoreceptor rows, whereas the control group not. Indeed, after 1 DIV, the statistical difference in the number of photoreceptor's layers is decreasing (**Table 4-16**).

Table 4-16. Mann-Whitney test p-values of comparison of the number of photoreceptor layers between each time-point in the group of *in vitro* RD explants (without RPE), * $p < 0.05$

Time-point	Mann-Whitney test in the noRPE group, between time-points PHOTORECEPTORS LAYERS			
	1 DIV	3 DIV	5 DIV	7 DIV
1 DIV		0.11	0.04*	0.03*
3 DIV			0.71	0.40
5 DIV				0.99
7 DIV				

Table 4-17. Mean number of positive cells in each day of fixation, in both groups. Comparison between groups, Mann-Whitney test value

		No RPE	With RPE	Mann-Whitney test	
		Time point	Mean value	Mean value	No RPE vs. with RPE
Number of photoreceptor layers (mean \pm SEM)	1 DIV	8.99 \pm 1.36	6.26 \pm 0.65	0.04*	
	3 DIV	7.19 \pm 0.67	6.66 \pm 0.57	0.32	
	5 DIV	6.24 \pm 0.61	5.74 \pm 0.52	0.25	
	7 DIV	7.11 \pm 0.76	7.42 \pm 0.98	0.98	
Number of TUNEL + cells (mean \pm SEM)	1 DIV	2.83 \pm 1.03	1.50 \pm 0.00	0.12	
	3 DIV	11.83 \pm 6.68	0.75 \pm 0.30	0.02*	
	5 DIV	11.03 \pm 2.50	3.75 \pm 0.83	0.02*	
	7 DIV	15.84 \pm 1.73	7.67 \pm 0.00	0.04*	
Number of AIF + cells (mean \pm SEM)	1 DIV	1.00 \pm 0.27	0.20 \pm 0.22	0.04*	
	3 DIV	8.60 \pm 0.57	0.60 \pm 0.27	0.02*	
	5 DIV	0.10 \pm 0.11	0.00 \pm 0.00	0.05	
	7 DIV	0.00 \pm 0.00	0.00 \pm 0.00	1.00	
Number of CDK4 + cells (mean \pm SEM)	1 DIV	2.01 \pm 0.75	0.00 \pm 0.00	0.02*	
	3 DIV	3.70 \pm 0.51	1.65 \pm 0.81	0.04*	
	5 DIV	3.93 \pm 2.93	1.13 \pm 0.00	0.06	
	7 DIV	4.73 \pm 0.86	1.58 \pm 0.12	0.02*	
Number of H3K27me ³ + cells (mean \pm SEM)	1 DIV	1.78 \pm 0.86	2.15 \pm 3.03	0.05	
	3 DIV	2.89 \pm 2.64	1.00 \pm 1.41	0.4	
	5 DIV	12.68 \pm 2.06	1.35 \pm 0.08	0.04*	
	7 DIV	9.24 \pm 1.98	4.07 \pm 2.73	0.04*	

RPE – retinal pigment epithelium, SEM – standard error of the mean, *p<0.05

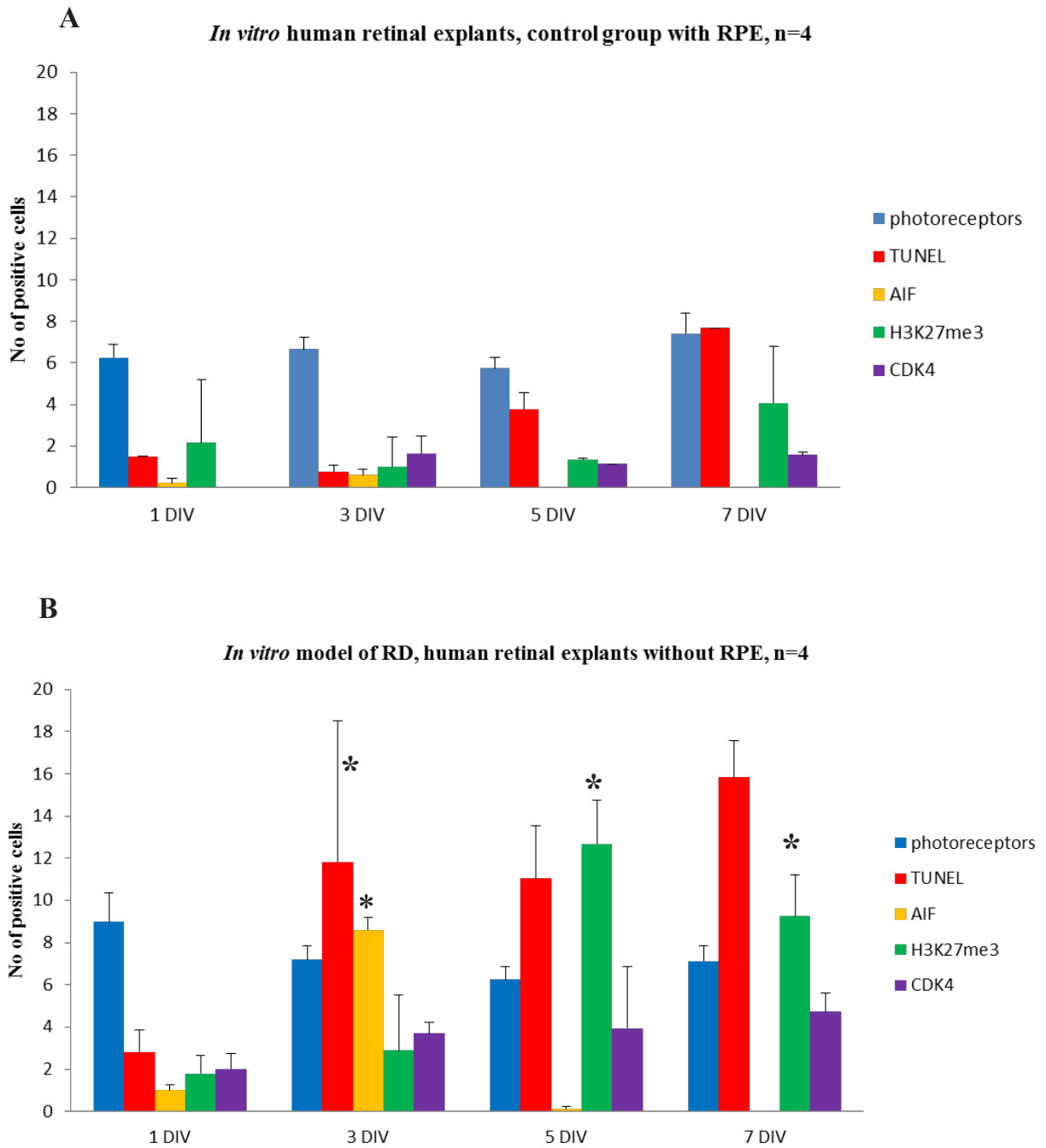


Figure 4-24 A-B. Figures showing summary data of all four human retinal explants, in two groups: *in vitro* control group (a) and *in vitro* RD group (b) for all five followed parameters. Note the significant difference between groups for all five parameters but at different time points. The most important differences are especially for an increase of TUNEL- and H3K27me3-positive photoreceptors over time in the RD group, AIF had a peak at 3DIV, following the peak of TUNEL positive cells, while the CDK4 is moderately more expressed in RD group, suggesting the cell-cycle re-entrance in certain cells.

4.5.3.2. TUNEL staining; cell death marker

TUNEL positive cells were present from the beginning of the experiment in low level in the control group despite the different postmortem delays (12h, 14h, 23h and 24h) and the dissection procedure of the tissue. The number of TUNEL-positive cells increases at 5DIV and peaked at 7 DIV (**Table 4-17, Figure 4-25**). For the RD group, a marked higher number was observed at 3 DIV with an increase of about 157% in comparison to the control group and remained stable (**Figure 4-25, Figure 4-26**). Interestingly, this peak of cell death coincides with this described for rhegmatogenous retinal detachment *in vivo*. (Hisatomi, Sakamoto et al. 2001, Arroyo, Yang et al. 2005) A significant 30% increase of TUNEL positive cells continues to occur between 3 DIV and 7DIV with a high variation at 5 days suggesting a biphasic cell death process (**Figure 4-24 A-B, Figure 4-25, Table 4-17, Table 4-18**). Considering the involvement of other described actors of cells death to those described for Caspase-3 pathway, we investigated in addition other potential actors as proteins of the cell cycle such as CDK4 as it was described to participate to some process of neuron (Yang, Geldmacher et al. 2001, Höglinger, Breunig et al. 2007) and photoreceptor death in another model of retinal degeneration. (Zencak, Schouwey et al. 2013)

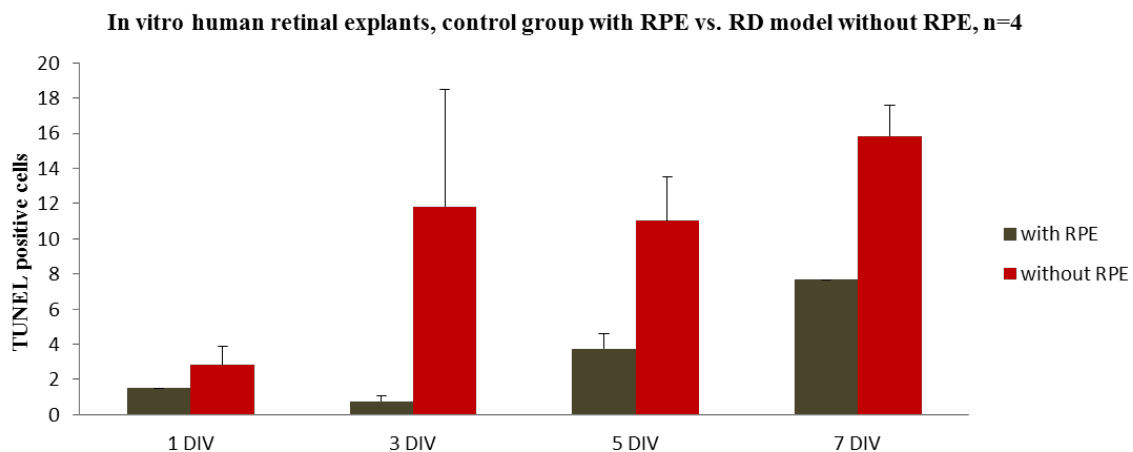


Figure 4-25. Comparison of TUNEL-positive cells between control group (human retinal explants with RPE) and *in vitro* model of RD (human retinal explants without RPE). Note the important difference in TUNEL positive cells between groups in all time points, notably highly expressed since 3rd day *in vitro*. n = 0.75 for the control group, and n = 11.83 for the group without RPE

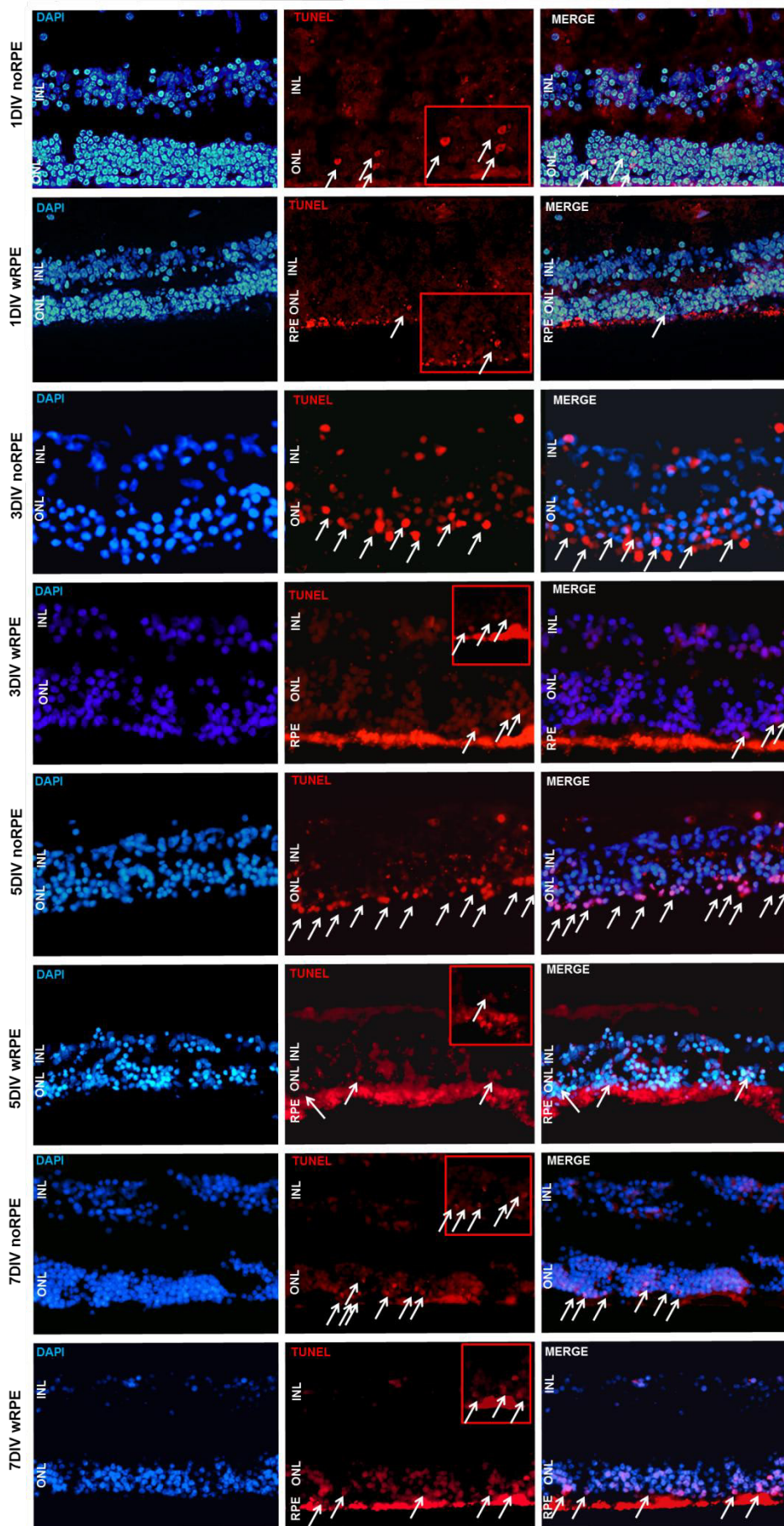


Figure 4-26. TUNEL positive cells (arrows) at 1DIV, 3 DIV, 5 DIV, 7 DIV, in the human *in vitro* RD model without RPE and in control group of human *in vitro* retinal tissue with RPE. The presence of RPE produced an artefact fluorescent background
ONL: outer nuclear layer
INL: inner nuclear layer
RPE: retinal pigment epithelium
Magnification: 400x
Calibration bar: 20µm

Table 4-18. Mann-Whitney test p-values of comparison of the number of TUNEL positive cells between each time-point in the group of *in vitro* RD explants (without RPE), *p<0.05

Time-point	Mann-Whitney test in the noRPE group, between time-points TUNEL			
	1 DIV	3 DIV	5 DIV	7 DIV
1 DIV		0.04*	0.02*	0.02*
3 DIV			0.28	0.14
5 DIV				0.08
7 DIV				

4.5.3.3. Caspase-3 expression

Caspase-3 is the final effector of apoptosis (Murakami, Notomi et al. 2013) and was chosen to reveal the extent of apoptotic events in the retina with and without RPE. Surprisingly, very few cells in the ONL were present in both groups and no peak of apoptosis was clearly identified (not shown).

4.5.3.4. Apoptosis-inducing factor (AIF) staining

AIF represents a caspase-independent apoptogenic factor. AIF is normally localized in mitochondria. During the cell death, i.e. apoptosis, it was observed that AIF translocates to the nucleus. (Hisatomi, Sakamoto et al. 2001, Hisatomi, Nakazawa et al. 2008) We checked for the expression of AIF in human *in vitro* model of RD. We observed that AIF was present in the ONL at 1DIV and with a marked peak at 3DIV in the RD group. The peak of AIF positive cells followed the peak of TUNEL positive cells observed at 3DIV (**Figure 4-24, Figure 4-27, Figure 4-28, Table 4-17**). At 5DIV and 7DIV there was no visible AIF positive cell.

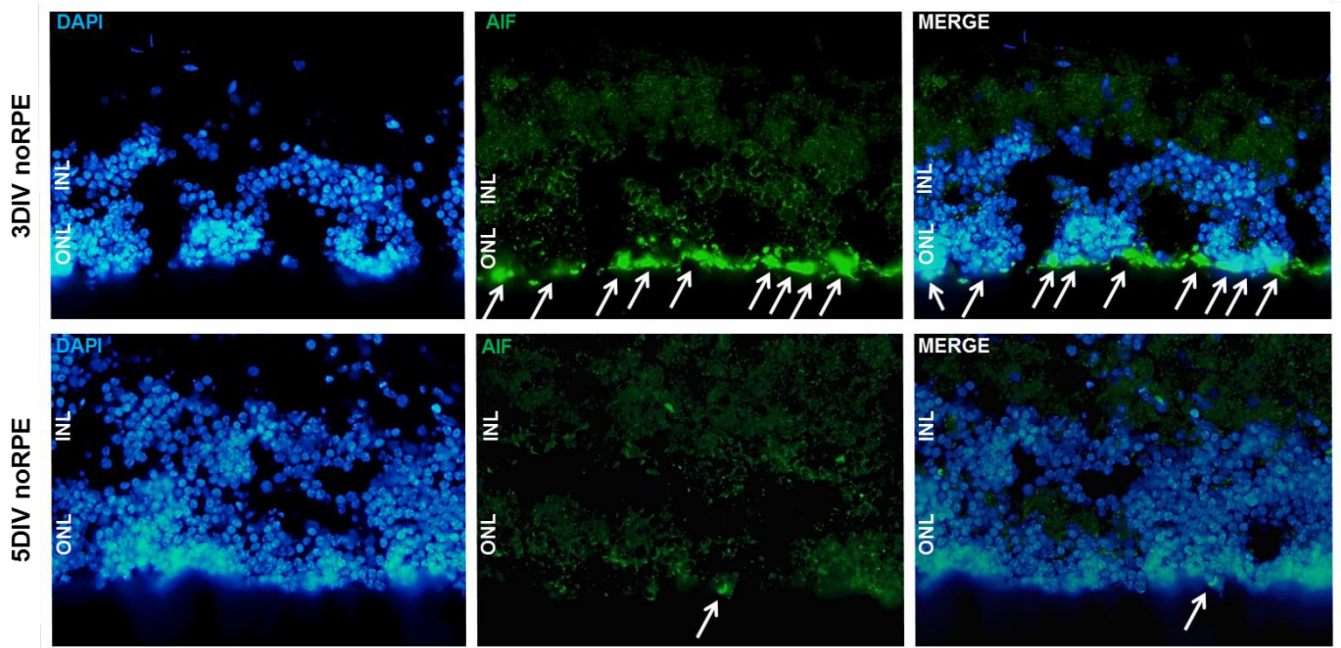


Figure 4-27. AIF positive cells at 3DIV in the human *in vitro* model of retinal detachment. At 5DIV there is only one AIF positive cell. *ONL*: outer nuclear layer, *INL*: inner nuclear layer
Magnification: 400x, Calibration bar: 20 μ m

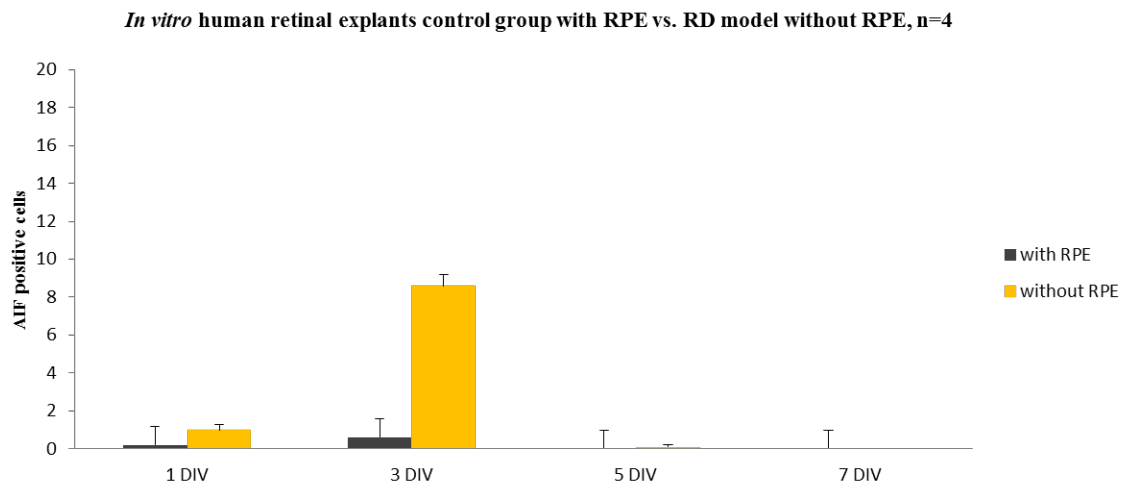


Figure 4-28. Comparison of AIF-positive cells between control group (human retinal explants with RPE) and *in vitro* model of RD (human retinal explants without RPE). Note the important difference in AIF positive cells between groups at 3DIV, when they were notably highly expressed. n = 0.60 for the control group, and n = 8.60 for the group without RPE

4.5.3.5. CDK4 staining; marker of cell cycle re-entrance

No CDK4 was observed in the control group after 1 DIV and only very rare cells expressed this protein between 3 to 7 DIV. In the RD group, CDK4 positive cells are present starting at 1 DIV (Figure 4-24 A-B, Figure 4-29, Table 4-17, Table 4-19) and the number remained very low and stable between 3 to 7 DIV. The mean number of CDK4 positive cells in the group of explants mimicking RD was 3.07 ± 2.31 , in all the time-points, while in the control group this number was 1.25 ± 1.38 . Note that the number of CDK4 positive cells is much lower in comparison to TUNEL-positive ones (Figure 4-30). Comparison between the two groups showed statistical difference at each time-point, except for 5DIV (Figure 4-24 A-B, Figure 4-29, Figure 4-30, Table 4-17).

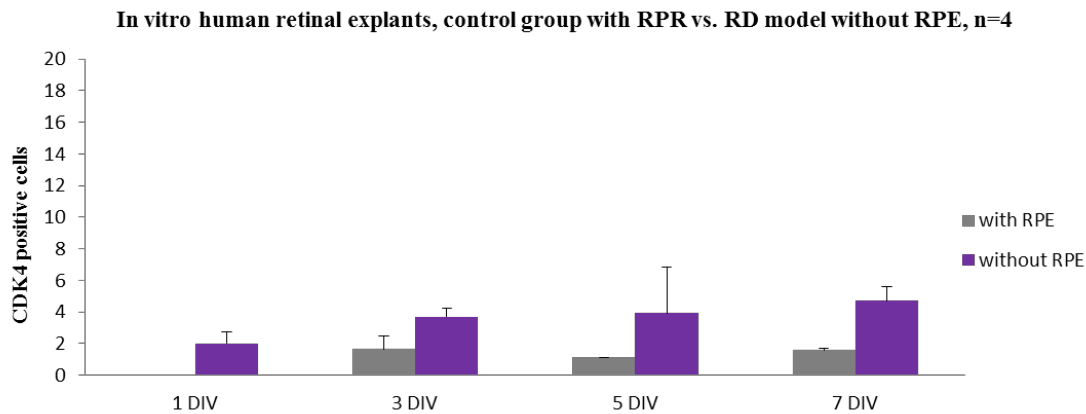


Figure 4-29. Comparison of CDK4 positive cells between control group (human retinal explants with RPE) and *in vitro* model of RD (human retinal explants without RPE). Note the very low number of CDK4 positive cells after 1 DIV in the control group, as well as its little increase over time in the RD group. n=1.65 at 3DIV for the control group, and n=3.70 at 3DIV and n=4.73 at 7DIV for the group without RPE

Table 4-19. Mann-Whitney test p-values of comparison of the number of CDK4 positive cells between each time-point in the group of *in vitro* RD explants (without RPE), *p<0.05

Time-point	Mann-Whitney test in the noRPE group, between time-points CDK4			
	1 DIV	3 DIV	5 DIV	7 DIV
1 DIV		0.04*	0.28	0.02*
3 DIV			0.50	0.08
5 DIV				0.50
7 DIV				

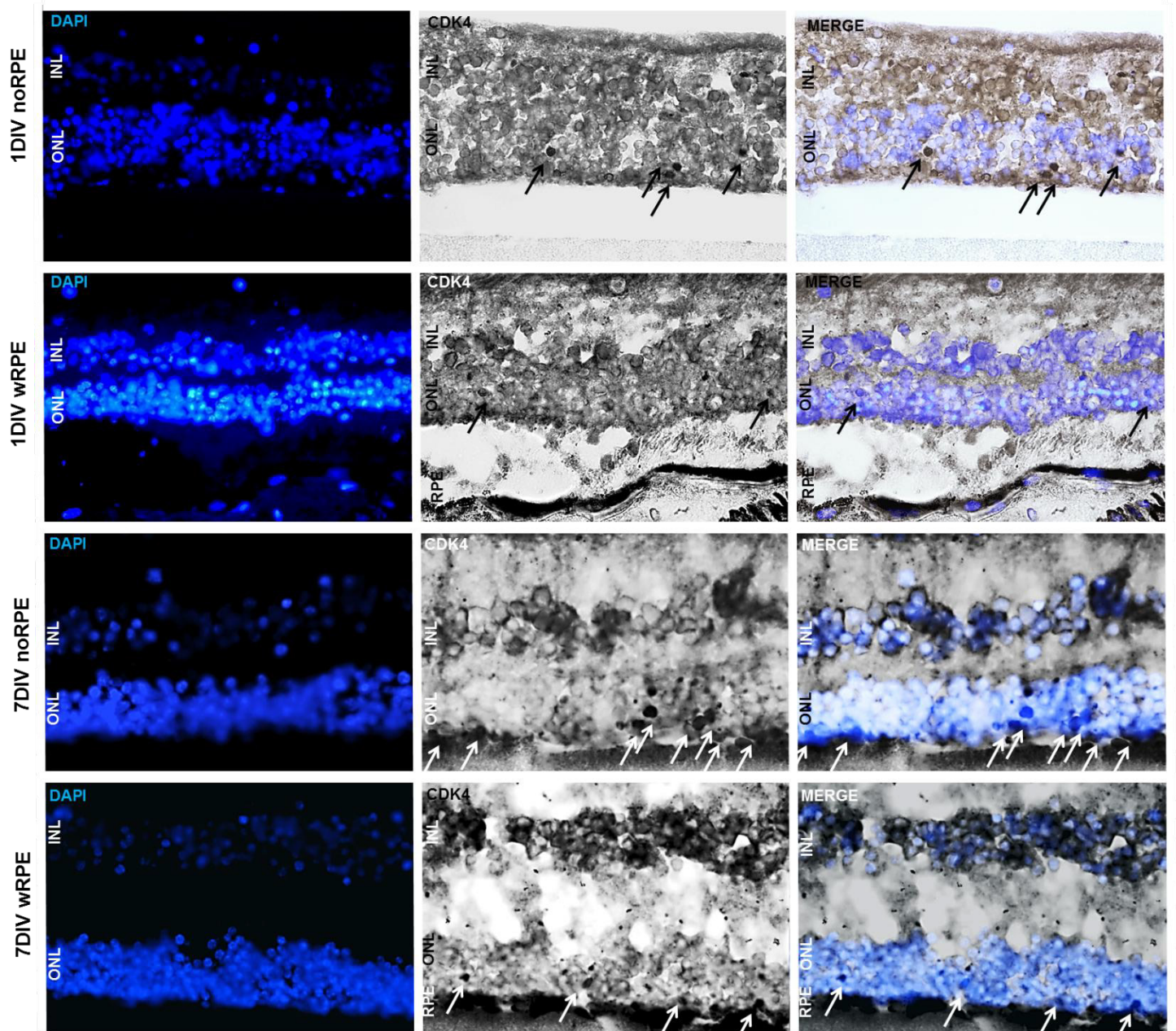


Figure 4-30. CDK4 positive cells (arrows) in the human *in vitro* model of retinal detachment (human retinal explants without RPE) and control group (human retinal explants with RPE), at 1DIV and at 7DIV. *ONL*: outer nuclear layer, *INL*: inner nuclear layer. Magnification: 400x. Calibration bar: 20µm

4.5.3.6. H3K27me3; epigenetic modifications

Observing that epigenetic modifications occur at the Histone level in some models of retinitis pigmentosa (unpublished data), we investigated the H3K27me3 mark known to regulate gene repression. (Wahlin, Enke et al. 2013) In the control group, the number of H3K27me3-positive cells in the ONL remained low until 5 DIV and showed a slight elevation at 7 DIV, whereas a marked increase of this mark was observed at 5 DIV in the RD group and stayed elevated at 7 DIV, although partially reduced (**Figure 4-24, Figure 4-31, Figure 4-32, Table 4-17, Table 4-20**). Note that the elevated number of H3K27me3-positive cells appears after the peak of TUNEL-positive cells.

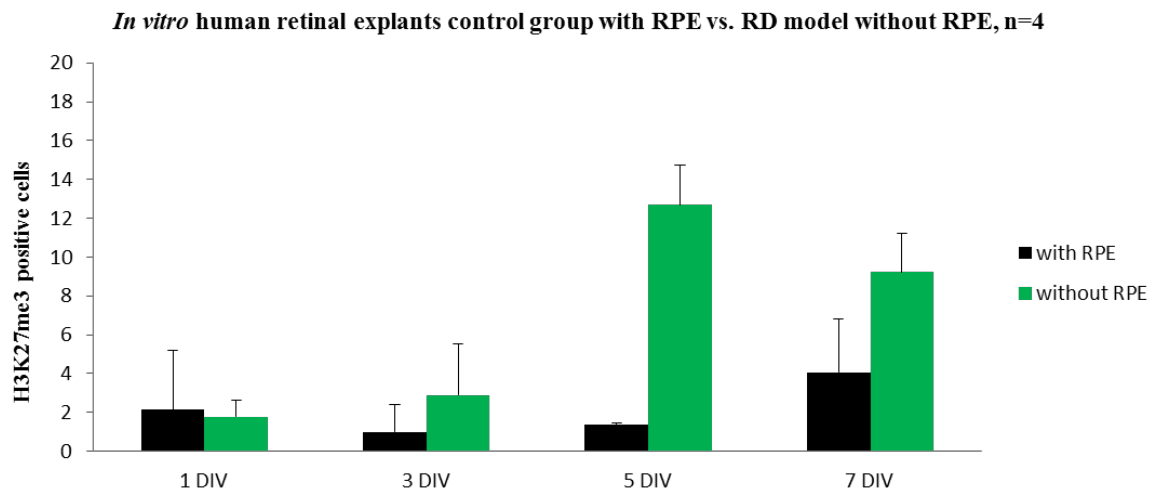


Figure 4-31. Comparison of H3K27me3 positive cells between control group (human retinal explants with RPE) and *in vitro* model of RD (human retinal explants without RPE). Note the increase in H3K27me3 positive cells level in RD model starting at 5 DIV. n=1.35 for the control group, and n=12.68 for the group without RPE

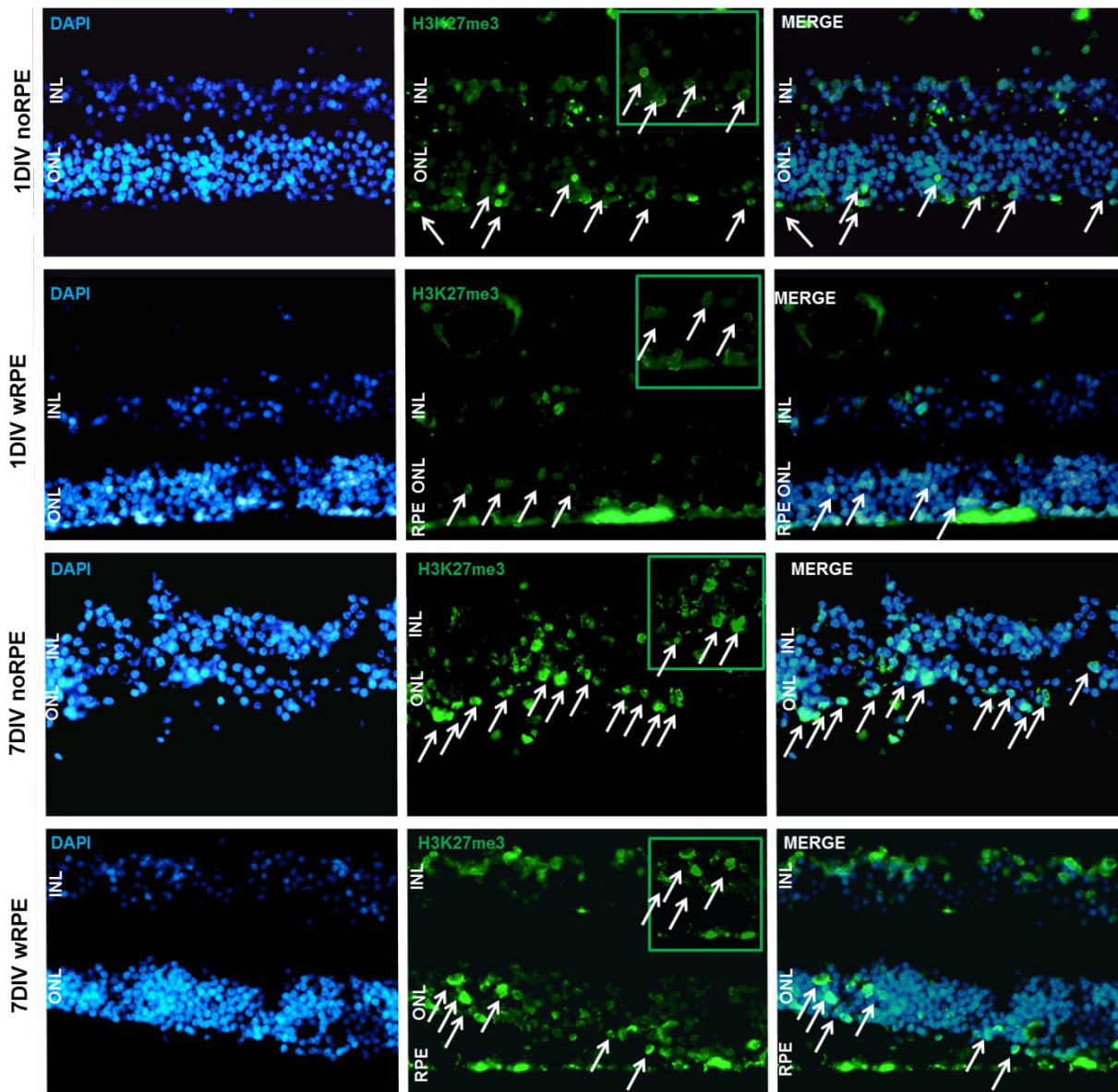


Figure 4-32. H3K27me³ positive cells at 1DIV and at 7DIV, in the human *in vitro* model of RD (without RPE) and human *in vitro* model of retinal tissue with RPE *ONL*: outer nuclear layer, *INL*: inner nuclear layer, *RPE*: retinal pigment epithelium. Magnification: 400x Calibration bar: 20µm

Table 4-20. Mann-Whitney test p-values of comparison of the number of H3K27me ³ positive cells between each time-point in the group of <i>in vitro</i> RD explants (without RPE), *p<0.05				
Time-point	Mann-Whitney test in the noRPE group, between time-points H3K27me³			
	1 DIV	3 DIV	5 DIV	7 DIV
1 DIV		0.41	0.02*	0.02*
3 DIV			0.02*	0.06
5 DIV				0.06
7 DIV				

4.5.4. Discussion

Very few studies investigated human samples to characterize and to study the process of cell death after retinal detachment. It is first time that cell death characterization without RPE were done on human retinal explants to model RD *in vitro*.

An original investigation performed with retinal samples obtained during surgery at different time after RD revealed that TUNEL-positive cells peaked at around 2 days after the separation of the retina from the RPE (Arroyo et al 2005). (Arroyo, Yang et al. 2005) The cell death time course observed is similar to those documented with animal models. (Hisatomi, Sakamoto et al. 2001, Sancho-Pelluz, Arango-Gonzalez et al. 2008) However, the mechanisms of the cell death process remains largely unknown in the human retina tissue. The present model of retina explant culture without the RPE is well in accordance with the cell death kinetic monitored in the human sample RD and animal models cited above.

This approach opens new perspectives to test first *in vitro* drugs to block a specific cell death pathway once the different pathways will be clearly identified probably decreasing the number of unsuccessful trials. The comprehension of the mechanisms is still necessary to correctly propose a protective approach for the injured photoreceptors.

Among the first clear demonstrations of apoptosis as a major form of photoreceptor cell death after RD was made by Cook and colleagues in a cat model of RD, (Cook, Lewis et al. 1995) following the establishment of TUNEL assay. (Gavrieli, Sherman et al. 1992) They showed that photoreceptor cells in the detached retina exhibit strong TUNEL reactivity as well as pyknotic morphological changes. Moreover, they demonstrated that the photoreceptor cell death after RD occurs in an earlier period than previously recognized: TUNEL-positive cells are detected as early as 1-3 days after RD, followed by a decline in their number over the next few weeks. This early activation of apoptosis, which begins within 1 day and peaks at 2-3 days after RD, has been confirmed in other animal models of RD with rhegmatogenous RD. (Hisatomi, Sakamoto et al. 2001, Arroyo, Yang et al. 2005)

In our *in vitro* model of human RD, we noticed the peak of TUNEL positive cells at 3 DIV, with a plateau until 7 DIV (latest time-point), thus underlining the need for urgent surgery of patients affected by retinal detachment. The presence of TUNEL positive cells even at 1 DIV time-point can be explained with the theory that retinal explantation is a traumatic event and the cultures therefore are displaying cell death (TUNEL assay) even under controlled conditions. Surprisingly, a post-mortem delay inferior to 24h (12h, 14h, 23h and 24h) had little effect on photoreceptor death. As a result of the culture situation, the

number of photoreceptor rows in the ONL *in vitro* is decreasing in the RD group more significantly than it would *in vivo*. (Hisatomi, Sakamoto et al. 2002, Sahaboglu, Paquet-Durand et al. 2013)(Sahaboglu et al., 2013) Note that in the present culture condition, no RPE are present at all, whereas in patients the RPE are present although at an unfavorable distance from the neuroretina.

Several works revealed in animal models that Caspase-3 is activated during RD. (Wenzel, Grimm et al. 2005, Sancho-Pelluz, Arango-Gonzalez et al. 2008, Trichonas, Murakami et al. 2010, Murakami, Notomi et al. 2013) We thus investigated the course of Caspase-3 appearance in our *in vitro* model. Surprisingly in both groups, only rare cells were positive for this enzyme suggesting alternative pathways to conduct the sensory cells to death.

Models of neurodegenerative disease show that neurons committed to cell death re-express cell-cycle related proteins especially CDK4. (Vincent, Rosado et al. 1996, Yang, Geldmacher et al. 2001, Nguyen, Boudreau et al. 2003, Höglinger, Breunig et al. 2007) Zencak et al. revealed that reactivation of cell cycle proteins is associated with photoreceptor death in five distinct models of retinal degeneration. This study showed in the *Rdl* mouse model that CDK4-positive cells were present starting from postnatal day 9 (P9) with the marked increase until P12, whereas almost no CDK4-positive cells were detected in the wild-type retina. (Zencak, Schouwey et al. 2013) The authors detected also the re-expression of CDK4 positive cells in acute model of retinal degeneration induced by light damage; with intense and widespread nuclear expression of CDK4 and CDK2 in the ONL 36h after light damage, when the cell death process reaches its peak and CDKs play a crucial role in the execution phase of photoreceptor death. (Wenzel, Grimm et al. 2005, Zencak, Schouwey et al. 2013) In view of the interesting observations made in animal models, we asked whether retinal degeneration is also linked to cell cycle proteins and machinery and tested the potential presence of cell cycle regulators in photoreceptor cell death.

On human retinal explants, on *in vitro* model of RD, CDK4 staining was performed. Following TUNEL staining results in our explants, CDK4 are present in all time points with higher peak at 7 DIV. This kinase is not present in control group, showing the significant difference between the two groups over time. However, the kinetic of CDK4 appearance did not correlate or precede the peak of cell death observed at 3 days. Moreover, the number of CDK4-positive cells is much lower than the number of TUNEL-positive cells which observation differs from this made in rodent models of retinal dystrophies. (Sancho-Pelluz, Arango-Gonzalez et al. 2008, Trifunovic, Sahaboglu et al. 2012, Zencak, Schouwey et al. 2013) These results suggest that CDK4 is probably not involved in the first peak of cell death

at 3 DIV and may little account for the continuation of photoreceptor degeneration in later time points

We found that H3K27me3 showed a massive increase at 5 DIV in the RD group, which expression is very low in the control group. Epigenetic modifications were poorly document for retinal diseases, nonetheless interestingly changes in DNA methylation was observed in retina of different mouse models of retinal degeneration. DNA methylation is generally associated with repression of transcription. (Jones and Liang 2009) DNA methylation is increased in dying photoreceptors. (Farinelli, Perera et al. 2014) In all of the models, and in line with the *Rdl* data, a sub-population of photoreceptors showed an increase of nuclear DNA methylation at PN7 to PN15 compared with wild type counterparts. This suggested increased DNA methylation as a common feature in all the analyzed models. The TUNEL assay for dying cells co-labeled the 5mC-positive cells (anti-5-methylcytosine antibody was used to analyze photoreceptor DNA methylation in situ) to a great extent, suggesting an intimate connection between increased DNA methylation and the degeneration of the photoreceptors. (Farinelli, Perera et al. 2014) Moreover, the various models have different degeneration kinetics, which leads to different numbers of dying photoreceptor cells at their respective peak of degeneration. (Chang, Hawes et al. 2002, Kaur, Mencl et al. 2011, Sahaboglu, Paquet-Durand et al. 2013) DNA methylation was found to be most prominent and to reach ‘catastrophic’ intensities during the final stages of cell death. (Farinelli, Perera et al. 2014) However, it cannot be excluded that hypermethylation of specific genes may be starting far earlier. (Farinelli, Perera et al. 2014) Our results with positive H3K27me3 well correlate with DNA methylation in photoreceptors. Indeed, EZH2, the enzyme that methylates H3 on lysine 27, is a component of the complex of the DNA-methyl transferase (DNMT) suggesting that EZH2 first initiates epigenetic changes which are reinforced then by DNMTs.

In addition, because a PcG protein, BMI1, was identified to be crucial for photoreceptor death (Zencak et al., 2013), H3K27me3 may thus be more relevant to identify genes involved in the process of cell death.

However, in the present study, the highest peak of H3K27me3 positive cells is expressed at 5 DIV, suggesting that the first wave of photoreceptor death is independent on EZH2 activity and that the continuation of the degeneration may be related to EZH2. If this is true, and needs to be confirmed by future studies with specific inhibitors, the medication to slowdown photoreceptor degeneration has to be adapted to each stage of the degenerative process to enhance the survival of the photoreceptors. These data also support the theory and clinical observations that the most important is to perform RD surgery in the first 3 days, in

order to have a good functional recovery. In view of our and previous published results, successive death pathways are activated after retinal detachment. Although we did not detect Caspase-3 activation, we cannot exclude that the early death peak at 3 DIV is mediated by apoptosis. AIF was shown in different models to be expressed during this peak.

Interestingly, the presence of AIF in photoreceptor nucleus was well detected 3 days after the culture without RPE and is almost absent from this organelle at 5 and 7 DIV, although several photoreceptors contained AIF in the cytoplasm around the nucleus. This observation perfectly fits with previous *in vivo* data and correlates with the appearance of the first peak of TUNEL positive cells in the human retina explants without RPE.

4.5.5. Conclusion

CDK4, H3K27me3 and AIF are expressed in an *in vitro* model of RD of human retinas. These first observations are suggesting possible overlapping mechanisms of cell death characterized in animal models of retinal degeneration, even though the expression of CDK4 positive cells are coming at a later stage than the peak of TUNEL positive cells. These results suggest that the re-entrance into the cell cycle is present, but is not the main pathway of photoreceptors' death in RD.

All these data, suggest that AIF mediates the first process of cell death and highlight that cell death occurring at a later stage of degeneration may be related to epigenetic modification, confirmed with the presence of H3K27me3 at 5DIV and 7DIV.

Further studies need to identify which genes are affected by such modification and if drugs inhibiting such pathways or modifications have a protective action on photoreceptors. The characterization and the interactions of the different cell death pathways occurring in human retina after retinal detachment is thus required to give adapted medication in the future if surgery cannot be performed during the early event of retinal detachment

5. DISCUSSION

The study covered the topic of retinal detachment from many aspects: clinical, epidemiological and experimental. Retinal detachment, with its sudden onset leads to inevitable blindness if not operated on time. The main hypothesis of the project was to determine if better characterization of the cell cycle proteins and apoptotic factors *in situ*, as well as cellular morphology of RD could help predict post-operative anatomical and functional recovery and subsequently patients' QoL.

In this prospective study we analyzed 194 patients with primary RD. We divided patients depending on the macular involvement (macula-ON and macula-OFF RD) that was confirmed by SD-OCT preoperatively. In both groups, significantly more often right eyes were affected (63.4% vs. 36.6%) and there were two times more men than women presenting with RD. Aside that univariate analysis showed positive correlation between age, lens status, AL and SE with RD, multivariate model demonstrated that a shorter AL and pseudophakic lens status were the only independent risk factors for macula-OFF RD (**Table 4-1**).

Furthermore, in 4.4% of RD patients, we identified a distinct new subgroup of RD: hemi-macular detachment (HMD). We described HMD clinical characteristics, with the particular preoperative shape forming a sub-foveal pocket of SRF becoming bullous outside the vascular arcades and postoperative watermark visible mostly in the ellipsoid layer and on EnFace OCT.

The birefringent OCT characteristics helped us to describe different evolution and recovery pathway of the choroid depending on the RD type. This has opened the door to many subclinical and physiological questions that are still unknown. We have demonstrated that in peripheral macula-ON RD the CT sub-foveally is thicker throughout follow up compared to the fellow eye (inter-eye difference; TE-FE) (**Table 4-10, Table 4-11**). Following paracentral macula-ON RD, sub-foveally, CT demonstrated thinning compared to the FE (**Table 4-10, Table 4-11**). In the macula-OFF RD, a marked thinning was observed in sub-foveal inter-eye difference of CT at M1 and M3 (**Table 4-10, Table 4-11**). The inter-eye difference in sub-foveal CT between peripheral macula-ON and paracentral macula-ON and between peripheral macula-ON and macula-OFF eyes was statistically different at M1 ($p=0.00$, $p=0.00$) and at M3 ($p=0.00$, $p=0.00$) (**Table 4-10, Table 4-11**).

Taking into account all the clinical results together, we observed that macula-OFF RDs were significantly less presented in medium to high myopes, as well, AL >25mm was much less observed in the macula-OFF group. Several reasons might be involved in these

results. These reasons are discussed in detail in the chapter 4.1.4. But, it is interesting to mention that highly myopic patients are better informed on RD symptoms during standard clinical care. Also, the answer could be that a thinner choroid may restrict retinal perfusion and thus it may inhibit accumulation of SRF having as a consequence slower progression of RD. This implicate that the negative relationship between AL and choroidal thickness may contribute to the higher rate of macula-OFF RD in shorter eyes. (Flores-Moreno, Lugo et al. 2013, Alshareef, Khuthaila et al. 2017, Iwase, Kobayashi et al. 2017, Sayman Muslubas, Hocaoglu et al. 2017)

The opportunity to examine photoreceptors *in vivo* gave us the possibility to detect and evaluate subclinical changes in retinal diseases and therefore it raised the possibility to understand, explain and even maybe predict the functional recovery. For the first time, we used experimental imaging, adaptive optics fundus camera, in patients with primary RD (macula-ON and macula-OFF) during postoperative follow up. On a precise and well described way (**refer to the chapter 4.4.2**) we were tracing cones and analyzing the same region of ineterst in one eye over time, matching the adequate ROI between treated and fellow eye (**Figure 4-17, Figure 4-18**). In order to eliminate the noise, we introduced for the first time, the way to express results as the inter-eye difference (fellow eye – treated eye). The inter-eye difference was used before in some glaucoma studies and rarely in some reports with macular hole surgery. Wide use of the inter-eye difference stayed aside. This is very important in assymetric diseases, such as RD (**refer to chapter 4.4.2, paragraph Inter-eye difference**). To ensure our methodology for AO analysis, we analyzed the stability of cone density in the healthy, fellow eye. With AO, the cone density was stable in FE between M1 and M3. As expected, the cone density was decreased in treated eyes compared to fellow eyes. Surprisengly, cone density was reduced also in macula-ON RD at M1. During the 3 months follow up, cone density increased in the macula-ON group, but not in the macula-OFF group. VA and type of RD (macular involvement) were independently positively correlated with the cone density.

For the first time, in this study, the alterations in cone topography were observed even in the macula-ON RD patients after PPV with gas tamponade. This unexpected firstly decrease at M1 after PPV and consequently increase at M3 in cone density in macula-ON RD patients is the most controversial. Several mechanisms could explain these observations. There are probably several factors influencing these results. In previous studies on healthy subjects, the cone “disappearing” on AO fundus camera was explained by the Stiles-Crawford effect, i.e. that in order to have a detectable cone on the AO, it is necessary that the light is

making 90° with the cone. (Stiles and Crawford 1933, Roorda, Romero-Borja et al. 2002, Miloudi, Rossant et al. 2015, Morris, Blanco et al. 2015) In RD, photoreceptors are detached from the RPE, which make them change their orientation and spacing. Even in peripheral macula-ON RDs, the photoreceptors' stretching is transmitted from periphery towards the macular region, more specifically to foveal region. This disarray of photoreceptors might be due to changes in their polarity. All this might result in less detectable cones on the AO fundus camera in both, macula-ON and macula-OFF RDs. This distress might have two origins, disease-based (due to RD itself) and iatrogenic, due to the surgery. All the analyzed patients had undergone the pars plana vitrectomy with gas tamponade. It is still unknown what is the effect of vitrectomy itself on the cones neither the effect of the substances for tamponade that are for some amount of time in a continuous contact with the retina. More studies *in vivo* (e.g. with AO fundus camera) have to be performed in order to better characterize these mechanisms. The explanation for the cone "recovery" after three months after PPV in macula-ON RD can be supported by the study of Hageman et al, who proved that the interphotoreceptor (cone) matrix very firmly adheres to the RPE; cone sheaths even being stretched but attached to the RPE surface, might give the impression of increasing cone density with time. (Hageman, Marmor et al. 1995) Three months after PPV, the cones are realigning and becoming again detectable on the AO fundus camera. (Roorda, Romero-Borja et al. 2002, Roorda and Williams 2002, Morris, Blanco et al. 2015)

Also, the cones vitality and realignment might be linked to the choroidal perfusion as the outer retina is blood supplied from the adjacent choroid (the metabolic exchange). (Forrester, Dick et al. 2015) Different pathways of choroidal perfusion and consequently choroid reaction to the different types of RD, as previously described (**Figure 4-10, Table 4-10**), might influence also the postoperative cone recovery. This is important to investigate further in future studies, in order to be able to follow subclinical changes in photoreceptors and in choroid in order to predict the postoperative functional recovery.

The entire above mentioned have strong influence on patients' QoL. Even after good postoperative anatomical success (retina completely reattached), the visual function is not always the best. Reasons for postoperative visual disturbances might be explained with our clinical results. To better understand the impact of RD on patients' everyday life and their ability to come back to their normal activities, we examined their vision-related QoL distributing the NEI VFQ-13 instrument, in several time-points (**Table 3-1**). Being sure that in this shorten version the concept of unidimensionality is respected, as well as the appropriate interval-level measurement, we analyzed the composite score and the subscales

scores (**Table 4-3, Table 4-4, Figure 4-3**). Preoperatively, macula-ON patients were the least concerned, with the important difference compared to macula-OFF RD patients. As expected, macula-OFF patients were improving over follow up period, mostly following the improvement of the visual recovery. In the macula-ON group, patients were concerned at one month after surgery; even their BCVA didn't change significantly. This disappeared three months after surgery. It is very important to highlight that it is the socioemotional subscale where the highest changes were observed, and not the visual functioning subscale. For the first time we were using the shorten version of NEI VFQ-25, NEI VFQ-13 instrument. For the first time, we were reporting the QoL results on a homogenous group of patients, who all underwent the same type of surgery and tamponade. We are among rare studies who compared macula-ON and macula-OFF RD patients' QoL with a follow up. There were few studies reporting QoL after RD. (Okamoto, Okamoto et al. 2008, Zou, Zhang et al. 2011, van de Put, Hoeksema et al. 2014, Smretschig, Falkner-Radler et al. 2016) Majority of them analyzed QoL in patients with macula-OFF RD at one time-point after surgery (cross-sectional), mixed different types of surgeries (PPV + gas, PPV + silicon, scleral buckling) and macula-ON and macula-OFF groups. Only one study is reporting preoperative vision-related QoL in macula-ON and macula-OFF RDs, but they also combined patients with all surgery types. (Zou, Zhang et al. 2011)

It is very important to analyze the vision-related QoL in RD patients, as BCVA is not enough representative for the visual function in total and, as seen previously, even with the good BCVA patients might be concerned with their vision. To have a homogenous group of RD patients to study QoL the long-term prospective studies are needed, in order to catch all the intergroup differences. The weakness of our study is that we don't have a big number of answered questionnaires that fulfilled the criteria (one type of surgery, one type of tamponade, macula-ON separated from macula-OFF, and the questionnaire completed in all 4 time-points). Also, we didn't take into account the socio-economical characteristics of our patients. Our study group might be also biased by the type of patients that were treated or referred to the Jules-Gonin Eye Hospital, as they might be more complicated than in other ophthalmological centers.

To understand and characterize why the surgery should be performed as soon as possible in patients with RD, especially in macula-ON patients, and what is the prognosis of surgery if the macula is detached several days, the cellular mechanisms should be studied and understood. If we understand what cellular processes are leading to the unrecoverable visual function and unrecoverable photoreceptors degeneration, we could have the new target for

new treatment agents. In order to try to better understand what processes are happening in photoreceptors during RD, we designed for the human *in vitro* model of RD. Known already that photoreceptors are dying in RD, and that the dominant pathway of cell death is the apoptosis, we examined if there is the overlapping mechanism in the cell death between previously described retinal degenerations and RD. We tested if there is the re-entering in the cell cycle (especially G1/S phase regulators), by testing the presence of CDK4, the cyclin-dependent kinase, demonstrated that it is reactivated and is bringing cell again into a cell-cycle and consequently into apoptosis (**Figure 4-23**). The CDK4 were discovered in rodent models of retinal degenerations as well as in the rodent light-damage model. (Höglinger, Breunig et al. 2007, Sancho-Pelluz, Arango-Gonzalez et al. 2008, Zencak, Schouwey et al. 2013) TUNEL-staining demonstrated that there is a peak in cell death after three days *in vitro* (3DIV), i.e. if the retina is detached for three days (**Figure 4-24**). This is related to the clinical well-known experience that the RD lasting for more than 3 days is more damaged and the postoperative functional recovery is not as good as if the surgery was performed before. (Burton 1982) For the first time, we can confirm that the CDK4 is expressed also in the human *in vitro* model of RD. It is important to notice that the number of CDK4 positive cells is much lower compared to the number of TUNEL positive cells, giving us a message that there are probably other mechanisms that are also implicated in the photoreceptors' cell death in RD and that cell-cycle re-entrance is not the main pathway. Furthermore, we investigated other pathways. We tested the caspase-3, as for the final effector of apoptosis. Surprisingly, very few cells in the ONL were present in both groups. Further investigation included testing for the epigenetic modifications at the histone level, as described in some models of retinitis pigmentosa. (Farinelli, Perera et al. 2014) The H3K27me3 was present with the highest peak at 5DIV and being stable at 7DIV (the latest time-point) (**Figure 4-31, Figure 4-32, Table 4-20**). Furthermore, we decided to analyze for the apoptosis-inducing factor (AIF). It was confirmed in rodent models of retinal diseases. (Hisatomi, Sakamoto et al. 2001) Our results can confirm the present peak of AIF positive cells at 3DIV. These results suggest that the AIF has probably the main role in the early cell death. At later stages, the epigenetic modifications may play an important role in photoreceptors' cell death in RD model. Further investigations are needed to completely understand the mechanisms underlying the photoreceptors cell death in RD, especially in human retina. Once the target mechanism is found, the inhibitor molecule should be tested in order to prevent the cell death and ensure the complete photoreceptor recovery.

6. CONCLUSIONS

The most important conclusions of this study are:

1. Pseudophakic lens status and shorter AL are associated with macula-OFF RD.
2. There is a statistical significance in QoL CS between patients with macula-ON and macula-OFF RD
3. There is a statistical significance in the socioemotional and visual functioning subscales' scores between patients with macula-ON and macula-OFF RD, pre-operatively and post-operatively
4. In patients with macula-ON RD there is a notable drop of patients' QoL satisfaction one month after surgery
5. In the patients with macula-OFF patients there is a positive progression in their QoL satisfaction in the whole postoperative period
6. The biggest changes in QoL are present in the socioemotional subscale
7. We defined and characterized more precisely HMD as a distinct subgroup of RDs, which occurs in 4.4% of primary retinal detachments
8. VA recovery in HMD is good, although most patients report residual visual disturbances in their central visual field most probably induced by the changes in the outer retina along the demarcation line through the fovea
9. We report choroidal changes in the sub-foveal and in the sub-macular choroid in relation to the different extension of RD.
10. We observed that CT is thinner than in the fellow eyes patients with paracentral RD.
11. We observed that CT is even thinner than in fellow eyes in patients with macula-OFF RD.
12. In eyes with peripheral RD the CT was thicker than in the fellow eye
13. In the patients with peripheral RD, the CT in the fellow eyes was markedly thinner than in those presenting with paracentral RD or macula-OFF RD, indicating that these patients may have a lower risk of developing macula-OFF RD due to thinner baseline CT.
14. There is a statistically significant inter-eye difference between macula-ON and macula-OFF groups in cone density and cone spacing following pars plana vitrectomy
15. We observed an improvement in cone density in the macula-ON group between month 1 and month 3 postoperatively and positive correlation with BCVA.

16. We observed a statistically significant and independent correlation between cone density, type of RD and postoperative BCVA over time.
17. In the human *in vitro* model of RD, CDK4, H3K27me3 and AIF are expressed.
18. The peak of TUNEL positive cells in the human *in vitro* model of RD is observed at 3DIV
19. AIF positive cells are present in the human *in vitro* model of RD with the peak at 3DIV, suggesting that AIF mediates the first process of cell death
20. H3K27me3 positive cells are present with the peak at 5DIV and being stable at 7DIV, suggesting that at a later stage of degeneration the cell death may be related to epigenetic modification.
21. CDK4 positive cells are present in the human *in vitro* model of RD, but at a later stage than the peak of TUNEL positive cells, suggesting that there are some common cell death pathways between retinal degenerations and RD, but that the re-entrance into the cell cycle is not the main pathway of photoreceptors' death in RD.

7. REFERENCES

- Aapola, U., I. Liiv and P. Peterson (2002). "Imprinting regulator DNMT3L is a transcriptional repressor associated with histone deacetylase activity." Nucleic acids research **30**(16): 3602-3608.
- Akkoyun, I. and G. Yilmaz (2014). "Choroidal thickness after scleral buckling surgery versus pars plana vitrectomy in macula-off rhegmatogenous retinal detachment." Klinische Monatsblätter für Augenheilkunde **231**(10): 1029-1033.
- Al-Ubaidi, M. R., J. G. Hollyfield, P. A. Overbeek and W. Baehr (1992). "Photoreceptor degeneration induced by the expression of simian virus 40 large tumor antigen in the retina of transgenic mice." Proceedings of the National Academy of Sciences **89**(4): 1194-1198.
- Alberts, B., A. Johnson, J. Lewis, D. Morgan, M. Raff, K. Roberts and P. Walter (2015). Molecular Biology of the Cell (Garland Science, New York, 2002).
- Alonso, J., M. Espallargues, T. F. Andersen, S. D. Cassard, E. Dunn, P. Bernth-Petersen, J. C. Norregaard, C. Black, E. P. Steinberg and G. F. Anderson (1997). "International applicability of the VF-14: An index of visual function in patients with cataracts." Ophthalmology **104**(5): 799-807.
- Alshareef, R. A., M. K. Khuthaila, M. Januwada, A. Goud, D. Ferrara and J. Chhablani (2017). "Choroidal vascular analysis in myopic eyes: evidence of foveal medium vessel layer thinning." Int J Retina Vitreous **3**: 28.
- Anderson, D. H., W. H. Stern, S. K. Fisher, P. A. Erickson and G. A. Borgula (1981). "The onset of pigment epithelial proliferation after retinal detachment." Investigative ophthalmology & visual science **21**(1): 10-16.
- Anderson, D. H., W. H. Stern, S. K. Fisher, P. A. Erickson and G. A. Borgula (1983). "Retinal detachment in the cat: the pigment epithelial-photoreceptor interface." Invest Ophthalmol Vis Sci **24**(7): 906-926.
- Arroyo, J. G., L. Yang, D. Bula and D. F. Chen (2005). "Photoreceptor apoptosis in human retinal detachment." Am J Ophthalmol **139**(4): 605-610.
- Aydin Kurna, S., A. Altun, T. Gencaga, S. Akkaya and T. Sengor (2014). "Vision related quality of life in patients with keratoconus." J Ophthalmol **2014**: 694542.
- Barski, A., S. Cuddapah, K. Cui, T.-Y. Roh, D. E. Schones, Z. Wang, G. Wei, I. Chepelev and K. Zhao (2007). "High-resolution profiling of histone methylations in the human genome." Cell **129**(4): 823-837.

Berger, S. L. (2007). "The complex language of chromatin regulation during transcription." Nature **447**(7143): 407-412.

Besirli, C. G., N. D. Chinskey, Q.-D. Zheng and D. N. Zacks (2011). "Autophagy activation in the injured photoreceptor inhibits fas-mediated apoptosis." Investigative ophthalmology & visual science **52**(7): 4193-4199.

Bowling, B. (2015). Kanski's clinical ophthalmology: A systematic approach, Elsevier Health Sciences.

Bowling, B. (2015). Kanski's clinical ophthalmology – a systematic approach, Saunders Ltd.

Boyer, L. A., K. Plath, J. Zeitlinger, T. Brambrink, L. A. Medeiros, T. I. Lee, S. S. Levine, M. Wernig, A. Tajonar and M. K. Ray (2006). "Polycomb complexes repress developmental regulators in murine embryonic stem cells." nature **441**(7091): 349-353.

Brown, G. C. (1999). "Vision and quality-of-life." Transactions of the American Ophthalmological Society **97**: 473.

Brown, J. S., D. I. Flitcroft, G. S. Ying, E. L. Francis, G. F. Schmid, G. E. Quinn and R. A. Stone (2009). "In vivo human choroidal thickness measurements: evidence for diurnal fluctuations." Invest Ophthalmol Vis Sci **50**(1): 5-12.

Burton, T. C. (1982). "Recovery of visual acuity after retinal detachment involving the macula." Trans Am Ophthalmol Soc **80**: 475-497.

Burton, T. C. (1989). "The influence of refractive error and lattice degeneration on the incidence of retinal detachment." Transactions of the American Ophthalmological Society **87**: 143.

Caputo, G., F. Metge, C. Arndt and J. Conrath (2012). Décollements de rétine: Rapport SFO 2011, Elsevier Health Sciences.

Carroll, J., D. B. Kay, D. Scoles, A. Dubra and M. Lombardo (2013). "Adaptive optics retinal imaging--clinical opportunities and challenges." Curr Eye Res **38**(7): 709-721.

Carvounis, P. E. and E. R. Holz (2005). "Management of retinal breaks and conditions predisposing to retinal detachment." Comprehensive ophthalmology update **7**(1): 13-22.

Chakraborty, R., S. A. Read and M. J. Collins (2011). "Diurnal variations in axial length, choroidal thickness, intraocular pressure, and ocular biometrics." Invest Ophthalmol Vis Sci **52**(8): 5121-5129.

Chang, B., N. Hawes, R. Hurd, M. Davisson, S. Nusinowitz and J. Heckenlively (2002). "Retinal degeneration mutants in the mouse." Vision research **42**(4): 517-525.

Chen, C. Y., C. Hooper, D. Chiu, M. Chamberlain, N. Karia and W. J. Heriot (2007). "Management of submacular hemorrhage with intravitreal injection of tissue plasminogen activator and expansile gas." Retina **27**(3): 321-328.

Chen, M., D. Rajapakse, M. Fraczek, C. Luo, J. V. Forrester and H. Xu (2016). "Retinal pigment epithelial cell multinucleation in the aging eye - a mechanism to repair damage and maintain homeostasis." Aging Cell **15**(3): 436-445.

Chen, S. N., B. Lian Ie and Y. J. Wei (2016). "Epidemiology and clinical characteristics of rhegmatogenous retinal detachment in Taiwan." Br J Ophthalmol **100**(9): 1216-1220.

Cheng, C.-Y., M.-Y. Yen, H.-Y. Lin, W.-W. Hsia and W.-M. Hsu (2004). "Association of ocular dominance and anisometric myopia." Investigative ophthalmology & visual science **45**(8): 2856-2860.

Chinskey, N. D., Q.-D. Zheng and D. N. Zacks (2014). "Control of photoreceptor autophagy after retinal detachment: the switch from survival to death." Investigative ophthalmology & visual science **55**(2): 688-695.

Choma, M., M. Sarunic, C. Yang and J. Izatt (2003). "Sensitivity advantage of swept source and Fourier domain optical coherence tomography." Opt Express **11**(18): 2183-2189.

Colin, J., A. Robinet and B. Cochener (1999). "Retinal detachment after clear lens extraction for high myopia: seven-year follow-up." Ophthalmology **106**(12): 2281-2285.

Cook, B., G. P. Lewis, S. K. Fisher and R. Adler (1995). "Apoptotic photoreceptor degeneration in experimental retinal detachment." Invest Ophthalmol Vis Sci **36**(6): 990-996.

Coyle, J. T. (1984). "Keratoconus and eye rubbing." Am J Ophthalmol **97**(4): 527-528.

Curcio, C. A., K. R. Sloan Jr, O. Packer, A. E. Hendrickson and R. E. Kalina (1987). "Distribution of cones in human and monkey retina: individual variability and radial asymmetry." Science **236**: 579-583.

Curcio, C. A., K. R. Sloan, R. E. Kalina and A. E. Hendrickson (1990). "Human photoreceptor topography." J Comp Neurol **292**(4): 497-523.

de Boer, J. F., B. Cense, B. H. Park, M. C. Pierce, G. J. Tearney and B. E. Bouma (2003). "Improved signal-to-noise ratio in spectral-domain compared with time-domain optical coherence tomography." Opt Lett **28**(21): 2067-2069.

Delolme, M. P., B. Dugas, F. Nicot, A. Muselier, A. M. Bron and C. Creuzot-Garcher (2012). "Anatomical and functional macular changes after rhegmatogenous retinal detachment with macula off." Am J Ophthalmol **153**(1): 128-136.

- Deramo, V. A., T. A. Cox, A. B. Syed, P. P. Lee and S. Fekrat (2003). "Vision-related quality of life in people with central retinal vein occlusion using the 25-item National Eye Institute Visual Function Questionnaire." Arch Ophthalmol **121**(9): 1297-1302.
- Dougherty, B. E. and M. A. Bullimore (2010). "Comparison of scoring approaches for the NEI VFQ-25 in low vision." Optometry and vision science: official publication of the American Academy of Optometry **87**(8): 543.
- Drexler, W. and J. G. Fujimoto (2008). Optical coherence tomography: technology and applications, Springer Science & Business Media.
- Drexler, W., U. Morgner, F. X. Kartner, C. Pitris, S. A. Boppart, X. D. Li, E. P. Ippen and J. G. Fujimoto (1999). "In vivo ultrahigh-resolution optical coherence tomography." Opt Lett **24**(17): 1221-1223.
- Eagling, E. M. (1974). "Ocular damage after blunt trauma to the eye. Its relationship to the nature of the injury." The British journal of ophthalmology **58**(2): 126.
- Edmund, J. (1968). "Analysis of the subretinal fluid. Measurement of the onkotic pressure." Acta Ophthalmol (Copenh) **46**(6): 1184-1193.
- Falkner-Radler, C. I., J. S. Myung, S. Moussa, R. V. Chan, E. Smretschmig, S. Kiss, A. Graf, J. D'Amico D and S. Binder (2011). "Trends in primary retinal detachment surgery: results of a Bicenter study." Retina **31**(5): 928-936.
- Farinelli, P., A. Perera, B. Arango-Gonzalez, D. Trifunovic, M. Wagner, T. Carell, M. Biel, E. Zrenner, S. Michalakakis and F. Paquet-Durand (2014). "DNA methylation and differential gene regulation in photoreceptor cell death." Cell death & disease **5**(12): e1558.
- Fayers, P. M. and D. Machin (2013). Quality of life: the assessment, analysis and interpretation of patient-reported outcomes, John Wiley & Sons.
- Fernandez, E. and P. Artal (2003). "Membrane deformable mirror for adaptive optics: performance limits in visual optics." Opt Express **11**(9): 1056-1069.
- Ferrari, K. J., A. Scelfo, S. Jammula, A. Cuomo, I. Barozzi, A. Stützer, W. Fischle, T. Bonaldi and D. Pasini (2014). "Polycomb-dependent H3K27me1 and H3K27me2 regulate active transcription and enhancer fidelity." Molecular cell **53**(1): 49-62.
- Ferris, F. L., A. Kassoff, G. H. Bresnick and I. Bailey (1982). "New visual acuity charts for clinical research." American journal of ophthalmology **94**(1): 91-96.
- Fisher, S. K., G. P. Lewis, K. A. Linberg and M. R. Verardo (2005). "Cellular remodeling in mammalian retina: results from studies of experimental retinal detachment." Prog Retin Eye Res **24**(3): 395-431.

Flores-Moreno, I., F. Lugo, J. S. Duker and J. M. Ruiz-Moreno (2013). "The relationship between axial length and choroidal thickness in eyes with high myopia." Am J Ophthalmol **155**(2): 314-319.e311.

Forrester, J. V., A. D. Dick, P. G. McMenamin, F. Roberts and E. Pearlman (2015). The eye: basic sciences in practice, Elsevier Health Sciences.

Fukuda, S., F. Okamoto, M. Yuasa, T. Kunikata, Y. Okamoto, T. Hiraoka and T. Oshika (2009). "Vision-related quality of life and visual function in patients undergoing vitrectomy, gas tamponade and cataract surgery for macular hole." Br J Ophthalmol **93**(12): 1595-1599.

Gabriele, M. L., G. Wollstein, H. Ishikawa, L. Kagemann, J. Xu, L. S. Folio and J. S. Schuman (2011). "Optical coherence tomography: history, current status, and laboratory work." Invest Ophthalmol Vis Sci **52**(5): 2425-2436.

Galluzzi, L., I. Vitale, J. Abrams, E. Alnemri, E. Baehrecke, M. Blagosklonny, T. M. Dawson, V. Dawson, W. El-Deiry and S. Fulda (2012). "Molecular definitions of cell death subroutines: recommendations of the Nomenclature Committee on Cell Death 2012." Cell Death & Differentiation **19**(1): 107-120.

Gavrieli, Y., Y. Sherman and S. A. Ben-Sasson (1992). "Identification of programmed cell death in situ via specific labelling of nuclear DNA fragmentation." Journal of cell Biology **119**: 493-493.

Gil, J. and G. Peters (2006). "Regulation of the INK4b–ARF–INK4a tumour suppressor locus: all for one or one for all." Nature reviews Molecular cell biology **7**(9): 667-677.

Globe, D. R., S. Levin, T. S. Chang, P. J. Mackenzie and S. Azen (2002). "Validity of the SF-12 quality of life instrument in patients with retinal diseases." Ophthalmology **109**(10): 1793-1798.

Go, S. L., C. B. Hoyng and C. C. Klaver (2005). "Genetic risk of rhegmatogenous retinal detachment: a familial aggregation study." Archives of Ophthalmology **123**(9): 1237-1241.

Golstein, P. and G. Kroemer (2007). "Cell death by necrosis: towards a molecular definition." Trends Biochem Sci **32**(1): 37-43.

Gonin, J. (1930). "The treatment of detached retina by searing the retinal tears." Archives of Ophthalmology **4**(5): 621-625.

Grizzard, W. S., G. F. Hilton, M. E. Hammer and D. Taren (1994). "A multivariate analysis of anatomic success of retinal detachments treated with scleral buckling." Graefes Arch Clin Exp Ophthalmol **232**(1): 1-7.

Group, S. S. T. R. (2003). "Responsiveness of the National Eye Institute Visual Function Questionnaire to changes in visual acuity: findings in patients with subfoveal choroidal neovascularization—SST Report No. 1." Archives of ophthalmology **121**(4): 531.

Guerin, C. J., G. P. Lewis, S. K. Fisher and D. H. Anderson (1993). "Recovery of photoreceptor outer segment length and analysis of membrane assembly rates in regenerating primate photoreceptor outer segments." Invest Ophthalmol Vis Sci **34**(1): 175-183.

Gutierrez, P., M. R. Wilson, C. Johnson, M. Gordon, G. A. Cioffi, R. Ritch, M. Sherwood, K. Meng and C. M. Mangione (1997). "Influence of glaucomatous visual field loss on health-related quality of life." Archives of ophthalmology **115**(6): 777-784.

Hageman, G. S., M. F. Marmor, X. Y. Yao and L. V. Johnson (1995). "The interphotoreceptor matrix mediates primate retinal adhesion." Arch Ophthalmol **113**(5): 655-660.

Hammer, M. E., T. G. Burch and D. Rinder (1986). "Viscosity of subretinal fluid and its clinical correlations." Retina **6**(4): 234-238.

Hassan, T. S., R. Sarrafizadeh, A. J. Ruby, B. R. Garretson, B. Kuczynski and G. A. Williams (2002). "The effect of duration of macular detachment on results after the scleral buckle repair of primary, macula-off retinal detachments." Ophthalmology **109**(1): 146-152.

Hassan, T. S., R. Sarrafizadeh, A. J. Ruby, B. R. Garretson, B. Kuczynski and G. A. Williams (2002). "The effect of duration of macular detachment on results after the scleral buckle repair of primary, macula-off retinal detachments." Ophthalmology **109**(1): 146-152.

Herrup, K. and Y. Yang (2007). "Cell cycle regulation in the postmitotic neuron: oxymoron or new biology?" Nature Reviews Neuroscience **8**(5): 368-378.

Hisatomi, T., T. Nakazawa, K. Noda, L. Almulki, S. Miyahara, S. Nakao, Y. Ito, H. She, R. Kohno and N. Michaud (2008). "HIV protease inhibitors provide neuroprotection through inhibition of mitochondrial apoptosis in mice." The Journal of clinical investigation **118**(6): 2025-2038.

Hisatomi, T., T. Sakamoto, Y. Goto, I. Yamanaka, Y. Oshima, Y. Hata, T. Ishibashi, H. Inomata, S. A. Susin and G. Kroemer (2002). "Critical role of photoreceptor apoptosis in functional damage after retinal detachment." Current eye research **24**(3): 161-172.

Hisatomi, T., T. Sakamoto, T. Murata, I. Yamanaka, Y. Oshima, Y. Hata, T. Ishibashi, H. Inomata, S. A. Susin and G. Kroemer (2001). "Relocalization of apoptosis-inducing factor in photoreceptor apoptosis induced by retinal detachment in vivo." Am J Pathol **158**(4): 1271-1278.

Ho, S., A. Fitt, K. Frimpong-Ansah and M. Benson (2006). "The management of primary rhegmatogenous retinal detachment not involving the fovea." Eye **20**(9): 1049-1053.

Hofer, H., P. Artal, B. Singer, J. L. Aragon and D. R. Williams (2001). "Dynamics of the eye's wave aberration." J Opt Soc Am A Opt Image Sci Vis **18**(3): 497-506.

Höglinger, G. U., J. J. Breunig, C. Depboylu, C. Rouaux, P. P. Michel, D. Alvarez-Fischer, A.-L. Boutillier, J. DeGregori, W. H. Oertel and P. Rakic (2007). "The pRb/E2F cell-cycle pathway mediates cell death in Parkinson's disease." Proceedings of the National Academy of Sciences **104**(9): 3585-3590.

Howie, A. R., E. Darian-Smith, P. L. Allen and B. Vote (2016). "Whole population incidences of patients presenting with rhegmatogenous retinal detachments within Tasmania, Australia." Clinical and Experimental Ophthalmology: 144-146.

Huang, D., E. A. Swanson, C. P. Lin, J. S. Schuman, W. G. Stinson, W. Chang, M. R. Hee, T. Flotte, K. Gregory, C. A. Puliafito and et al. (1991). "Optical coherence tomography." Science **254**(5035): 1178-1181.

Ikuno, Y., I. Maruko, Y. Yasuno, M. Miura, T. Sekiryu, K. Nishida and T. Iida (2011). "Reproducibility of retinal and choroidal thickness measurements in enhanced depth imaging and high-penetration optical coherence tomography." Investigative ophthalmology & visual science **52**(8): 5536-5540.

Imamura, Y., T. Fujiwara, R. Margolis and R. F. Spaide (2009). "Enhanced depth imaging optical coherence tomography of the choroid in central serous chorioretinopathy." Retina **29**(10): 1469-1473.

Ioannidis, A. S., L. Speedwell and K. K. Nischal (2005). "Unilateral keratoconus in a child with chronic and persistent eye rubbing." Am J Ophthalmol **139**(2): 356-357.

Iwase, T., M. Kobayashi, K. Yamamoto, K. Yanagida, E. Ra and H. Terasaki (2017). "Change in choroidal blood flow and choroidal morphology due to segmental scleral buckling in eyes with rhegmatogenous retinal detachment." Sci Rep **7**(1): 5997.

Jablonski, M. M., J. Tombran-Tink, D. A. Mrazek and A. Iannaccone (2000). "Pigment epithelium-derived factor supports normal development of photoreceptor neurons and opsin expression after retinal pigment epithelium removal." Journal of Neuroscience **20**(19): 7149-7157.

Jenuwein, T. and C. D. Allis (2001). "Translating the histone code." Science **293**(5532): 1074-1080.

Jones, P. A. (2012). "Functions of DNA methylation: islands, start sites, gene bodies and beyond." Nature Reviews Genetics **13**(7): 484-492.

Jones, P. A. and G. Liang (2009). "Rethinking how DNA methylation patterns are maintained." Nature Reviews Genetics **10**(11): 805-811.

- Kaluzny, J. (1970). "Myopia and retinal detachment." Pol Med J **9**(6): 1544-1549.
- Karabatsos, G. (2001). "The Rasch model, additive conjoint measurement, and new models of probabilistic measurement theory." Journal of applied measurement **2**(4): 389-423.
- Kaur, J., S. Mencl, A. Sahaboglu, P. Farinelli, T. Van Veen, E. Zrenner, P. Ekström, F. Paquet-Durand and B. Arango-Gonzalez (2011). "Calpain and PARP activation during photoreceptor cell death in P23H and S334ter rhodopsin mutant rats." PLoS One **6**(7): e22181.
- Keilhauer, C. N. and F. C. Delori (2006). "Near-infrared autofluorescence imaging of the fundus: visualization of ocular melanin." Invest Ophthalmol Vis Sci **47**(8): 3556-3564.
- Khadka, J., C. McAlinden and K. Pesudovs (2013). "Quality assessment of ophthalmic questionnaires: review and recommendations." Optometry & Vision Science **90**(8): 720-744.
- Kimura, M., A. Nishimura, H. Yokogawa, T. Okuda, T. Higashide, Y. Saito and K. Sugiyama (2012). "Subfoveal choroidal thickness change following segmental scleral buckling for rhegmatogenous retinal detachment." American journal of ophthalmology **154**(5): 893-900.
- Kitaguchi, Y., K. Bessho, T. Yamaguchi, N. Nakazawa, T. Mihashi and T. Fujikado (2007). "In vivo measurements of cone photoreceptor spacing in myopic eyes from images obtained by an adaptive optics fundus camera." Jpn J Ophthalmol **51**(6): 456-461.
- Klein, B. E., R. Klein and S. E. Moss (1998). "Self-rated health and diabetes of long duration. The Wisconsin Epidemiologic Study of Diabetic Retinopathy." Diabetes Care **21**(2): 236-240.
- Klein, R., S. E. Moss, B. E. Klein, P. Gutierrez and C. M. Mangione (2001). "The NEI-VFQ-25 in people with long-term type 1 diabetes mellitus: the Wisconsin Epidemiologic Study of Diabetic Retinopathy." Arch Ophthalmol **119**(5): 733-740.
- Kobayashi, M., T. Iwase, K. Yamamoto, E. Ra, K. Murotani and H. Terasaki (2017). "Perioperative factors that are significantly correlated with final visual acuity in eyes after successful rhegmatogenous retinal detachment surgery." PLoS One **12**(9): e0184783.
- Koh, H. J., L. Cheng, B. Kosobucki and W. R. Freeman (2007). "Prophylactic intraoperative 360 laser retinopexy for prevention of retinal detachment." Retina **27**(6): 744-749.
- Koizumi, H., T. Yamagishi, T. Yamazaki, R. Kawasaki and S. Kinoshita (2011). "Subfoveal choroidal thickness in typical age-related macular degeneration and polypoidal choroidal vasculopathy." Graefes Arch Clin Exp Ophthalmol **249**(8): 1123-1128.
- Kolb, H. (2003). "How the retina works." American scientist **91**(1): 28-35.
- Kontos, A. and T. H. Williamson (2016). "Rate and risk factors for the conversion of fovea-on to fovea-off rhegmatogenous retinal detachment while awaiting surgery." Br J Ophthalmol.

Korobelnik Jean-François, T. R. (2014). Décollement de la rétine / Chirurgie maculaire. Paris, Médecine Sciences Publications Lavoisier.

Kouzarides, T. (2007). "Chromatin modifications and their function." Cell **128**(4): 693-705.

Kreissig, I., H. Lincoff, B. Witassek and G. Kolling (1981). Color vision and other parameters of macular function after retinal reattachment. Current Concepts in Diagnosis and Treatment of Vitreoretinal Diseases, Karger Publishers: 77-85.

Kroemer, G., L. Galluzzi, P. Vandenabeele, J. Abrams, E. Alnemri, E. Baehrecke, M. Blagosklonny, W. El-Deiry, P. Golstein and D. Green (2009). "Classification of cell death: recommendations of the Nomenclature Committee on Cell Death 2009." Cell Death & Differentiation **16**(1): 3-11.

Kubay, O. V., D. G. Charteris, H. S. Newland and G. L. Raymond (2005). "Retinal detachment neuropathology and potential strategies for neuroprotection." Surv Ophthalmol **50**(5): 463-475.

Kunchithapautham, K. and B. Rohrer (2007). "Apoptosis and autophagy in photoreceptors exposed to oxidative stress." Autophagy **3**(5): 433-441.

Kunchithapautham, K. and B. Rohrer (2007). "Autophagy is one of the multiple mechanisms active in photoreceptor degeneration." Autophagy **3**(1): 65-66.

Kur, J., E. A. Newman and T. Chan-Ling (2012). "Cellular and physiological mechanisms underlying blood flow regulation in the retina and choroid in health and disease." Progress in retinal and eye research **31**(5): 377-406.

Laatikainen, L., E. M. Tolppanen and H. Harju (1985). "Epidemiology of rhegmatogenous retinal detachment in a Finnish population." Acta ophthalmologica **63**(1): 59-64.

Lecleire-Collet, A., M. Muraine, J. F. Menard and G. Bresseur (2006). "Evaluation of macular changes before and after successful retinal detachment surgery using stratus-optical coherence tomography." Am J Ophthalmol **142**(1): 176-179.

Lee, K. E., B. E. Klein, R. Klein, Z. Quandt and T. Y. Wong (2009). "Association of age, stature, and education with ocular dimensions in an older white population." Archives of ophthalmology **127**(1): 88-93.

Lee, P. P., S. M. Whitcup, R. D. Hays, K. Spritzer and J. Javitt (1995). "The relationship between visual acuity and functioning and well-being among diabetics." Qual Life Res **4**(4): 319-323.

Lee, T. I., R. G. Jenner, L. A. Boyer, M. G. Guenther, S. S. Levine, R. M. Kumar, B. Chevalier, S. E. Johnstone, M. F. Cole and K.-i. Isono (2006). "Control of developmental regulators by Polycomb in human embryonic stem cells." Cell **125**(2): 301-313.

Lees, E. (1995). "Cyclin dependent kinase regulation." Current opinion in cell biology 7(6): 773-780.

Leitgeb, R., C. Hitzenberger and A. Fercher (2003). "Performance of fourier domain vs. time domain optical coherence tomography." Opt Express 11(8): 889-894.

Lewis, G., D. Charteris, C. Sethi and S. Fisher (2002). Animal models of retinal detachment and reattachment: identifying cellular events that may affect visual recovery, Nature Publishing Group.

Lewis, G. P., C. J. Guérin, D. H. Anderson, B. Matsumoto and S. K. Fisher (1994). "Rapid changes in the expression of glial cell proteins caused by experimental retinal detachment." American Journal of Ophthalmology 118(3): 368-376.

Liang, J., D. R. Williams and D. T. Miller (1997). "Supernormal vision and high-resolution retinal imaging through adaptive optics." J Opt Soc Am A Opt Image Sci Vis 14(11): 2884-2892.

Liem, A. T., J. E. Keunen, G. J. van Meel and D. van Norren (1994). "Serial foveal densitometry and visual function after retinal detachment surgery with macular involvement." Ophthalmology 101(12): 1945-1952.

Lina, G., Q. Xuemin, W. Qinmei and S. Lijun (2016). "Vision-related quality of life, metamorphopsia, and stereopsis after successful surgery for rhegmatogenous retinal detachment." Eye (Lond) 30(1): 40-45.

Lincoff, H. and R. Gieser (1971). "Finding the retinal hole." Arch Ophthalmol 85(5): 565-569.

Linder, M., T. S. Chang, I. U. Scott, D. Hay, K. Chambers, L. M. Sibley and E. Weis (1999). "Validity of the visual function index (VF-14) in patients with retinal disease." Arch Ophthalmol 117(12): 1611-1616.

Linsenmeier, R. A. and L. Padnick-Silver (2000). "Metabolic dependence of photoreceptors on the choroid in the normal and detached retina." Invest Ophthalmol Vis Sci 41(10): 3117-3123.

Lombardo, M., S. Serrao, P. Ducoli and G. Lombardo (2013). "Eccentricity dependent changes of density, spacing and packing arrangement of parafoveal cones." Ophthalmic Physiol Opt 33(4): 516-526.

Lumbroso, B., D. Huang, A. Romano, M. Rispoli and G. Coscas (2013). Clinical en face OCT atlas, JP Medical Ltd.

Lundström, M. and E. Wendel (2006). "Assessment of vision-related quality of life measures in ophthalmic conditions." Expert review of pharmacoeconomics & outcomes research **6**(6): 691-724.

Machemer, R. and U. H. Steinhorst (1993). "Retinal separation, retinotomy, and macular relocation: I. Experimental studies in the rabbit eye." Graefes Arch Clin Exp Ophthalmol **231**(11): 629-634.

Machemer, R. and U. H. Steinhorst (1993). "Retinal separation, retinotomy, and macular relocation: II. A surgical approach for age-related macular degeneration?" Graefes Arch Clin Exp Ophthalmol **231**(11): 635-641.

Mackenzie, P. J., T. S. Chang, I. U. Scott, M. Linder, D. Hay, W. J. Feuer and K. Chambers (2002). "Assessment of vision-related function in patients with age-related macular degeneration." Ophthalmology **109**(4): 720-729.

Mallinson, T. (2007). "Why measurement matters for measuring patient vision outcomes." Optometry & Vision Science **84**(8): E675-E682.

Mangione, C. M., S. Berry, K. Spritzer, N. K. Janz, R. Klein, C. Owsley and P. P. Lee (1998). "Identifying the content area for the 51-item National Eye Institute Visual Function Questionnaire: results from focus groups with visually impaired persons." Archives of Ophthalmology **116**(2): 227-233.

Mangione, C. M., P. P. Lee, P. R. Gutierrez, K. Spritzer, S. Berry and R. D. Hays (2001). "Development of the 25-item National Eye Institute Visual Function Questionnaire." Arch Ophthalmol **119**(7): 1050-1058.

Mangione, C. M., P. P. Lee, J. Pitts, P. Gutierrez, S. Berry and R. D. Hays (1998). "Psychometric properties of the National Eye Institute Visual Function Questionnaire (NEI-VFQ). NEI-VFQ Field Test Investigators." Arch Ophthalmol **116**(11): 1496-1504.

Margolis, M. K., K. Coyne, T. Kennedy-Martin, T. Baker, O. Schein and D. A. Revicki (2002). "Vision-specific instruments for the assessment of health-related quality of life and visual functioning: a literature review." Pharmacoeconomics **20**(12): 791-812.

Margolis, R. and R. F. Spaide (2009). "A pilot study of enhanced depth imaging optical coherence tomography of the choroid in normal eyes." Am J Ophthalmol **147**(5): 811-815.

Massof, R. W. and D. C. Fletcher (2001). "Evaluation of the NEI visual functioning questionnaire as an interval measure of visual ability in low vision." Vision Res **41**(3): 397-413.

Massof, R. W. and G. S. Rubin (2001). "Visual function assessment questionnaires." Survey of ophthalmology **45**(6): 531-548.

Matsumoto, H., J. W. Miller and D. G. Vavvas (2013). "Retinal detachment model in rodents by subretinal injection of sodium hyaluronate." JoVE (Journal of Visualized Experiments)(79): e50660-e50660.

Menu dit Huart, L., O. Lorentz, O. Goureau, T. Leveillard and J. A. Sahel (2004). "DNA repair in the degenerating mouse retina." Mol Cell Neurosci **26**(3): 441-449.

Mermoud, J. E., S. P. Rowbotham and P. D. Varga-Weisz (2011). "Keeping chromatin quiet: how nucleosome remodeling restores heterochromatin after replication." Cell cycle **10**(23): 4017-4025.

Mikkelsen, T. S., M. Ku, D. B. Jaffe, B. Issac, E. Lieberman, G. Giannoukos, P. Alvarez, W. Brockman, T.-K. Kim and R. P. Koche (2007). "Genome-wide maps of chromatin state in pluripotent and lineage-committed cells." Nature **448**(7153): 553-560.

Miller, D., O. Kocaoglu, Q. Wang and S. Lee (2011). "Adaptive optics and the eye (super resolution OCT)." Eye **25**(3): 321.

Miller, D. T., D. R. Williams, G. M. Morris and J. Liang (1996). "Images of cone photoreceptors in the living human eye." Vision Res **36**(8): 1067-1079.

Miloudi, C., F. Rossant, I. Bloch, C. Chaumette, A. Leseigneur, J. A. Sahel, S. Meimon, S. Mrejen and M. Paques (2015). "The Negative Cone Mosaic: A New Manifestation of the Optical Stiles-Crawford Effect in Normal Eyes." Invest Ophthalmol Vis Sci **56**(12): 7043-7050.

Mitry, D., M. A. Awan, S. Borooah, A. Syrogiannis, C. Lim-Fat, H. Campbell, A. F. Wright, B. W. Fleck, D. G. Charteris and D. Yorston (2012). "Long-term visual acuity and the duration of macular detachment: findings from a prospective population-based study." British Journal of Ophthalmology: bjophthalmol-2012-302330.

Mitry, D., M. A. Awan, S. Borooah, A. Syrogiannis, C. Lim-Fat, H. Campbell, A. F. Wright, B. W. Fleck, D. G. Charteris, D. Yorston and J. Singh (2013). "Long-term visual acuity and the duration of macular detachment: findings from a prospective population-based study." Br J Ophthalmol **97**(2): 149-152.

Mitry, D., J. Chalmers, K. Anderson, L. Williams, B. W. Fleck, A. Wright and H. Campbell (2010). "Temporal trends in retinal detachment incidence in Scotland between 1987 and 2006." British Journal of Ophthalmology: bjo. 2010.172296.

Mitry, D., D. G. Charteris, B. W. Fleck, H. Campbell and J. Singh (2010). "The epidemiology of rhegmatogenous retinal detachment: geographical variation and clinical associations." Br J Ophthalmol **94**(6): 678-684.

Mitry, D., D. G. Charteris, B. W. Fleck, H. Campbell and J. Singh (2010). "The epidemiology of rhegmatogenous retinal detachment: geographical variation and clinical associations." British Journal of Ophthalmology **94**(6): 678-684.

Mitry, D., D. G. Charteris, D. Yorston, M. R. Siddiqui, H. Campbell, A.-L. Murphy, B. W. Fleck, A. F. Wright and J. Singh (2010). "The epidemiology and socioeconomic associations of retinal detachment in Scotland: a two-year prospective population-based study." Investigative ophthalmology & visual science **51**(10): 4963-4968.

Mitry, D., J. Singh, D. Yorston, M. A. Siddiqui, A. Wright, B. W. Fleck, H. Campbell and D. G. Charteris (2011). "The predisposing pathology and clinical characteristics in the Scottish retinal detachment study." Ophthalmology **118**(7): 1429-1434.

Mitry, D., S. Tuft, D. McLeod and D. G. Charteris (2011). "Laterality and gender imbalances in retinal detachment." Graefes Arch Clin Exp Ophthalmol **249**(7): 1109-1110.

Miura, M., G. Arimoto, R. Tsukahara, R. Nemoto, T. Iwasaki and H. Goto (2012). "Choroidal thickness after scleral buckling." Ophthalmology **119**(7): 1497-1498.

Morey, L. and K. Helin (2010). "Polycomb group protein-mediated repression of transcription." Trends in biochemical sciences **35**(6): 323-332.

Morgan, I. G., K. Ohno-Matsui and S. M. Saw (2012). "Myopia." Lancet **379**(9827): 1739-1748.

Morris, H. J., L. Blanco, J. L. Codona, S. L. Li, S. S. Choi and N. Doble (2015). "Directionality of individual cone photoreceptors in the parafoveal region." Vision Res **117**: 67-80.

Mrejen, S., T. Sato, C. A. Curcio and R. F. Spaide (2014). "Assessing the cone photoreceptor mosaic in eyes with pseudodrusen and soft Drusen in vivo using adaptive optics imaging." Ophthalmology **121**(2): 545-551.

Mrejen, S. and R. F. Spaide (2013). "Optical coherence tomography: imaging of the choroid and beyond." Surv Ophthalmol **58**(5): 387-429.

Mruthyunjaya, P., S. S. Stinnett and C. A. Toth (2004). "Change in visual function after macular translocation with 360 degrees retinectomy for neovascular age-related macular degeneration." Ophthalmology **111**(9): 1715-1724.

Murakami, T., F. Okamoto, Y. Sugiura, Y. Okamoto, T. Hiraoka and T. Oshika (2017). "Changes in metamorphopsia and optical coherence tomography findings after successful retinal detachment surgery." Retina.

- Murakami, Y., S. Notomi, T. Hisatomi, T. Nakazawa, T. Ishibashi, J. W. Miller and D. G. Vavvas (2013). "Photoreceptor cell death and rescue in retinal detachment and degenerations." Progress in retinal and eye research **37**: 114-140.
- Murakami, Y., S. Notomi, T. Hisatomi, T. Nakazawa, T. Ishibashi, J. W. Miller and D. G. Vavvas (2013). "Photoreceptor cell death and rescue in retinal detachment and degenerations." Prog Retin Eye Res **37**: 114-140.
- Musch, D. C., A. A. Farjo, R. F. Meyer, M. N. Waldo and N. K. Janz (1997). "Assessment of health-related quality of life after corneal transplantation." Am J Ophthalmol **124**(1): 1-8.
- Muthiah, M. N., C. Gias, F. K. Chen, J. Zhong, Z. McClelland, F. B. Sallo, T. Peto, P. J. Coffey and L. da Cruz (2014). "Cone photoreceptor definition on adaptive optics retinal imaging." Br J Ophthalmol **98**(8): 1073-1079.
- Narendran, V., A. Kothari, S. Charles, V. Saravanan and I. Kreissig (2014). Principles and Practice of Vitreoretinal Surgery, JP Medical Ltd.
- Nassiri, N., S. Mehravaran, K. Nouri-Mahdavi and A. L. Coleman (2013). "National Eye Institute Visual Function Questionnaire: usefulness in glaucoma." Optom Vis Sci **90**(8): 745-753.
- Nguyen, M. D., M. Boudreau, J. Kriz, S. Couillard-Després, D. R. Kaplan and J.-P. Julien (2003). "Cell cycle regulators in the neuronal death pathway of amyotrophic lateral sclerosis caused by mutant superoxide dismutase 1." Journal of Neuroscience **23**(6): 2131-2140.
- Nickla, D. L. and J. Wallman (2010). "The multifunctional choroid." Prog Retin Eye Res **29**(2): 144-168.
- Nordmann, J. P., M. Viala, K. Sullivan, B. Arnould and G. Berdeaux (2004). "Psychometric Validation of the National Eye Institute Visual Function Questionnaire - 25 (NEI VFQ-25) French version: in a population of patients treated for ocular hypertension and glaucoma." Pharmacoeconomics **22**(3): 197-206.
- Odrobina, D., I. Laudanska-Olszewska, P. Gozdek, M. Maroszynski and M. Amon (2013). "Influence of scleral buckling surgery with encircling band on subfoveal choroidal thickness in long-term observations." Biomed Res Int **2013**: 586894.
- Okamoto, F., Y. Okamoto, S. Fukuda, T. Hiraoka and T. Oshika (2010). "Vision-related quality of life and visual function after vitrectomy for various vitreoretinal disorders." Invest Ophthalmol Vis Sci **51**(2): 744-751.
- Okamoto, F., Y. Okamoto, T. Hiraoka and T. Oshika (2008). "Vision-related quality of life and visual function after retinal detachment surgery." Am J Ophthalmol **146**(1): 85-90.

Okamoto, F., Y. Sugiura, Y. Okamoto, T. Hiraoka and T. Oshika (2013). "Changes in contrast sensitivity after surgery for macula-on rhegmatogenous retinal detachment." Am J Ophthalmol **156**(4): 667-672.

Ophthalmology, A. A. o. (2016). Retina and Vitreous Basic and Clinical Science Course.

Orr, P., A. M. Rentz, M. K. Margolis, D. A. Revicki, C. M. Dolan, S. Colman, J. T. Fine and N. M. Bressler (2011). "Validation of the National Eye Institute Visual Function Questionnaire-25 (NEI VFQ-25) in age-related macular degeneration." Invest Ophthalmol Vis Sci **52**(6): 3354-3359.

Osterberg, G. (1935). "Topography of the layer of rods and cones in the human retina." Acta ophthalmol **13**: 6-97.

Otteson, D. C. (2011). "Eyes on DNA methylation: current evidence for DNA methylation in ocular development and disease." Journal of ocular biology, diseases, and informatics **4**(3): 95-103.

Pallant, J. F. and A. Tennant (2007). "An introduction to the Rasch measurement model: an example using the Hospital Anxiety and Depression Scale (HADS)." British Journal of Clinical Psychology **46**(1): 1-18.

Pan, C. W., D. Ramamurthy and S. M. Saw (2012). "Worldwide prevalence and risk factors for myopia." Ophthalmic Physiol Opt **32**(1): 3-16.

Park, D. H., K. S. Choi, H. J. Sun and S. J. Lee (2017). "FACTORS ASSOCIATED WITH VISUAL OUTCOME AFTER MACULA-OFF RHEGMATOGENOUS RETINAL DETACHMENT SURGERY." Retina.

Park, S. J., S. C. Cho, N.-K. Choi, K. H. Park and S. J. Woo (2017). "Age, sex, and time-specific trends in surgical approaches for rhegmatogenous retinal detachment: A Nationwide, Population-Based Study Using the National Claim Registry." Retina.

Parrish, R. K., 2nd, S. J. Gedde, I. U. Scott, W. J. Feuer, J. C. Schiffman, C. M. Mangione and A. Montenegro-Piniella (1997). "Visual function and quality of life among patients with glaucoma." Arch Ophthalmol **115**(11): 1447-1455.

Pastor, J. C., I. Fernandez, E. Rodriguez de la Rúa, R. Coco, M. R. Sanabria-Ruiz Colmenares, D. Sanchez-Chicharro, R. Martinho, J. M. Ruiz Moreno, J. Garcia Arumi, M. Suarez de Figueroa, A. Giraldo and L. Manzananas (2008). "Surgical outcomes for primary rhegmatogenous retinal detachments in phakic and pseudophakic patients: the Retina 1 Project--report 2." Br J Ophthalmol **92**(3): 378-382.

Pesudovs, K. (2010). "Item banking: a generational change in patient-reported outcome measurement." Optometry & Vision Science **87**(4): 285-293.

Pesudovs, K., J. M. Burr, C. Harley and D. B. Elliott (2007). "The development, assessment, and selection of questionnaires." Optometry & Vision Science **84**(8): 663-674.

Pesudovs, K., L. E. Caudle, G. Rees and E. L. Lamoureux (2008). "Validity of a visual impairment questionnaire in measuring cataract surgery outcomes." Journal of Cataract & Refractive Surgery **34**(6): 925-933.

Pesudovs, K., V. K. Gothwal, T. Wright and E. L. Lamoureux (2010). "Remediating serious flaws in the National Eye Institute Visual Function Questionnaire." Journal of Cataract & Refractive Surgery **36**(5): 718-732.

Podoleanu, A., J. Rogers, D. Jackson and S. Dunne (2000). "Three dimensional OCT images from retina and skin." Opt Express **7**(9): 292-298.

Podoleanu, A. G. and R. B. Rosen (2008). "Combinations of techniques in imaging the retina with high resolution." Prog Retin Eye Res **27**(4): 464-499.

Ra, E., Y. Ito, K. Kawano, T. Iwase, H. Kaneko, S. Ueno, S. Yasuda, K. Kataoka and H. Terasaki (2017). "Regeneration of Photoreceptor Outer Segments After Scleral Buckling Surgery for Rhegmatogenous Retinal Detachment." Am J Ophthalmol **177**: 17-26.

Rahman, W., F. K. Chen, J. Yeoh, P. Patel, A. Tufail and L. Da Cruz (2011). "Repeatability of manual subfoveal choroidal thickness measurements in healthy subjects using the technique of enhanced depth imaging optical coherence tomography." Investigative ophthalmology & visual science **52**(5): 2267-2271.

Ramkissoon, Y. D., S. A. Aslam, S. P. Shah, S. C. Wong and P. M. Sullivan (2010). "Risk of iatrogenic peripheral retinal breaks in 20-G pars plana vitrectomy." Ophthalmology **117**(9): 1825-1830.

Rasch, G. (1960). "Probabilistic models for some intelligence and achievement tests." Copenhagen: Danish Institute for Educational Research.

Rashid, S., S. Pilli, E. K. Chin, R. J. Zawadzki, J. S. Werner and S. S. Park (2013). "Five-year follow-up of macular morphologic changes after rhegmatogenous retinal detachment repair: Fourier domain OCT findings." Retina **33**(10): 2049-2058.

Ratnam, K., J. Carroll, T. C. Porco, J. L. Duncan and A. Roorda (2013). "Relationship between foveal cone structure and clinical measures of visual function in patients with inherited retinal degenerations." Invest Ophthalmol Vis Sci **54**(8): 5836-5847.

Remé, C. E. and M. Sulser (1977). "Diurnal variation of autophagy in rod visual cells in the rat." Albrecht von Graefes Archiv für klinische und experimentelle Ophthalmologie **203**(3-4): 261-270.

Renieri, G., S. Pitz, N. Pfeiffer, M. E. Beutel and R. Zwerenz (2013). "Changes in quality of life in visually impaired patients after low-vision rehabilitation." Int J Rehabil Res **36**(1): 48-55.

Roorda, A., F. Romero-Borja, W. Donnelly Iii, H. Queener, T. Hebert and M. Campbell (2002). "Adaptive optics scanning laser ophthalmoscopy." Opt Express **10**(9): 405-412.

Roorda, A. and D. R. Williams (2002). "Optical fiber properties of individual human cones." J Vis **2**(5): 404-412.

Rose, NR., Klose RJ (2014). "Understanding the relationship between DNA methylation and histone lysine methylation." Biochim Biophys Acta. **1839**(12):1362-72.

Rosman, M., T. Y. Wong, S. G. Ong and C. L. Ang (2001). "Retinal detachment in Chinese, Malay and Indian residents in Singapore: a comparative study on risk factors, clinical presentation and surgical outcomes." International ophthalmology **24**(2): 101-106.

Ross, W., A. Lavina, M. Russell and D. Maberley (2005). "The correlation between height of macular detachment and visual outcome in macula-off retinal detachments of ≤ 7 days' duration." Ophthalmology **112**(7): 1213-1217.

Ross, W. H. and D. W. Kozy (1998). "Visual recovery in macula-off rhegmatogenous retinal detachments." Ophthalmology **105**(11): 2149-2153.

Rossi, G. C., G. Milano and C. Tinelli (2003). "The Italian version of the 25-item National Eye Institute Visual Function Questionnaire: translation, validity, and reliability." J Glaucoma **12**(3): 213-220.

Rowe, J. A., J. C. Erie, K. H. Baratz, D. O. Hodge, D. T. Gray, L. Butterfield and D. M. Robertson (1999). "Retinal detachment in Olmsted County, Minnesota, 1976 through 1995." Ophthalmology **106**(1): 154-159.

Ruiz-Medrano, J., I. Flores-Moreno, P. Pena-Garcia, J. A. Montero, J. S. Duker and J. M. Ruiz-Moreno (2014). "Macular choroidal thickness profile in a healthy population measured by swept-source optical coherence tomography." Invest Ophthalmol Vis Sci **55**(6): 3532-3542.

Ryan, B. and T. H. MARGRAIN (2008). "Measuring low vision service outcomes: Rasch analysis of the seven-item National Eye Institute Visual Function Questionnaire." Optometry & Vision Science **85**(2): 112-121.

Sahaboglu, A., O. Paquet-Durand, J. Dietter, K. Dengler, S. Bernhard-Kurz, P. A. Ekström, B. Hitzmann, M. Ueffing and F. Paquet-Durand (2013). "Retinitis pigmentosa: rapid neurodegeneration is governed by slow cell death mechanisms." Cell death & disease **4**(2): e488.

Saleh, M., G. Debellemanni, M. Meillat, P. Tumahai, M. Bidaut Garnier, M. Flores, C. Schwartz and B. Delbosc (2014). "Quantification of cone loss after surgery for retinal detachment involving the macula using adaptive optics." Br J Ophthalmol **98**(10): 1343-1348.

Salicone, A., W. E. Smiddy, A. Venkatraman and W. Feuer (2006). "Visual recovery after scleral buckling procedure for retinal detachment." Ophthalmology **113**(10): 1734-1742.

Sancho-Pelluz, J., B. Arango-Gonzalez, S. Kustermann, F. J. Romero, T. van Veen, E. Zrenner, P. Ekstrom and F. Paquet-Durand (2008). "Photoreceptor cell death mechanisms in inherited retinal degeneration." Mol Neurobiol **38**(3): 253-269.

Sayman Muslubas, I., M. Hocaoglu, M. G. Ersoz, S. Arf and M. Karacorlu (2017). "Choroidal thickness in chronic rhegmatogenous retinal detachment before and after surgery, and comparison with acute cases." Int Ophthalmol.

Sayman Muslubas, I., M. Karacorlu, M. Hocaoglu, S. Arf and O. Uysal (2016). "Subfoveal choroidal thickness change after pars plana vitrectomy in recent onset rhegmatogenous retinal detachment." Retina **36**(12): 2371-2376.

Schocket, L. S., A. J. Witkin, J. G. Fujimoto, T. H. Ko, J. S. Schuman, A. H. Rogers, C. Baumal, E. Reichel and J. S. Duker (2006). "Ultrahigh-resolution optical coherence tomography in patients with decreased visual acuity after retinal detachment repair." Ophthalmology **113**(4): 666-672.

Schocket, L. S., A. J. Witkin, J. G. Fujimoto, T. H. Ko, J. S. Schuman, A. H. Rogers, C. Baumal, E. Reichel and J. S. Duker (2006). "Ultrahigh-resolution optical coherence tomography in patients with decreased visual acuity after retinal detachment repair." Ophthalmology **113**(4): 666-672.

Scoles, D., J. A. Flatter, R. F. Cooper, C. S. Langlo, S. Robison, M. Neitz, D. V. Weinberg, M. E. Pennesi, D. P. Han, A. Dubra and J. Carroll (2016). "Assessing photoreceptor structure associated with ellipsoid zone disruptions visualized with optical coherence tomography." Retina **36**(1): 91-103.

Sengoku, T. and S. Yokoyama (2011). "Structural basis for histone H3 Lys 27 demethylation by UTX/KDM6A." Genes Dev **25**(21): 2266-2277.

Sherr, C. J. (2006). "Divorcing ARF and p53: an unsettled case." Nature Reviews Cancer **6**(9): 663-673.

Sherr, C. J. and J. M. Roberts (1999). "CDK inhibitors: positive and negative regulators of G1-phase progression." Genes & development **13**(12): 1501-1512.

Sherr, C. J. and J. M. Roberts (2004). "Living with or without cyclins and cyclin-dependent kinases." Genes & development **18**(22): 2699-2711.

Sheu, S.-J., L.-P. Ger and J.-F. Chen (2007). "Male sex as a risk factor for pseudophakic retinal detachment after cataract extraction in Taiwanese adults." Ophthalmology **114**(10): 1898-1903. e1891.

Sheu, S.-J., L.-P. Ger and W.-L. Ho (2010). "Late increased risk of retinal detachment after cataract extraction." American journal of ophthalmology **149**(1): 113-119. e111.

Sheu, S. J., L. P. Ger and W. L. Ho (2010). "Late increased risk of retinal detachment after cataract extraction." Am J Ophthalmol **149**(1): 113-119.

Smretschnig, E., C. I. Falkner-Radler, S. Binder, J. Sporn, R. Ristl, C. Glittenberg and K. Krepler (2016). "Vision-related quality of life and visual function after retinal detachment surgery." Retina **36**(5): 967-973.

Spaide, R. F., H. Koizumi and M. C. Pozzoni (2008). "Enhanced depth imaging spectral-domain optical coherence tomography." American journal of ophthalmology **146**(4): 496-500.

Stangos, A. N., I. K. Petropoulos, C. G. Brozou, A. D. Kapetanios, A. Whatham and C. J. Pournaras (2004). "Pars-plana vitrectomy alone vs vitrectomy with scleral buckling for primary rhegmatogenous pseudophakic retinal detachment." Am J Ophthalmol **138**(6): 952-958.

Staurenghi, G., S. Sadda, U. Chakravarthy and R. F. Spaide (2014). "Proposed lexicon for anatomic landmarks in normal posterior segment spectral-domain optical coherence tomography: the IN*OCT consensus." Ophthalmology **121**(8): 1572-1578.

Steinberg, E. P., J. M. Tielsch, O. D. Schein, J. C. Javitt, P. Sharkey, S. D. Cassard, M. W. Legro, M. Diener-West, E. B. Bass, A. M. Damiano and et al. (1994). "National study of cataract surgery outcomes. Variation in 4-month postoperative outcomes as reflected in multiple outcome measures." Ophthalmology **101**(6): 1131-1140; discussion 1140-1131.

Steinberg, E. P., J. M. Tielsch, O. D. Schein, J. C. Javitt, P. Sharkey, S. D. Cassard, M. W. Legro, M. Diener-West, E. B. Bass, A. M. Damiano and et al. (1994). "The VF-14. An index of functional impairment in patients with cataract." Arch Ophthalmol **112**(5): 630-638.

Stiles, W. and B. Crawford (1933). "The luminous efficiency of rays entering the eye pupil at different points." Proceedings of the Royal Society of London. Series B, Containing Papers of a Biological Character **112**(778): 428-450.

Subramanian, M. L. and T. M. Topping (2004). "Controversies in the management of primary retinal detachments." International ophthalmology clinics **44**(4): 103-114.

Sugawara, T., A. Hagiwara, A. Hiramatsu, K. Ogata, Y. Mitamura and S. Yamamoto (2010). "Relationship between peripheral visual field loss and vision-related quality of life in patients with retinitis pigmentosa." Eye (Lond) **24**(4): 535-539.

Sugawara, T., E. Sato, T. Baba, A. Hagiwara, A. Tawada and S. Yamamoto (2011). "Relationship between vision-related quality of life and microperimetry-determined macular sensitivity in patients with retinitis pigmentosa." Jpn J Ophthalmol **55**(6): 643-646.

Takeuchi, A., G. Kricorian and M. F. Marmor (1996). "When vitreous enters the subretinal space. Implications for subretinal fluid protein." Retina **16**(5): 426-430.

Tani, P., D. M. Robertson and A. Langworthy (1980). "Rhegmatogenous retinal detachment without macular involvement treated with scleral buckling." Am J Ophthalmol **90**(4): 503-508.

Tani, P., D. M. Robertson and A. Langworthy (1981). "Prognosis for central vision and anatomic reattachment in rhegmatogenous retinal detachment with macula detached." Am J Ophthalmol **92**(5): 611-620.

Tesio, L. (2003). "Measuring behaviours and perceptions: Rasch analysis as a tool for rehabilitation research." Journal of rehabilitation medicine **35**(3): 105-115.

Trevor, G. and C. M. Fox (2007). Applying the Rasch Model: fundamental measurement in the human sciences, L. Erlbaum.

Trichonas, G., Y. Murakami, A. Thanos, Y. Morizane, M. Kayama, C. M. Debouck, T. Hisatomi, J. W. Miller and D. G. Vavvas (2010). "Receptor interacting protein kinases mediate retinal detachment-induced photoreceptor necrosis and compensate for inhibition of apoptosis." Proceedings of the National Academy of Sciences **107**(50): 21695-21700.

Trifunovic, D., A. Sahaboglu, J. Kaur, S. Mencl, E. Zrenner, M. Ueffing, B. Arango-Gonzalez and F. Paquet-Durand (2012). "Neuroprotective strategies for the treatment of inherited photoreceptor degeneration." Current molecular medicine **12**(5): 598-612.

Turner, J. R. and M. Gellman (2013). Encyclopedia of Behavioral Medicine, Springer.

van de Put, M. A., L. Hoeksema, W. Wanders, I. M. Nolte, J. M. Hooymans and L. I. Los (2014). "Postoperative vision-related quality of life in macula-off rhegmatogenous retinal detachment patients and its relation to visual function." PLoS One **9**(12): e114489.

Van de Put, M. A., J. M. Hooymans, L. I. Los and D. R. R. D. S. Group (2013). "The incidence of rhegmatogenous retinal detachment in the Netherlands." Ophthalmology **120**(3): 616-622.

Veckeneer, M., L. Derycke, E. W. Lindstedt, J. van Meurs, M. Cornelissen, M. Bracke and E. Van Aken (2012). "Persistent subretinal fluid after surgery for rhegmatogenous retinal detachment: hypothesis and review." Graefes Arch Clin Exp Ophthalmol **250**(6): 795-802.

Veckeneer, M., K. Van Overdam, D. Bouwens, E. Feron, D. Mertens, E. Peperkamp, P. Ringens, P. Mulder and J. Van Meurs (2001). "Randomized clinical trial of cryotherapy

versus laser photocoagulation for retinopexy in conventional retinal detachment surgery." Am J Ophthalmol **132**(3): 343-347.

Vincent, I., M. Rosado and P. Davies (1996). "Mitotic mechanisms in Alzheimer's disease?" Journal of Cell Biology **132**(3): 413-426.

Vuong, V. S., E. Moisseiev, D. Cunefare, S. Farsiu, A. Moshiri and G. Yiu (2016). "Repeatability of choroidal thickness measurements on enhanced depth imaging optical coherence tomography using different posterior boundaries." American journal of ophthalmology **169**: 104-112.

Wahlin, K. J., R. A. Enke, J. A. Fuller, G. Kalesnykas, D. J. Zack and S. L. Merbs (2013). "Epigenetics and cell death: DNA hypermethylation in programmed retinal cell death." PloS one **8**(11): e79140.

Wakabayashi, T., Y. Oshima, H. Fujimoto, Y. Murakami, H. Sakaguchi, S. Kusaka and Y. Tano (2009). "Foveal microstructure and visual acuity after retinal detachment repair: imaging analysis by Fourier-domain optical coherence tomography." Ophthalmology **116**(3): 519-528.

Wakabayashi, T., Y. Oshima, H. Fujimoto, Y. Murakami, H. Sakaguchi, S. Kusaka and Y. Tano (2009). "Foveal microstructure and visual acuity after retinal detachment repair: imaging analysis by Fourier-domain optical coherence tomography." Ophthalmology **116**(3): 519-528.

Wang, J., D. McLeod, D. B. Henson and P. N. Bishop (2003). "Age-dependent changes in the basal retinovitreal adhesion." Investigative ophthalmology & visual science **44**(5): 1793-1800.

Wassle, H., U. Grunert, J. Rohrenbeck and B. B. Boycott (1990). "Retinal ganglion cell density and cortical magnification factor in the primate." Vision Res **30**(11): 1897-1911.

Weichel, E. D., A. Martidis, M. S. Fineman, J. A. McNamara, C. H. Park, J. F. Vander, A. C. Ho and G. C. Brown (2006). "Pars plana vitrectomy versus combined pars plana vitrectomy-scleral buckle for primary repair of pseudophakic retinal detachment." Ophthalmology **113**(11): 2033-2040.

Wenzel, A., C. Grimm, M. Samardzija and C. E. Reme (2005). "Molecular mechanisms of light-induced photoreceptor apoptosis and neuroprotection for retinal degeneration." Prog Retin Eye Res **24**(2): 275-306.

Wickham, L., M. Connor and G. W. Aylward (2004). "Vitrectomy and gas for inferior break retinal detachments: are the results comparable to vitrectomy, gas, and scleral buckle?" Br J Ophthalmol **88**(11): 1376-1379.

Williams, D. R. (2011). "Imaging single cells in the living retina." Vision Res **51**(13): 1379-1396.

Williamson, T. H., M. Shunmugam, I. Rodrigues, M. Dogramaci and E. Lee (2013). "Characteristics of rhegmatogenous retinal detachment and their relationship to visual outcome." Eye (Lond) **27**(9): 1063-1069.

Wojtkowski, M., V. Srinivasan, J. G. Fujimoto, T. Ko, J. S. Schuman, A. Kowalczyk and J. S. Duker (2005). "Three-dimensional retinal imaging with high-speed ultrahigh-resolution optical coherence tomography." Ophthalmology **112**(10): 1734-1746.

Wolfensberger, T. J. (2004). "Foveal reattachment after macula-off retinal detachment occurs faster after vitrectomy than after buckle surgery." Ophthalmology **111**(7): 1340-1343.

Wolfensberger, T. J. and M. Gonvers (2002). "Optical coherence tomography in the evaluation of incomplete visual acuity recovery after macula-off retinal detachments." Graefes Arch Clin Exp Ophthalmol **240**(2): 85-89.

Wright, B. D. and M. Mok (2000). "Understanding Rasch measurement: Rasch models overview." Journal of applied measurement.

Yang, Y., D. S. Geldmacher and K. Herrup (2001). "DNA replication precedes neuronal cell death in Alzheimer's disease." Journal of Neuroscience **21**(8): 2661-2668.

Yokota, S., S. Ooto, M. Hangai, K. Takayama, N. Ueda-Arakawa, Y. Yoshihara, M. Hanebuchi and N. Yoshimura (2013). "Objective assessment of foveal cone loss ratio in surgically closed macular holes using adaptive optics scanning laser ophthalmoscopy." PLoS One **8**(5): e63786.

Yonemoto, J., H. Ideta, K. Sasaki, S. Tanaka, A. Hirose and C. Oka (1994). "The age of onset of posterior vitreous detachment." Graefes Arch Clin Exp Ophthalmol **232**(2): 67-70.

Yu, J., R. Peng, H. Chen, C. Cui and J. Ba (2012). "Elucidation of the Pathogenic Mechanism of Rhegmatogenous Retinal Detachment with Proliferative Vitreoretinopathy by Proteomic Analysis Proteomic Analysis Pathogenic Metabolism of PVR." Investigative ophthalmology & visual science **53**(13): 8146-8153.

Yun, C., J. Ahn, M. Kim, J. T. Kim, S. Y. Hwang, S. W. Kim and J. Oh (2017). "Characteristics of retinal vessels in surgically closed macular hole: an optical coherence tomography angiography study." Graefes Arch Clin Exp Ophthalmol **255**(10): 1923-1934.

Yuzawa, M., K. Fujita, E. Tanaka and E. C. Wang (2013). "Assessing quality of life in the treatment of patients with age-related macular degeneration: clinical research findings and recommendations for clinical practice." Clin Ophthalmol **7**: 1325-1332.

Zacks, D. N., Y. Han, Y. Zeng and A. Swaroop (2006). "Activation of signaling pathways and stress-response genes in an experimental model of retinal detachment." Investigative ophthalmology & visual science **47**(4): 1691-1695.

Zawadzki, R. J., S. S. Choi, S. M. Jones, S. S. Oliver and J. S. Werner (2007). "Adaptive optics-optical coherence tomography: optimizing visualization of microscopic retinal structures in three dimensions." J Opt Soc Am A Opt Image Sci Vis **24**(5): 1373-1383.

Zawadzki, R. J., S. M. Jones, S. S. Olivier, M. Zhao, B. A. Bower, J. A. Izatt, S. Choi, S. Laut and J. S. Werner (2005). "Adaptive-optics optical coherence tomography for high-resolution and high-speed 3D retinal in vivo imaging." Opt Express **13**(21): 8532-8546.

Zencak, D., K. Schouwey, D. Chen, P. Ekstrom, E. Tanger, R. Bremner, M. van Lohuizen and Y. Arsenijevic (2013). "Retinal degeneration depends on Bmi1 function and reactivation of cell cycle proteins." Proc Natl Acad Sci U S A **110**(7): E593-601.

Zencak, D., K. Schouwey, D. Chen, P. Ekström, E. Tanger, R. Bremner, M. van Lohuizen and Y. Arsenijevic (2013). "Retinal degeneration depends on Bmi1 function and reactivation of cell cycle proteins." Proceedings of the National Academy of Sciences **110**(7): E593-E601.

Zhang, J., B. Rao and Z. Chen (2005). "Swept source based fourier domain functional optical coherence tomography." Conf Proc IEEE Eng Med Biol Soc **7**: 7230-7233.

Zhang, T., P. Godara, E. R. Blanco, R. L. Griffin, X. Wang, C. A. Curcio and Y. Zhang (2015). "Variability in Human Cone Topography Assessed by Adaptive Optics Scanning Laser Ophthalmoscopy." Am J Ophthalmol **160**(2): 290-300.e291.

Zhang, Y., J. Rha, R. Jonnal and D. Miller (2005). "Adaptive optics parallel spectral domain optical coherence tomography for imaging the living retina." Opt Express **13**(12): 4792-4811.

Ziccardi, L., D. Giannini, G. Lombardo, S. Serrao, R. Dell'Omo, A. Nicoletti, M. Bertelli and M. Lombardo (2015). "Multimodal Approach to Monitoring and Investigating Cone Structure and Function in an Inherited Macular Dystrophy." Am J Ophthalmol **160**(2): 301-312.e306.

Zou, H., X. Zhang, X. Xu, H. Liu, L. Bai and X. Xu (2011). "Vision-related quality of life and self-rated satisfaction outcomes of rhegmatogenous retinal detachment surgery: three-year prospective study." PLoS One **6**(12): e28597.

LIST OF ABBREVIATIONS

RD – retinal detachment

RPE – retinal pigment epithelium

SRF – subretinal fluid

VA – visual acuity

BCVA – best corrected visual acuity

PVD – posterior vitreous detachment

OCT – optical coherence tomography

EDI OCT – enhance depth optical coherence tomography

SD OCT – spectral domain optical coherence tomography

QoL – quality of life

NEI VFQ – National Eye Institute Visual Functioning Questionnaire

PPV – pars plana vitrectomy

SB – scleral buckling

ILM – internal limiting membrane

NFL – nerve fiber layer

GCL – ganglion cell layer

IPL – inner plexiform layer

INL – inner nuclear layer

OPL – outer plexiform layer

ONL – outer nuclear layer

OLM – outer limiting membrane

PL – photoreceptor layer

CT – choroidal thickness

AO – adaptive optics fundus camera

DIV – day(s) in vitro

CDK4 – cyclin-dependent kinase 4

H3K27me³ – histone methylation on the amino (N) terminal tail of the core histone H3

AIF – apoptosis-inducing factor

TUNEL – Terminal deoxynucleotidyl transferase (TdT) dUTP Nick-End Labeling

DAPI – 4',6-diamidino-2-phenylindole, a fluorescent stain that binds strongly to A-T rich regions in DNA

B27 – culture medium supplement, serum-free neurobasal medium

FBS – fetal bovine serum

P/S – penicillin/streptomycin solution

DMEM/F12 – Dulbecco's Modified Eagle Medium/Nutrient mixture F12; basal medium for supporting the growth of many different mammalian cells

ANNEXES

Jules-Gonin questionnaire de fonctionnement visuel pour détachement de rétine

version 2015

INSTRUCTIONS :

Ce questionnaire est lié au sujet des problèmes qui impliquent votre vision ou les sentiments que vous avez sur un problème de vision.

Après chaque question, il y a une liste de réponses possibles. S'il vous plaît, choisissez la réponse qui décrit le mieux votre situation.

S'il vous plaît, répondez à toutes les questions comme si vous portiez vos lunettes ou de lentilles de contact (le cas échéant).

S'il vous plaît, prenez autant de temps que vous deviez pour répondre à chaque question.

Toutes vos réponses sont confidentielles.

Afin de mieux connaître vos problèmes de vision et comment ils affectent votre qualité de vie, vos réponses doivent être aussi précises que possible, dans cette enquête.

Rappelez-vous, si vous portiez des lunettes ou des lentilles de contact pour une activité particulière, s'il vous plaît, répondez à toutes les questions suivantes comme si vous les portiez.

Jules-Gonin questionnaire de fonctionnement visuel

1ère PARTIE - ETAT DE SANTE GENERAL ET VUE (Entourez un chiffre)

1. Actuellement, lorsque vous regardez avec les deux yeux en même temps, vous diriez que votre vue avec la meilleure correction optique (avec lunettes ou lentilles, si vous les portez) est excellente, bonne, mauvaise, ou très mauvaise, ou bien êtes-vous complètement aveugle ?

Excellente	Bonne	Mauvaise	Très mauvaise
(1)	(2)	(3)	(4)

2. Avez-vous du mal à lire les caractères d'imprimerie de taille normale dans les journaux, avec la meilleure correction optique que vous portez?

Pas du tout	Un peu	Enormément	Arrêté de le faire à cause de votre vue
(1)	(2)	(3)	(4)

3. Avez-vous du mal à faire certaines tâches ou certains passe-temps qui exigent de bien voir de près, comme faire la cuisine, de la couture, bricoler dans la maison ou utiliser des petits outils ?

Pas du tout	Un peu	Enormément	Arrêté de le faire à cause de votre vue
(1)	(2)	(3)	(4)

4. A cause de votre vue, avez-vous du mal à retrouver quelque chose sur une étagère encombrée ?

Pas du tout	Un peu	Enormément	Arrêté de le faire à cause de votre vue
(1)	(2)	(3)	(4)

5. Avez-vous du mal à lire les panneaux de circulation ou les enseignes de magasins dans la rue ?

Pas du tout	Un peu	Enormément	Arrêté de le faire à cause de votre vue
(1)	(2)	(3)	(4)

6. A cause de votre vue, avez-vous du mal à descendre des marches, un escalier ou les rebords de trottoirs la nuit ou quand l'éclairage est faible ?

Pas du tout	Un peu	Enormément	Arrêté de le faire à cause de votre vue
(1)	(2)	(4)	(4)

7. A cause de votre vue, avez-vous du mal à rendre visite à des gens, à aller dans des soirées ou au restaurant ?

Pas du tout	Un peu	Enormément	Arrêté de le faire à cause de votre vue
(1)	(2)	(3)	(4)

2^{ème} PARTIE; VOS REACTIONS A VOS PROBLEMES DE VUE

Les questions suivantes portent sur ce qui vous arrive peut-être à cause de votre vue. Pour chaque question, entourez le chiffre qui indique si, dans votre situation, cette question est vraie en permanence, très souvent, rarement ou jamais. (Entourez un chiffre)

8. Faites-vous moins de choses que vous ne le voudriez à cause de votre vue ?

Jamais (1)	Rarement (2)	Très souvent (3)	En permanence (4)
-----------------------------	-------------------------------	-----------------------------------	------------------------------------

9. Etes-vous limité(e) dans le temps que vous pouvez consacrer à votre travail ou à vos activités à cause de votre vue ?

Jamais (1)	Rarement (2)	Très souvent (3)	En permanence (4)
-----------------------------	-------------------------------	-----------------------------------	------------------------------------

Pour chacune des phrases suivantes, entourez le chiffre qui indique si, dans votre situation, c'est entièrement vrai, plutôt vrai, plutôt faux ou entièrement faux. (Entourez un chiffre)

10. Je reste chez moi la plupart du temps à cause de ma vue

Entièrement faux (1)	Plutôt faux (2)	Plutôt vrai (3)	Entièrement vrai (4)
-----------------------------	------------------------	------------------------	-----------------------------

11. Je maîtrise beaucoup moins bien ce que je fais à cause de ma vue

Entièrement faux (1)	Plutôt faux (2)	Plutôt vrai (3)	Entièrement vrai (4)
-----------------------------	------------------------	------------------------	-----------------------------

12. A cause de ma vue, je dois trop compter sur ce que me disent les autres

Entièrement faux (1)	Plutôt faux (2)	Plutôt vrai (3)	Entièrement vrai (4)
-----------------------------	------------------------	------------------------	-----------------------------

13. Je m'inquiète à l'idée de faire des choses embarrassantes pour moi-même ou pour les autres, à cause de ma vue

Entièrement faux (1)	Plutôt faux (2)	Plutôt vrai (3)	Entièrement vrai (4)
-----------------------------	------------------------	------------------------	-----------------------------

Annex 2: Laboratory protocols - Globe dissection

Protocole pour la dissection de globe humain

Le globe arrive dans la solution de NaCl.

La dissection du globe doit se faire dans la salle P2 proche de l'entrée, sous la hotte (dans la solution de NaCl)

Faire la paracentèse. Continuer à couper respectant le limbe.

Enlever la cornée, l'iris et le cristallin. Enlever la vitrée.

Couper la sclère avec la rétine dans la forme de fleur (4 coupes).

Décoller la rétine **en prélevant l'épithélium pigmentaire** avec la rétine (contrôle pour le décollement de rétine).

Pour le **modèle *in vitro* de décollement de rétine, enlever le RPE**. Couper la rétine périphérique dans les petites tranches, le minimum 5x5mm.

Mettre les explants avec les RPE sur la membrane de l'insert Millipore et puis dans une plaque de 6 puits contenant 1.5mL de milieu (le milieu pénètre par capillarité à travers le filtre).

Suivant les instructions et les milieux disponibles :

Utiliser le milieu suivant :

B27 [1x]_f [50x]_i

FBS [1%]_f [100%]_i

P/S [100 x]_f [1x]_i

DMEM/F12

Ou le milieu R16 complet.

Protocole DR

1. Groupe de rétine sans RPE (DR *in vitro*)
2. Groupe contrôle avec RPE

Fixer les rétines aux temps différents :

1. Time 0 (tout de suite)
2. Time 1 (24h DIV)
3. Time 3 (3 DIV)
4. Time 5 (5 DIV)
5. Time 7 (7 DIV)

Laisser les plaques à 37°. Changer le milieu chaque 2 jour.

La rétine est fixée selon le protocole : 2h 4% PAF

2h 10% Sucrose

Laisser dans 30% Sucrose

Montage des explants selon le protocole dans le Yazulla, puis congeler à -20°

B27 - neuronal cell culture supplement, B-27 Supplement is an optimized serum-free supplement used to support the low- or high-density growth and short- or long-term viability of embryonic, post-natal, and adult hippocampal and other CNS neurons. B-27 Supplement is provided as a 50X liquid and is intended for use with Neurobasal Medium or Neurobasal-A Medium for neuronal cell culture without the need for an astrocyte feeder layer. It is a modification of serum-free Neurobasal medium.

FBS – fetal bovine serum is the most widely used serum-supplement for the in vitro cell culture of eukaryotic cells. This is due to it having a very low level of antibodies and containing more growth factors, allowing for versatility in many different cell culture applications. Bovine serum albumin is the major component of the fetal bovine serum.

P/S - Penicillin/Streptomycin Solution is a 5mL 100x solution designed to aid in reducing risks of contamination in research. It consists of 10,000 units/mL of Penicillin and 10,000 µg/mL of Streptomycin in saline solution.

DMEM/F12 - Dulbecco's Modified Eagle Medium/Nutrient Mixture F-12 is a widely used basal medium for supporting the growth of many different mammalian cells.

PAF – paraformaldehyde

Annex 3: Laboratory protocols - TUNEL staining protocol

TUNEL Roche* en Texas-Red adapté

*In Situ Cell Death Detection Kit , TMR red de Roche (cat. Ref 12 156 792 910)
Stock -20°C

Sortir les lames du -20°C et les laisser sécher 15 minutes
Hydrater au PBS 10 min, laver 1x 10 min

Prétraitement : 0.2% Triton X-100 in PBS 15 min T. amb.
Rincer les lames 3x au PBS
Incuber 45 min. avec le Blocking : 10% serum w/o Triton

TUNEL solution :

2 µl (tube blue cap= enzyme) + 38 µl (tube red cap) + 140 µl PBS (= 180 ul ... adapter!)

Incuber 50 min - 1h à 37°C

Laver 3x 5 minutes au PBS

Faire le DAPI

Monter

Annex 4: Laboratory protocols - DAPI staining protocol

DAPI Sigma D9542

The new **stock**: 1mg/ml is kept at -20°C, in the 2nd antibodies drawer (aluminium box).

There is aliquots of 100 µl and others just under these are aliquots of 500 µl.

The tube (stock: 1mg/ml) we thaw is kept in the **dark** at 4°C (small tube in the door's frige) :this stock is stable for several weeks.

Solution ready to use 0,1µg/ml :

stock is diluted 1000x , can be **stable 2-3 weeks** in the **dark**. You will find this tube at the usual place at 4°C

Can be also diluted 10.000x

Annex 5: Laboratory protocols - CDK4 DAB staining protocol

<u>ID:</u>	C9	
<u>Antigen:</u>	CDK4 (h-22)	
<u>Ordering information:</u>	Santacruz #sc-601	
<u>Staining:</u>		
<u>Host:</u>	Rabbit	
<u>Specificity:</u>	H,M,R	
<u>Storage:</u>	4°C	
	Tissue	Cells
<u>Pre-treatment:</u>	0.3% triton in PBS 20min RT	
<u>Blocking:</u>	5% NGS 3% BSA 0.3% triton in PBS	
<u>Duration:</u>	1h	
<u>Temperature:</u>	RT	
<u>Block endog. peroxidases :</u>	0.3% H2O2 5 min RT	
<u>Wash:</u>	4x3 min PBS	
<u>First antibody:</u>	C9 1:75	
<u>Buffer:</u>	Blocking	
<u>Duration:</u>	1h RT then ON 4°C	
<u>Temperature:</u>		
<u>Wash:</u>	3x5min PBS	
<u>Secondary antibody:</u>	Biotinylated GAR 1:200	
<u>Buffer:</u>	PBS	
<u>Duration:</u>	1h (!after 30 min prepare ABC solution, leave 30 min before use!)	
<u>Temperature:</u>	RT	
<u>Wash:</u>	3x3min PBS	
<u>ABC Substrate:</u>	Vector kit 1 drop A + 1 drop B in 4 ml PBS, incubate 30 min RT	
<u>Wash:</u>	3x5 min PBS	
<u>DAB staining:</u>	20 ul / ml DAB Buffer reveal 1-2 min	
<u>Wash:</u>	H2O	
<u>(Nuclei counterstaining</u>	DAPI 5-10 min RT)	
<u>Wash:</u>	3X5minutes PBS	
<u>Mount:</u>	with Mowiol	
<u>Comments:</u>	Ok DW 28.04.16 (Yvan approved)	
	Control + : mouse Rd1 P13	
<u>Reference person & date:</u>	Jelena 22.10.2014	

Annex 6: Laboratory protocols - H3K27me³ staining protocol

<u>ID:</u>	H3	
<u>Antigen:</u>	H3K27me3	
<u>Ordering information:</u>	MerckMillipore #07-449	
<u>Staining:</u>	Histone H3 trimethylated at Lys27, trimethyl-histone H3 (Lys27)	
<u>Host:</u>	Rabbit	
<u>Specificity:</u>	H, M, Ce	
<u>Storage:</u>	minus 20°C 4ul par tube	
	Tissue	Cells
<u>Equilibration:</u>	20 min @ RT in PBS	
<u>Pre-treatment:</u>	Antigen retrieval:	
	Buffer: 10 mM citrate pH 6.0 home made	
	200ml in blue plastic blox filled with 12 slides (use blank slides to reach 12)	
	Heat in a microwave oven 5mn @696W (Medium power set-up) NON-STOP	
	Cool down the cryosection 30mn @ RT - see recipe below	
<u>Wash:</u>	Rinse 3X with PBS 1X then 0.3%triton in PBS 30min RT	
<u>Blocking:</u>	5% NGS 1%BSA 0.3% Tx in PBS	
<u>Duration:</u>	1h30	
<u>Temperature:</u>	RT	
<u>First antibody:</u>	1:200 for 1h or 1:400 for O.N.	
<u>Buffer:</u>	Blocking	
<u>Duration:</u>	ON 4°C or 1h 37°C	
<u>Temperature:</u>		
<u>Wash:</u>	3x5min PBS	
<u>Secondary antibody:</u>	GAR 1:2000	
<u>Buffer:</u>	PBS	
<u>Duration:</u>	1h	
<u>Temperature:</u>	RT	
<u>Wash:</u>	3x5min PBS	
<u>Nuclei counterstaining</u>	DAPI 5-10minutes RT	
<u>Wash:</u>	3x5minutes PBS	
<u>Mount:</u>	with Mowiol	
<u>Comments:</u>	Citrate homemade: 0.840g of citric acid monohydrate (C8) in 400ml dH2O adjust pH to 6 with NaOH	
<u>Reference person & date:</u>	MM 05.06.14	

Annex 7: Laboratory protocols - Active Caspase 3 staining protocol

<u>ID:</u>	C40	
<u>Antigen:</u>	Active Caspase 3	
<u>Ordering information:</u>	BD Pharmingen #559565	
<u>Staining:</u>	mort cellulaire	
<u>Host:</u>	Rabbit	
<u>Specificity:</u>	Human Mouse	
<u>Storage:</u>	4°C	
	Tissue	Cells
<u>Pre-treatment:</u>	no	
<u>Blocking:</u>	5%NGS 0.2%triton in PBS	
<u>Duration:</u>	1h	
<u>Temperature:</u>	RT	
<u>First antibody:</u>	C40 1:75	
<u>Buffer:</u>	Blocking	
<u>Duration:</u>	ON	
<u>Temperature:</u>	4°C	
<u>Wash:</u>	3x5minutes	
<u>Secondary antibody:</u>	Alexa Fluor GAR 1:2000	
<u>Buffer:</u>	Blocking	
<u>Duration:</u>	1h30	
<u>Temperature:</u>	RT	
<u>Wash:</u>	3x5minutes	
<u>Nuclei counterstaining</u>	DAPI 5-10minutes RT	
<u>Wash:</u>	3x5minutes PBS	
<u>Mount:</u>	with Moviol	
<u>Comments:</u>	Fixation: 1h PAF4% RT	
<u>Reference person & date:</u>	AC for SD. 2014-2015	

Annex 8: Laboratory protocols - AIF staining protocol

ID:	A10	
Antigen:	AIF (Apoptosis Inducing Factor)	
Ordering information:	Abcam #ab32516	
Staining:	mitochondrial marker	
Host:	Rabbit monoclonal	
Specificity:	Mouse, human, rat	
Storage:	-20 C	
	Tissue	Cells
Pre-treatment:	Antigen retrieval (Citrate 10mM pH 6 5 min micro-wave @696V, cool 30 min)	
Wash:	PBS 3 x 5 min	
Blocking:	5%NGS +2% BSA + 0.3% TritonX in PBS	
Duration:	1h30	
Temperature:	RT	
First antibody:	A10 1:250	
Buffer:	Blocking	
Duration:	ON	
Temperature:	4°C	
Wash:	PBS 3 x 5 minutes	
Secondary antibody:	GAR 1:2000	
Buffer:	PBS	
Duration:	1h	
Temperature:	RT	
Wash:	PBS 3 x 5 minutes	
Nuclei counterstaining:	DAPI 5-10minutes RT	
Wash:	3x5minutes PBS	
Mount:	with Moviol	
Comments:	Positive control = Rd1 PN12	
Reference person & date:	Dana et Jelena février 2018	

CURRICULUM VITAE

Jelena Potić was born on the 21st March 1985. in Belgrade, Serbia, where she finished primary school “Vladislav Ribnikar” and The Third Belgrade High School.

Jelena Potić started studies in medicine in 2003, at the School of Medicine, University of Belgrade. She graduated in 2009, as the best student in the generation, with the average grade 9.91 (grade system: 5 – failure, 6 – the lowest passing grade, 10 – the highest). During her studies, Jelena was students` tutor – demonstrator in the Physiology Department during 2 years (2005/2006. and 2006/2007.), president of the Center for students` research, skilled and scientific work at the School of Medicine, University of Belgrade, member of the Council for the science and she was representing Medical School and University of Belgrade on many occasions such as: “X International Intensive Course – Bioethics at the Frontiers of Biomedicine”, Prague, Czech Republic, in July 2006, professional students` exchange (IFMSA) in Hospital Laval – Department of Cardiology, University Laval, Quebec City, Canada, in august 2008 and in the Hospital Virgen de la Victoria – Department of Gynecology and Obstetrics, University of Malaga, Spain in August 2009.

Jelena has gained many awards and scholarships: awards for the best student (each scholar year, starting with 2004.) and award of the Foundation “Nikola Spasic” for the best student in 2nd year of the School of Medicine (December 2005.), Scholarship of the Ministry of Education of the Republic of Serbia (academic years 2004/2005, 2006/2007, 2007/2008.), scholarship of the Republic Fondation for the Scientific and Artistic Youth, Ministry of Education, Republic of Serbia (academic year 2005/2006.), scholarship of the City of Belgrade (academic 2005/2006, 2006/2007, 2007/2008), scholarship of Ministry of Youth and Sports of the Republic of Serbia - Young Talents Fund - scholarships for 1000 best graduate students from Serbia (academic year 2008/2009.), EFG Eurobank scholarship for 100 best graduate students from Serbia (academic year 2008/2009.).

After graduation, Jelena has been awarded with the award „Crown of Success“ for the academic year 2008/2009, for the best student of the University of Belgrade. She has finished the academic studies in ophthalmology, at the Medical Faculty of Belgrade (2009/2010.) and defended with excellence the final Academic work entitled: “The time of absorption of submacular fluid comparing to the duration of macula-off rhegmatogenous retinal detachment after successful scleral buckle surgery, diagnosed with Optical coherence tomography”, under the mentorship of Prof. Dr I. Stefanovic (31.03.2011.). In 2010, Jelena has started PhD studies in epidemiology and ophthalmology, at the School of Medicine, University of Belgrade.

Jelena Potic started her residency in Ophthalmology in April 2012 and she passed the final national exam of Ophthalmology with excellence in April 2016.

In 2014, Jelena Potic was awarded from ARVO (Association for Research in Vision and Ophthalmology) Foundation “2014 Developing Country Eye Researcher Travel Fellowship” for the scientific poster. In the same year, she passed ICO exams (International Council of Ophthalmology): Basic Science & Optics and Refraction. In the same year, Jelena gained the Swiss Government Excellence Scholarship for the academic year 2014/2015 (University of Lausanne, Switzerland). Since then, Jelena is an

active collaborator with the University of Lausanne and Eye Hospital Jules-Gonin, where she spent two years to perform the PhD research. Currently she participates on three ongoing projects in Jules-Gonin Eye Hospital, University of Lausanne, Switzerland: “Anatomical and functional recovery of patients with retinal detachment and their quality of life”, “Retinal detachments in advanced retinoblastoma patients” and “Pathway of photoreceptor cell death in *in-vitro* model of retinal detachment”.

Jelena Potic was the National Representative of Serbia in the European Society of Ophthalmology – Young Ophthalmologists (2013-2017) and now she is the active Young Ophthalmologists (SOE YO) Committee member, elected in June 2017. Jelena has founded the Swiss-Serbian Association of Swiss Government Excellence Scholarship holders in June 2017. Since 2016, Jelena is Serbian Medical Chamber Collaborator for cooperation with UEMS (European Union of Medical Specialists) and also she is member of the Serbian Delegation in UEMS.

Jelena Potic was the invited speaker on several conferences: ARVO 2016 (Association for Research in Vision and Ophthalmology, Seattle, USA, May 2016), 2nd EMOYO 2016 (European Meeting of Young Ophthalmologists, held in June 2016 in Oviedo, Spain), and in conferences “Jeudi Jules-Gonin” in Lausanne, Switzerland (May 2017 and May 2018).

Currently, Jelena Potic is a specialist in Ophthalmology with the special interest in vitreoretinal surgery, eye trauma, retinal diseases, and retinoblastoma. She is employed in the Clinic for eye diseases, Clinical Center of Serbia, Belgrade, since February 2010, as a medical doctor and since April 2016 she works at the Eye Trauma Unit. Jelena Potic actively participates in clinical work (surgery, consultation and ultrasound diagnostics) and scientific work at the Clinic for Eye Diseases, Clinical Center of Serbia. She has been the author and/or coauthor on 36 scientific works published in extenso or presented on International or National Conferences. She is member of the Serbian Society of Ophthalmologists, Swiss Society of Ophthalmologists, European Society of Ophthalmologists, French Society of Ophthalmologists, Euretina (European Society of Retina Specialists) and ARVO (Association for Research in Vision and Ophthalmology).

Jelena speaks fluently three foreign languages French, English and Italian and was awarded for French language on several occasions: 1st place at the Republic Competition in French language of Serbian High schools in the year 2003 and the award of the French Government in the summer 2003. in Paris; she passed DALF exams in French language.

Izjava o autorstvu

Potpisani-a Jelena Potic

broj upisa EP-II-08/10

Izjavljujem

da je doktorska disertacija pod naslovom :

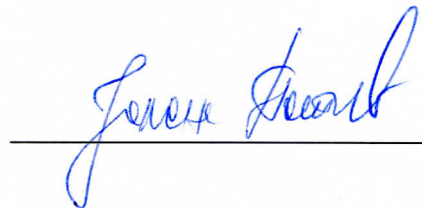
Characterization of the Mechanisms of Photoreceptor Degeneration during Retinal Detachment; the Evaluation of Postoperative Anatomical and Functional Recovery

(Карактеризација механизма дегенерације фоторецептора након аблације ретине; евалуација анатомског и функционалног постоперативног опоравка)

- rezultat sopstvenog istraživačkog rada,
- da predložena disertacija u celini ni u delovima nije bila predložena za dobijanje bilo koje diplome prema studijskim programima drugih visokoškolskih ustanova,
- da su rezultati korektno navedeni i
- da nisam kršio/la autorska prava i koristio intelektualnu svojinu drugih lica.

Potpis doktoranda

U Beogradu, 20.02.2018.



Izjava o istovetnosti štampane i elektronske verzije doktorskog rada

Ime i prezime autora : Jelena Potic

Broj upisa EP-II-08/10

Studijski program : EPIDEMIOLOGIJA

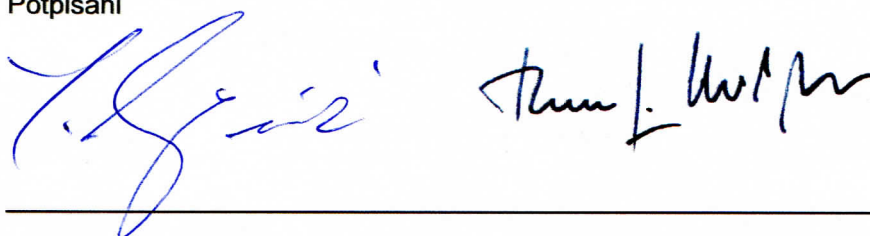
Naslov rada

Characterization of the Mechanisms of Photoreceptor Degeneration during Retinal Detachment; the Evaluation of Postoperative Anatomical and Functional Recovery

(Карактеризација механизма дегенерације фоторецептора након аблације ретине; евалуација анатомског и функционалног постоперативног опоравка)

Mentori Prof. Yvan Arsenijevic, Prof. Thomas J. Wolfensberger

Potpisani



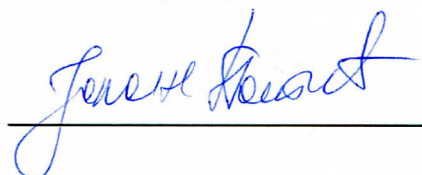
izjavljujem da je štampana verzija mog doktorskog rada istovetna elektronskoj verziji koju sam predao/la za objavljivanje na portalu **Digitalnog repozitorijuma Univerziteta u Beogradu**.

Dozvoljavam da se objave moji lični podaci vezani za dobijanje akademskog zvanja doktora nauka, kao što su ime i prezime, godina i mesto rođenja i datum odbrane rada.

Ovi lični podaci mogu se objaviti na mrežnim stranicama digitalne biblioteke, u elektronskom katalogu i u publikacijama Univerziteta u Beogradu.

Potpis doktoranda

U Beogradu, 20.02.2018.



Statement on the identity of the printed and electronic version of doctoral dissertation

Author's name and surname: Jelena Potic

Index number: EP-II-08/10

Study program: EPIDEMIOLOGY

Title of the thesis:

Characterization of the Mechanisms of Photoreceptor Degeneration during Retinal Detachment; the Evaluation of Postoperative Anatomical and Functional Recovery

(Карактеризација механизма дегенерације фоторецептора након аблације ретине; евалуација анатомског и функционалног постоперативног опоравка)

Mentors Prof. Yvan Arsenijevic, Prof. Thomas J. Wolfensberger

Signed

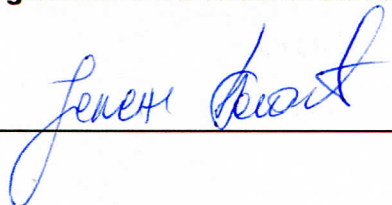
I declare that the printed version of my doctoral thesis is identical to the electronic version I submitted for publication on the portal of the **Digital Repository of the University of Belgrade**.

I authorize the publication of my personal information regarding the academic title of Doctor of Science, such as name, surname, age and place of birth, and date of defense of thesis.

These personal data can be published on the digital library's web pages, in the electronic catalog and in the publications of the University of Belgrade.

Signature of the doctoral student

In Belgrade, 20th February 2018.



Izjava o korišćenju

Ovlašćujem Univerzitetsku biblioteku „Svetozar Marković“ da u Digitalni repozitorijum Univerziteta u Beogradu unese moju doktorsku disertaciju pod naslovom:

Characterization of the Mechanisms of Photoreceptor Degeneration during Retinal Detachment; the Evaluation of Postoperative Anatomical and Functional Recovery

(Карактеризација механизма дегенерације фоторецептора након аблације ретине; евалуација анатомског и функционалног постоперативног опоравка)

koja je moje autorsko delo.

Disertaciju sa svim priložima predao/la sam u elektronskom formatu pogodnom za trajno arhiviranje.

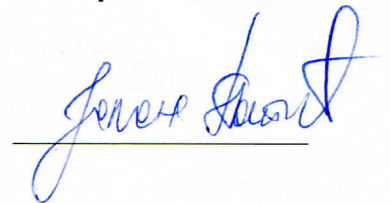
Moju doktorsku disertaciju pohranjenu u Digitalni repozitorijum Univerziteta u Beogradu mogu da koriste svi koji poštuju odredbe sadržane u odabranom tipu licence Kreativne zajednice (Creative Commons) za koju sam se odlučio/la.

1. Autorstvo
2. Autorstvo - nekomercijalno
3. Autorstvo – nekomercijalno – bez prerade
4. Autorstvo – nekomercijalno – deliti pod istim uslovima
5. Autorstvo – bez prerade
6. Autorstvo – deliti pod istim uslovima

(Molimo da zaokružite samo jednu od šest ponuđenih licenci, kratak opis licenci dat je na poleđini lista).

U Beogradu, 20.02.2018.

Potpis doktoranda



1. Autorstvo - Dozvoljavate umnožavanje, distribuciju i javno saopštavanje dela, i prerade, ako se navede ime autora na način određen od strane autora ili davaoca licence, čak i u komercijalne svrhe. Ovo je najslobodnija od svih licenci.
2. Autorstvo – nekomercijalno. Dozvoljavate umnožavanje, distribuciju i javno saopštavanje dela, i prerade, ako se navede ime autora na način određen od strane autora ili davaoca licence. Ova licenca ne dozvoljava komercijalnu upotrebu dela.
3. Autorstvo - nekomercijalno – bez prerade. Dozvoljavate umnožavanje, distribuciju i javno saopštavanje dela, bez promena, preoblikovanja ili upotrebe dela u svom delu, ako se navede ime autora na način određen od strane autora ili davaoca licence. Ova licenca ne dozvoljava komercijalnu upotrebu dela. U odnosu na sve ostale licence, ovom licencom se ograničava najveći obim prava korišćenja dela.
4. Autorstvo - nekomercijalno – deliti pod istim uslovima. Dozvoljavate umnožavanje, distribuciju i javno saopštavanje dela, i prerade, ako se navede ime autora na način određen od strane autora ili davaoca licence i ako se prerada distribuira pod istom ili sličnom licencom. Ova licenca ne dozvoljava komercijalnu upotrebu dela i prerada.
5. Autorstvo – bez prerade. Dozvoljavate umnožavanje, distribuciju i javno saopštavanje dela, bez promena, preoblikovanja ili upotrebe dela u svom delu, ako se navede ime autora na način određen od strane autora ili davaoca licence. Ova licenca dozvoljava komercijalnu upotrebu dela.
6. Autorstvo - deliti pod istim uslovima. Dozvoljavate umnožavanje, distribuciju i javno saopštavanje dela, i prerade, ako se navede ime autora na način određen od strane autora ili davaoca licence i ako se prerada distribuira pod istom ili sličnom licencom. Ova licenca dozvoljava komercijalnu upotrebu dela i prerada. Slična je softverskim licencama, odnosno licencama otvorenog koda.